UNIVERSITY OF SOUTHAMPTON

FACULTY OF MEDICINE

School of Medicine

The influence of the environment on cell-cell communication in the epithelial–mesenchymal trophic unit.

by

Fabio Bucchieri, MD

Thesis for the degree of Doctor of Philosophy

March 2012

ABSTRACT

UNIVERSITY OF SOUTHAMPTON
ABSTRACT
FACULTY OF MEDICINE
SCHOOL OF MEDICINE
Doctor of Philosophy
THE INFLUENCE OF THE ENVIRONMENT ON CELL-CELL COMMUNICATION IN THE EPITHELIAL–MESENCHYMAL TROPHIC UNIT.
by Fabio Bucchieri

Rationale: A key factor involved with the progressive decline in lung function in severe asthma is airway remodelling. This involves collagen deposition within the *lamina reticularis*, matrix deposition in the submucosa, smooth muscle hyperplasia, and microvascular and neuronal proliferation.

Aims: The main aim of this thesis was to test the hypothesis that *epithelial susceptibility to environmental injury and a prolonged tissue repair response result in activation of the epithelial mesenchymal trophic unit (EMTU) that in turn promotes airway wall remodelling*.

Methods: Investigation of epithelial mesenchymal signalling involved use of cells derived from normal or asthmatic volunteers and cultured *in vitro*. These were tested in simple monocultures and then a 'tissue engineered' construct was developed to enable assessment of responses in a complex cell model that closely mimics the human bronchial mucosa.

Results: Infection of asthmatic bronchial epithelial cells (AS PBEC) with RV-16 caused significantly less apoptosis when compared to infection of bronchial epithelial cells obtained from healthy controls (HC PBEC). As a consequence of this RV replicated more in AS PBEC; this defect may explain the higher susceptibility of the lower airways to RV infection in asthmatic subjects.
Using primary bronchial fibroblast cultures, collagen type I and fibronectin significantly increased adhesion rates, while laminin reduced differentiation of fibroblasts into myofibroblasts. None of the ECM components that were evaluated affected fibroblast survival. Although asthmatic fibroblasts expressed more αSMA than normal fibroblasts, no significant difference in terms of fibroblast differentiation was found when different ECM components, of relevance to asthma pathogenesis, were studied. When bronchial fibroblasts were exposed to conditioned media obtained from PBEC infected with RV16, there was no effect on markers of remodelling but there was a marked amplification of the epithelial inflammatory response, mainly due to increased release of IL8, IL6, RANTES and IP-10, suggesting that during a virus-induced exacerbation the fibroblasts promote inflammation. To investigate susceptibility to oxidant stress, PBEC were treated with 20% cigarette smoke extract (CSE). AS PBECs were more susceptible to CSE with a significant increase of early apoptotic (EA) cells compared to HS PBEC. Reduced glutathione protected both HS and AS PBEC from CSE-induced cell death causing a significant increase in cell viability, with a concomitant decrease in apoptosis. Oxidative stress-induced apoptosis in PBECs did not follow the canonical caspase pathways, but rather depended on a more direct mitochondrial damage pathway. The ECM also appeared to play a role in oxidative stress-induced cell death, with collagen IV being most effective in reducing H_2O_2-induced apoptosis. Finally, we developed and characterised a novel 3D *in vitro* model of human bronchial mucosa that proved to be very similar to the normal *in vivo* counterpart with a well differentiated epithelial layer composed of ciliated and goblet cells producing mucus and supported by a functional basement membrane which separated the epithelium from a mesenchymal layer containing fibroblasts dispersed in a well organised ECM. This model allowed investigation of the long term effects of CSE exposure which showed that CSE caused many characteristic signs of remodelling such as thickening of the basement membrane, disarray of the ECM, loss of ciliated cells and hyperproduction of mucus. These effects occurred in the absence of inflammatory or immune cells.

Conclusions: The finding that epithelial cells from asthmatic donors have increased susceptibility to viral and oxidative stress emphasises the importance of tissue susceptibility in asthma. These findings, together with the observations that there is substantial cross talk between epithelial cells and fibroblasts supports the concept that abnormal function of the EMTU is an important contributory factor for asthma pathogenesis.

For my wife, Johanna, who has always been there through the hard times and has changed my life in ways I would have never dreamed possible.

"To whom I owe the leaping delight
That quickens my senses in our waking time
And the rhythm that governs the repose of our sleeping time,
The breathing in unison

Of lovers whose bodies smell of each other
Who think the same thoughts without need of speech
And babble the same speech without need of meaning.

No peevish winter wind shall chill
No sullen tropic sun shall wither
The roses in the rose-garden which is ours and ours only."
(T.S.Eliot)

List of Contents

Preface

"There is nothing like looking, if you want to find something.
You certainly usually find something, if you look,
but it is not always quite the something you were after."
J. R. R. Tolkien –

This thesis is based on studies conducted between January 2003 and September 2006 at the Roger Brooke Laboratory, Division of Infection, Inflammation and Immunity, School of Medicine, University of Southampton, UK. Even though work and family related commitments have since taken up much of my time, the completion of my thesis has never been far from my thoughts, and I am delighted to have at last been able to put this final version together, mostly thanks to many kind concessions made by several people.

I would like to express my utmost gratitude for her unwavering support, and for always believing in me, to my PhD supervisor, friend, surrogate mother and boss Professor Donna E. Davies. Without her patience, competent guidance on more occasions than I can remember, and inspirational input on my ideas this thesis would never have become a reality.

A special thank you is in order for the person under whose supervision I first started to learn about cell culture techniques, Dr. Anna Merendino. Thank you, Anna, for continuing to work with me over the years, as well as for your highly valued friendship.

I would also like to thank all of the colleagues with whom I have had the pleasure to work with at the Brooke Labs, especially Dr. James Lordan and Professor Peter Wark. Another one of the said colleagues, Dr. Sarah Puddicombe, will always hold a special place in my heart, not only because of our professional collaboration, but also because of her and her husband Richard's friendship that was invaluable to me during those first few months in a foreign country where I knew no-one.

The logistical help and support, as well as the professional advice and dialogue, provided by my colleague and friend Professor Francesco Cappello in my native Palermo, have been paramount to successfully carrying out my research work abroad for extended periods of time.

Moreover, two young researchers, Dr. Anna Ribbene and Dr. Antonio Noto, who have continued to build on some of my results described in this thesis, have been of great help to me while writing the final draft of this thesis.

I certainly need thank my Italian boss, Professor Giovanni Zummo, for letting me take up the opportunity to work and study in one of the leading European research facilities in Southampton, as well as for always providing inspiration and infallible guidance not only to me, but to all young researchers who are lucky enough to work with him.

I would also like to express my sincere gratitude to Professor Stephen Holgate for offering me the chance to come to work in the UK, and for the scientific advice, guidance and motivation he has subsequently provided me with.

Last, but not least, this thesis is dedicated, *In Memoriam*, to Professor Maurizio Vignola, whose diligent research work has always been a great source of inspiration to me. Sadly, this remarkable individual, idealistic leader, and, first and foremost, a human being with a beautiful soul and spirit as well as a brilliant mind, lost his battle against a serious illness at the age of only 40 in 2004. His premature loss still immensely grieves those of us who had the pleasure of knowing him. Hope you are still smiling watching down on us, dear Maurizio!

Palermo, March 2012

Fabio Bucchieri

LIST OF FIGURES

Definitions and abbreviations

ΔΔCT	Delta Delta Cycle Treshold
15-HETE	5-hydroxy-5, 8, 11, 13-eicosatetraenoate
HCl	Hydrochloric Acid
2D	Bi-dimensional
3D	Three-dimensional
3-NT	3-Nitrotyrosine
7AAD	7-amino-actimycin D
AA	Ascorbic Acid
Ab	Antibody
Ac-DEVD-CHO	Acetyl-aspartyl-glutamyl-valyl-aspartal (a caspase-3 inhibitor)
AIF	Apoptosis-Inducing Factor
AM	Acetoxethylester
AP	Activator Protein
AS	Asthmatic Subject
As	Arsenic
AxV	Annexin V
BAL	Bronchoalveolar Lavage
BCECF	Bis-carboxymethyl-carboxyfluorescein
BDP	Beclomethasone
BEBM	Bronchial Epithelial Basal Medium
BEGM	Bronchial Epithelial Growth Medium
BHR	Bronchial Hyperresponsiveness
BSA	Bovine Serum Albumin
C3I	Caspase-3 Inhibitor
Ca^{2+}	Calcium
CAMP	Childhood Asthma Management Program
CBA	Cytometric Bead Array
CCL5	Chemokine (C-C motif) Ligand 5
CD	Cluster of Differentiation
CK	Cytokeratin
CM-RV	Conditioned Medium-Rhinovirus
CM-SFM	Conditioned Medium-Serum Free Medium
CO2	Carbon Dioxide
COL1A1	Collagen Type I, Alpha 1
COPD	Chronic Obstructive Pulmonary Disease
CPE	Cytopathic Effect
CS	Cigarette Smoke
CSE	Cigarette Smoke Extract
CTGF	Connective Tissue Growth Factor
Cu,Zn-SOD	Cu,Zn Superoxide Dismutase
DCVC	Dichlorovinylcysteine
DEP	Diesel Exhaust Particles
DMEM	Dulbecco's Modified Minimum Essential Medium
DMSO	Dimethyl Sulphoxide
DNase	Deoxyribonuclease
dNTP	Deoxynucleoside 5'-Triphospate
EA	Early Apoptosis
ECM	Extracellular Matrix
EDTA	Ethylendiaminetetraacetic Acid
EEM	Epon Embedding Media
EGFR	Epidermal Growth Factor Receptor
EMTU	Epithelial-Mesenchymal Trophic Unit
ET-1	Endothelin-1
ETS	Environmental Tobacco Smoke
FACS	Fluorescence Activated Cell Sorter

FAK	Focal Adhesion Kinase
FAM	6-carboxyfluorescein
FBS	Fetal Bovine Serum
FEV1	Forced Espiratory Volume in One Second
FGF	Fibroblast Growth Factor
FITC	Fluorescein Isothiocyanate
FU	Fluorescent Unit
GM-CSF	Granulocyte Macrophage Colony –Stimulating Factor
GSH	Glutathione
GSSG	Glutathione Disulfide
GTPase	Guanosine 5'-Triphosphatase
H_2O_2	Hydrogen Peroxide
HBSS	Hank's Balanced Salt Solution
HC	Healthy Controls
HEPES	4-(2-hydroxyethyl)-1-piperazine-ethanesulfonic acid
ICAM-1	Intercellular Adhesion Molecule-1
ICS	Inhaled Corticosteroids
IFN	Interferon
IGF	Insulin Growth Factor
IgG	Immunoglobulin G
IL	Interleukin
ITS	Insulin, Transferrin and Sodium Selenite Supplement
LDH	Lactate Dehydrogenase
MCP-1	Monocyte Chemoattractant Protein 1
MFI	Mean Fluorescence Intensity
Mg^{2+}	Magnesium
MgCl2	Magnesium Chloride
MIT	Methylisothiazolinone
MMP	Matrix Metalloproteinase
MOI	Multiplicity of Infection
MPO	Myeloperoxidase
MSMB	Microseminoprotein Beta
NaOH	Sodium Hydroxide
NO	Nitric Oxide
p21waf	Cyclin-Dependent Protein Kinase Inhibitor
Pb	Lead
PBEC	Primary Bronchial Epithelial Cells
PBS	Phosphate-Buffered Saline
PCNA	Proliferating Cell Nuclear Antigen
pCO2	Carbon Dioxide Partial Pressure
PCR	Polymerase Chain Reaction
PDGF	Platelet-Derived Growth Factor
PE	Phycoerythrin
PG	Prostaglandin
PhaCo	Phase Contrast Microscopy
PI	Propidium Iodide
PM	Particulate Matter
PO	Propylene Oxide
pO2	Oxygen Partial Pressure
RANTES	Regulated on Activation, Normal T Expressed and Secreted
RhoA	Ras homolog gene family, member A
RNS	Reactive Nitrogen Species
ROS	Reactive Oxygen Species
RT-PCR	Real Time Polymerase Chain Reaction
RV	Rhinovirus
SCID	Severe Combined Immunodeficiency
SEM	Scanning Electron Microscope
SFM	Serum Free Medium
SOD	Superoxide Dismutase
SRF	Serum Response Factor

STAT-1	Signal Tranducer, Activation of Transcription-1
TAMRA	6-carboxy- N,N,N9,N9-tetramethyl-rhodamine
TCID	Tissue Culture Infectious Dose
TEM	Transmission Electron Microscope
TGF	Transforming Growth Factor
TH	T Helper
TLR	Toll-like Receptor
TRITC	Tetramethylrhodamine Isothiocyanate
UBC	Ubiquitin C
VEGF	Vascular Endothelial Growth Factor
Z-LEHD-FMK	Z-Leu-Glu(OMe)-His-Asp(OMe)-FMK TFA (a caspase-9 inhibitor)
α SMA	Alpha Smooth Muscle Actin

DECLARATION OF AUTHORSHIP

I, Fabio Bucchieri

declare that the thesis entitled:

The influence of the environment on cell-cell communication in the epithelial – mesenchymal trophic unit.

and the work presented in the thesis are both my own, and have been generated by me as the result of my own original research. I confirm that:

- this work was done wholly or mainly while in candidature for a research degree at this University;
- where any part of this thesis has previously been submitted for a degree or any other qualification at this University or any other institution, this has been clearly stated;
- where I have consulted the published work of others, this is always clearly attributed;
- where I have quoted from the work of others, the source is always given. With the exception of such quotations, this thesis is entirely my own work;
- I have acknowledged all main sources of help;
- where the thesis is based on work done by myself jointly with others, I have made clear exactly what was done by others and what I have contributed myself;
- parts of this work have been published as:

  - Peter AB Wark, Sebastian L Johnston, **Fabio Bucchieri**, Robert Powell, Sarah Puddicombe, Vasile Laza-Stanca, Stephen T Holgate & Donna E Davies. Asthmatic bronchial epithelial cells have a deficient innate immune response to infection with rhinovirus. *J Exp Med*. 2005 Mar 21;201(6):937-47.
  - Wark PA, **Bucchieri F**, Johnston SL, Gibson PG, Hamilton L, Mimica J, Zummo G, Holgate ST, Attia J, Thakkinstian A, Davies DE.IFN-gamma-induced protein 10 is a novel biomarker of rhinovirus-induced asthma exacerbations. J Allergy Clin Immunol. 2007 Sep;120(3):586-93. Epub 2007 Jul 12.
  - Haitchi HM, Bassett DJ, **Bucchieri F**, Gao X, Powell RM, Hanley NA, Wilson DI, Holgate ST, Davies DE. Induction of a disintegrin and metalloprotease 33 during embryonic lung development and the influence of IL-13 or maternal allergy. J Allergy Clin Immunol. 2009 Sep;124(3):590-7, 597.e1-11. Epub 2009 Aug 8.

Signed: ……..

Date:……

.

1. INTRODUCTION

1.1 Historical background.

Asthma was described for the first time in 1859 by Henry Hide Salter, as a "disease of reversible airway obstruction"; in 1960, the bronchial hyperresponsiveness (BHR) was to be added to the description. By 1997, the National Heart, Lung, and Blood Institute defined asthma as "a chronic inflammatory disorder of the airways in which many cells play a role, in particular mast cells, eosinophils, and T lymphocytes. In susceptible individuals this inflammation causes recurrent episodes of wheezing, breathlessness, chest tightness, and cough particularly at night and/or in the early morning. These symptoms are usually associated with widespread but variable airflow limitation that is at least partially reversible, either spontaneously or with treatment. The inflammation also causes an associated increase in airway responsiveness to a variety of stimuli."

This development in the description of asthma over the last 40 years illustrates the rapid progress made in understanding this complex disease. To a certain extent, this is due to advances in the techniques used to study the disease. Initially, the limited methods used for investigating asthma only included the measurement of airway obstruction and inflammatory cell numbers in peripheral blood, whereas much of the early pathologic work relied on the use of post-mortem samples. The introduction of the fiberoptic bronchoscope finally allowed the detailed pathology of asthma to be examined in a systematic manner. Currently, fiberoptic bronchoscopy is a technique commonly utilized in the field of respiratory disease research, as it allows the collection of biopsy specimens, bronchial brushing samples, and bronchoalveolar lavage fluid for immunochemical or molecular analysis and, more recently, for the establishment of in vitro models, enabling functional studies intended for defining underlying disease mechanisms.

1.2. The role of inflammation and remodeling in asthma.

Immunohistochemical analysis of bronchial biopsy specimens has contributed to a detailed description of the inflammatory cells of asthmatic airways. These infiltrates are characterized by the presence of mast cells, basophils, eosinophils, monocytes, and T lymphocytes of a TH inflammatory profile (Howarth et al., 1991). Subsequently, treatments have been developed to suppress this inflammatory response for therapeutic benefit (Djukanovic, 2002). Some success has been achieved with the use of corticosteroids, leukotriene receptor antagonists, and mast cell stabilizers (The Global Initiative for Asthma, 2002). However, there are still many asthmatic patients with chronic symptoms for whom anti-inflammatory therapy is inadequate and who account for up to 50% of the health costs of this disease (Van Ganse, 2002). Although inflammation undoubtedly plays a central role in asthma, it does not explain many of the characteristic features of this chronic and recurrent disease (Holgate, 2002). Eosinophils have been considered to have a pivotal role in the pathogenesis of this disease for a long time; however, studies with recombinant human IL-12 (Bryan et al., 2000) or an anti–IL-5 blocking mAb (Leckie et al. 2000; Flood-Page et al., 2002) have so far been unsuccessful in terms of proving the efficacy of these agents, despite the fact that the results show an evident reduction in circulating (by approximately 90%), sputum (by approximately 60%-80%), and tissue (by approximately 55%) eosinophil numbers in the case of anti–IL-5. Thus, even though atopy and airway eosinophilia are clearly associated with asthma, having been linked to asthma severity and exacerbations, they cannot be considered as explicit requirements for disease expression. Atopy and BHR have also been shown to have different genetic inheritance patterns (Skadhuage et al., 1999), suggesting that locally operating factors may be responsible for predisposing individuals to asthma (Holgate, 1999); these findings could also help understand the epidemiologic evidence identifying several environmental factors, including pollutant exposure (Rahman and Macnee, 2000; COMEAP, 1995), diet (Soutar et al., 1997) and respiratory virus infection (Message and Johnston, 2002), all of which are

considered key risk factors in this disease due to their ability to increase oxidant stress in the airways.

The relevance of airway remodeling, the other main histologic characteristic of asthma, in the disease pathogenesis is still controversial, since traditionally inflammation was thought to be the sole cause of asthma, causing airway remodeling to receive considerably less attention. Yet changes involving epithelial goblet cell hyperplasia and metaplasia, collagen deposition and thickening of the lamina reticularis, smooth muscle hyperplasia, as well as proliferation of airway blood vessels and nerves are all common hallmarks of chronic asthma, also frequently found in postmortem asthmatic airways (Dunnill, 1971; Carroll et al., 1993). Morphometric studies have revealed that mucosal and adventitial thickening of asthmatic airways is theoretically able to explain a large component of BHR and excessive airway narrowing, both of which are commonly observed in established disease (Wiggs et al., 1992). These structural changes in established asthma are poorly responsive to corticosteroids.

Airway remodeling also provides an explanation for corticosteroid-resistant BHR (Sont et al., 1999) and the accelerated decline in lung function observed over time in adult asthma (Lange et al., 1998). If BHR and bronchial inflammation respond fairly well to conventional therapy such as bronchodilators and anti-inflammatory drugs, airways smooth muscle remodelling remains insensitive to these treatments (Girodet et al., 2011).

According to the Childhood Asthma Management Program study on children aged 5 to 11 years old, the initial beneficial effect, seen during the first year of treatment, of inhaled corticosteroids on the postbronchodilator improvement in airway function, did not last beyond the first three years of treatment (The Childhood Asthma Management Program Research Group, 2000). The fact that airway remodeling is insensitive to corticosteroids may best explain this observation. In a biopsy study, collagen deposition in the lamina reticularis and underlying fibroblast proliferation, rather than eosinophil infiltration, have been described as diagnostic features of asthma (Cokugras et al., 2001); this finding highlights the significance of tissue remodeling as an early and consistent element of childhood asthma. Although long-term inflammation has been thought to cause airway tissue remodeling, biopsy studies in young children have revealed that tissue restructuring can be present up to

4 years prior to the onset of symptoms (Pohunek et al., 2000), implying that this process begins in the early stages of the development of asthma, and might occur in parallel with inflammation or even be required for the establishment of persistent inflammation. While pathologic abnormalities are scarcely found in bronchial biopsies from infants with virus–associated wheezing, epithelial injury and thickening of the lamina reticularis is evident by the time these subjects reach three years of age (Saglani et al., 2005 and 2007). Due to the fact that the thickening of the lamina reticularis, very common in asthma, does not relate to asthma duration, it still remains to be verified whether this has a strong impact on airwall remodeling (Kim et al., 2007). However, it has been shown that the degree of thickening follows disease severity (Bourdin et al., 2007), and can be observed in subjects with both atopic and non-allergic asthma. The deposition of new extracellular matrix in the lamina reticularis could prove to be another marker of chronic epithelial damage, given its distinctive occurrence in the airways of asthmatic as well as lung transplant patients (Law et al., 2005).

1.3. Surfacing of new theories for asthma pathogenesis.

During the last three decades, the prevalence of asthma has increased dramatically, and although the disease has been shown to have a strong genetic basis, this period has been much too short for recent genetic changes to be responsible for the increase. Considering this notion, it has been hypothesised that environmental changes could have exposed a pre-existing susceptibility within the population. Environmental noxae affect the bronchial epithelium, the protective layer of cells that lines the airways, thus any difference in the ability of the asthmatic epithelium to withstand environmental insults would provide a plausible, local gene-environment interface.

A new paradigm, called the “epithelial-mesenchymal trophic unit” (EMTU), in which exaggerated inflammation and remodeling in the airways result from abnormal injury and repair responses caused by the bronchial epithelium’s susceptibility to components of the inhaled environment, has been proposed to explain the pathogenesis of asthma (Holgate et al., 2009). The changes involved affect the correct functioning of the epithelium, as well as its ability to communicate

with the underlying mesenchymal cells necessary to achieve an appropriate microenvironment for promoting tissue remodeling and for sustaining the persistent inflammatory responses characteristic of chronic asthma. This theory positions atopy or TH2-mediated inflammation in parallel with the altered tissue response rather than sequential to it, thus explaining why asthma does not develop in a significant proportion of atopic individuals, and why some asthmatic subjects respond to steroid therapy (inflammation dominating) and others are more resistant to it (remodeling dominating).

Figure 1.1 Illustration of normal human bronchial epithelium.

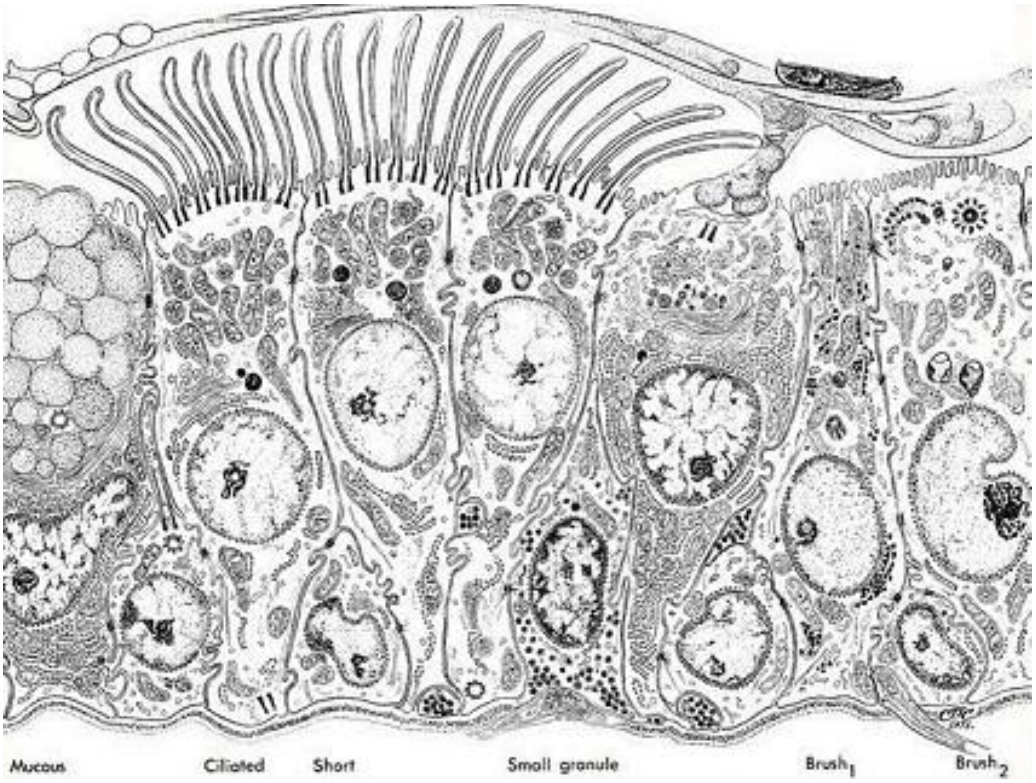

1.4. The modulating role of the airway epithelium in inflammation and remodelling.

The normal differentiated bronchial epithelium is a pseudo-stratified structure that incorporates a columnar layer composed of ciliated and secretory cells supported by basal cells (Figure 1.1). The most important role of this polarised structure is to act as a material barrier to guard the internal milieu of the lungs from inhaled pollutants, infectious agents and other particulate matter. The bronchial epithelium actively protects the airways by secreting mucus and cytoprotective molecules that trap and inactivate inhaled substances, which are subsequently removed by means of ciliary beat activity. The bronchial epithelium also responds to environmental stimuli by signalling to, and interacting with, cells of the innate and adaptive immune systems through secretion of cytokines and chemokines, as well as through expression of adhesion molecules such as ICAM-1 and CD40 (Chung and Barnes, 1999; Merendino et al., 2006). As a result of these interactions, the epithelium and the immune system act together when the natural epithelial barrier is compromised, allowing extra protection to be employed. Tissue repair can be facilitated by the immune and inflammatory cells, once activated, which can remove cell debris and provide a transient supply of locally acting growth factors.

The asthmatic epithelium displays evidence of activation associated with structural damage and goblet cell metaplasia. Signs of epithelial stress can include extensive activation of the transcription factors nuclear factor-kB (NF-kB), activator proteins (e.g. AP-1) and signal transducer, activation of transcription-1 (STAT-1) and increase in the expression of heat shock proteins and the cyclin-dependent kinase inhibitor, p21waf. Compatibly with an injured phenotype, the asthmatic epithelium is an important source of autacoid mediators, chemokines and growth factors (Chung and Barnes, 1999), which sustain ongoing inflammation.

It has been hypothesised that the epithelial damage seen in asthma is artefactual. However, research carried out in Southampton shows enhanced expression of the epidermal growth factor receptor (EGFR, HER1, c-erbB1) (Puddicombe et al., 2000) and the epithelial isoform of CD44 (Lackie et al., 1997), indicating that injury has occurred in vivo, as it is unlikely that these proteins are up-regulated sufficiently rapidly (within minutes) prior to fixation, following tissue

disruption occurring as a consequence of bronchoscopic biopsy (Holgate and Davies, 2001). It has also been shown that EGFR expression in asthma increases depending on severity of the disease, being evident throughout the epithelium that in turn suggests that the stress and damage is widespread (Lackie et al., 1997).

While the extent of injury may imply that the damage is caused by immune cell products, the fact that EGFR expression levels remain high even after corticosteroid treatment suggests the presence of corticosteroid-resistant epithelial pathways, linked to stress and injury, that may contribute to disease chronicity.

More recently, Xiao and colleagues have shown that bronchial biopsies obtained from asthmatic subjects have disruptions in their tight junctions, concluding that bronchial epithelial barrier in asthma is defective and this could facilitate the passage of allergens and/or other agents in the lamina propria determining immune activation (Xiao et al., 2011).

These structural modifications seem to imply the presence of a chronic wound scenario, characteristic not only of adulthood asthma, but also found in asthmatic children's airways (Fedorov et al., 2005). Recently, it has been demonstrated that airway epithelial cells of atopic children with asthma have an inherently impaired injury repair ability, compared to that of cells of normal atopic children; this could be due to the presence of a defect linked to a marked up-regulation of plasminogen activator inhibitor-1 (Stevens et al., 2008). A dysfunctional epithelial repair process can also stimulate the release of profibrogenic growth factors, as recently shown in a murin model of naphthalene-induced epithelial injury (Snyder et al., 2009).

Even though it is difficult to experimentally determine, in vivo, whether there are any intrinsic differences in the susceptibility of the asthmatic bronchial epithelium to environmental noxae, back in 2002 I showed that cultures of asthmatic bronchial epithelial cells grown in vitro were more susceptible to oxidant-induced apoptosis than normal (Bucchieri et al., 2002), while Bayram et al. have demonstrated that bronchial epithelial cells from mild atopic asthmatics release more IL-8 and GM-CSF than those from non-asthmatic individuals, when stimulated with Diesel Exhaust Particles (DEPs) (Bayram et al., 1998). Given that these alterations remain unchanged through several in vitro generations, it is unlikely they are a

secondary effect of airway inflammation. The theory that the effects of environmental stimuli may provide a triggering mechanism for the induction of epithelial activation and damage in asthma could be plausible given the results of epidemiological studies, identifying multiple, interacting risk factors for asthma, such as diet low in anti-oxidants and inhalant pollutants (e.g. particulate matter (PM10) and ozone. The initiation of this proposed triggering mechanism is thought to result in inflammatory cell influx, causing secondary damage through production of endogenous reactive oxygen; this has led to the formulation of a new theory, according to which a susceptible asthmatic epithelium creates a microenvironment capable of supporting chronic cycles of injury and inflammation after exposure to the relevant environmental trigger(s) (Swindle et al., 2009; Holgate et al., 2009).

1.5. Phenotypic heterogeneity of airway (myo)fibroblasts and smooth muscle cells.

Fibroblasts are a particularly diverse family of cells, comprehensively present in all tissues. These cells exhibit several essential differences in their structure, physiology, replicative behaviour, type of biosynthetic products and surface antigens (Sappino et al., 1990; Spanakis et al., 1995; Spanakis et al., 1997). The presence of fibroblastic subpopulations, characterised by different phenotypes and functions, even among lung fibroblasts, has been reported in mice (Derdak et al., 1991; Phipps et al., 1989). Lung fibroblasts, cultured in vitro, should be considered as permanently activated cells. In fact, the specific phenotypic features observed, in vivo, in activated myofibroblasts are present even in resting post-confluent fibroblasts (Schmitt-Graff et al., 1994). One of the fundamental steps in wound repair is the infiltration of fibroblasts from surrounding tissue to an extracellular matrix (ECM) of fibronectin, collagens, laminins, vitronectin and fibrin. Within the ECM, fibroblasts proliferate and differentiate into cells called myofibroblasts, which possess phenotypic and behavioural characteristics resembling those of fibroblasts and smooth muscle cells (Serini and Gabbiani, 1999). Under normal conditions, myofibroblasts play a decisive role in ECM deposition and the following wound contraction, subsequently disappearing as the fibrotic response diminishes and

normal structure and function is regained (Gailit and Clark, 1994; Welch et al., 1990; Phan, 1996).

In diseases like asthma, the consequences of repeated inflammation include structural remodelling of the airway wall, which is in part characterized by exaggerated ECM deposition and excessive subepithelial collagen deposition (Roche et al., 1989; Brewster et al., 1990; Johnson et al., 2004; Westergren-Thorsson et al., 2010).

Further evidence suggest that myofibroblasts play a key role in the EMTU, by propagating and amplifying signals from the bronchial epithelium into the deeper layers of the submucosa through release of soluble mediators (Richter et al., 2001). Myofibroblasts, being more contractile than fibroblasts, are likely to contribute to the alignment and stiffening of the airway ECM by secretion of collagens (Pepe et al., 2005; Kelly et al., 2005; Westergren-Thorsson et al., 2010).

Supporting these observations, immunohistochemistry and electron microscopy clearly show that airway myofibroblasts and smooth muscle bundles lie in close physical proximity in asthma (Jeffery, 1998). There is also an increase in the number of myofibroblast-like cells in the lamina reticularis of asthmatic subjects after allergen challenge (Gizycki et al., 1997). This seems to imply that when the epithelium is exposed to allergens, myofibroblasts migrate toward the smooth muscle, or smooth muscle cells migrate from the muscle bundles toward the lamina reticularis, in response to myofibroblast-derived chemoattractants and this determines activation of T lymphocytes (Ramos-Barbón et al., 2010). Because the phenotype of myofibroblasts is essentially an intermediate between that of a fibroblast and a smooth muscle cell, it could be hypothesised that myofibroblasts contribute directly to the increased smooth muscle mass due to their phenotypic plasticity (Gabbiani, 2003; Johnson et al., 2004)

Microscopic analysis shows that myofibroblasts are elongated cells containing intracellular filaments, abundant rough endoplasmic reticulum, and irregularly shaped nuclei (Gizycki et al., 1997). While there are no known markers specific for fibroblasts, myofibroblasts are generally characterized by the presence of filaments of αsmooth muscle actin (α SMA). Nonetheless, the definition of myofibroblast is more complex than this. In several in vivo situations, myofibroblasts do not express αSMA (Hinz et al., 2001; Tomasek et al., 2002), whilst still

expressing stress fibers containing non-muscle actins and myosins. Therefore, two subclasses have been proposed to categorise different myofibroblast phenotypes: proto-myofibroblasts (characterised by the presence of stress fibers, containing cytoplasmic actins) and differentiated myofibroblasts (characterised by the presence of stress fibers containing αSMA) (Tomasek et al., 2002). Additionally, myofibroblasts can express other smooth muscle proteins, such as heavy-chain myosin and calponin. Smooth muscle cells express further muscle-associated proteins, such as smooth muscle α-actin (Quian et al., 1996), muscarinic M3 receptor (Billington and Penn, 2002), and desmin (Sappino et al., 1990).

The origin of the myofibroblast in vivo is not fully understood. In granulation tissue, the most likely progenitor cells are local fibroblasts, since myofibroblasts have been shown to revert back to a fibroblast phenotype after wound closure (Darby et al., 1990). Other in vitro studies have reported smooth muscle cells acquiring morphologic and functional characteristics of the myofibroblast (Chamley et al., 1977), including collagen gene expression. Research carried out on obstructed rabbit bladders has shown that myofibroblasts can, under certain conditions, express αSMA, heavy-chain myosin and desmin, suggesting that it is possible for myofibroblasts to differentiate into a bona fide smooth muscle phenotype (Buoro et al., 1993). These examples display the plastic nature of the myofibroblast phenotype, which appears to shift toward a fibroblastic or smooth muscular phenotype depending on the microenvironment.

Factors affecting fibroblast phenotype that can be reliably used to manipulate the fibroblast phenotype in vitro have been subject of numerous studies. For instance, airways smooth muscle cells can release biologically active TGF-β, which is involved in various structural alterations such as epithelial changes, subepithelial fibrosis, mucus hypersecretion, goblet cell hyperplasia, and angiogenesis (Halwani et al., 2011). Members of the TGF-β family are indeed the most potent mediators of fibroblast-myofibroblast transformation (Boxall et al., 2006), and TGF- β has been reported to prolong the longevity of myofibroblasts by blocking IL-1 β –induced apoptosis (Zhang and Phan, 1999). It has been suggested that IL-4 can induce αSMA expression in fibroblasts, although other studies have revealed these cytokines to be poor differentiation factors when compared with TGF-β (Richter et al., 2001), whose

levels are increased in asthmatic bronchoalveolar lavage fluid (Redington et al., 1997; Larsen et al., 2006).

Mast cell histamine and tryptase also up-regulate αSMA expression in human foreskin fibroblasts. Mechanical influences would appear to have a considerable effect on the regulation of the myofibroblast phenotype as well. For instance, in splinted wounds, where the fibroblast population is under mechanical tension, myofibroblastic features have been show to appear earlier than in control wounds (Hinz et al., 2001). This observation has been confirmed in vitro with free-floating and tethered collagen lattices (Mochitate et al., 1991). In a similar study, Yang and colleagues grew undifferentiated mesenchymal cells on a collagen-coated silicon membrane, which was stretched once the cells had reached the desired confluency (Yang et al., 2000).

Sustained stretching induced the expression of smooth muscle proteins and accelerated smooth muscle myogenesis. This stretch-induced myogenesis was shown to be due to alternative splicing of serum response factor (SRF). SRF is a transcription factor known to be critical for the induction of muscle-specific gene expression. An alternatively spliced variant, SRF 5, was found to down-regulate bronchial myogenesis, whereas the full transcript was observed to promote myogenesis. When undifferentiated smooth muscle cells are starved of serum for 7 days, approximately 15% of the cells return to a contractile phenotype. This variation has been attributed to SRF cellular location, since responses were seen only when SRF was located in the nucleus (Camoretti-Mercado et al., 2000). Therefore, the fibroblast phenotype may potentially be influenced by the continuous expansion and contraction of the airways; the possible implications of this observation could be particularly valuable in the ongoing research on BHR and asthma (Swartz et al., 2001; Tschumperlin and Drazen, 2001). More recently, using microtubules formation inhibitors, it has been demonstrated that in airways smooth muscle cells, cell alignment results from the interplay of microtubules and actin stress fibers acting in tandem to maintain a homeostatic pre-strain in the cytoskeleton (Morioka et al., 2011). These findings reinforce the hypothesis that pathological alterations in the mechanical properties of the underlying extracellular matrix can be responsible for the onset of diseases such as asthma.

1.6. Role of the extracellular matrix in mesenchymal cell survival and differentiation.

Although factors involved in regulation of the expression and fate of myofibroblasts in the lung remain obscure, alterations in the expression of a variety of growth factors and cytokines during the inflammatory and postinflammatory states probably contribute. Recent evidence suggests the ECM may control these mechanisms. ECM acts as a scaffold onto, and within which tissues can organize; it also contains immense amounts of information that regulate cell shape, cytoskeletal organization, cell motility and polarity, gene expression, proliferation, and survival.

The ECM is more represented in asthmatic biopsies (Begueret et al., 2007), as a result of increased deposition of ECM proteins by airway resident cells, such as epithelial cells, fibroblasts, myofibroblasts, and smooth muscle cells, and its composition is different from that of nonasthmatics (Araujo et al., 2008).

Extensive research data is available on the smooth muscle phenotype and the importance of extracellular matrix (ECM) in mesenchymal cell survival (Freyer et al., 2001) and differentiation. Collagen I and IV, fibronectin, vitronectin, and, in particular, laminin have been found to maintain the contractile phenotype of the smooth muscle cell in vitro (Hayward et al., 1995; Zhang et al., 1999). An interesting research by Beqaj and colleagues suggested a mechanism by which laminin 2 could regulate smooth muscle differentiation (Beqaj et al., 2002). Their observations showed that before smooth muscle differentiation, a small GTPase-signaling protein called RhoA inhibits smooth muscle gene expression, whilst after differentiation RhoA maintained the smooth muscle phenotype. RhoA levels were shown to decrease rapidly when cells were grown on laminin 2, and thus smooth muscle differentiation was more prevalent on cultures grown on laminin. Moreover, degradation of ECM components could be less effective in moderating airways smooth muscle shortening (Meiss, 1999; McParland et al., 2003) but on the other hand, thickening of the airway wall and an increase in ECM deposition also increase airway stiffness and decrease airway compliance (Wilson et al., 1993) enabling the

airways to resist to dynamic compression. Also, deposition of connective tissue acts as mechanical impedance to contraction (McParland et al., 2003).

ECM components are also linked with the differentiating myofibroblast phenotype. For example, the ECM component vitronectin and its integrins have been shown to down-regulate myofibroblast transformation (Scaffidi et al., 2001).

1.7. Integrins in tissue inflammation and injury

Cell-ECM interactions are mediated by specific cell-surface receptors or integrins. Integrins, which are heterodimeric transmembrane glycoproteins that comprise of α and β chains, have important roles in a number of biological processes, such as wound healing and cell growth and survival (Hynes, 1992).

Ligation of specific integrins has been determined to be indispensable for cell survival (Frisch and Francis, 1994; Guadagno et al., 1993), differentiation and establishing cell polarity, as well as for the activation of a large number of genes (Fang et al., 1996; Werb et al., 1989). At least eight different integrins, that appear to form specific spatial patterns (Sheppard 1996), have been found to be constitutively expressed in normal human bronchial epithelial cells. However, expression of at least two other integrins (α5β1 and αvβ6) can be induced following damage and/or exposure to growth factors (Sheppard 1996).

Integrins have been found on fibroblasts from different organs, including the skin and intestine, but much less is known about their distribution on pulmonary fibroblasts. Nevertheless, β1 and β3 integrins have been confirmed to be present under normal conditions, as well as possibly upregulated by growth factors.

Practically nothing is known about the role and regulation of integrins in the repair processes of human airways. The little information available suggests that the profile of integrins expressed in human bronchial epithelium is comparable with that found in skin wound models (Gailit and Clark, 1994). Epithelial damage was found to be associated with early expression of αv, α5, β5 and β6 integrins in a project where human bronchial xenografts were explante into the skin of SCID mice; during the later stages of repair, the α5 expression diminished. In addition, the α2 integrin appeared to redistribute within the repairing cells (Pilewski et al., 1997). A study

using a human nasal epithelial cell culture, where maximal epithelial proliferation was coincident with an upregulated expression of fibronectin and its receptor, α5β1, produced analogous results (Herard et al., 1996). This is backed up further by an in vivo animal model of restricted epithelial damage (Horiba and Fukuda, 1994). The use of genetically manipulated mice has produced perhaps the most convincing data so far confirming that integrins play a role in airway inflammation. For instance, a study conducted on the lungs of β6 integrin knockout mice found that activated lymphocytes accumulate around the conducting airways, as well as showing evidence of airway hyperresponsiveness (Huang et al., 1996 and 1998). Similarly, the same lymphocyte accumulation can be observed in mice engineered to overexpress β1 integrins. Overall, these results would seem to imply a possible involvement of some integrin subunits in dampening the local inflammatory response (β6), while other subunits could play a role in increasing the inflammation (β1) (Sheppard, 1996). Recently, it has been suggested that β1-integrin shedding produced by repetitive allergen challenges in guinea-pigs is associated with collagen deposition in the sub-epithelial region of bronchi and bronchioles, along with inflammatory cells infiltration and BHR development (Bazán-Perkins et al., 2009); and also that the interaction of bronchial asthmatic fibroblasts with T cells, involving CD40L/α5-β1, increases the production of profibrogenic cytokine IL-6, suggesting that crosstalk between T cells and structural cells in asthma could be responsible for maintaining local mucosal inflammation (Loubaki et al., 2010).

Along with the integrins, recent reports have described several membrane molecules localizing to focal contacts, including proteoglycans (Woods and Couchman, 1994; Woods and Couchman, 1998; Woods et al., 2000; Zimmermann and David, 1999), glycosaminoglycan receptors (Bono et al., 2001; Borowsky and Hynes, 1998), as well as signaling molecules (Myohanen et al., 1993; Tang et al., 1998; Wei et al., 1999; Yebra et al., 1999); however, the type of involvement of these components in the mediation and/or regulation of adhesion remains unclear.

1.8. Phenotypic plasticity and mesenchymal cell abnormalities in asthma.

The mesenchymal cells of the asthmatic EMTU show signs of functional abnormalities similarly to the bronchial epithelium. Studies conducted in Southampton have found that fibroblasts from asthmatic patients, contrarily to those from healthy patients, proliferate in vitro in the absence of exogenous growth factors (Chaudhary et al., 2001). Johnson et al. reported a similar phenotype in asthmatic smooth muscle cells, although in their study, growth was still supported by the presence of serum factors (Johnson et al., 2001; Johnson and Burgess, 2004). This shared hyperproliferative property could be explained by the theory that the cells arise from a common mesenchymal progenitor cell population (i.e. stem cells), that carries an acquired or inherited defect. Such an abnormality might explain the increased number of myofibroblasts in the lamina reticularis and the increase in smooth muscle mass; both of these features are characteristic of the remodeled airways in asthma. However, at present we do not exactly know whether these progenitor cells follow a linear pathway of differentiation, becoming myofibroblasts and then smooth muscle cells, or whether committed progenitor cells (transit amplifying cells) are derived to provide a precursor pool for either cell type. It is likely that commitment and subsequent differentiation involves instructive signals from growth factors, as occurs during vessel development (Yamashita et al., 2000).

Recently, Michalik and colleagues have investigated fibroblast to myofibroblast transition in human bronchial fibroblasts and have found that the intensity of the transition induced by TGF-β1 is enhanced in asthmatic compared to non-asthmatic cells and that blocking N-cadherin with a specific blocking antibody, resulted in the inhibition of the transition, suggesting that loss of cell-cell adhesions in asthmatic fibroblasts could be important for the completion of fibroblast to myofibroblast transition (Michalik et al., 2011)

1.9. The epithelial mesenchymal trophic unit and airway remodeling.

Under normal conditions, the epithelium releases primarily factors that suppress mesenchymal cells, such as prostaglandin (PG) E2 and 15-HETE. The production of PGE2 and 15-HETE is diminished after the epithelium sustains injury or damage, and the ensuing repair responses could promote airway remodeling by activating the fibroblasts/myofibroblasts that lie directly under the epithelial layer in the lamina reticularis (Brewster et al., 1990). This signaling between the epithelium and fibroblasts involves the provision of growth factors and survival of mesenchymal cells likely to contribute to the component of asthma that is unresponsive to corticosteroids. In vitro studies have shown that injury to epithelial monolayers results in increased release of fibroproliferative and profibrogenic growth factors including fibroblast growth factor (FGF-2), insulin growth factor (IGF-1), platelet-derived growth factor (PDGF), endothelin (ET-1), and transforming growth factor (TGF)- β2. In asthma, the epithelium has increased susceptibility to oxidant injury through the activation of the caspase-3/apoptosis pathway. This feature also carries over into cultured asthmatic epithelial cells in vitro (Bucchieri et al., 2002). Impaired epithelial repair is another feature of asthma, and it is linked to the increased production of profibrotic growth factors such as TGF-β/or FGF-2, as evidenced by a low expression of cell markers of proliferation (e.g., proliferating cell nuclear antigen [PCNA]). This reaction can be reproduced in vitro by slowing epithelial repair in the presence of a selective tyrphostin inhibitor of the EGFR tyrosine kinase. This markedly augments the release of TGF-β2 (Puddicombe et al., 2000), which may play a key role in converting fibroblasts into myofibroblasts. Overexpression of EGFR (c-erb B1) in asthmatic bronchial epithelium in vivo, or in vitro after injury, remains unaffected by corticosteroid treatment (Holgate et al., 2003; Hamilton et al., 2005). The overexpression also increases in proportion to disease severity and chronicity. Expression of the related c-erbB2 and B3 receptors, as well as their ligands EGF, heparin-binding EGF-like growth factor (HB-EGF), TGF β, and amphiregulin appear unaltered in both asthmatic and normal epithelium

immunostaining. Inhaled corticosteroids (ICS) reduced airway inflammation and levels of IGF-1 in moderate-to-severe asthma, but minimal improvement was observed in BHR. Moreover, ICS had little or no effect on either latent or active TGF-β levels (Puddicombe et al., 2000). As corticosteroid treatment typically reduces inflammation, persistently high TGF-β is most likely to derive from the injured and repairing epithelium and the associated matrix turnover, rather than from infiltrating leukocytes such as eosinophils. Because both epithelial EGFR expression and TGF-β production are refractory to corticosteroids, the combined effects of the remodeling of these signalling pathways have been suggested to elucidate the incomplete resolution of pulmonary function with ICS as seen in chronic asthma (Holgate et al., 2003).

Recently, in an allergen-induced (house dust mite) epithelial barrier impairment model, it has been shown that TGF-β prolonged EGFR phosphorylation and inhibited ligand-induced EGFR internalisation/degradation, decreasing epithelial resistance and promoting junction disassembly (Heijink et al., 2010). The increased EGFR signaling may reduce epithelial integrity, impair epithelial repair and therefore enhance vulnerability of the epithelium. It has also been shown that damage in differentiated epithelial cultures results in TGF-β release that becomes sustained when epithelial cells and fibroblasts are co-cultured (Thompson et al., 2006). An increased synthesis of interstitial collagen close to the epithelial basal surface was also observed in this study. Using other types of epithelial damage, such as pneumatic compression (Tschumperlin et al., 2000; Tschumperlin et al., 2003) or dynamic lateral compression (Choe et al., 2006); activation of fibroblasts has also been shown e.g. by an increase in proliferation, differentiation into myofibroblasts, or ECM components synthesis.

Although myofibroblasts are recognized as key effector cells in tissue fibrosis because of their enhanced ability to synthesize interstitial collagens, those from asthmatic bronchial biopsy specimens also release greater amounts of ET-1 and vascular endothelial growth factor (Richter et al., 2001), which are mitogens for smooth muscle and vascular endothelial cells respectively. Using a panel of cell markers, including α-smooth muscle actin, heavy chain of myosin, and an early smooth muscle differentiation marker SM-22, Richter and colleague have demonstrated that mesenchymal transformation in the presence of TGF-β creates a

cell almost indistinguishable from a smooth muscle cell. When this kind of cell is grown from asthmatic airway tissue and compared with cells derived from normal airways, their proliferative response in the absence of exogenous growth factors is enhanced due to autocrine production of proliferative factors.

Communication between the epithelium and the subepithelial fibroblast sheath appears similar to the processes that drive physiologic remodeling of the airways during embryogenesis, when the epithelium and mesenchyme act as a "trophic unit" to regulate airway growth and branching (Warburton et al., 2000). Consequently, it is plausible to propose that the EMTU becomes activated or that the communication becomes abnormal in asthma to promote pathologic remodeling and smooth muscle proliferation (Holgate et al., 2000; Holgate et al., 2009). In subjects with asymptomatic BHR, longitudinal studies have shown that those who progress to asthma show parallel changes in inflammation and remodeling (Laprise et al., 1999).

In bronchial biopsy specimens, a thickening of the lamina reticularis has been observed in young children several years before the clinical manifestation of asthma (Pohunek et al., 1997). This feature is pathognomonic of asthma and, although it probably reflects activation of the EMTU, it should not be regarded as remodeling per se. The downstream consequences of EMTU activation affect the remodelling events of altered airway structure and function more directly. During foetal lung development, epithelial and mesenchymal growth is regulated in part by the balance of EGF, FGF, and TGF-β BMP signaling (Warburton et al., 2000). Environmental factors may interact with the EMTU to initiate structural changes in the airways (premodeling) in early life in individuals susceptible to asthma. This may explain the decrease in pulmonary function observed in young children susceptible to early wheezing (Dezateux and Stocks, 1997) and the loss of corticosteroid responsiveness on baseline pulmonary function observed in the CAMP study. Thus, for asthma to fully develop, bronchial epithelial susceptibility may precede, or occur in parallel with, factors predisposing to TH2-mediated inflammation and be an essential requirement for establishing the microenvironment that allows inflammation to become persistent in the airways, and for remodeling to occur.

AIMS

The main aim of this thesis is to investigate epithelial mesenchymal signalling using *in vitro* models of asthma with particular attention to the environmental influences.

Our hypothesis is that epithelial susceptibility to environmental injury and a prolonged tissue repair response result in activation of the epithelial mesenchymal trophic unit (EMTU) to promote airway wall remodelling. This could happen because in asthma the bronchial mucosa, comprised of both epithelial and fibroblast cells, has an abnormal response(s) to environmental stress. This could in turn cause resistance to induction of apoptosis with prolonged and augmented pro-inflammatory responses and a consequent exacerbation of asthma symptoms. To test this hypothesis our main models of environmental stress will be represented by cigarette smoke and rhinovirus (RV) infection.

As RV are associated with both asthma exacerbations and disease pathogenesis, we postulate that epithelial infection with RV could result in production of soluble mediators that stimulate inflammatory or remodelling responses in bronchial fibroblasts. Fibroblast responses will also be studied taking into account the eventual role that different ECM components can have on modulating fibroblast activity.

Our final purpose will be to undertake 'tissue engineering' to enable assessment of the aforementioned responses in a complex cell model that mimics, as closely as possible, the human bronchial mucosa.

2. METHODS

2.1 CELL CULTURES

All media and supplements were from Invitrogen unless otherwise specified. Cells, explants and outgrowths were grown in a humidified Heraeus incubator at 37°C, 5% CO_2.

2.1.1. Primary cells.

2.1.1.1. Fiberoptic bronchoscopy.

Epithelial brushings were obtained by bronchoscopy using a fiberoptic bronchoscope (FB-20D; Olympus, Tokyo, Japan) in accordance with standard published guidelines (Hurd, 1991) and ethical approval was obtained from the Southampton and South West Hampshire Local Research Ethics Committee. Bronchial epithelial cells were obtained using a standard sterile single-sheathed nylon cytology brush (BC 9C-26101; Olympus). On average, five to six consecutive brushings were sampled from the bronchial mucosa of the second and third generation bronchi. Cells were harvested into 5 ml sterile phosphate-buffered saline (PBS) after each brushing. At the completion of the procedure, 5 ml RPMI with 10% fetal bovine serum (FBS) was added and the sample centrifuged at 150 x *g* for 5 min to harvest the cells. Epithelial cell purity was assessed by performing differential cell counts of the harvested cell suspension. On average two to three biopsies were sampled from the opposite bronchi and transferred into 5 ml sterile PBS.

2.1.1.2. Primary Bronchial Epithelial Cells (PBEC).

Primary epithelial cultures were established by seeding freshly brushed bronchial epithelial cells into culture dishes containing 3 ml of serum-free hormonally supplemented Bronchial Epithelium Growth Medium (BEGM; Clonetics) containing 50 IU/ml penicillin and 50µg/ml streptomycin. When

confluent, the cells were passaged (p1) using trypsin and were allowed to further expand until used for experimentation at passage 2 or 3; control experiments confirmed that there was no significant difference between the responses of the cells at p2 or p3. The epithelial nature of cells was assessed by immunocytochemistry using a pan-CK antibody and antibodies specific for CK13 and CK18.

2.1.1.3. Primary Fibroblasts

Primary fibroblasts were obtained by outgrowth from bronchial biopsies. Biopsies from each subject were placed in a Petri dish coated with Collagen type I 5μg/ml with Dulbecco's modified Minimum Essential Medium (DMEM) supplemented with 10% v/v heat inactivated foetal bovine serum (FBS), 50 IU/ml penicillin, 50 μg/ml streptomycin, 1x non-essential amino acids, 1mM sodium pyruvate and 2mM glutamine. The tissue was chopped into pieces and scored onto the Petri dish using two sterile scalpel blades, to aid attachment of the fibroblasts. The tissues were incubated in a humidified incubator at 37°C, 5% CO_2 for approximately one week during which time fibroblasts migrated from the tissue and proliferated on the base of the culture dish.

The fibroblasts cultures were passaged 1:10-1:20, according to their rate of growth. Cultures were used for assays up until P10.

2.1.2. Trypsinisation of confluent cell monolayers

Trypsin-EDTA concentrate (10x) was diluted to a 1x solution with Hank's balanced salt solution (HBSS) without Ca^{2+} and Mg^{2+}. Prior to use, all media and trypsin was pre-warmed at room temperature. The cell monolayer was washed twice with HBSS to remove traces of serum. Approximately 1-2 ml 1x trypsin-EDTA was added to a T75 flask, enough to cover the bottom surface. Primary fibroblasts were removed by incubation at room temperature for approximately 60 seconds, followed by tapping of the flask. For PBEC this period was extended to around 2 minutes. The action of the trypsin was halted by the addition of growth medium supplemented

with 10% FBS. The cells were then spun at 150g for 5 minutes to remove the trypsin and the cell pellet was re-suspended in the required growth medium.

2.1.3. Counting and seeding of cells

Cell clumps were disrupted by aspiration through a 25gauge needle before plating out in order to obtain a single cell suspension. Cells and cell viability were counted using the trypan blue exclusion method. The dye can enter cells whose membranes are not intact i.e. non-viable cells and turn them blue. Thus this method gives a viable cell count (trypan blue excluded cells) and a total cell count (including blue cells).

A small aliquot of cell suspension (20µl) was added to 30µl of HBSS and 50µl 0.4%(w/v) trypan blue. The cells were counted using an improved Neubauer haemocytometer (depth 0.1mm, 400mm^2). The mean of the cells in the two central 1mm2 squares was calculated. The count is equivalent to 0.1 mm^3. The number of cells per ml is calculated by multiplying the mean count by 5 (dilution factor) x 10^4.

2.1.3.1 LDH assay

Cell were first resuspended in 200 µl of RPMI media and plated on a 96-well plate; after 24 hours, the remaining media was removed from the wells and 200 ul of lysis buffer (25 mM Hepes, 5 mM MgCl2, 1 mM EGTA + 1:200 pefabloc) was added to the cells. After 20 minutes of incubation (on a rocking table), 30 ul of lysate was pipetted up/down and transferred into a non-sterile 96well plate where 30 ul of LDH mixed reagent (1:45 mixture of A+B, Roche kit) was added.. After 10 minutes 15 ul 1N HCl was added and absorbance (LDH activity) measured (dual wavelength, 492 nm, background 690 nm).

2.1.4. Cryogenic storage.

Frozen aliquots of primary cells were routinely prepared to maintain stocks. Trypsinised cells were placed into media to neutralise the action of the trypsin. The cells were centrifuged at 150xg and the media discarded. The cells were re-

suspended in chilled growth media supplemented with 10% FBS and with 10% DMSO, the latter acts as a cryoprotectant. Approximately 1ml cell solution was placed into a cryotube (Invitrogen), frozen overnight at -80°C and then placed into liquid nitrogen vapour at -150°C for long-term storage.

To regenerate the cells, the cryotubes were rapidly thawed and placed into 10ml of warmed media in a T75cm² flask. The flask was placed in the incubator for 6 hours until the cells had adhered. The media was then replaced with fresh growth media to remove all traces of DMSO.

2.1.5 Treatments.

Prior to each treatment, cells were starved of growth factors for 24 hours to make them quiescent. This ensured that all the cells were synchronised in the same phase of the cell cycle and that when stimulated their responses would be similar. Two different media were used to make PBEC and primary fibroblasts quiescent: PBEC were starved with Bronchial Epithelial Basal Medium (BEBM; Clonetics) containing insulin, transferrin and sodium selenite supplement (ITS; Sigma) and 1mg/ml bovine serum albumin (BSA). Primary fibroblasts were starved with UltraCulture serum-free medium supplemented with 50 IU/ml penicillin and 50µg/ml streptomycin. All subsequent treatments were carried out in the same starving media for the required time points.

Most of the experiments were performed on ECM coated plates. This was achieved by coating trays or flasks for 2 hours prior to use with 5 µg/ml of Vitrogen collagen type I (Cohesion technologies inc., California, USA), 1µg/ml of collagen type I (from rat tail), collagen type IV, laminin (from human placenta), vitronectin and fibronectin (from human plasma) (all from Sigma-Aldrich, UK). The ECM was then removed and cells seeded as described above.

After 24 hours of starvation cells were then treated with the following stimuli.

2.1.5.1. Oxidants, anti-oxidants and cigarette smoke extracts (CSE).

Hydrogen peroxide (H_2O_2; Sigma, UK) was used to induce cell death (apoptosis and necrosis) in PBEC at 400μM for 24 hours. The eventual protective effect of different anti-oxidants was investigated using reduced glutathione (GSH; Sigma, UK) 1mM and ascorbic acid (AA; Sigma, UK) 250μM. PBEC were pre-treated with anti-oxidants for 30 minutes prior to the addition of H_2O_2 to the BEBM. At the same time the involvement of caspases in the apoptotic death induced by the H_2O_2 was evaluated using specific caspases inhibitors. Caspase-3 inhibitor (Ac-DEVD-CHO) and caspase-9 inhibitor (Z-LEHD-FMK) were purchased from BD Biosciences and both used at 120nM in the presence or absence of H_2O_2 or CSE.

CSE were prepared by a modification of the method of Carp and Janoff. (Carp et al., 1978). Briefly, smoke from two Kentucky 1R4F research cigarettes (University of Kentucky, Lexington, KY) whose filters were removed was bubbled through 50 mL of BEBM for 60-70 s. The resulting suspension was adjusted to pH 7.4 with concentrated NaOH, filtered through a 0.22-μM Millex-GS (Millipore, Watford, UK) filter and used immediately on PBEC at a concentrantion range of 1-30% in the presence or absence of anti-oxidants or caspases inhibitors.

2.1.5.2. Rhinovirus-16 (RV-16).

RV-16 stocks were provided by Dr Peter Wark. These were generated by infecting cultures of Ohio HeLa cells as previously described (Papi et al., 1999); cells and supernatants were harvested, cells were disrupted by freezing and thawing, cell debris was pelleted by low speed centrifugation and the clarified supernatant frozen at –70°C.

RV titration was performed by exposing confluent monolayers of HeLa cells in 96-well plates to serial 10-fold dilutions of viral stock and cultured for 5 days at 37°C in 5% CO_2. Cytopathic effect (CPE) was assessed by LDH assay and the tissue culture infective dose of 50% ($TCID_{50}$/ml) was then determined and the multiplicity of infection (MOI) derived (Papi et al., 1999). As a negative control for all experiments RV-16 was inactivated by exposure to UV irradiation at 1200μJ/cm^2 UV

light for 30 minutes. Inactivation was confirmed by repeating viral titrations in HeLa cells.

The desired concentration of RV-16 was applied to cells that were gently shaken at 150rpm at room temperature for 1 hour. The medium was then removed and the wells washed twice with 1ml Hanks Balanced Salt Solution. Fresh medium was then applied and the cells cultured at 37.5°C and 5% CO_2 for the desired time. As negative controls cells were treated with medium alone and UV inactivated RV-16. Confirmation of infection of epithelial cells and quantification of viral production was assessed by HeLa titration assay (Papi et al., 1999).

2.1.5.3. TGF-β.

TGF-β2 (PeproTech, USA) was used in most experiments at 10ng/ml. This dose was chosen as being the most effective in inducing fibroblast differentiation after pilot dose-response experiments.

2.1.6. Three-dimensional outgrowths.

Bronchial biopsies, were obtained from patients referred to the Unit of Respiratory Medicine of the University of Southampton. The following adopted procedures, conforming to the relevant ethical guidelines for human research, were in agreement with the Helsinki Declaration of 1975 as revised in 1983 and were approved by the Ethic Council of the University of Southampton, UK.

The biopsies were washed several times in sterile PBS, subsequently they were cut using a sterile scalpel in 0,5 mm^3 pieces, placed onto 6.5 mm BD Falcon™ cell culture inserts for 24-well plates (0.4 μm pores, transparent nylon membrane) in middle position upon the nylon membrane (Becton Dickinson, Franklin Lakes, NJ, USA), embedded in 60 μl of Matrigel (Becton Dickinson) and transferred into a 24 well plate (Corning Life Sciences) to constitute a Transwell system. Matrigel is a gelatinous protein mixture secreted by Engelbreth-Holm-Swarm (EHS) mouse sarcoma cells. This mixture resembles the complex extracellular environment found

in many tissues and is considered as a good substrate for 3D cell culture for its heterogeneous composition. The major components of Matrigel are basement membrane proteins such as laminin, entactin, and collagen IV which present cultured cells with the adhesive peptide sequences that they would encounter in their natural environment (Hughes, 2010). Matrigel constitutes a uniform and controllable structure very important for accuracy and reproducibility of an in vitro model usable to test compounds (Moharamzadeh et al., 2008).

The plates were put at 37°C for 5 minutes to facilitate the matrigel jellification and 330 µl of growth medium mix was added to each well after these 5 minutes. This mix was constituted of (Bronchial Epithelium Growth Medium/ Dulbecco's modified Minimum Essential Medium) BEGM/DMEM 10% foetal bovine serum FBS (1:1) The growth medium was replaced every 48 hours. The outgrowths were cultured at 37°C in a 5% CO2 atmosphere. An inverted light microscope equipped with phase contrast rings (LEICA DM-IRB, Leica Microsystems Srl) was used to monitor the outgrowths. At specific time points (after 1, 2 and 3 months in culture) the nylon membrane was detached from the insert and split in four pieces for characterisation through scanning electron microscopy, transmission Electron Microscopy and immunostaining.

2.2. PHASE CONTRAST MICROSCOPY.

Cells were routinely photographed before and after treatment to record any morphological changes occurring in the cells. An inverted light microscope equipped with phase contrast rings (LEICA DM-IRB) was used to visualise changes in cell size, shape and orientations and this was recorded by digital photography.

2.3. FLUORESCENCE MICROSCOPY.

Fluorescence microscopy is used to detect structures, molecules or proteins within the cell. Fluorescent molecules absorb light at one wavelength and emit light at another, longer wavelength. When fluorescent molecules absorb a specific absorption wavelength for an electron in a given orbital, the electron moves to a

higher energy level (the excited) state. Electrons in this state are unstable and will return to the ground state, releasing energy in the form of light and heat. This emission of energy is fluorescence. Because some energy is lost as heat, the emitted light contains less energy and therefore is a longer wavelength than the absorbed (or excitation) light.

In fluorescence microscopy, a cell is stained with a dye and the dye is illuminated with filtered light at the absorbing wavelength; the light emitted from the dye is viewed through a filter that allows only the emitted wavelength to be seen. The dye glows brightly against a dark background because only the emitted wavelength is allowed to reach the eyepieces or camera port of the microscope.

Among the common fluorescence dyes are fluorescein, which emits green light when exited with blue light and rhodamine, which emits deep red fluorescence when excited by green-yellow light. The fluorescence microscopes are equipped with three fluorescent filter cubes, each containing specific barrier filters and a beam-splitting mirror.

2.3.1. ApoAlert™ kit

The induction of apoptosis in cells infected with RV16 was confirmed by demonstrating altered mitochondrial membrane permeability using the ApoAlert Mitochondrial Membrane sensor (Clontech, Palo Alto Ca, USA). The MitoSensor present in this kit is a cationic dye that fluoresces differently in apoptotic and nonapoptotic cells. Normally, the dye is taken up in the mitochondria, where it forms aggregates that exhibit intense red fluorescence. In apoptotic cells, the dye cannot accumulate in the mitochondria because of altered mitochondrial membrane permeability. As a result, the dye remains in monomeric form in the cytoplasm, where it fluoresces green.

Briefly, cells were gently rinsed with serum-free media. Immediately prior to use, 1 µl MitoSensor Reagent was added to 1 ml Incubation Buffer (final concentration: 5 µg/ml). The mix was vortexed and centrifuged for 5 min at 14,000 rpm to remove possible aggregates. Cells were then covered with the supernatant obtained earlier. 1 ml of diluted reagent was used for each well of a 6-well plate.

Samples were incubated at 37°C in a 5% CO_2 incubator for 15–20 min and gently rinsed with 1X PBS. Cells were finally examined under a fluorescence microscope using a band-pass filter.

2.4. ELECTRON MICROSCOPY.

I was extensively trained in electron microscopy at the Human Anatomy Section of the Experimental Medicine Department, University of Palermo, Italy, after receiving my degree in Medicine and Surgery. During this training period I was tutored by Prof. Giovanni Zummo.

All reagents were ordered from Electron Microscopy Sciences (EMS, PA) unless otherwise specified.

2.4.1. Scanning Electron Microscopy (SEM)

Outgrowths were pre-fixed for 1 hour in paraformaldehyde 2% and glutaraldehyde 0.5% in Milloning buffer pH 7.3. Samples were washed once in the same buffer and then post-fixed in osmium tetroxide 1% in Milloning buffer for 2 hours on a shaker. After this period, samples were washed again with Milloning buffer and then dehydrated in an ascending ethanol series (30, 50, 70, 95 and 100%): each step repeated four times for 5 minutes. The ethanol 100% was then substituted with CO_2 at the critical point. The samples were then bound to the stubs of the scanning electron microscope (JSM-6301F; JEOL, Japan) with a silver tape, metallized with gold and observed.

2.4.2. Transmission Electron Microscopy (TEM)

Outgrowths were pre-fixed for 1 hour in paraformaldehyde 2% and glutaraldehyde 0.5% in Milloning buffer pH 7.3. Samples were washed once in the same buffer and then post-fixed in osmium tetroxide 1% in Milloning buffer for 2

hours on a shaker. After this period samples were washed again with Milloning buffer and then dehydrated with ascending ethanol series (30, 50, 70, 95 and 100%): each step repeated four times for 5 minutes. The ethanol was then substituted by Propylene oxide (PO) for 30 minutes, 3 parts PO and 1 part of Epon Embedding Media (EEM; Electron Microscopy Sciences, USA) for 30 minutes, 2 parts PO and 2 parts EEM for 30 minutes, 1 part PO and 3 parts EEM for 30 minutes and finally only EEM for 24 hours. The specimens were then put in embedding containers in fresh EEM for 48 hours at 60°C. Ultrathin (50nm) sections of the embedded samples were cut with an ultramicrotome and placed on grids of Cu/Rh. Before the observation with the transmission electron microscope (JEM-1220; JEOL, Japan) the specimens were contrasted with uranyl-acetate 7% in methanol and Reynold's lead citrate.

2.5. IMMUNOSTAINING.

2.5.1. Immunofluorescence.

Cells (primary fibroblasts and PBEC) were seeded at $5x10^4$/well in 24 well trays (NUNC) coated with different ECM components, grown to 80% confluence in the appropriate growth media, starved with the respective starving media (Ultraculture and BEBM) and then treated as required for the different experiments. 3D outgrowths were stained in situ after the appropriate treatments and time points. At the end of the treatment cells or outgrowths were washed once with 1ml/well of HBSS and fixed *in situ* in 500µl/well of ice-cold absolute methanol for 20 minutes at –20°C. Cells or outgrowths, inside their plastic supports, were then left to dry in a laminar flow cabinet for 30 minutes and stored at –20°C. Trays were defrosted at room temperature, and washed twice with 1ml/well of phosphate buffered saline (PBS), permeabilised with 500µl/well of Triton X-100 (Sigma, UK) 0.1% in PBS for 3 minutes on ice and washed once with 1ml/well of PBS. Unspecific binding sites were blocked with 250µl/well of DMEM 10% FBS for 15 minutes. During this period the primary Abs were diluted in incubation buffer (DMEM 10%, Tween-20 0.1% and Sodium Azide 0.1% in PBS). The blocking buffer was then removed and

without washing the diluted Abs were added to the wells for 45 minutes. Wells were then washed twice with 1ml/well of incubation buffer and when needed secondary Abs were diluted in incubation buffer and applied to the wells for 45 minutes. Secondary Abs were conjugated with different fluorochromes.

The following primary Abs were used:

- anti-αsmooth muscle actin (αSMA) monoclonal FITC conjugated Ab (clone 1A4, working dilution 1:100) purchased from Sigma, UK.
- anti-apoptosis-inducing factor (AIF) rabbit polyclonal Ab (clone H-300, working dilution 1:100), purchased from Santa Cruz Biotechnology, USA.
- anti-cytokeratin13 (CK13) monoclonal IgG1 Ab (clone 1C7, working dilution 1:100) purchased from Abnova, USA.
- anti-cytokeratin18 (CK18) monoclonal IgG Ab (clone KRT18, working dilution 1:200) purchased from Abnova, USA.
- Anti-Collagen I monoclonal IgG1 Ab (clone 5D8-G9, working dilution 1:50) purchased from Millipore, UK.
- Anti-Laminin monoclonal IgG1 Ab (clone 2G6/A2, working dilution 1:200) purchased from Millipore, UK.

The secondary Abs were:

A secondary Alexa Fluor546–conjugated goat anti-rabbit Ab (1:500; Molecular Probes, USA) was used to reveal AIF positivity.

A secondary FITC-conjugated goat anti-mouse IgG Ab (working dilution 1:400, purchased from Sigma, UK) was used to reveal CK13 and Collagen I positivity.

A secondary TRITC-conjugated goat anti-mouse IgG Ab (working dilution 1:500, purchased from Sigma, UK) was used to reveal CK18 and Laminin positivity.

At the end of the 45 minutes incubation step with the secondary Abs, wells were washed twice with 1 ml of PBS and coverslips mounted with MOVIOL® (DABCO) mounting medium. The trays were then ready to be observed under the fluorescent light of a LEICA inverted fluorescent microscope.

2.6. FLOW CYTOMETRY.

Flow cytometry involves the use of a beam of laser light projected through a liquid stream that contains cells, or other particles, which when struck by the focussed light give out signals which are picked up by detectors. These signals are then converted for computer storage and data analysis, and can provide information about various cellular properties.

The term "flow cytometry" derives from the measurement (meter) of single cells (cyto) as they flow past a series of detectors. The fundamental concept is that cells flow one at a time through a region of interrogation where multiple biophysical properties of each cell can be measured at rates of over 1000 cells per second. These biophysical properties are then correlated with biological and biochemical properties of interest. The high through-put of cells allows for rare cells, which may have inherent or inducible differences, to be easily detected and identified from the remainder of the cell population.

In order to make the measurement of biological/biochemical properties of interest easier, the cells are usually stained with fluorescent dyes that bind specifically to cellular constituents. The dyes are excited by the laser beam, and emit light at longer wavelengths. Detectors pick up this emitted light, and these analogue signals are converted to digital so that they may be stored, for later display and analysis.

2.6.1. Annexin-V staining.

Apoptosis and necrosis were measured according to the technique of Vermes and coworkers (Vermes et al., 1995), in which binding of annexin-V (AxV) was used to detect phosphatidylserine, which is externalized on the outer leaflet of the plasma membrane of cells during early stages of the apoptotic process. Propidium iodide (PI) is used to discriminate necrotic cells. This fluorescent dye is passively up-taken by cells whose cytoplasmic membrane is damaged.

Cells (PBEC and fibroblasts) (5 x 10^4/well) were grown to 70-80% confluence in 24-well plates (Nunc, Fisher Scientific, Loughborough, UK). The growth media were then replaced with the appropriate starvation media (BEBM and Ultraculture for PBEC and fibroblasts respectively) for 24 hours to render the cells quiescent before exposure to the different treatments as detailed in the Results section. Adherent cells were then harvested with trypsin in Ca^{2+} and Mg^{2+}-free Hanks' balanced salt solution and combined with nonadherent cells for analysis. After washing twice in cold PBS, the cells were resuspended at a density of 1 x 10^5 cells/100 µl of binding buffer (10 mM HEPES pH 7.4, 140 mM NaCl, 2.5 mM $CaCl_2$) in 5 ml propylene FACS tubes. AxV-FITC (1 µg/ml) and PI (2.5 µg/ml) were added to the tubes and incubated in the dark for 15 min, after which 400 µl of cold binding buffer was added and cells analyzed using a FACScan flow cytometer (Becton and Dickinson, Oxford, UK). Control tubes lacking AxV-FITC, PI, or both were included for the acquisition. Analysis of dotplots of FL1(AxV-FITC) versus FL2 (PI) was performed using WinMDI 2.8. The degree of early apoptosis was expressed as the number of AxV^+/PI^- cells shown as a percentage of total cells.

2.6.2 αSMA staining

Primary bronchial fibroblasts were seeded at 5x10^4 cells/ml onto 24 wells trays (NUNC) in DMEM 10% FBS and allowed to adhere to the plastic or different ECM components for 24 hours. The growth medium was then changed with Ultraculture in order to make them quiescent. After 24 hours this medium was replaced with fresh Ultraculture +/- $TGF\beta_2$ 10ng/ml, RV-16 or inactivated RV-16. At 24, 48 and 72 hours after the treatment, cells were harvested and transferred to FACS tubes at a dilution of 2x10^5/tube. Cells were washed with PBS, fixed with absolute methanol for 20 minutes at 0°C, washed once with PBS, permeabilised with 200µl/tube of Triton X-100 (Sigma, UK) 0.1% in PBS for 3 minutes on ice and washed once with 2ml/tube of PBS. Unspecific binding sites were blocked with 50µl/tubes of DMEM 10% FBS for 15 minutes. During this period monoclonal anti-αSMA FITC-conjugated antibody (clone 1A4 from Sigma, UK) was diluted in incubation buffer (DMEM 10%, Tween-20 0.1% and Sodium Azide 0.1% in PBS). 100 µl of the diluted antibody were then added to each tube and cells incubated for

45 minutes. After this period, cells were washed twice with 2ml/tube of PBS and finally cells were resuspended in 400 µl of PBS for FACS analysis. Control tubes were prepared substituting the anti-αSMA FITC-conjugated antibody with an isotype control mouseIgG1/FITC-conjugated (DAKO, UK) at the same concentration. 10000 events were acquired using BD CellQuest™ software (BD Biosciences) and subsequently analysed with the same software. Histograms were then plotted to quantify mean fluorescence intensities and percentages of positive cells.

2.6.3. Cytometric bead array immunoassay.

Cytokines and Chemokines were determined by Becton Dickinson (BD) Cytometric Bead Array (CBA). Six (cytokines) or five (chemokines) bead populations with distinct fluorescence intensities have been coated with capture antibodies (Ab) specific coupled with phycoerythrin (PE) which emits at 585 nm. The Calibrators (standards ranging from 0 to 5000 pg/ml. for the assay system), composed of capture Ab-bead and detector Ab–PE reagents, are mixtures of all cytokines and chemokines.

For each sample and cytokine or chemokine standard mixture, 50 µl of sample or standard was added to a mixture of 50 µl each of capture Ab-bead reagent and detector Ab–PE reagent. The final mixture (150 µl) was subsequently incubated for 3hrs at room temperature, and washed to remove unbound detector Ab–PE reagent before data acquisition using flow cytometry. A two-color flow cytometric analysis was then performed using a FACSCalibur flow cytometer (Becton and Dickinson, Oxford, UK). Data were acquired and analyzed using BD CBA.software. Forward vs. side scatter gating was employed to exclude any sample particles other than the 7.5-mm polystyrene beads. Data were displayed as two-color dot plots (FL-2 vs. FL-3) such that the six discrete FL-3 microparticle dye intensities were distributed along the *Y*-axis. Standard curves were plotted [cytokine calibrator concentration vs. FL-2 mean fluorescence intensity (MFI)] using a four-parameter logistic curve fitting model. Cytokine and chemokine concentrations were determined from these standard curves.

2.7. QUANTITATIVE PCR

RNA was extracted using TRIzol reagent (Life Technologies, Paisley, UK) and contaminating DNA removed using DNase (Ambion, Austin, USA) according to the manufacturer's instructions. 1 µg total RNA was reverse transcribed using 1 mM dNTP (Invitrogen, Paisley, UK), 3 ng random hexamer primer (MWG Biotech, Milton Keynes, UK), and 100 U MMLV RT enzyme (Promega, Chilworth, UK) according to the manufacturers' instructions. Real-time detection used an iCyclerIQ detection system using a PCR protocol as follows: 95°C for 10 minutes followed by 42 cycles of denaturation at 95°C for 15 seconds and annealing/extension at 60°C for 1 minute. For detection of actin, alpha 2, smooth muscle, aorta (*ACTA2*), interleukin 8 (*IL8*), collagen type I, alpha 1 (*COL1A1*) and connective tissue growth factor (*CTGF*) we used primers and fluorogenic probes labelled with reporter dye 6-carboxyfluorescein (FAM) and the quencher dye 6-carboxy- N,N,N9,N9-tetramethyl-rhodamine (TAMRA) (PremierDesign). The sequences were as shown in table 2.1. All genes were normalized to ubiquitin C (*UBC*) and phospholipase A2 (*A2*) genes and relative quantification performed using the ΔΔCT method (Wicks et al., 2006).

Table 2.1 Primers and probes for gene expression

Gene	Sense primer	Anti-sense primer	Probe
IL-8	CAGAGACAGC AGAGCACAC	AGCTTGGAAGT CATGTTTACAC	tggtggaCTAGGACA AGAGCCAGGAAG AAACCACCG
ACTA2	AAGCACAGAG CAAAAGAGGA AT	ATGTCGTCCCAG TTGGTGAT	CTGACCCTGAAGT ACCCGATAGAACA TGGCATggtcag
CTGF	CCCAGACCCA ACTATGATTA GAG	AGGCGTTGTCAT TGGTAACC	tCCCATCCCACAGG TCTTGGAACAGGC Gagatggg
COL1A1	AGACAGTGAT TGAATACAAA ACCA	GGAGTTTACAG GAAGCAGACA	tCAAGACCTCCCGC CTGCCCATCATCG Tgtcttga

2.8. FLUORESCENCE-BASED CELL ADHESION ASSAY.

Fluorescence-based adhesion assays involve labelling cells with a fluorescent dye, allowing cells to adhere to immobilised ligand, washing away non-adherent cells, and measuring the fluorescent signal of adherent cells with a fluorimetric plate reader. Cells were labelled with fluorescein derivatives such as bis-carboxymethyl-carboxyfluorescein (BCECF) and calcein in their acetoxymethylester (AM) form. The fluorescent dyes were taken up by cells and hydrolysed by cellular esterases. Calcein is recommended due to its pH-independence, superior retention by cells and photostability (Haughland et al., 1996). Also, calcein-AM does not affect lymphocyte adhesion, proliferation, or granulocyte chemotaxis (De Clerk et al., 1999).

2.8.1. Calcein-AM

96 well trays (NUNC) were coated with different ECM components as detailed in the Results section. Primary fibroblasts were harvested with trypsin-EDTA, centrifuged at 150g and resuspended in DMEM (no additives) at $1x10^7$/ml. Calcein-AM (BD Biosciences Pharmingen) was added to give a final 2μM concentration, and cells were incubated at room temperature in the dark for 30 minutes. Halfway during this period the tubes were inverted to mix. Cells were then washed three times by centrifuging them at 200 x g and resuspending in cold DMEM. At the end of the washings, cells were resuspended at $2x10^6$/ml in DMEM containing 2% FBS. Cells were then allowed to adhere to the different ECM components by adding 0.1ml of cell suspension per well and incubating at 37°C for 5, 15, 30, 45 and 60 minutes. At the end of each time point the wells were washed gently three times with DMEM at room temperature to remove non-adherent cells. 0.1ml of DMEM 2% FBS was then added in each well and the plate was read in a fluorescent plate reader Cytofluor II (PerSeptive Biosystems) at an excitation wavelength of 480nm and an emission wavelength of 530nm. In each experiment fluorescent units (FU) in 0.1ml of cells (total) and FU released into the supernatants during the assay (spontaneous) were determined. Percent cell bound fluorescence was then calculated as 100 x bound FU/total FU-spontaneous FU.

2.9. STATISTICS

Data were analysed using SPSS version 17 for Windows (SPSS Inc). As sample size was small and variables were not normally distributed the differences between the groups have been analysed using non-parametric tests; differences between two dependent variables were analysed using the signed rank test, for independent variables was used the Wilcoxon rank sum test and for multiple comparisons the Kruskal Wallis test. Correlations between two variables were assessed using Spearmans' rank correlation. A p value of <0.05 was considered significant.

3. RESULTS – EFFECTS OF RHINOVIRUS ON EMTU.

The aim of this chapter is to focus on the effects of rhinovirus-16 (RV16) infection on the epithelial-mesenchymal trophic unit paying particular attention to the differences between healthy and asthmatic subjects.

I first studied the responses of PBEC to such infection; this was followed by the analysis of human bronchial fibroblast responses to conditioned media from epithelial cells treated with RV-16. The functional responses of human bronchial fibroblasts to different ECMs were also studied.

3.1. RHINOVIRUS INFECTION AND PBEC RESPONSES.

It is believed that 85% of asthma exacerbations can be attributed to respiratory viral respiratory tract infections (Johnston et al., 1995; Nicholson et al., 1993), including the most severe cases that require hospitalisation (Johnston et al., 1996). It is of concern that viral infections can trigger severe asthma exacerbations even when there is good asthma control in compliant patients taking optimal doses of inhaled corticosteroids (Reddel et al., 1999). The most common pathogen associated with asthma exacerbations is rhinovirus (RV). Infection with RV leads to the release of inflammatory mediators (Doull et al., 1997) and increased bronchial responsiveness (Fraenkel et al., 1995). Subjects with asthma do not appear to be more susceptible to acquiring viral respiratory tract infections, but they do exhibit more severe lower respiratory tract symptoms in response to infection (Grunberg et al., 1997). Although RV is known to infect bronchial epithelial cells (Corne et al., 2002) and has been isolated from the lower airways (Gern et al., 1997; Papadopoulos et al., 2000), the reasons why the lower respiratory tract of asthmatic subjects is more prone to the effects of RV infection are still unclear (Proud, 2011).

3.1.1. Aims.

My hypothesis is that asthmatic bronchial epithelial cells have an abnormal response(s) to RV infection that could cause resistance to induction of apoptosis with prolonged and augmented pro-inflammatory responses; this may lead to a consequent exacerbation of asthma symptoms. In order to test this hypothesis, I set up a primary culture model where PBEC from asthmatic and healthy patients were infected with RV-16 and the obtained responses were evaluated in terms of:

- cell morphology;
- cell survival;
- efficacy of infection;
- caspases activation.

3.1.2. Morphological observations: effects of RV16 infection on PBEC morphology.

PBEC were plated onto 24 well trays at $5x10^4$/well and grown until 80% confluent. Cells were then serum starved for 24 hours before being infected with RV16 MOI 2. The medium was then removed and the wells washed twice with 1ml Hanks Balanced Salt Solution. Fresh medium was then applied and the cells cultured at 37.5°C and 5% CO_2 for the desired time. After 0 and 24 hours phase contrast photographs of the cells were taken with a JVC video camera. As shown in figure 3.1, after 24 hours, infection with RV-16 could be determined by the appearance of many characteristic signs of necrotic cell death. Cells displayed a swollen cytoplasm with enlarged nuclei mainly due to the cytopathic effect (CPE) of the virus.

3.1.3. Optimum time and dose response with RV-16 in primary bronchial epithelial cells.

To determine the optimum dose of RV-16 to elicit a reduction of viability and morphological changes in PBEC, a subject with mild asthma and a healthy control were selected. Cells were infected with RV-16 at an MOI ranging from 0.5 to 6. The impact on cell cytotoxicity was then assessed by measuring the activity of LDH in the supernatant. LDH activity rose considerably by 24 hours in cells treated with an MOI of 2 or greater. The subject with mild asthma however had high levels of LDH activity throughout all wells, including the negative controls at 48 hours with an increase in indiscriminate cell loss seen. The reason for this was unclear but makes it impossible to draw conclusions from the data from this time point. (Figure 3.2).

Figure 3.1

Morphological appearance of PBEC after 24 hrs of treatment.

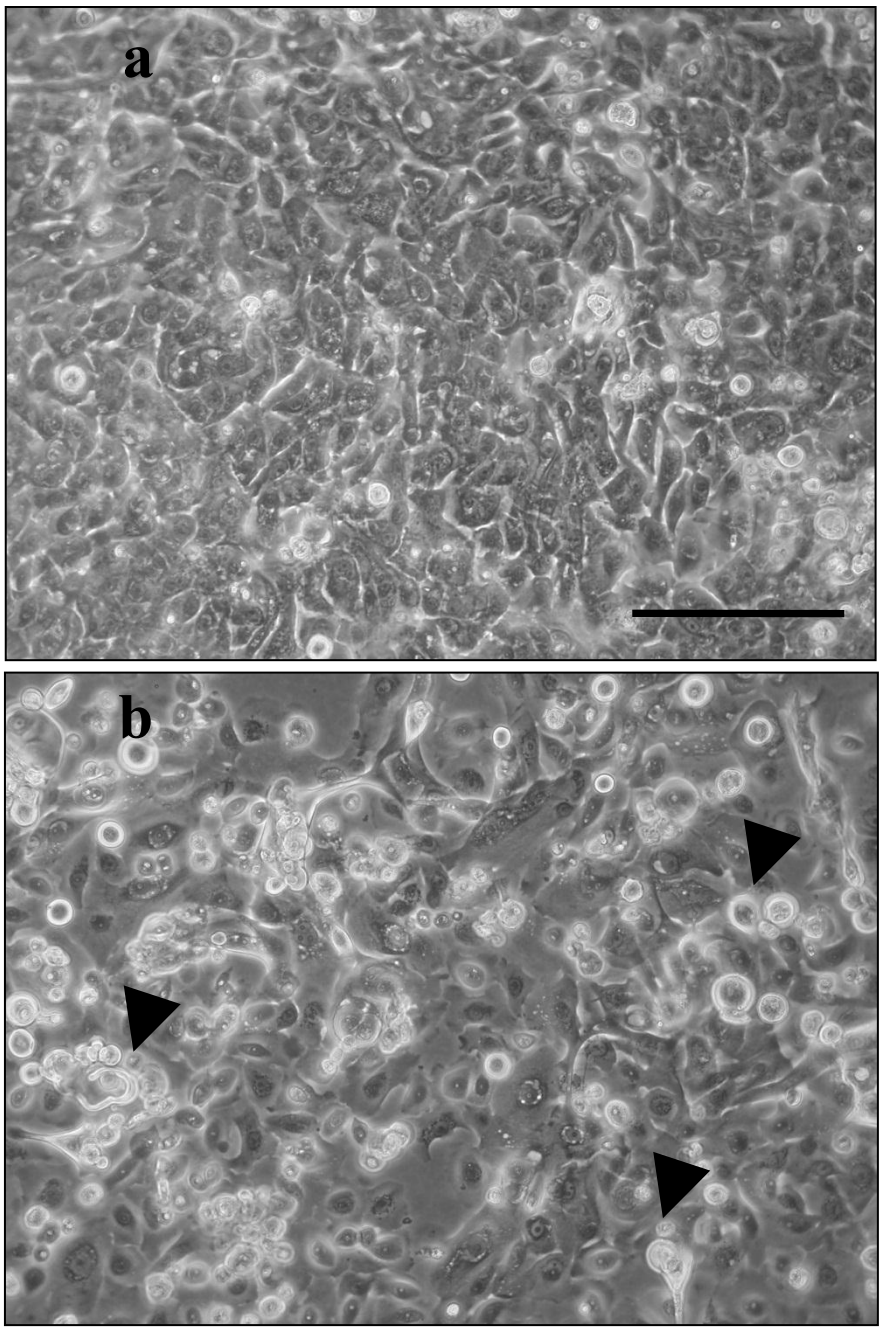

PBEC were serum starved for 24 hrs before being treated with serum free medium (a) or infected with RV-16 MOI2 (b) for a further 24 hrs. Arrowheads indicate swollen necrotic cells; bar = 100μm.

Figure 3.2

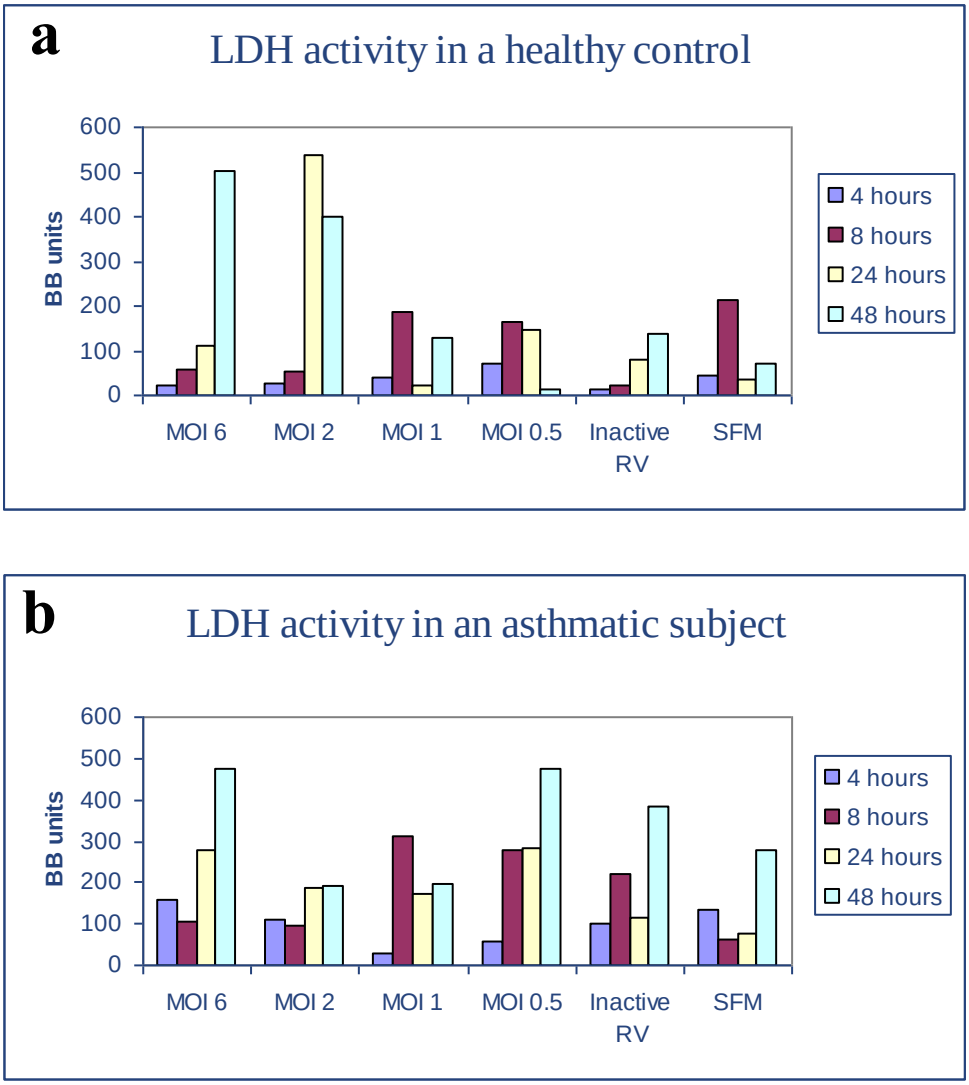

LDH activity is measured in BB units. A rise in LDH activity appears to be present by 24 hours and continuing to rise by 48 hours at an MOI of 2 or greater. The subject with mild asthma however had high levels of LDH activity throughout all wells including the negative controls at 48 hours with an increase in indiscriminate cell loss seen. The reason for this was unclear but makes it impossible to draw conclusions from the data from this time point.

3.1.4. Infection and viral yield from primary bronchial epithelial cells

Following RV-16 infection of PBEC, recovery of viable RV was determined by transmission of infection and CPE on Ohio HeLa cells from the infected supernatant of PBEC. CPE was not seen using supernatants obtained up to 8h after infection of the primary cultures, but thereafter rose steadily up to 48h. Asthmatic PBEC had a significantly greater increase in RV-16 detected by 24h and 48h as measured by $TCID_{50}$ (Figure 3.3a). This was preceded by an increase in viral replication 8h post infection in AS compared to HC (Figure 3.3b).

Figure 3.3

a **Viral yeld from bronchial epithelial cells**

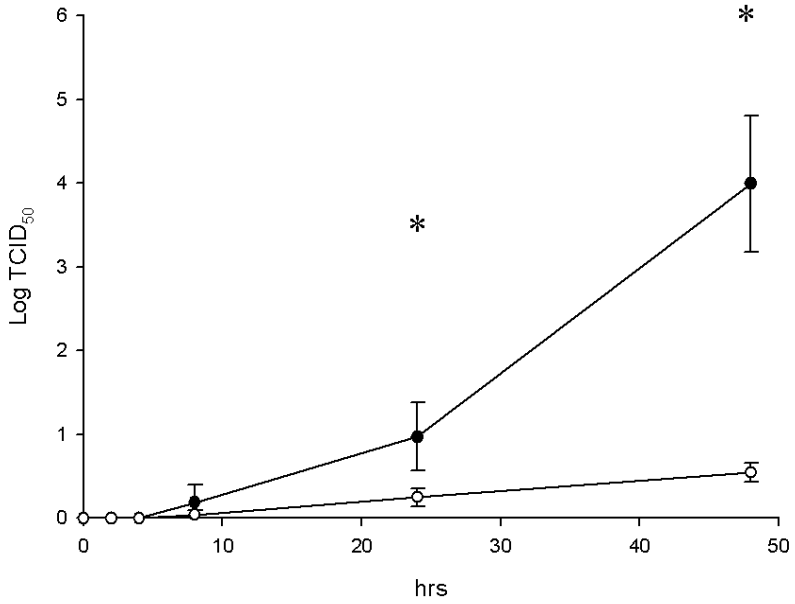

b **Production of RV-16 mRNA 8hrs after infection**

RV-16 replication and release from normal and asthmatic PBECs. (a): RV-16 release into the supernatant of infected cells was determined by calculating the TCID50 x104/ml by titration assay in Ohio HeLa cells. The supernatant from 14 ICS requiring asthmatics and 10 healthy controls were examined on individual titration plates. Data points represent the mean and the standard deviation. By 48h significantly more RV was detected from asthmatic cells with a mean TCID50 x104/ml of 3.99 (0.8), compared to 0.54 (0.12) in healthy control cells (p=0.001). **(b):** RV-16 vRNA production was measured by qPCR after 8h of infection. Median (IQR) production (x 106) from asthmatic cells was significantly increased at 2.1 (0.16, 9.7) compared to 0.04 (0.009, 0.06) from healthy controls (p= 0.007).

3.1.5. Evaluation of cell death: normal vs asthma differences with RV-16 infection.

As apoptosis is a natural defence mechanism that protects against virus replication, I continued by characterizing the nature of cell death in response to RV-16 using Annexin-V staining. PBEC obtained from 20 subjects (10 HC and 10 AS; table 3.1) were infected with RV-16 and flow cytometric analysis revealed that there was a significant reduction in viable cell number 8 hours following RV-16 infection of normal PBEC. This was not seen in cells treated with medium alone or UV inactivated RV-16 suggesting a direct link between infection and cell death (Figure 3.4a). In contrast, infection of asthmatic PBEC with RV-16 had a smaller effect on viability at 8h (Figure 3.4a). By comparing $AxV^{+}/7AAD^{-}$ cells (i.e. apoptotic cells) and $AxV^{+}/7AAD^{+}$ cells (i.e. necrotic cells), the difference in overall viability between normal and asthmatic PBEC was found to be due to a significant increase in apoptosis in the normal cultures (Figure 3.4b).

The induction of apoptosis in infected cells was confirmed by demonstrating altered mitochondrial membrane permeability using the ApoAlert Mitochondrial Membrane sensor (Clontech, Palo Alto Ca, USA) (Figure 3.5). The MitoSensor present in this kit is a cationic dye that fluoresces differently in apoptotic and nonapoptotic cells. Normally, the dye is taken up in the mitochondria, where it forms aggregates that exhibit intense red fluorescence. In apoptotic cells, the dye cannot accumulate in the mitochondria because of altered mitochondrial membrane permeability. As a result, the dye remains in monomeric form in the cytoplasm, where it fluoresces green. As shown in figure 3.5b, after infection for 8 hours with RV-16 at MOI2 most of asthmatic PBEC exhibit a diffuse green fluorescence in their cytoplasm (altered mitochondrial membrane potential) as opposed to cells exposed to UV inactivated RV (figure 3.5a) whose cytoplasm is bright red.

Table 3.1 Clinical characteristics of volunteers.

10 subjects with moderately severe asthma and 10 healthy controls were recruited.

Subject characteristics

	Asthma	Normal	P values
Number	10	10	NA
Sex (% male)	69%	60%	P=0.6
Mean age (range)	32 (21-58)	29 (24-38)	P=0.4
Mean FEV1% predicted (SD)	77.3 (15.5)	110.3 (13.6)	P< 0.001

Subjects with asthma had mild to moderate disease, the majority (8/10) were on inhaled corticosteroids (ICS) and had relatively preserved lung function.

Characteristics of subjects with asthma

	Mild intermittent	Mild persistent	Moderate persistent
Number	2	5	3
Inhaled steroids (yes)	0	4 (80%)	3 (100%)
Mean (sd) Dose ICS BDP/day		300 (115)	617 (256)
Mean (sd) FEV1 % predicted	92.4 (6.2)	86.9 (6.6)	77.7 (17.9)

Values for FEV1 as a percentage of the predicted FEV1 are given as a mean and standard deviation of the mean. Inhaled corticosteroid dose is given as amount of beclomethasone (BDP) used per day, expressed as the mean and sd.

Figure 3.4

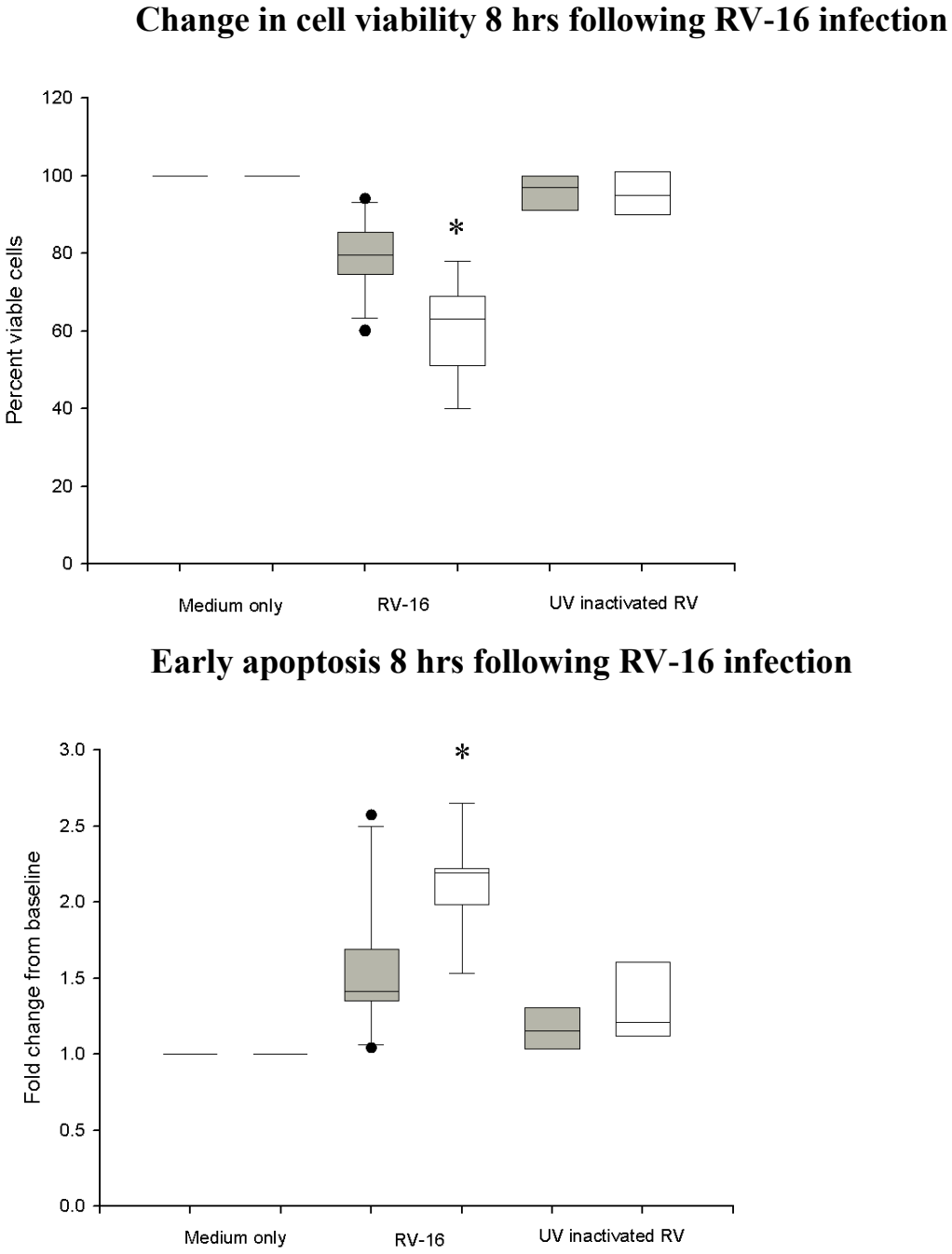

Differences in cell viability and apoptotic response following RV-16 infection in asthmatic and normal bronchial epithelial cells. **Panel (a):** Viable (AxV-/7AAD-) cell number was determined 8hrs after infection and expressed as % viability compared with cells treated with medium alone. Infection with RV-16 led to a significant reduction in median (IQR) cell viability in both asthmatic (grey boxes) and control (white boxes) cells compared to both medium alone (p=0.03 and 0.02 respectively) and UV inactivated RV-16 (p=0.02 and 0.001 respectively). In asthmatic cells there was significantly better viability, median 80% (74, 86)%, compared to healthy controls 63% (51, 69)% (p=0.02). **Panel (b):** Apoptotic (AxV+/7AAD-) cells were also analysed 8h following RV-16 infection. Data are expressed as median (IQR) fold change in apoptosis from baseline. There was a significant and virus-specific increase in cell apoptosis in response to infection in cells from both groups, however, this response was significantly impaired in asthmatic cells with a fold increase of only 1.4 (1.3, 1.7), compared to 2.2 (2.1, 2.3) in healthy controls (p=0.02).

Figure 3.5

Altered mitochondrial membrane permeability after RV infection

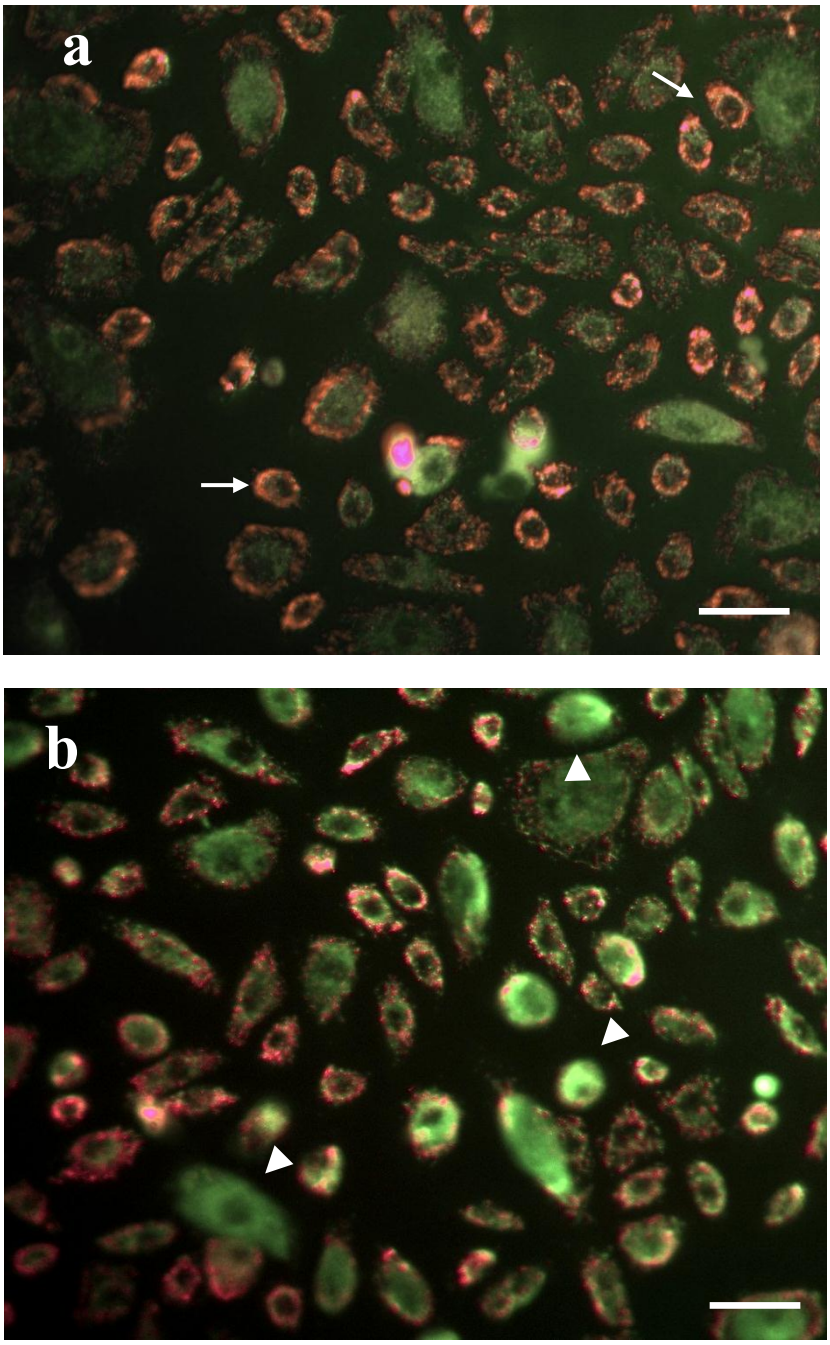

PBEC obtained from a representative asthmatic subject were infected with RV16 at MOI2 for 8 hrs (b) or with the same dose of UV inactivated RV (a). After washing with PBS cells were incubated with a cationic dye that fluoresces differently in apoptotic and nonapoptotic cells. Normally, the dye is taken up in the mitochondria, where it forms aggregates that exhibit intense red fluorescence (arrows). In apoptotic cells, the dye cannot accumulate in the mitochondria because of altered mitochondrial membrane permeability. As a result, the dye remains in monomeric form in the cytoplasm, where it fluoresces green (arrowheads). Bar = 25μM

3.1.6. Effects of inhibition of apoptosis and RV-16 production

As increased virion production by asthmatic PBEC was associated with reduced apoptosis, I investigated whether suppression of apoptosis in RV-16 infected normal PBEC was sufficient to enhance virion production. Thus, PBEC were treated with the caspases-3 inhibitor (C3I), Ac-DEVD-CHO, before and following infection with RV- 16. The inhibitor led to a marked reduction in apoptosis in the healthy control cells but had minimal effect on asthmatic cells compared to infection alone (Figure 3.6a). Treatment of cells from healthy controls with C3I also had a direct impact on RV-16 production, with a significant increase in transmissible infection at 48h, a similar increase was not seen in asthmatic cells treated with C3I (Figure 3.6b). These data provided a direct link between inhibition of early apoptosis and increased viral yield.

Figure 3.6

a **The effect of the Caspase 3 inhibitor ZVDfmk on apoptosis following infection**

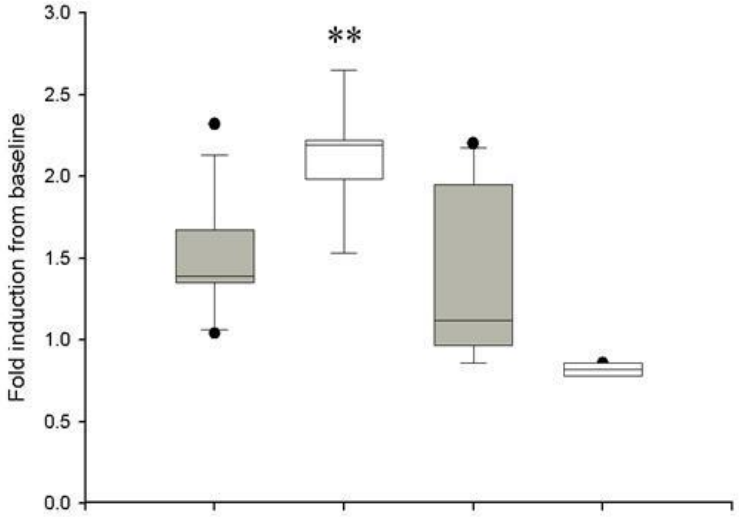

b **Modification of RV-16 production by inhibition of Caspase 3**

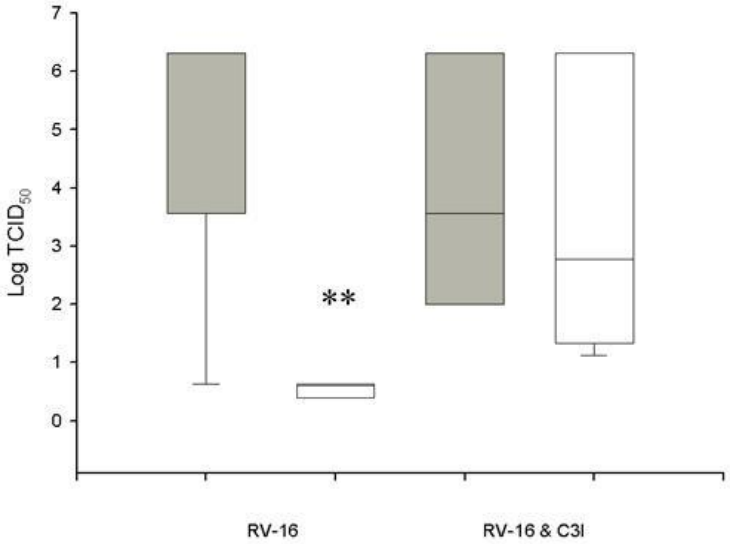

Inhibition of caspase activity inhibits apoptosis and increases RV-16 replication. (**a**): Cells were treated with RV-16 alone or with ZVD-fmk, before and after infection with RV-16. Results are expressed as the fold change in apoptotic cells compared to cells treated with medium alone. In asthmatic cells were there was a median (IQR) induction of apoptosis above baseline of 1.4 (1.3, 1.7) with RV-16 alone; pre-treatment of cells with the ZVD-fmk, had little effect on apoptosis (median (IQR) = 1.12 (1.01, 1.8); (p=0.4). However, in healthy controls cells, RV-16 infection resulted in a median (IQR) fold induction of apoptosis above baseline of 2.2 (2.1,2.3) and this was abolished by pre-treatment with ZVD-fmk (median (IQR) 0.82 (0.76, 0.86); p=0.03). (**b**): The effect of caspase-3 inhibition on RV-16 production was measured by HeLa titration assay on the BEC supernatant removed after 48h of infection. There was no difference seen in the TCID50 x104/ml in the supernatant removed from asthmatic cells infected with RV-16 (median (IQR) = 3.56 (3.50-3.62) compared to infected cells treated with ZVD-fmk (median (IQR) = 3.5 (3.45-3.62); p=0.94). However for healthy control BECs, the TCID50 x104/ml increased greater than 4 fold, from a median (IQR) value of 0.6 (0.4, 0.63) with infection alone to 2.78 (0.63, 6.32) (p=0.01) in the presence of RV-16 and ZVD-fmk.

3.1.7. Conclusions.

The results presented herein are part of a broader research project that was conducted in collaboration with Dr Peter Wark at the Brooke Labs.

My results show that infection of PBEC with RV-16 induced a significant reduction in cell viability with a subsequent increase in early apoptosis in healthy subjects when compared to asthmatic patients. These data were confirmed by evaluating the mitochondrial membrane potential. The increase in apoptosis was accompanied by a higher viral replication rate. Moreover, using a specific caspase inhibitor to block apoptosis led to a marked reduction in apoptosis in the healthy control cells but had minimal effect on asthmatic cells compared to infection alone, as well as having a direct impact on RV-16 production, with a significant increase in transmissible infection at 48h that was not seen in asthmatic cells treated with the same inhibitor. Using the same experimental model, together with Dr Wark we found that viral RNA expression and late virus release into supernatant was increased 50 fold and 7 fold respectively in asthmatic cells compared to healthy controls, and that virus infection induced late cell lysis in asthmatic cells but not in normal cells. More importantly, examination of early innate immune responses revealed profound impairment of virus induced interferon-β mRNA expression in asthmatic cultures that produced >2.5 times less interferon-β protein.

In view of the data obtained in collaboration with Dr Wark, my results suggest that in infected asthmatic cells, exogenous interferon-β induced apoptosis and reduced virus replication, and therefore it is possible to demonstrate a causal link between deficient interferon-β, impaired apoptosis and increased viral replication. Epidemiological evidence demonstrates that asthmatic subjects develop more severe lower respiratory symptoms and reduction in lung function when infected with RV (Corne et al., 2002); however, the mechanisms behind this increased susceptibility to rhinovirus infection were unknown. The data presented in this chapter together with the results obtained with Dr Wark seem to indicate that impaired type 1 interferon production is likely to be an important mechanism.

These results offer a logical explanation for asthmatic subjects having lower respiratory tract symptoms and reductions in lung function of greater severity and

duration as a consequence of RV infection. While infection of bronchial epithelial cells is limited in non-asthmatic subjects by an innate antiviral response and induction of apoptosis in infected cells, a deficiency of IFN-β in asthma could facilitate virus replication and cytolysis with increased infection of neighbouring cells. Exaggerated inflammatory responses are likely to result in asthmatics *in vivo*, consequent upon the increased replication and the cytolytic effects of the virus infection.

3.2. ROLE OF ECM IN MODULATING LUNG (MYO)FIBROBLASTS ACTIVITY.

Prior to studying the responses of fibroblasts to conditioned media obtained by PBECs infected with RV16, I characterised the bronchial fibroblast culture model in terms of susceptibility to the different ECMs and intrinsic phenotypic differences between fibroblasts obtained from normal or asthmatic subjects. Cell-ECM interactions have a pivotal function in several cellular processes, such as migration, proliferation, differentiation and survival. ECM was previously thought of a passive supportive structure, essential for the formation and maintenance of tissues. Today, it is widely recognised that it is a dynamic structure that modulates a range of cell processes due to its organization and composition. Altering its molecular composition may therefore profoundly affect cell function.

Pulmonary fibroblasts have been shown to have a wider variety of functions aside from being target structural cells, such as directly contributing to pulmonary inflammation and ultimately to airway wall remodelling. The various compounds these fibroblasts release can substantially alter the surrounding environment (Mutsaers et al., 1997). These cells are also associated with the deposition and remodelling of lung ECM, being the primary cellular source of collagens I and III; which are released in response to IL-1β and growth factors, such as TGF-β, responsible for activating pro-collagen gene expression (McAnulty et al., 1995). Surprisingly, other fibroblast-related cytokines (e.g. IL-6) generate a reverse outcome by releasing matrix metalloproteinases, including MMP-2 (collagenase) and MMP-9 (gelatinase), which may lead to ECM remodelling. Moreover, it has been demonstrated that lung fibroblasts release a membrane type-1 matrix metalloprotease whose collagenolytic activity has been correlated with ECM remodelling in acute and chronic lung diseases (Rowe et al., 2011).

Both fibroblast proliferation and collagen synthesis are profoundly influenced by cellular adhesion. In normal fibroblasts, cell division requires anchorage to a substratum. The more firmly anchored the cells, the greater their proliferation (Grinnell 1994; Guadagno et al., 1991) and production of collagen (Dhawan et al., 1990 and 1991). Fibroblast cell lines derived from normal lung conform to this pattern. However, fibroblast cell lines generated from individuals with idiopathic pulmonary fibrosis have been found to continue to proliferate on a soft substrate, in

an anchorage-independent manner (Torry et al., 1994). Whether this change is related to alterations in fibroblast integrins or other factors, has not yet been fully determined. This finding suggests that fibroblast responsiveness to influences from the ECM is a critical component that restricts fibroblast activity in the normal lung. A recent study using in vivo mouse models that mimic airway remodeling, coupled with conditional deletion in adult fibroblasts, has shown that integrin αvβ8–mediated TGF-β activation plays a critical role in both airway fibrosis and inflammation (Kitamura et al., 2011).

The degree of adhesion between the cells and ECM depends on the state of differentiation of the cells, as well as their location and any surrounding conditions that can be sensed by the cells. The huge variety of complex *in vivo* microenvironments poses a major hurdle for achieving a thorough understanding of the cell-matrix adhesion process.

3.2.1. AIMS

The goal of the present study was to determine whetherdifferent ECM components might modify human lung fibroblast activity in culture. Specifically, my hypothesis was that matrices involved in the composition of the basement membrane of the bronchial mucosa, such as collagen type I and IV, fibronectin and laminin could affect cell morphology, adhesion, differentiation and survival. In order to verify this hypothesis, I set up a primary culture model of human bronchial fibroblasts where the responses of these cells to the abovementioned matrix components were evaluated.

3.2.2. Morphological observations: fibroblasts appearance and adhesion on different ECMs.

Primary bronchial fibroblasts were plated onto 24 well trays at $5x10^4$/well and grown on laminin, fibronectin, collagen I, collagen IV or charged plastic for 72 hours; digital photographs were taken at 2, 24 and 72 hours. Figure 3.7 shows that

after 2 hrs in culture cells grown on charged plastic only (a) were attaching more slowly to the substratum as demonstrated by the lower number of cells spread on the plastic per microscopic field and the higher number of rounded cells (floating) when compared to all the ECM components. On collagen IV (e) cells did not spread as well as with fibronectin (c) or laminin (b). After 24 hours the fibroblasts were spread uniformly to the substratum even though the cells on plastic were still slightly less in number (Figure 3.8). After 72 hours fibroblasts reached confluency and there was no significant difference in the number of cells attached to the different components (Figure 3.9). At all time-points and with the different ECM components studied it was not possible to identify any particular difference in the morphology of these cells.

Figure 3.7

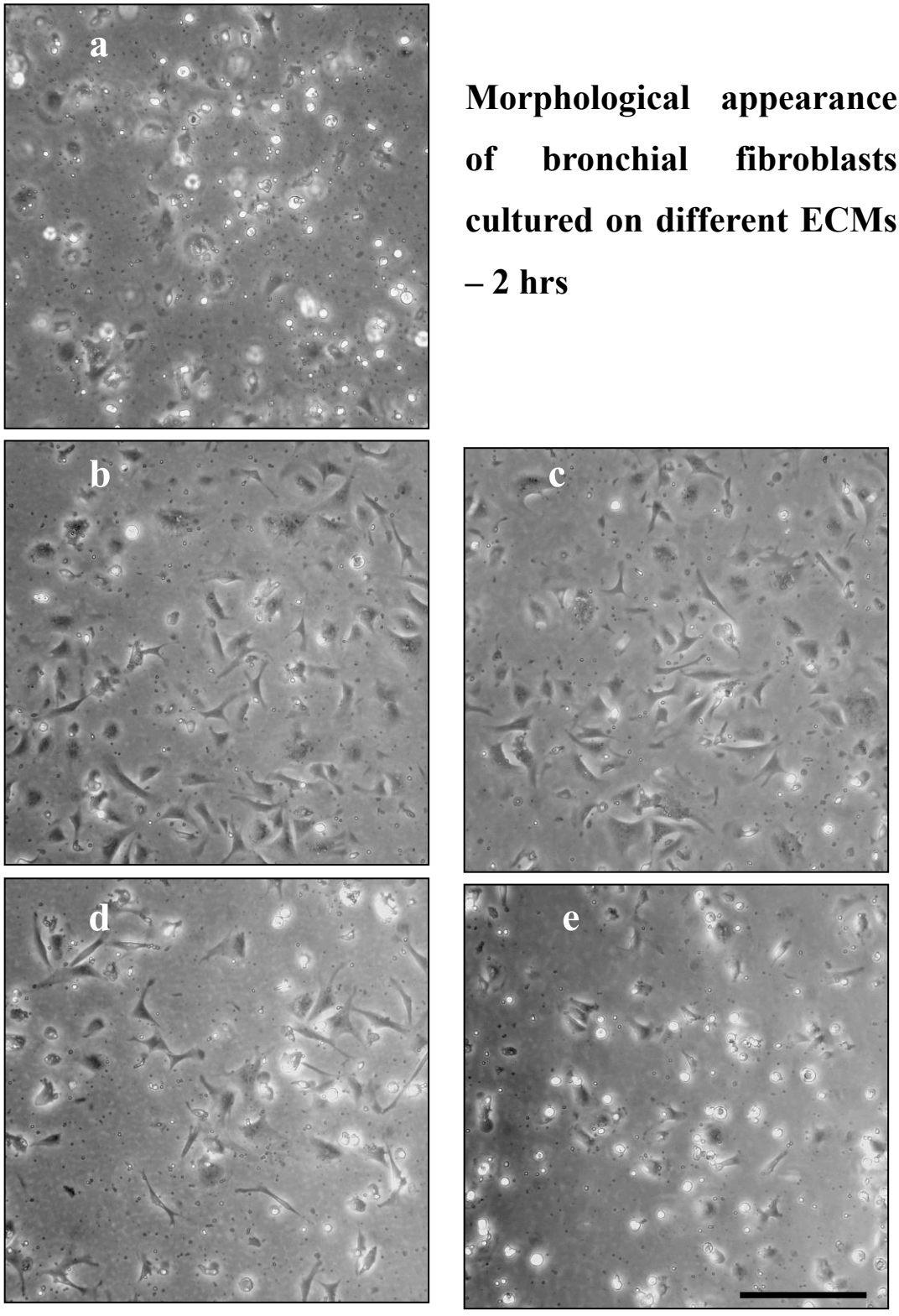

Morphological appearance of bronchial fibroblasts cultured on different ECMs – 2 hrs

Fibroblasts were plated onto 24 well trays and grown on charged plastic coated with PBS only (a), laminin (b), fibronectin (c), collagen type I (d) or collagen type IV (e) all at 1μg/ml. Photographs were taken at 2 hr.; bar = 100μm. Cells in panels a and e show a delayed adhesion velocity to their substrates when compared to the other cells. Cell morphology is identical in all the different conditions.

Figure 3.8

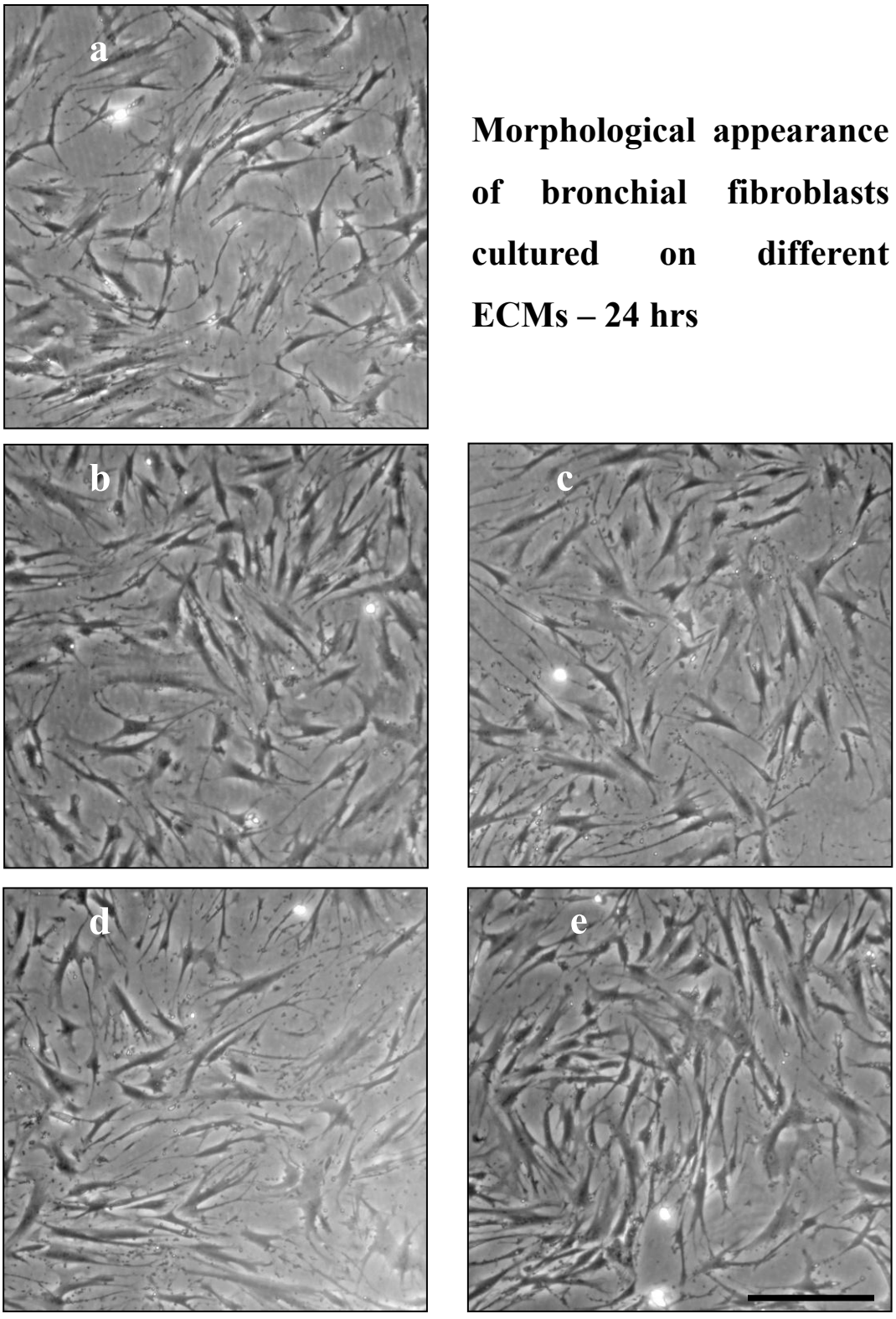

Morphological appearance of bronchial fibroblasts cultured on different ECMs – 24 hrs

Fibroblasts were plated onto 24 well trays and grown on charged plastic coated with PBS only (a), laminin (b), fibronectin (c), collagen type I (d) or collagen type IV (e) all at 1μg/ml. Photographs were taken at 24 hr.; bar = 100μm. By this time point all cells show a similar level of adhesion to their substrate and an identical morphology in all conditions.

Figure 3.9

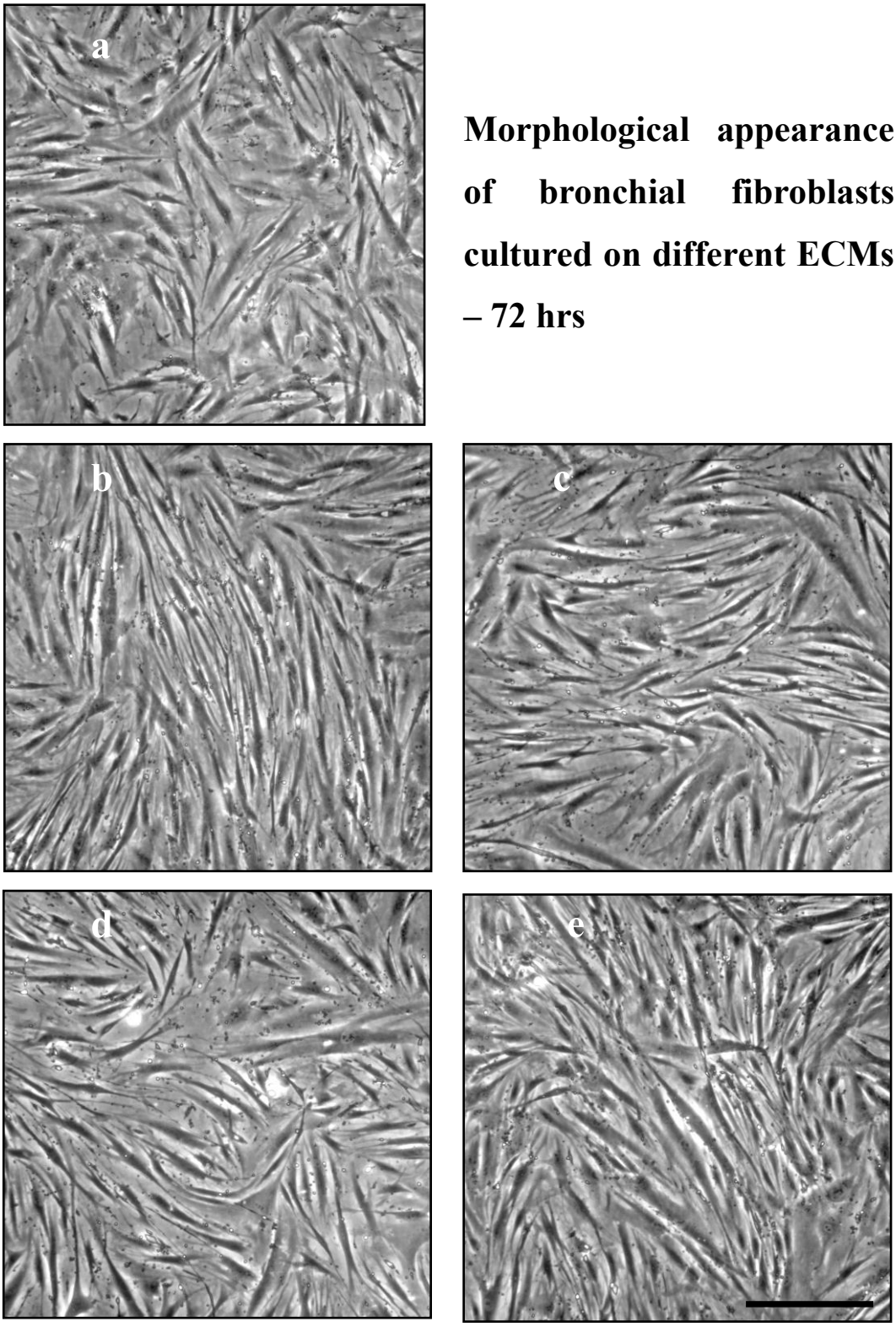

Morphological appearance of bronchial fibroblasts cultured on different ECMs – 72 hrs

Fibroblasts were plated onto 24 well trays and grown on charged plastic coated with PBS only (a), laminin (b), fibronectin (c), collagen type I (d) or collagen type IV (e) all at 1μg/ml. Photographs were taken at 72 hr.; bar = 100μm. After reaching cell confluency, fibroblasts are still failing to show any difference in morphology.

3.2.3. Cell adhesion: calcein-AM to assay adhesion of fibroblasts to different ECMs.

To evaluate whether the different ECMs might condition the ability of primary bronchial fibroblast to adhere to their substratum, a fluorescence-based adhesion assay (Calcein-AM) was performed. Primary bronchial fibroblasts were seeded onto 96-well trays at $2x10^5$/well; wells were coated with laminin, fibronectin, collagen I, or charged plastic. Cells were allowed to adhere for 5, 15, 30, 45 and 60 minutes. A different tray had to be prepared for each different time point. At the end of each time point the tray was collected and cells stained with calcein-AM. The plate was then read in a fluorescent plate reader Cytofluor II (PerSeptive Biosystems) at an excitation wavelength of 480nm and an emission wavelength of 530nm. In each experiment fluorescent units (FU) in 0.1ml of cells (total) and FU released into the supernatants during the assay (spontaneous) were determined. Percent cell bound fluorescence was then calculated as 100 x bound FU/(total FU)-(spontaneous FU). Figure 3.10 shows an example of this staining after 1 hour. It is possible to appreciate the different levels of spreading of cells into the substratum, with collagen I being the one that caused the cells to spread the most followed by fibronectin, laminin and plastic. The overall number of cells however did not significantly vary between the different conditions.

The graph in figure 3.11 shows the percent cell bound fluorescence at the different time points and with the different ECM components in primary bronchial fibroblasts obtained from 4 healthy subjects. At all time points collagen I and fibronectin caused a statistically significant increase of percent cell bound fluorescence when compared to charged plastic alone ($p<0.02$ for both). Coating the wells with laminin instead did not change significantly the ability of fibroblasts to adhere to the plastic substratum when compared to charged plastic alone.

Figure 3.10

Calcein-AM assay

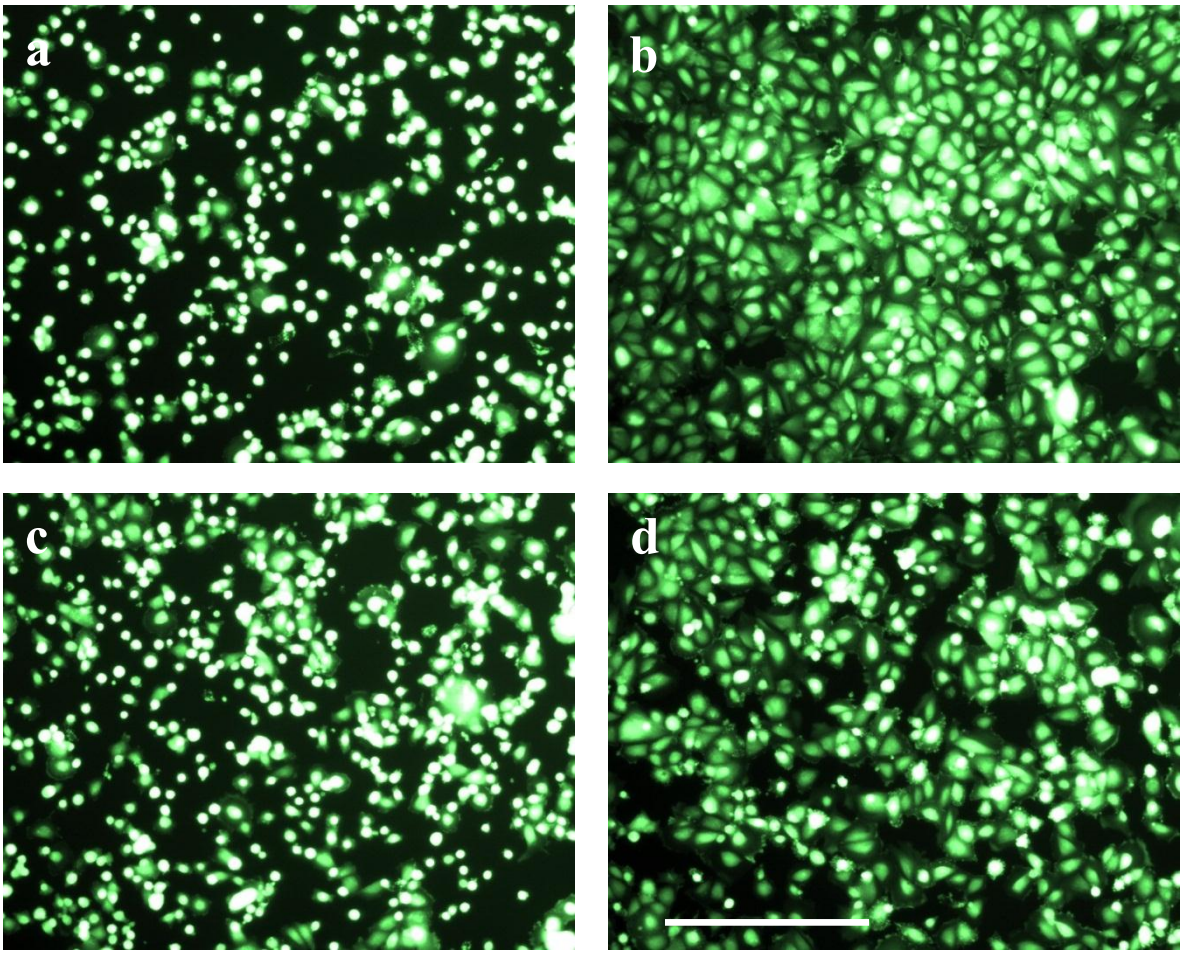

96 well trays (NUNC) were coated with charged plastic (a), collagen type I (b), laminin (c) or fibronectin (d). Primary fibroblasts were harvested, centrifuged and resuspended in DMEM (no additives) at $1x10^7$/ml. Calcein-AM was added to give a final 2µM concentration, and cells were incubated at room temperature in the dark for 30 minutes. Cells were then washed and at the end of the washings resuspended at $2x10^6$/ml in DMEM containing 2% FBS. Cells were then allowed to adhere to the different ECM components by adding 0.1ml of cell suspension per well and incubating at 37°C for 60 minutes. At the end of this time point the wells were washed gently to remove non-adherent cells. 0.1ml of DMEM 2% FBS was then added in each well and digital photographs were taken. Bar = 100 µm.
It is possible to appreciate the different levels of spreading of cells into the substrata, with collagen I being the one that cause the cells to spread the most followed by fibronectin, laminin and plastic. The overall number of cells however does not differ between the different ECMs.

Figure 3.11

Calcein-AM assay quantification

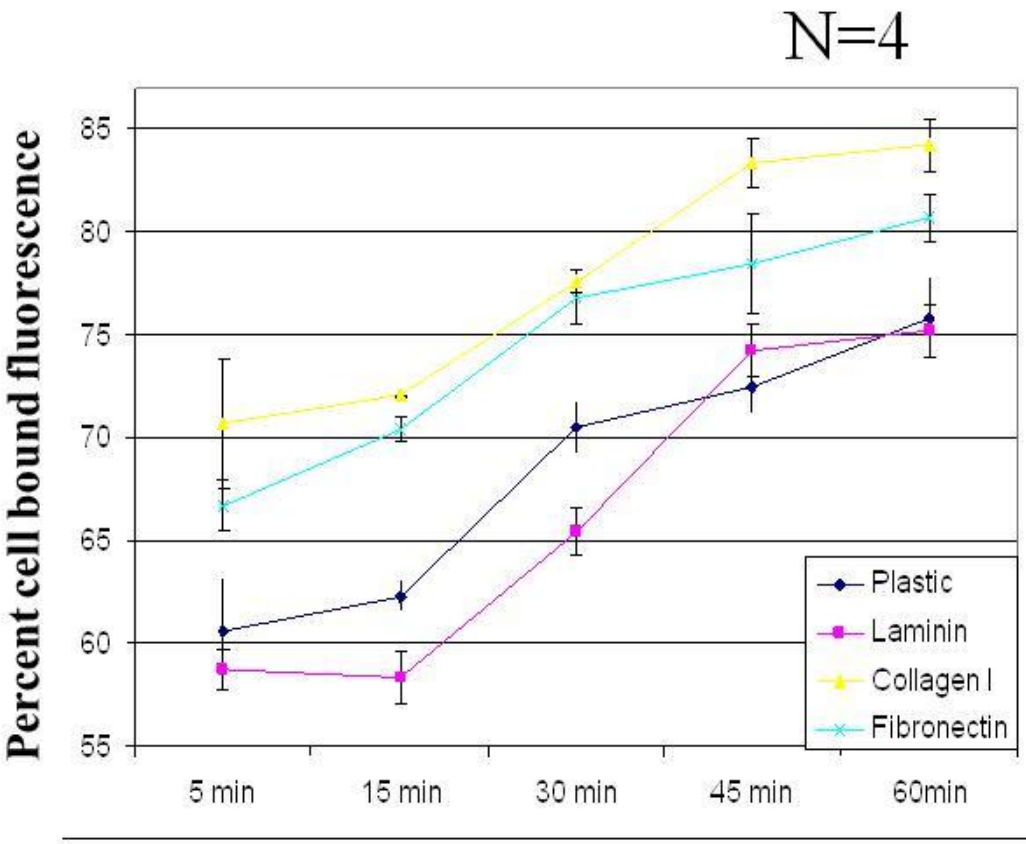

96 well trays were coated with charged plastic alone, collagen type I, laminin or fibronectin. Primary fibroblasts were harvested and resuspended at $1x10^7$/ml. Calcein-AM was added to give a final 2mM concentration, and cells were incubated at room temperature in the dark for 30 minutes. Cells were washed three times and resuspended at $2x10^6$/ml in DMEM containing 2% FBS. Cells were then allowed to adhere to the different ECM components by adding 0.1ml of cell suspension per well and incubating at 37°C for 5, 15, 30, 45 and 60 minutes. At the end of each time point the wells were washed gently to remove non-adherent cells. 0.1ml of DMEM 2% FBS was then added in each well and the plate was read in a fluorescent plate reader Cytofluor II (PerSeptive Biosystems) at an excitation wavelength of 480nm and an emission wavelength of 530nm. In each experiment fluorescent units (FU) in 0.1ml of cells (total) and FU released into the supernatants during the assay (spontaneous) were determined. Percent cell bound fluorescence was then calculated as 100 x bound FU/total FU-spontaneous FU. N=4.
At all time points collagen I and fibronectin determined a statistically significant increase of percent cell bound fluorescence when compared to charged plastic alone ($p<0.02$ for both).

3.2.4. Differentiation of fibroblasts into myofibroblasts: Immunofluorescence and FACS analysis to study αSMA expression in fibroblasts cultured on different ECMs.

In order to verify whether the ECM could play a role in the differentiation of primary bronchial fibroblasts into myofibroblasts, we immunostained fibroblasts from healthy subjects with a monoclonal antibody FITC-conjugated directed towards alpha smooth muscle actin (αSMA). Although there are no known specific markers for fibroblasts, myofibroblasts are classically characterized by the presence of filaments of αSMA. As TGF-β_2 is a well-known inducer of fibroblast differentiation into myofibroblasts, we treated cells with this growth factor in order to obtain a positive control. Nuclei were counterstained with PI. Figure 3.12 shows a high magnification photograph of a myofibroblast, stained for αSMA, presenting the characteristic stress fibers. Figure 3.13 shows that, as expected, treatment with TGF-β_2 at 10 ng/ml induced an increase in the number of fibroblasts positive for αSMA when compared to untreated fibroblasts grown on plastic (uncoated).

However, out of the three ECM components tested, collagen I, fibronectin and laminin, only the latter seemed to be able to determine a slight reduction in the number of αSMA positive cells. To quantify both percentage of positive cells and mean fluorescence intensity (MFI) of αSMA, fibroblasts were also analysed with flow cytometry. Primary bronchial fibroblasts obtained from 8 healthy subjects were immunostained for FACS analysis as detailed in the Methods section. Figure 3.14 shows a typical example of a histogram plot obtained with this method. In this case the treatment with TGF-β_2 induced a 34% increase in the number of fibroblasts positive for αSMA when compared to its serum free medium (SFM) control. At the same time the MFI has more than doubled showing that the treatment has also induced an increase of the number of αSMA molecules per cell. Collagen-I and fibronectin failed to induce any significant change both in the number of fibroblasts expressing αSMA and in the MFI (data not shown). The presence of laminin instead significantly reduced the number of αSMA positive cells when compared to plastic alone (12.14-/+7.3 vs 9.05-/+7.1, p=0.036) (Figure 3.15). The MFI instead was not significantly changed (65-/+21.06 vs 58.74-/+23.15, p=0.161).

Figure 3.12

αSMA immunostaining

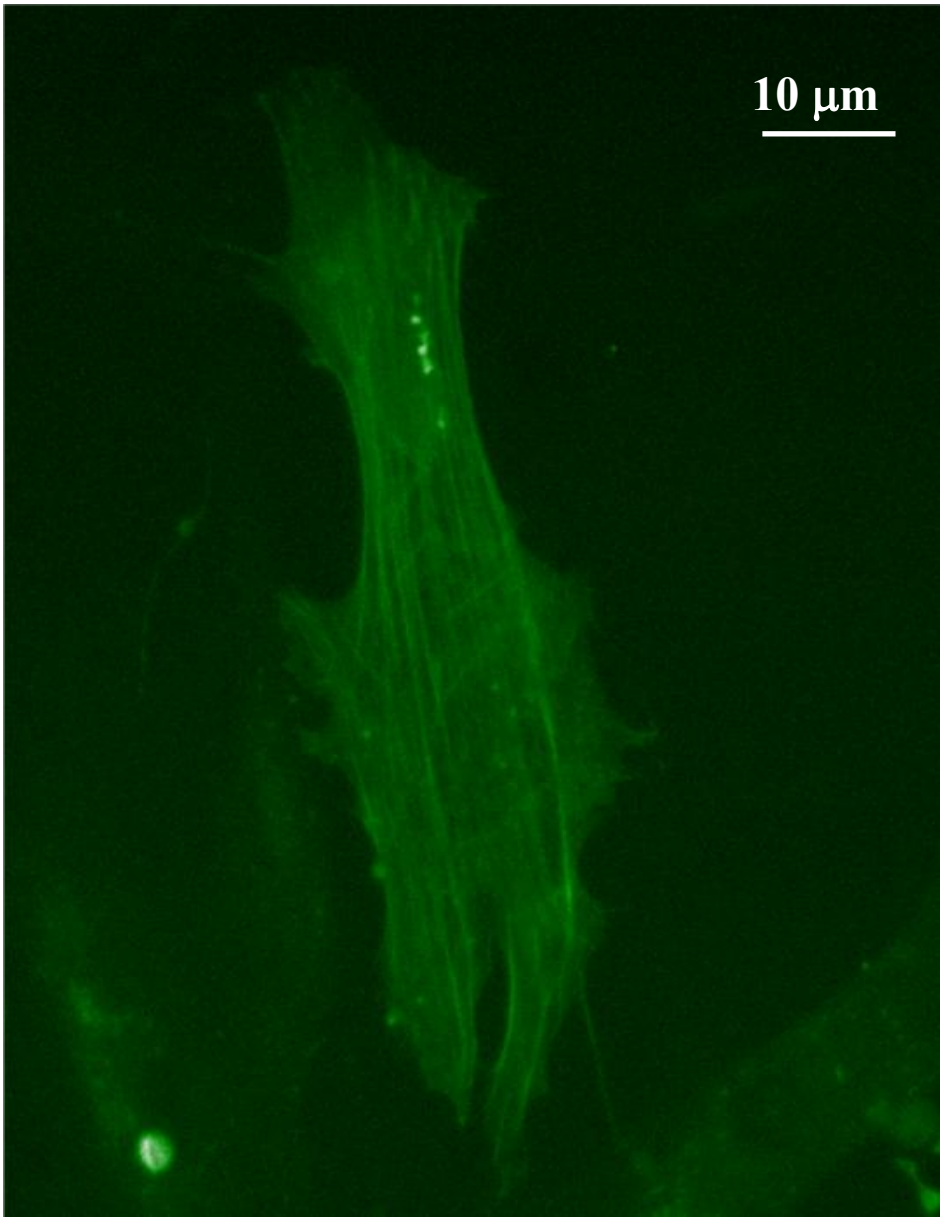

Primary fibroblasts were seeded at $5x10^4$/well in 24 well trays coated with different ECM components, grown to 80% confluence in the appropriate growth media and then treated as required for the different experiments. At the end of the treatment cells were washed, fixed, permeabilised and stained with a monoclonal anti-α smooth muscle actin FITC-conjugated antibody as reported in the Materials and methods section. This image is a high magnification photograph of a myofibroblast presenting the characteristic stress fibers. Bar = 10 μm.

Figure 3.13
αSMA immunostaining

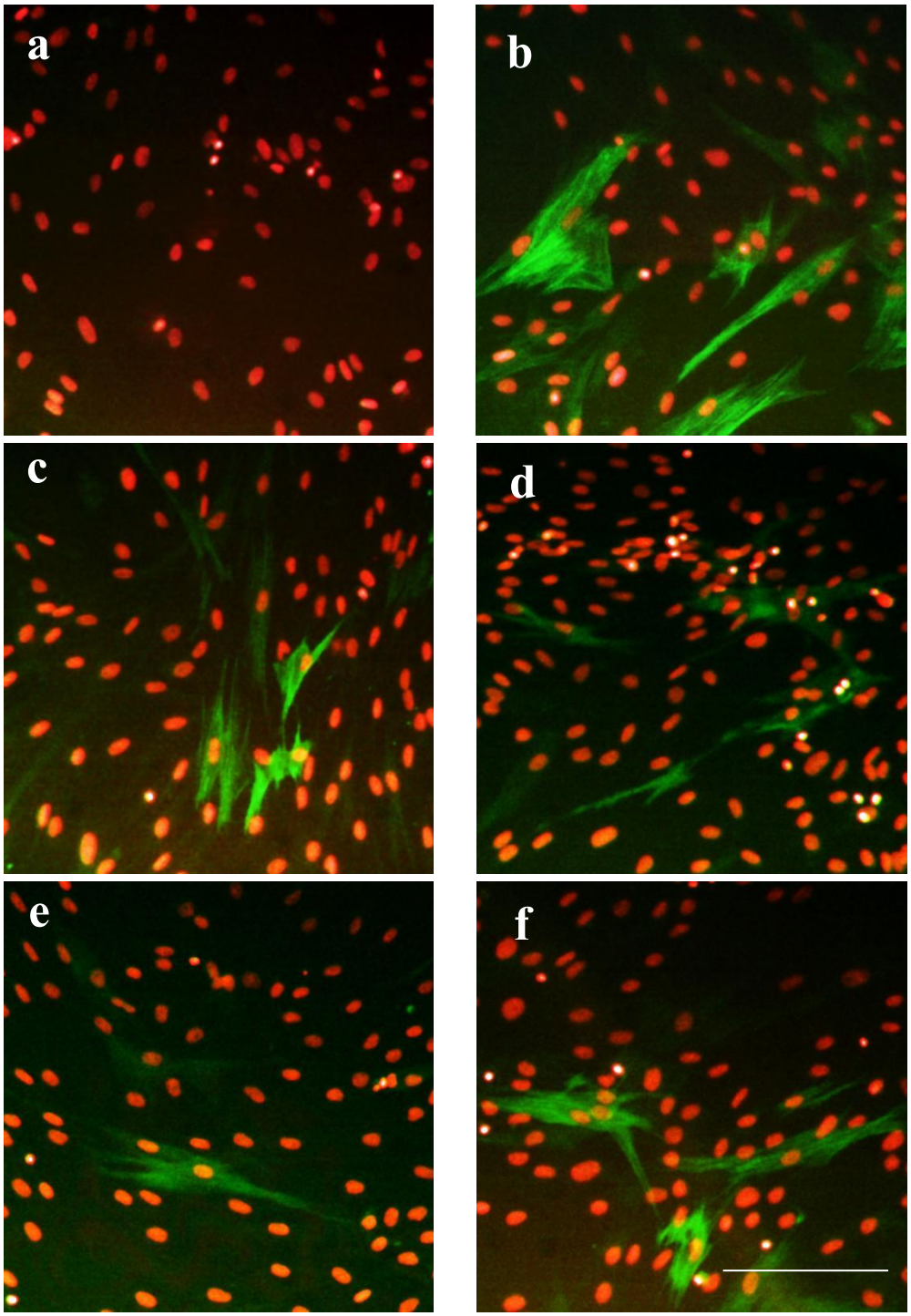

Primary fibroblasts were seeded at 5x104/well in 24 well trays coated with different ECM components charged plastic only (**c**), collagen type I (**d**), laminin (**e**), fibronectin (**f**), grown to 80% confluence in the appropriate growth media and then treated as required for the different experiments. At the end of the treatment cells were washed, fixed, permeabilised and stained with a monoclonal anti-α smooth muscle actin FITC-conjugated antibody as reported in the Materials and methods section. Nuclei were counterstained with PI. Panel a shows the appropriate isotype control, whereas panel b is a postive control obtained by treating the same cells with TGF-β2 10ng/ml. Bar = 100 μm.

Figure 3.14

αSMA expression analysis by flow cytometry

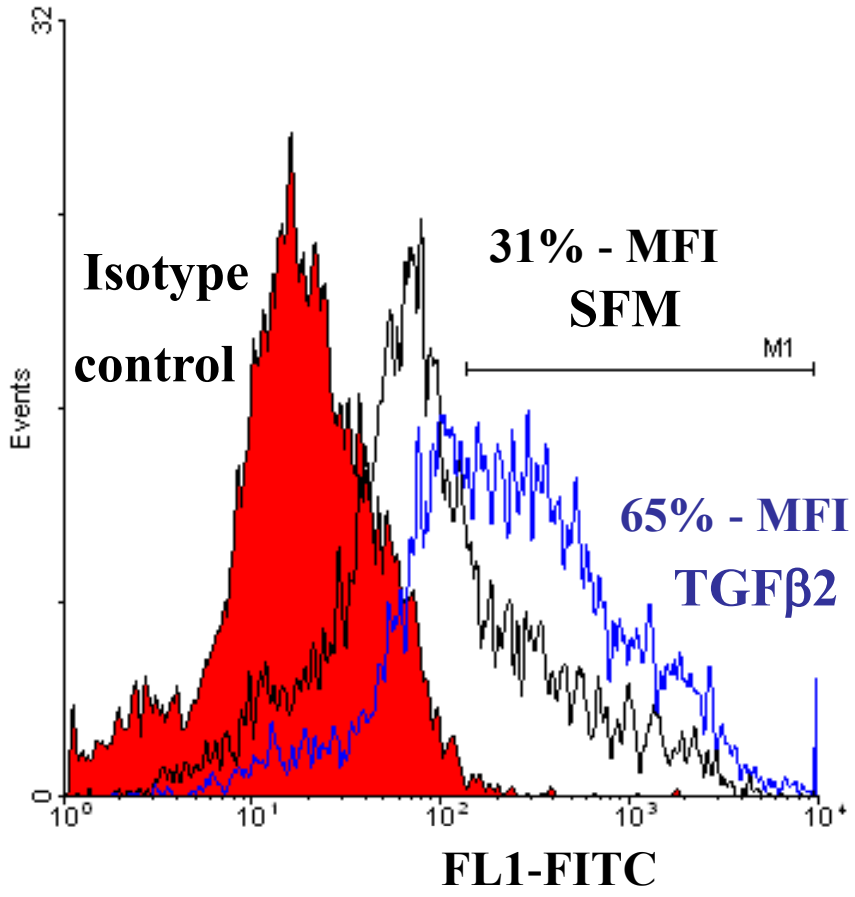

Typical example of a histogram plot for αSMA staining. Filled red = Isotype control. Black line = Untreated control (SFM). Blue line = TGFβ2 positive control. Marker M1 is positioned at the end of the isotype control histogram and the percentage of staining for all the other conditions are relative to this marker. MFI is instead calculated on the whole distribution of the events for the different histograms.

Treatment with TGF-β2 has induced a two folds increase in the number of fibroblasts positive for αSMA when compared to its serum free medium (SFM) control. At the same time the MFI has more than doubled showing that the treament has also induced an increase of the number of αSMA molecules per cell.

Figure 3.15

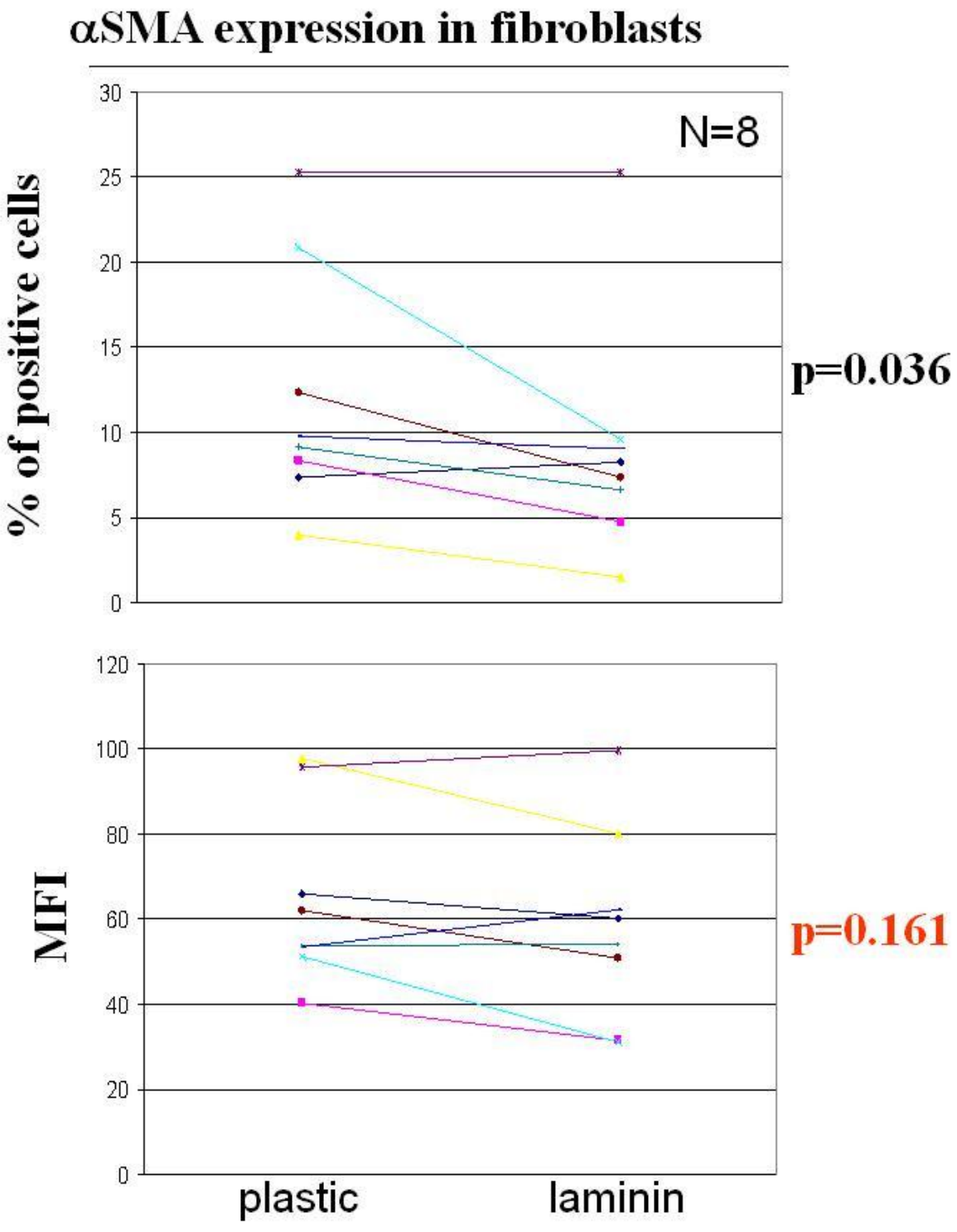

Primary bronchial fibroblasts obtained from 8 healthy subjects were immunostained for FACS immunofluorescent analysis as detailed in the Methods section. The presence of laminin has significantly reduced the number of αSMA positive cells when compared to plastic alone (12.14-/+7.3 vs 9.05-/+7.1, p=0.036). The MFI instead was not significantly changed (65-/+21.06 vs 58.74-/+23.15, p=0.161).

3.2.5. Cell survival: Evaluation of cell death levels in fibroblasts with Annexin-V/PI staining.

In order to evaluate whether different ECM components were able to modify cell survival, primary bronchial fibroblasts obtained from four healthy subjects were seeded onto 24-well trays at $5x10^4$/well; wells were coated with laminin, fibronectin, collagen I, or charged plastic only. After a starvation period of 24 hours, cells were harvested, collected in FACS tubes and stained with Annexin-V/PI in order to evaluate basal levels of apoptosis and necrosis. Figure 3.16 shows that the ECMs studied were not able to induce any significant change in basal levels of viability or early apoptosis when compared to charged plastic alone. Fibroblasts were then treated with hydrogen peroxide to evaluate eventual differences induced by the ECMs in response to a proapoptotic factor. A dose of 100 μM and a time point of 24 hours were chosen based on preliminary dose-response experiments that indicated these as the optimal dose and time to get a good number of apoptotic cells. Figure 3.17 shows that even during oxidative stress conditions the different ECMs did not play any significant role in protecting fibroblasts from hydrogen peroxide-induced apoptosis.

Figure 3.16

Effects of the ECM on cell viability and apoptosis - I

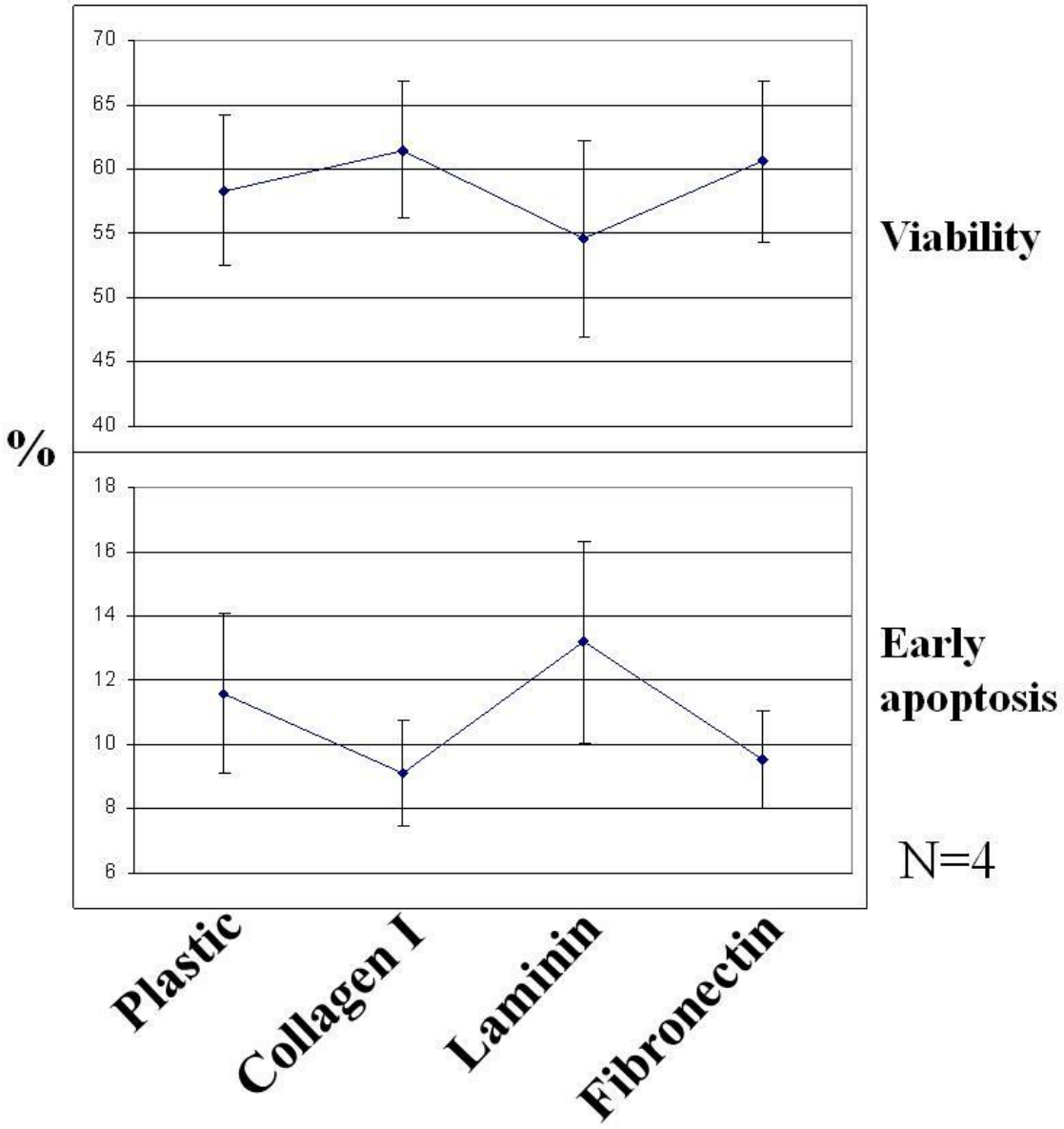

Annexin-V/PI FACS staining. Primary bronchial fibroblasts obtained from four healthy subjects were seeded onto 24-well trays at 5x104/well; wells were coated with laminin, fibronectin, collagen I, or charged plastic only. After a starvation period of 24 hours, cells were harvested, collected in FACS tubes and stained with Annexin-V/PI in order to evaluate basal levels of total viability, apoptosis and necrosis.
As shown by this graph, all the ECMs studied failed to induce any significant change in basal levels of viability or early apoptosis when compared to charged plastic alone. N=4.

Figure 3.17

Effects of the ECM on cell viability and apoptosis - II

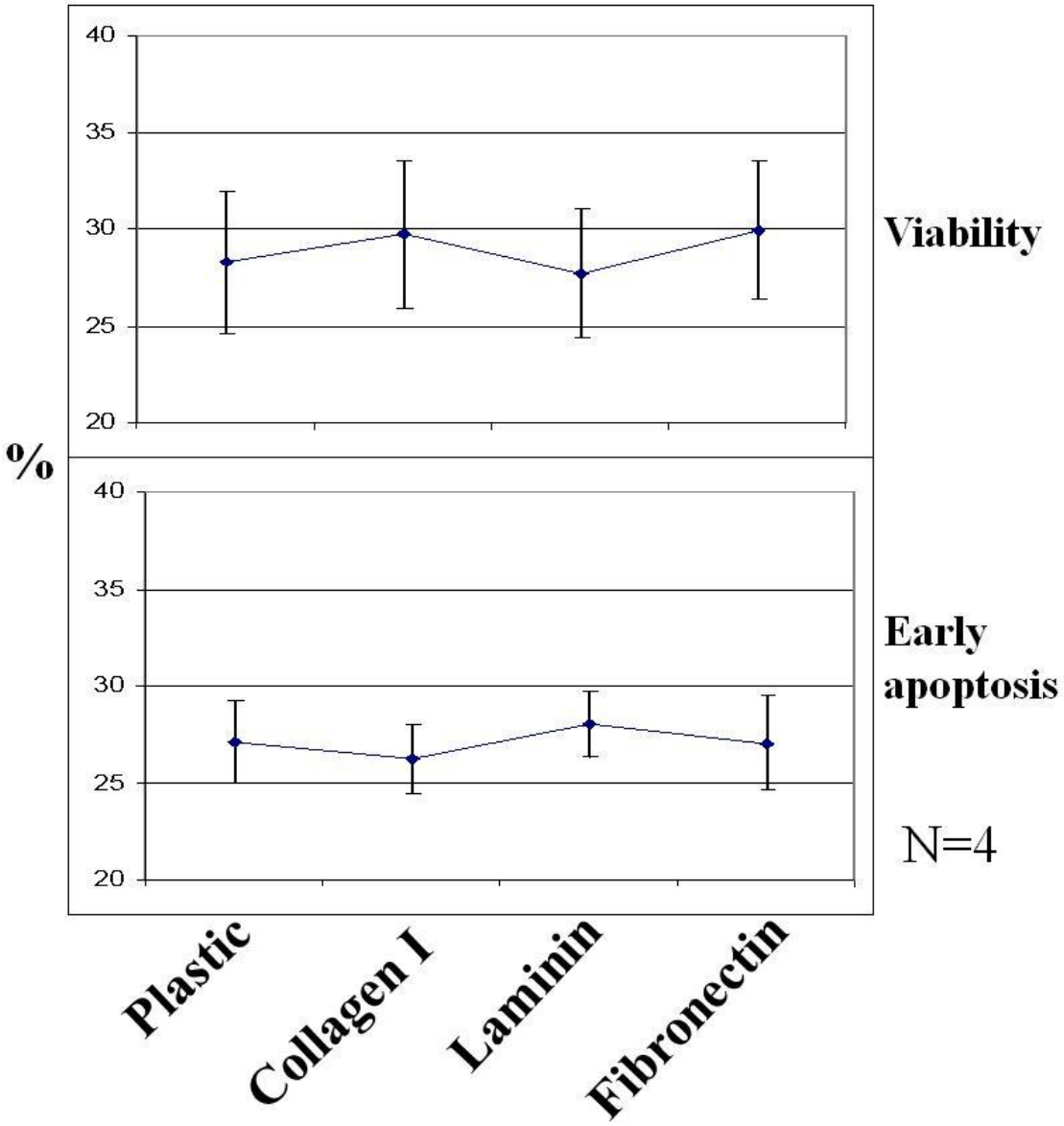

Annexin-V/PI FACS staining. Primary bronchial fibroblasts obtained from four healthy subjects were seeded onto 24-well trays at 5x104/well; wells were coated with laminin, fibronectin, collagen I, or charged plastic only. After a starvation period of 24 hours, cells were treated with hydrogen peroxyde 100 μM for 24 hours, harvested, collected in FACS tubes and stained with Annexin-V/PI in order to evaluate levels of total viability, apoptosis and necrosis.
As shown by this graph, all the ECMs studied failed to induce any significant protective effect on oxidant-induced cell death when compared to charged plastic alone. N=4.

3.2.6. Conclusions

The interaction of activated fibroblasts with the surrounding ECM and their modification by cytokines and growth factors is an important issue for understanding the complex events underlying the sup-epithelial fibrosis typical of asthma.

Many cytokines and mechanical factors can be responsible for the activation of fibroblasts, and the mechanisms responsible for their activation underlie specific feedback controls that originate due to the recognition of the surrounding ECM molecules mediated mainly by integrins. Having recognized defined portions of the ECM components, these receptors are able to mediate signals depending on the specific integrin that was expressed at the cell surface site (Beate et al., 2000).

These important signals are required for fibroblasts to adapt their biosynthetic machinery to the ever changing biological requirements (Beate et al., 2000).

My results show that adhesion dynamics seemed to be different depending on the substrate used. Initial phase contrast observations showed that when lung fibroblasts were allowed to adhere to charged plastic only, for the first few hours they attached more slowly to their substratum when compared to all the evaluated ECM components. Moreover, on collagen IV cells did not spread as well as on fibronectin or laminin. However, at later time points, there was no significant difference in the number of cells attached to the different components. Also, it was not possible to identify any particular difference in the morphology of the fibroblasts at all time-points and with the different ECM components. I therefore proceeded with the evaluation of cell adhesion using a calcein-AM assay under a fluorescent microscope that showed that collagen type I was the ECM component in which the cells spread most, but the overall number of cells attached to the culture plates was not significantly affected by the different components. When calcein-AM assay was quantified with a fluorescent plate reader, at all time points collagen I and fibronectin were found to cause a statistically significant increase of percent cell bound fluorescence when compared to charged plastic alone. However, I found that the accuracy of this assay is limited by the fact that the degree of spreading of cells into the substratum will affect the fluorescence levels recorded by the reader that does not necessarily reflect the actual number of cells. A method to normalize cell numbers in relation to spreading degree should therefore be employed in future studies.

To investigate fibroblast differentiation with the different ECM components, cells were immunostained for αSMA and quantification carried out by flow cytometry. As expected, treatment with TGF- β2, that was used as positive control, induced an increase in the number of αSMA positive fibroblasts. However, out of the ECM components studied, only laminin coating significantly reduced the number of αSMA positive cells when compared to plastic alone, suggesting that this ECM protein might determine a reduction in fibroblasts to myofibroblasts transition.

Finally, I evaluated, by Annexin V assay, eventual differences in cell death levels with the different ECM components. None of the ECM components studied induced any significant change in viability or early apoptosis, whether in basal conditions or after oxidative stress, when compared to charged plastic alone. The physiological ECM in the airways is mainly composed of collagen type I and III with fibronectin and laminin playing an important role during remodelling (Chakir et al., 1996; Royce et al., 2009). Fibronectin and laminin are also involved in increased resistance of lung cells, including fibroblasts, to ionizing radiations and cytotoxic drugs, suggesting a potential role in carcinogenesis (Cordes et al., 2003) but also in fibrosis. An interesting manuscript published in 2006 by Kim and his colleagues suggest that during experimental lung injury, that exposes ECM components such as laminin and fibronectin, there could be evidence of lung alveolar epithelial-to-mesenchymal transition (EMT). When these authors cultured primary alveolar epithelial cells on fibronectin or fibrin, those cells underwent robust EMT via integrin-dependent activation of endogenous latent TGF-β_1. In contrast, the same cells cultured on laminin/collagen mixtures do not activate the TGF-β_1 pathway and, if exposed to active TGF-β_1, undergo apoptosis rather than EMT (Kim et al., 2006). These data implicate that the provisional ECM could act as a key regulator of epithelial transdifferentiation during fibrogenesis. As stated before, in my experimental setup, none of the studied ECM components caused any statistically significant modification in cell survival rates or cell adhesion/differentiation.

However, independently from any potential limitations and/or methodological flaws of my study, considering that the main *in vivo* function of fibroblasts is to lay the ECM, it is likely that these cells, when cultured *in vitro*, will start layering their own ECM components thus modifying whatever artificial substrate applied. For this reason, in order to examine fibroblast function, it is

essential to develop novel cell culture models where these cells can be grown in an environment that mimics the bronchial mucosa as closely as possible.

3.3. DIFFERENCES IN FIBROBLASTS ACTIVITY BETWEEN HEALTHY SUBJECTS AND ASTHMATICS.

A plethora of studies have investigated functional differences in inflammatory cells of healthy or asthmatic subjects. Ironically, much less is known about the structural cells that constitute most of the lung parenchyma. The ability of structural cells to synthesise a wide array of inflammatory mediators, including proinflammatory cytokines and chemokines, implicate these cells as effector cells with the capacity to regulate inflammatory responses in asthmatic airways. Researchers are becoming increasingly more aware of the potentially important roles played by these cells in the pathogenesis of asthma and other chronic inflammatory diseases; however, the exact contribution of specific structural cell types, especially fibroblasts, to the overall process is still unclear.

3.3.1. Aims

The main aim of this study was to extend the methods already applied in the characterization of fibroblast differentiation to the evaluation of eventual functional differences between healthy and asthmatic subjects, taking into account the possible role played by the ECM. More specifically, my hypothesis was that fibroblasts obtained from asthmatic subjects might be more differentiated towards a myofibroblastic lineage and that ECM could affect cell differentiation. In order to test this theory fibroblasts obtained from healthy and asthmatic subjects were evaluated for αSMA expression and the effect of different ECM components was assessed.

3.3.2. Morphological observations: phenotypical differences and αSMA staining.

Primary human bronchial fibroblasts from healthy and asthmatic subjects were plated onto 24 well trays coated with collagen type I (1μg/ml) at $5x10^4$/well and grown until 80% confluence. Cells were then serum starved for 24 hours before

being fixed and stained with a monoclonal anti-αSMA FITC-conjugated antibody as specified in the Methods section. At the end of the staining, phase contrast and fluorescent photographs of the same microscopic fields were taken with a JVC video camera. Phase contrast and fluorescent images were then overlayed using Adobe Photoshop CS2 layers merging function (screen mode).

Figure 3.18 shows that fibroblasts from asthmatic subjects (panel b) displayed a protomyofibroblastic phenotype with evident stress fibers (white arrowheads) and a flat cytoplasm. The αSMA staining (white arrows) confirmed the myofibroblastic nature of most of the asthmatic fibroblasts. Cells obtained from healthy subjects instead resembled morphologically *bona fide* fibroblasts with fewer αSMA-positive cells. Interestingly, in the asthmatic fibroblasts (panel b) is possible to identify cells with stress fibers that are negative for αSMA (white arrowheads).

3.3.3. αSMA expression: flow cytometric analysis.

In order to quantify the differences in terms of αSMA expression between normal and asthmatic fibroblasts, flow cytometric analysis was performed. At the same time the possible role of the ECM was also analysed. Sixteen subjects (8 healthy controls –HC- and 8 asthmatic subjects –AS-) were recruited for this study. Fibroblasts obtained from bronchial biopsies were plated onto 24 well trays, coated with collagen type I, fibronectin, laminin or charged plastic alone at $5x10^4$/well and grown until 80% confluent. Cells were then serum starved for 24 hours before being fixed and stained for the flow cytometric analysis of αSMA expression as detailed in the Methods section. Figure 3.19 shows that on uncoated charged plastic, αSMA expression was significantly increased in the AS group when compared with the HC group (12.1±7.3 vs 40.3± 15.8, p=0.004). With all the ECMs tested the situation was similar albeit with slightly different values of significance (i.e. with laminin p = 0.010). When comparing the effects of the ECM within the same groups it was interesting to note that laminin failed to reach statistical significance in the AS group (plastic vs laminin; . 46±15.9 vs 28.2±15.6, p=0.069). The fibroblasts grown on collagen type I and fibronectin behaved similarly.

Figure 3.18

Morphological appearance of HC and AS fibroblasts

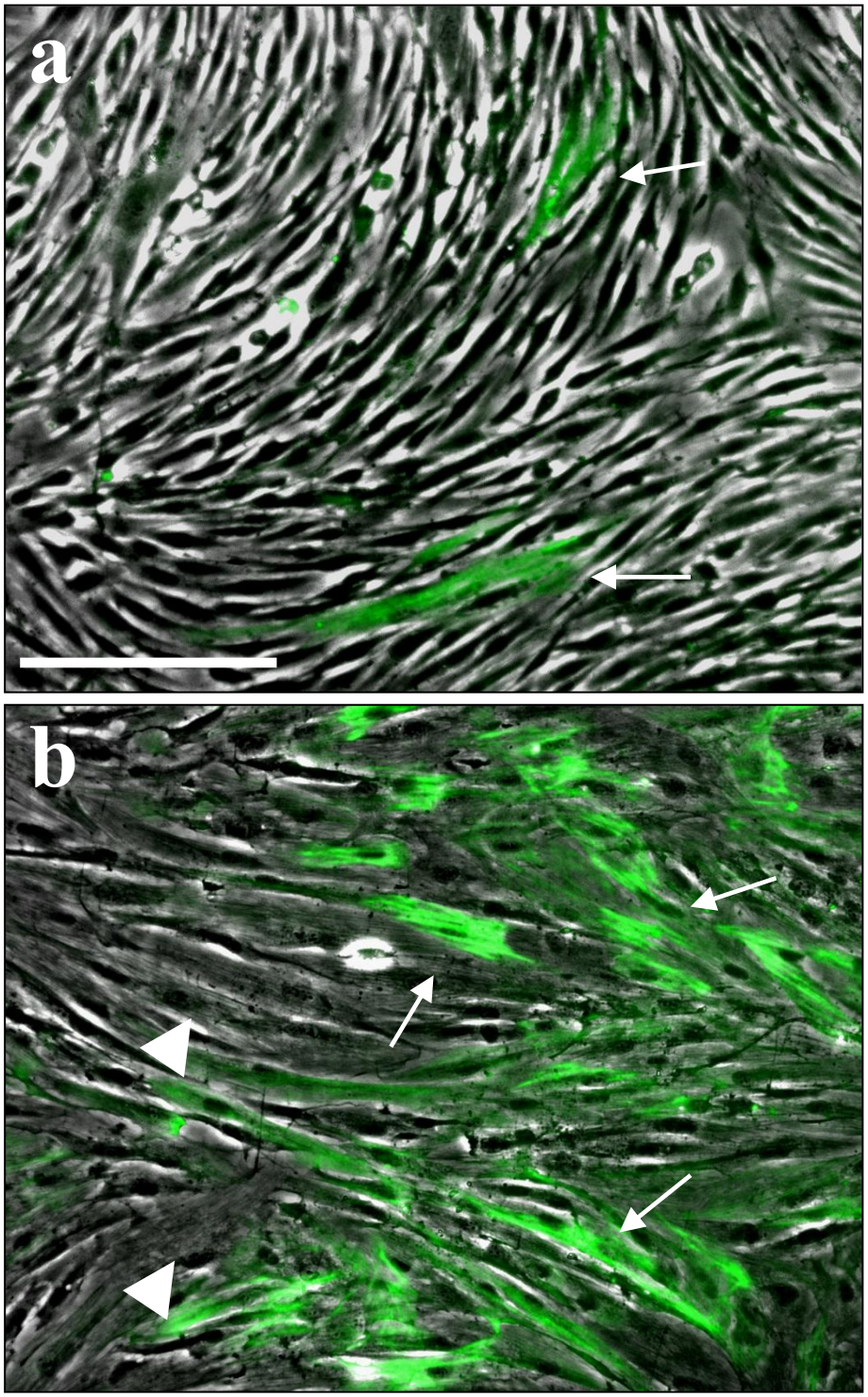

Fibroblasts from HC (a) and AS (b) subjects were fixed and stained with a monoclonal anti-αSMA FITC-conjugated Ab as specified in the Methods section. Phase contrast and fluorescent images were then overlayed. Bar=100 μm. The figure shows that asthmatic fibroblasts displayed a proto-myofibroblastic phenotype with stress fibers (arrowheads) and a flat cytoplasm. The αSMA staining (arrows) confirmed the myofibroblastic nature of most of the asthmatic fibroblasts. Cells obtained from HS instead resembled morphologically *bona fide* fibroblasts with fewer αSMA-positive cells.

Figure 3.19

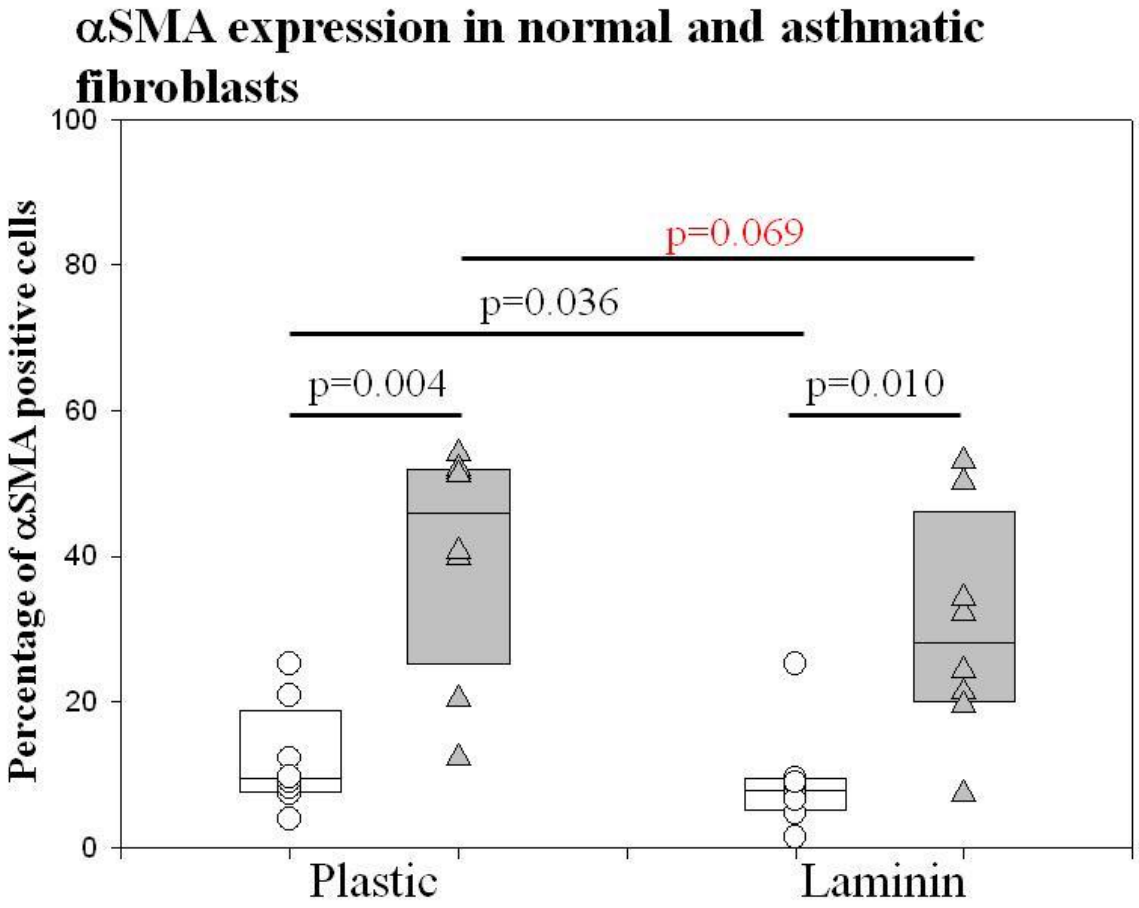

Fibroblasts obtained from 8 HC (white boxes) and 8 AS (grey boxes) were fixed and stained for flow cytometric analysis of αSMA expression as detailed in the Methods section The results are displayed as a box plot showing median, interquartile range and 5-95% confidence intervals from 8 HC (white circles) and 8 AS (greyed triangles). P values are reported above the plots. AS vs HC differences were analysed by Mann Whitney U test, whereas ECM effects within the same group by Wilcoxon Signed Rank tests.
On uncoated plastic, αSMA expression was significantly increased in the AS group when compared with the HC group (9.5+/-7.3 vs 46+/-15.8, p=0.004). With all the ECMs tested the situation was similar albeit with slightly different values of significance (i.e. with laminin p was 0.010).
When comparing the effects of the ECM within the same groups it was interesting to note that laminin failed to reach statistical significance in the AS group.

3.3.4. Conclusions

My results show that primary human bronchial fibroblasts obtained from asthmatic subjects presented a higher number of cells committed to a myo-fibroblastic differentiating lineage when compared with healthy controls. Interestingly, both subclasses of the myofibroblast phenotype, the proto-myofibroblasts and the differentiated myofibroblasts, were present in asthma-derived fibroblasts, whereas the proto-myofibroblasts seemed to be missing from the healthy controls, suggesting that it may be this subclass that is responsible for the high numbers of differentiated myo-fibroblasts found in asthmatic subjects.

Pertinent to asthma, we know that parenchymal fibroblasts release RANTES and eotaxin upon stimulation with TNF-β (Teran et al., 1999). Interestingly, low concentrations of IL-4, but not IFN-γ, synergise with TNF-β to release eotaxin in amounts that far exceed that observed with epithelial cells. These data suggest that Th2 cytokines, in particular IL-4, released in the bronchial tissues in asthma may polarise lung fibroblasts to produce substantial amounts of eotaxin in asthmatic lungs. Lung fibroblasts also express mRNA for other eosinophil activating chemokines, including MCP-3 or MCP-4, upon stimulation with TNF-β (or IL-4 (Teran et al., 1999). Additionally, human lung fibroblasts synthesize IL-6 and MCP-1 upon stimulation with IL-4 or IL-13. MCP-1 expression is increased in asthmatic airways and may be involved in the activation and the recruitment of macrophages and basophils. Finally, fibroblasts are a potential source of GM-CSF and stem cell factor known to promote differentiation, activation and survival of eosinophils and mast cells, respectively. More recently, it has been shown that incubation of human bronchial epithelial cells with TGF-beta1 induces de novo expression of αSMA and increased formation of stress fibers (Zhang et al., 2009). Moreover, bronchial fibroblasts from asthmatic subjects display, *in vitro,* a high potential to differentiate into myofibroblasts (Wicks et al., 2006; Michalik et al., 2009)

In my experiments, ECM did not seem to play a significantrole in fibroblast differentiation with the exclusion of laminin that caused a decrease in the number of myofibroblasts in both normal and asthmatic cells. As stated in the previous chapter, fibroblasts are the main cell type responsible for the production of the ECM and therefore it is plausible that these cells form their own matrix once in culture. This

could explain the absence of any real significant difference with the different ECMs tested.

3.4. RESPONSE OF FIBROBLASTS TO RV16-INFECTED EPITHELIAL CELLS CONDITIONED SUPERNATANTS.

Apart from the immediate pro-inflammatory consequences of infection with RV, it is unclear whether infection also influences the process of airway wall remodelling. For some time, a relationship between severe viral induced bronchiolitis and persistent wheezing in children has been known (Sigurs 2002), but a clear causal link has not been established. However, with RV infection, subjects with asthma do demonstrate evidence of prolonged and increased tissue inflammation compared to normals (Fraenkel et al., 1995). While acute virus-induced exacerbations increase airway inflammation, subjects have persistently lower lung function after this has returned to baseline compared with asthmatics with non-virus triggered exacerbations (Wark et al., 2002). Infection of airway epithelium by rhinovirus (RV) is the most common cause of asthma exacerbations in both children and adults (Lachowicz-Scroggins et al., 2010) leading to increased lower airway inflammation and increased bronchial responsiveness (Wark P et al., 2005). In fact, infection of airway epithelial cells induces the production of a number of mediators involved in inflammatory and immune processes that may exacerbate airway inflammation (Zaheer et al., 2009).

Primary human bronchial epithelial cells (PBECs) exposed to RV show interleukins release as IL8, IL-6, IL1β, of IFN-β, granulocyte macrophage colony – stimulating factor (GM-CSF) , TNFα, RANTES and IP-10 (Wark et al., 2007; Korpi-Steiner et al., 2010). Human RV infection affects the upper and lower airway and induces the release of elevated levels of monocyte chemoattractant protein 1 (MCP-1) after infection (Korpi-Steiner et al., 2010). Previous studies of RV infection of PBECs have shown virus specific induction and release of RANTES or CCL5 (Schroth et al., 1999). RANTES is a chemoattractant for eosinophils recruitment, which may represent a central event in the pathogenesis of virus-induced asthma exacerbations (Papadopoulos et al 2001). RANTES is probably not specific to viral infections, since its expression is dependent on viral replication (Bedke N et al., 2009).

The mediator showing the strongest response to RV-16 infection is interferon gamma-inducible protein 10 (IP-10) (Spurrell et al., 2005). IP-10 is a chemokine ligand with a close link to RV replication, but it is not dependent on prior induction

of type 1 interferons (Spurrell JC 2005). Induction of IP-10 gene expression by RV-16 depended on activation of NF-kB and levels of IP-10 correlated with symptom severity, viral titer as well as with elevated numbers of lymphocytes in airway secretions (Korpi-Steiner et al., 2010). Subjects with virus-induced acute asthma show high levels of IP-10 and IL-10 mRNA expression in sputum correlated to mRNA expression of TLR2 and TLR3, underlining that signalling via TLRs may play an important role in mediating airway inflammation (Wood LG et al 2010). The presence of RV was associated with increased levels of IP-10 in bronchoalveolar lavage (BAL) of patients with serious acute respiratory illness (Sumino KC et al., 2010) and serum IP-10 was proposed as a biomarker of human rhinovirus infection and exacerbation of COPD and asthma (Wark et al., 2007, Quint JK et al., 2010). Moreover, IP-10 may be induced by fragments of the extracellular matrix component hyaluronan utilizing the NF-kB pathway, suggesting the emerging role of airway epithelium as a regulator of local inflammation and immune responses (Boodoo et al., 2006).

In addition to up-regulation of genes related to inflammation, infected PBEC cells of asthmatic subjects reveal a higher expression of genes related to airway repair and remodelling, along with a lower expression of an interferon response gene (*IF144*) and tumor suppressor genes microseminoprotein beta (*MSMB*) (Bochkov et al., 2010).

In vitro studies demonstrate that bronchial fibroblasts are also involved in the response to RV infection by producing transient mRNA for IL-8, IL6 and TNFα and a more sustained production of RANTES gene expression (Bedke et al., 2009). Moreover, fibroblasts, rather than the epithelium, may play a key role in VEGF mediated vascular responses after rhinovirus infection (De Silva et al., 2006).

3.4.1. Aims.

Epithelial mesenchymal signalling plays a critical role during embryonic development. It is also implicated in controlling normal cellular homeostasis in adult tissues and is activated in response to injury. As rhinoviruses (RV) are associated with asthma pathogenesis, I postulated that epithelial infection with RV results in

production of soluble mediators that stimulate inflammatory or remodelling responses in bronchial fibroblasts.

In order to verify this hypothesis, I set up a simple culture model where fibroblasts were exposed to conditioned media obtained by PBEC infected with RV16. Eighteen subjects (6 healthy controls –HC- and 12 asthmatic subjects –AS-) were recruited for this study. Fibroblasts obtained as outgrowths from bronchial biopsies were plated onto 24 well trays, coated with collagen type I, at $5x10^4$/well and grown until 80% confluence. Cells were then serum starved for 24 hours before being treated with conditioned media that were UV irradiated to prevent direct infection of the fibroblasts with RV (CM-RV, diluted 1:4 in Ultraculture). These conditioned media were initially obtained from a single HC donor of PBECs infected with RV-16 at MOI of 2 for 24 hours; non-infected epithelial conditioned medium (CM-SFM, diluted 1:4 in Ultraculture) was used as control. However, in order to verify possible differences in fibroblast responses following exposure to media conditioned from PBEC obtained from either healthy subjects or asthmatic patients, a second set of experiments was designed where conditioned media were obtained by pooling media acquired after infection of six different PBEC cultures obtained from healthy subjects and six from asthmatic subjects. In both sets of experiments, after 24 hours, the conditioned media from the fibroblasts were collected, aliquoted and stored at -80°C until the cytobead array assay while the cells were harvested, lysed and prepared for mRNA analysis. Myofibroblast differentiation was assessed by induction of αSMA, CTGF and COL1A1 gene expression determined by real-time quantitative RT-PCR, while proinflammatory responses were determined using BD cytobead arrays.

3.4.2. αSMA expression: flow cytometry and taqman analysis.

Treatment of fibroblasts, obtained from 6 HC and 6 AS, with conditioned medium from virally infected epithelial cells had no significant effect on induction of αSMA at both mRNA or protein expression level (data not shown). This is surprising, considering that infection of bronchial epithelial cells with RV-16 has

been shown to determine a significant increase in TGF-β_2 mRNA and protein (Dosanij 2006). In fact, considering the potent differentiating effect of TGF-β2 on fibroblasts (Wicks et al., 2006), I was expecting that conditioned media obtained from PBEC after RV-16 infection would cause a significant change in αSMA expression. For this reason, it would be important to evaluate TGF-β2 expression in PBEC conditioned media at both transcriptional and translational levels during future studies.

3.4.3. CTGF and COL1A1 gene expression.

To determine whether conditioned media from virally infected normal and asthmatic epithelial cells could promote an increase of a remodelling response independent from αSMA expression, induction of CTGF and COL1A1 gene expression were determined by real-time quantitative RT-PCR. Figure 3.20 shows that treatment of fibroblasts, both normal and asthmatic, for 24hrs, with conditioned media from virally infected normal or asthmatic epithelial cells had no significant effect on gene expression when compared to baseline levels. Based on these data, we could hypothesise that there was no increase in the number of subepithelial myofibroblasts nor in the deposit of interstitial collagen. This confirmed what was suggested by the αSMA expression data.

3.4.3. Cytokines release: Cytobead arrays

Subsequently, we decided to investigate whether RV-16 conditioned media could cause a change in pro-inflammatory cytokine release by fibroblasts. Eleven chemokines and cytokines, of particular relevance in lung chronic inflammatory diseases, were studied: IP-10, MCP-1, MIG, RANTES, IL12, TNFα, IL10, IL6, IL1β and IL8. The cytobead array procedure is detailed in the Methods section. Figure 3.21 shows a typical example of a FL2 vs FL3 dotplot for a chemokine cytobead array. Figure 3.22 shows a few time-course curves graphs relative to IL-6, IL-8, RANTES and IP-10 levels in RV-16 infected epithelial conditioned media. These

experiments were necessary to evaluate the more appropriate infection time point for the successive experiments on the fibroblasts. Based on these results a 24 hours time point was considered appropriate.

Figure 3.20

Coll1 and cTGF mRNA expression in HC and AS fibroblasts.

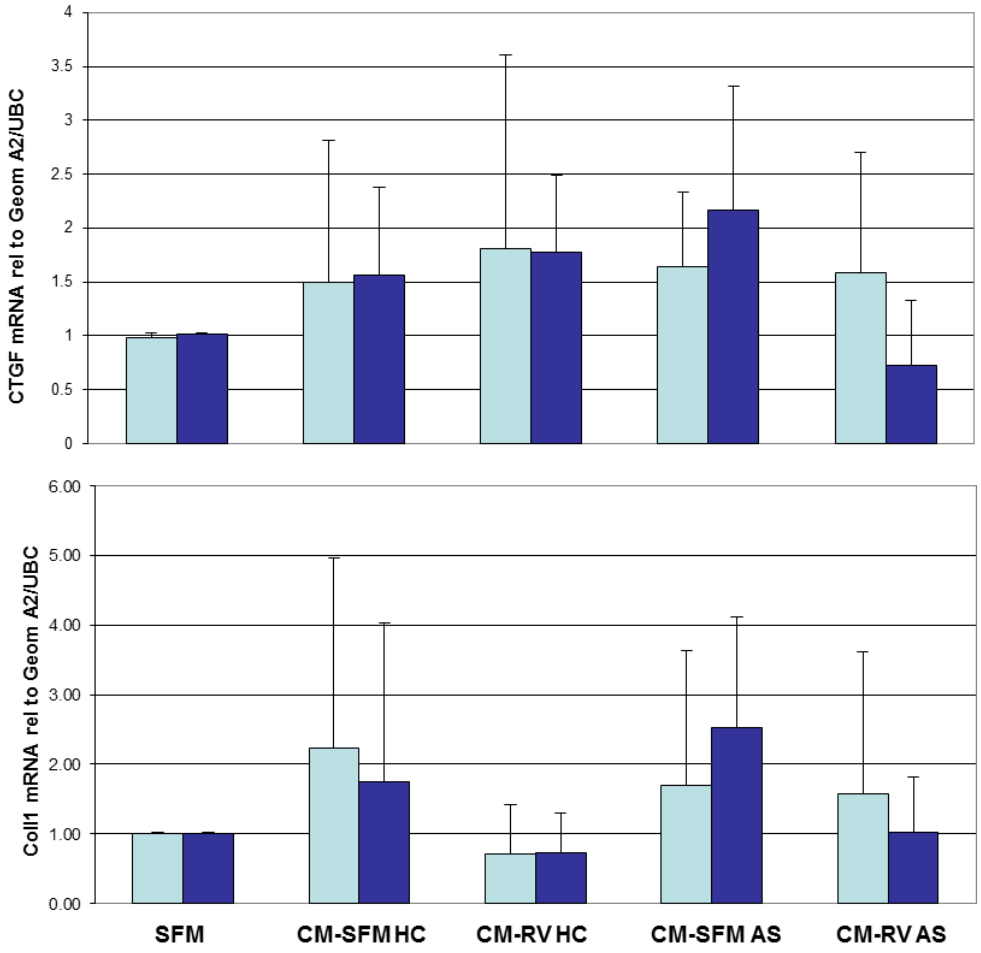

Fibroblasts obtained from 6 healthy controls (HC, light blue boxes) and 12 asthmatic subjects (AS, dark blue boxes) were exposed to conditioned media acquired by PBEC from healthy controls (CM-RV HC) or asthmatic subjects (CM-RV AS) infected with RV-16 at MOI of 2 for 24 hours. Non-infected epithelial conditioned media (CM-SFM HC or AS, diluted 1:4 in Ultraculture) were used as control of the infected conditioned media, whereas SFM represent fibroblasts that were not treated. After 24 hours, fibroblasts were harvested, lysed, and prepped for mRNA analysis. Graphs show CTGF and Coll1 mRNA levels after normalization for ubiquitin C (UBC) and phospholipase A2 (A2) genes and relative quantification performed using the ΔΔCT method . No statistically significant differences were observed.

Figure 3.21

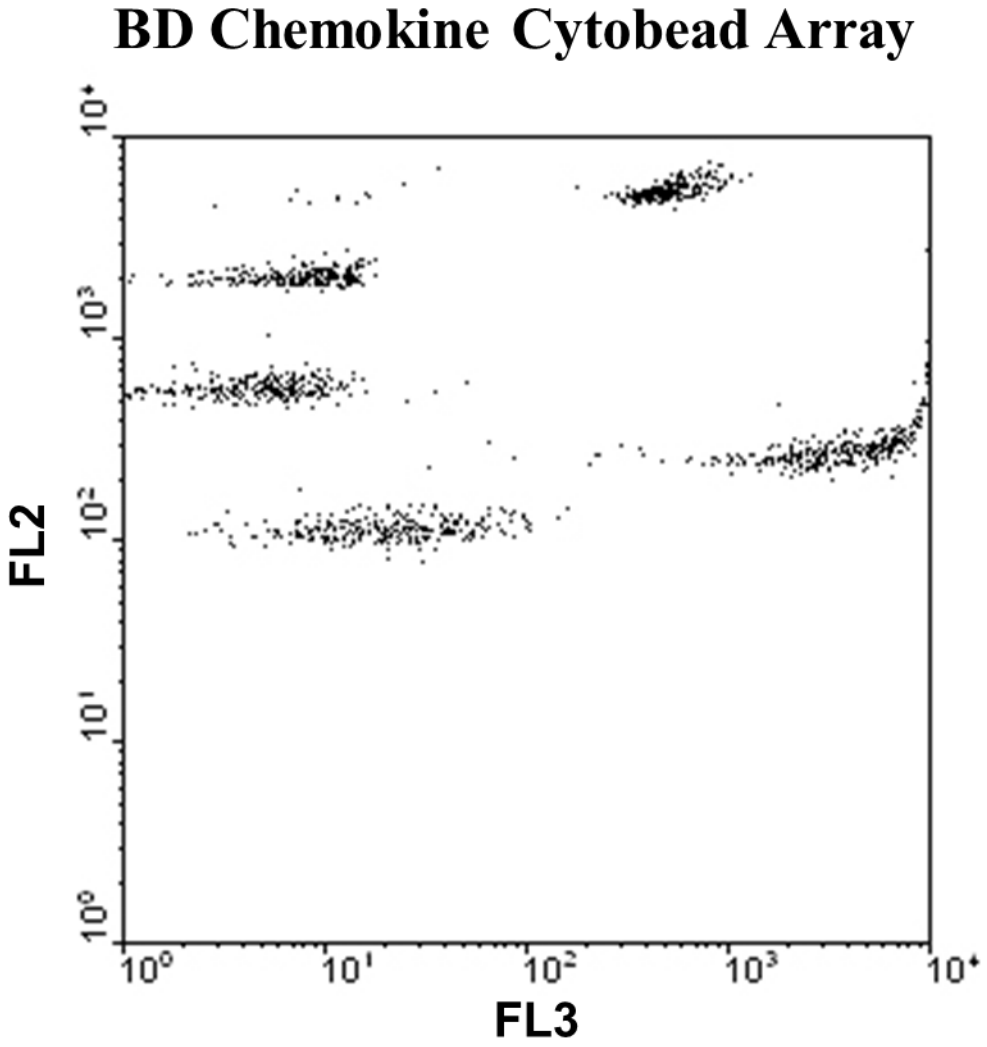

Typical FL2 vs FL3 dotplot showing the distribution of the beads in a chemokine cytobed array.
Each cluster of beads represents a single cytokine or chemokine. The level of MFI in FL3 is directly correlated with the protein amount released in the supernatants.
See Methods section for a more detailed description.

Figure 3.22

Time-course graphs for cytokines release.

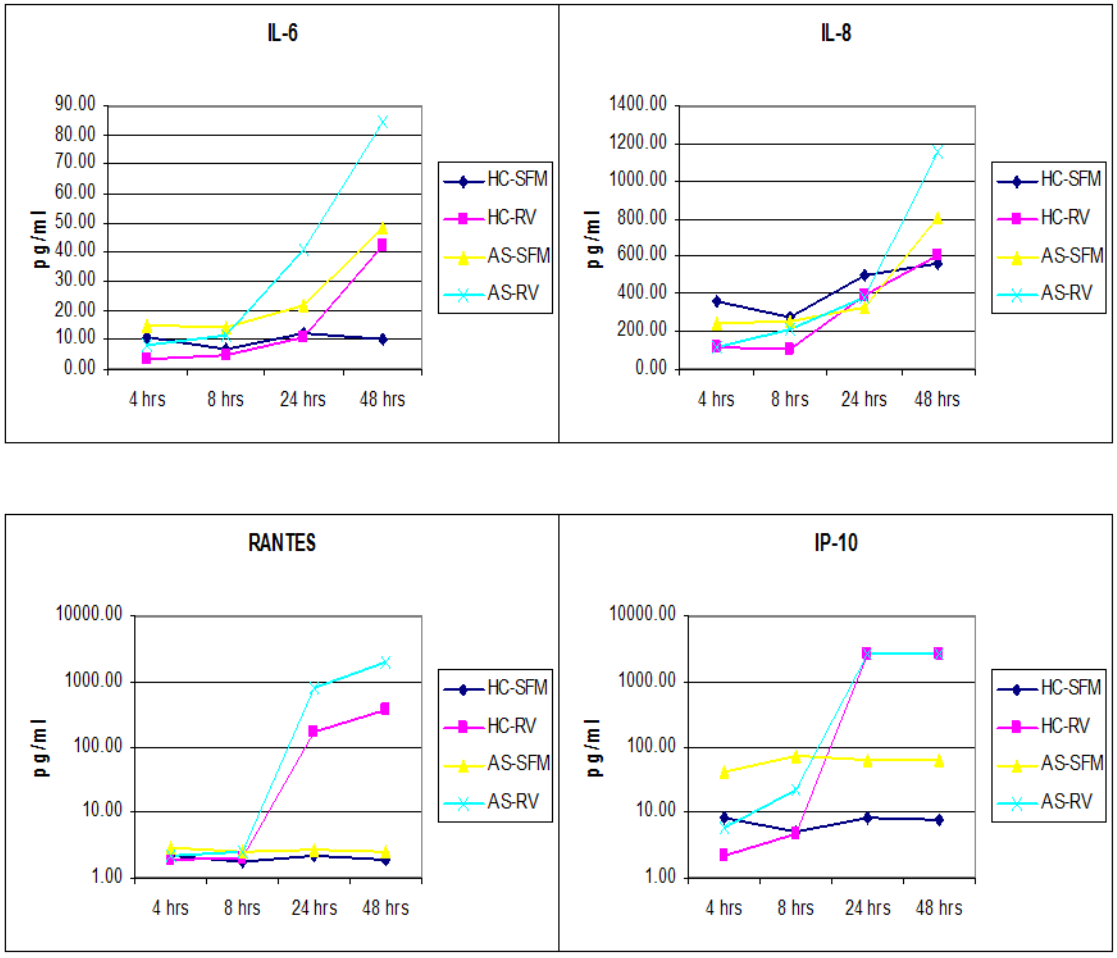

Time-course curves relative to IL-6, IL-8, RANTES and IP-10 levels in RV-16 infected PBEC conditioned media. These experiments were necessary to evaluate the more appropriate infection time point for the successive experiments on the fibroblasts. Based on these results a 24 hours time point was considered appropriate.

3.4.4. Effects of RV16-conditioned media from HC PBEC on cytokines and chemokines release by HC and AS fibroblasts.

Since we wanted to isolate the responses eventually obtained from the many variables possibly arising with the use of PBEC conditioned media obtained from both healthy subjects and asthmatic patients, at first we evaluated only fibroblast responses to conditioned media acquired from a single HC PBEC. This clearly exemplified our experimental setup making it easier to analyse the eventual responses.

Figures 3.23 and 3.24 show that, with this experimental setup, IL6, IL8, RANTES and IP-10 release from fibroblasts was clearly affected by the RV16-conditioned media. In particular, it is possible to notice a more or less striking, but always statistically significant, effect of the CM-RV for all four proteins when compared to both CM-SFM ($p < 0.005$) or SFM alone ($p < 0.05$). Interestingly and expectedly, even CM-SFM alone had a significant effect on both HC and AS fibroblasts when compared to SFM alone, with the exclusion of RANTES.

It was not possible however to detect any statistically significant difference in the responses of HC vs AS fibroblasts, with the exclusion of IP-10 where AS fibroblasts released significantly lower amounts of this protein when treated with either CM-SFM ($p=0.025$) or CM-RV ($p=0.004$) (Fig.3.24). These results are particularly relevant especially in view of the current knowledge base already highlighted in the introduction of this chapter.

We are omitting the results obtained with the other 7 molecules studied because although detected, their levels were not significantly altered either by conditioned media (both SFM or RV) or between the groups.

Figure 3.23

Cytokines release in conditioned media-treated fibroblasts

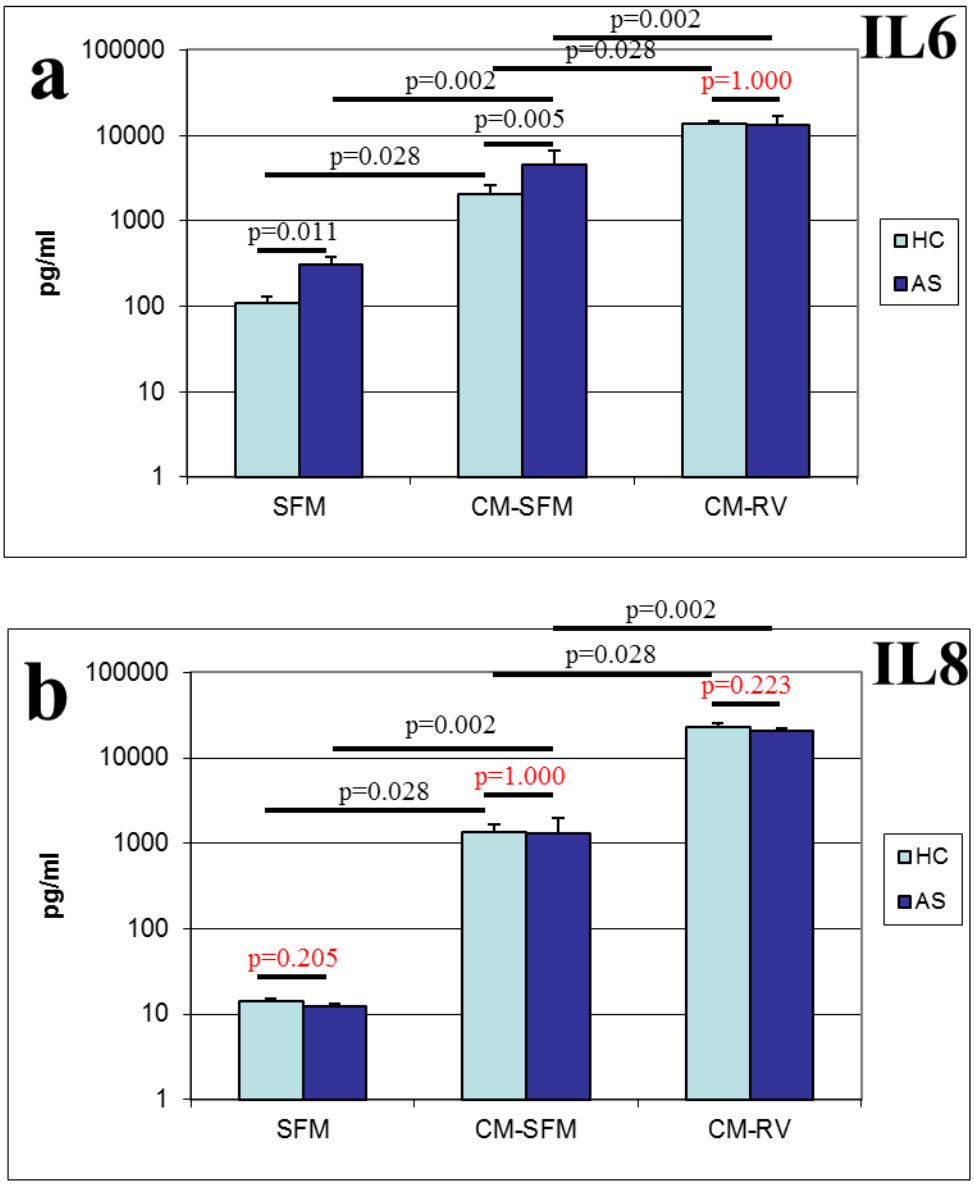

Fibroblasts obtained from 6 healthy controls (HC, light blue boxes) and 12 asthmatic subjects (AS, dark blue boxes) were exposed to conditioned media acquired by PBEC from a single healthy control (CM-RV) infected with RV-16 at MOI of 2 for 24 hours. Non-infected epithelial conditioned media (CM-SFM, diluted 1:4 in Ultraculture) were used as control of the infected conditioned media, whereas SFM represent fibroblasts that were not treated. After 24 hours, fibroblasts growth media were collected and analysed with the cytobead arrays system. Graphs show IL6 and IL8 protein levels (pg/ml) after correction for the relative amount of proteins found in the PBEC conditioned media.

Figure 3.24

Chemokines release in conditioned media-treated fibroblasts

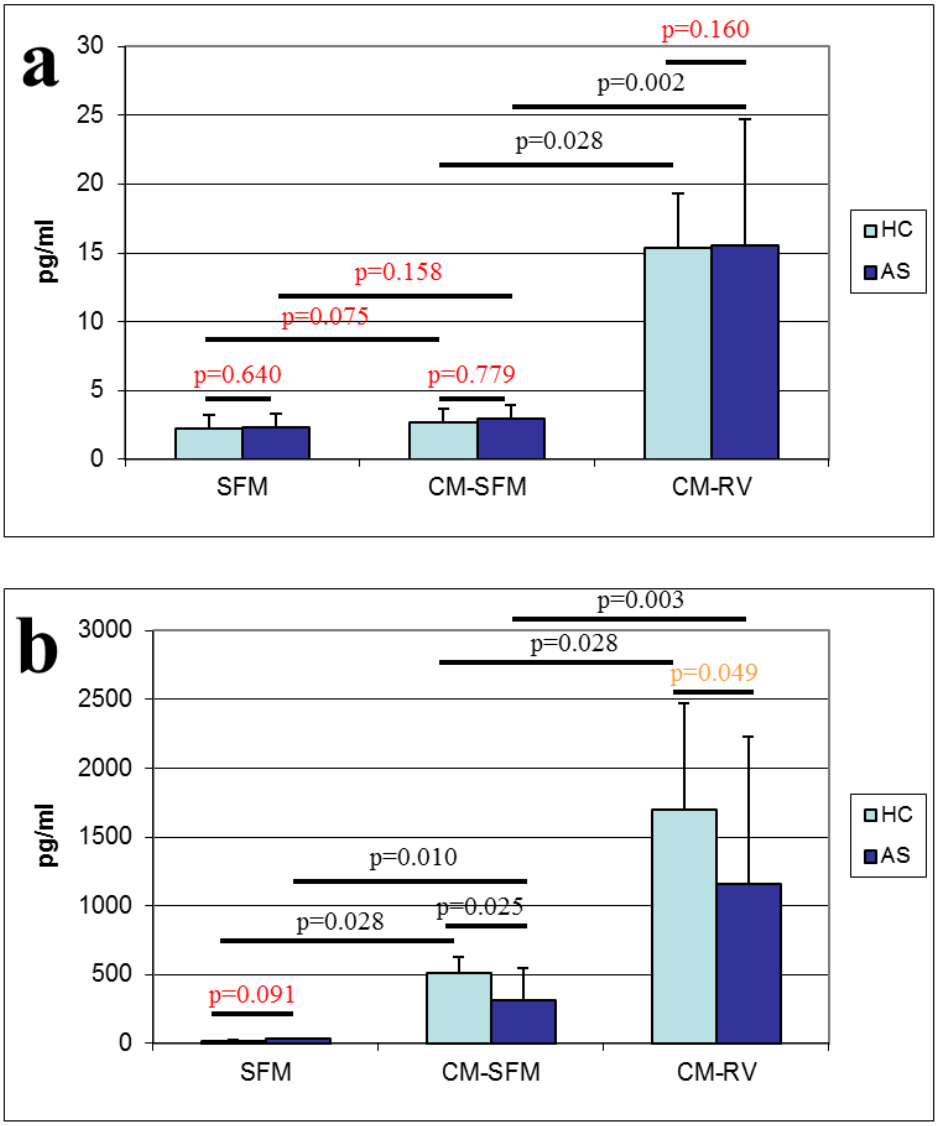

Fibroblasts obtained from 6 healthy controls (HC, light blue boxes) and 12 asthmatic subjects (AS, dark blue boxes) were exposed to conditioned media acquired by PBEC from a single healthy control (CM-RV) infected with RV-16 at MOI of 2 for 24 hours. Non-infected epithelial conditioned media (CM-SFM, diluted 1:4 in Ultraculture) were used as control of the infected conditioned media, whereas SFM represent fibroblasts that were not treated. After 24 hours, fibroblasts growth media were collected and analysed with the cytobead arrays system. Graphs show RANTES and IP-10 protein levels (pg/ml) after normalization for the relative amount of proteins found in the PBEC conditioned media.

3.4.5. Effects of HC and AS PBEC RV16-conditioned media on cytokines release by fibroblasts.

As said earlier, in order to verify possible differences in HC and AS fibroblast responses following exposure to PBEC media conditioned from either healthy controls or asthmatic patients, a second set of experiments was designed where conditioned media were obtained by pooling media acquired after infection of six different PBEC cultures obtained from healthy controls or from asthmatic subjects.

Fig 3.25 shows IL-8 and IL-6 levels in supernatants of HC and AS fibroblasts treated with non-infected (CM-SFM) and RV16-infected (CM-RV) conditioned media obtained from HC and AS PBEC. The concentrations in pg/ml of mediators released by fibroblasts after conditioned media treatments (CM-SFM and CM-RV) are corrected for the level of mediators present in the PBEC-conditioned media.

IL-8 release was significantly increased in healthy and asthmatic fibroblasts treated with either CM-RV or CM-SFM from HC or AS PBEC when compared to their respective SFM controls. Moreover, CM-RV treatment resulted in a statistically significant increase of IL8 release when compared to CM-SFM in all studied conditions. However, no significant differences were observed using CM-RV or CM-SFM obtained from HC PBEC or AS PBEC, with the only exception that CM-SFM induced release of IL8 in HC fibroblasts was significantly lower than CM-SFM from AS donors. Finally, it is important to notice that the amount of IL8 released by both HC and AS fibroblasts following CM-RV treatment was greatly increased compared to what was released in the CM-RV by the PBEC (around 20000 pg/ml vs 3000 pg/ml).

IL6 release followed a somewhat similar pattern to what described for IL8, albeit the overall levels were significantly lower (Fig. 3.25). Moreover, IL6 release from both HC and AS fibroblasts following CM-SFM and CM-RV stimulation was significantly higher in conditioned media obtained from AS PBEC.

Release of the other cytokines (IL12, TNFα, IL10, IL6 and IL1β) was not significantly modified in all the studied conditions.

Figure 3.25
IL8 and IL6 release in conditioned media-treated fibroblasts

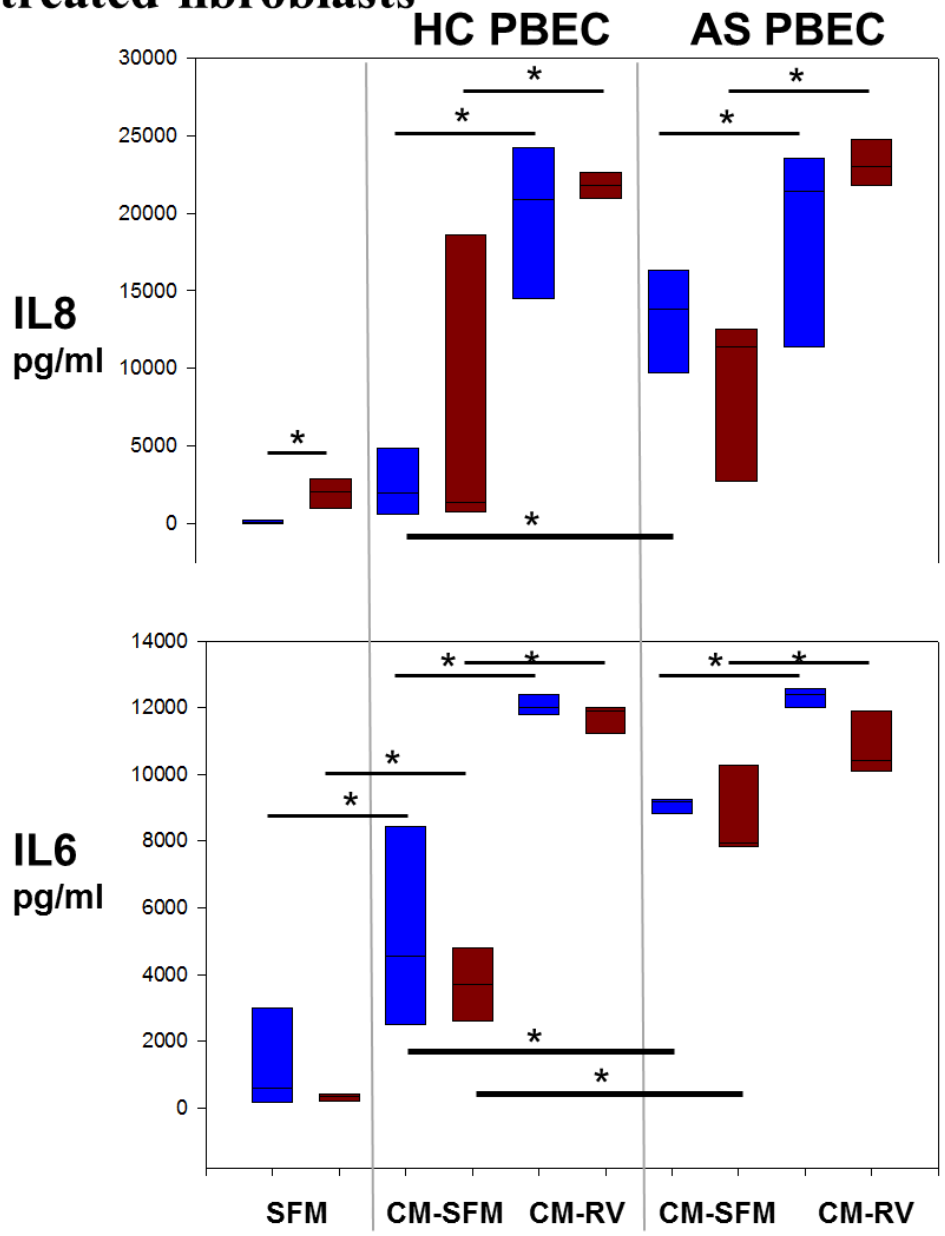

Fibroblasts obtained from 6 healthy controls (blue boxes) and 6 asthmatic subjects (brown boxes) were exposed to conditioned media acquired by either HC PBEC or AS PBEC infected with RV-16 at MOI of 2 for 24 hours (CM-RV). Non-infected epithelial conditioned media (CM-SFM, diluted 1:4 in Ultraculture) were used as control of the infected conditioned media, whereas SFM represent fibroblasts that were untreated. After 24 hours, fibroblasts growth media were collected and analysed with the cytobead arrays system. Graphs show IL8and IL6 protein levels (pg/ml) after correction for the relative amount of proteins found in the PBEC conditioned media. * = $p<0.05$.

3.4.6. Effects of HC and AS PBEC RV16-conditioned media on chemokines release by fibroblasts.

The chemokines that we studied were IP-10, RANTES, MCP-1 and MIG. Only the first two however showed significant results. Figure 3.26 shows release of RANTES and IP-10 by HC and AS fibroblasts untreated, treated with CM-SFM or CM-RV obtained from HC or AS PBEC. The concentrations in pg/ml of mediators released by fibroblasts after conditioned media treatments (CM-SFM and CM-RV) were corrected for the level of mediators present in the PBEC-conditioned media.

Overall RANTES release from fibroblasts was much more contained than what was previously observed with IL8 or IL6, with a maximum peak observed in AS PBEC CM-RV treated HC fibroblasts ranging around 50 pg/ml. In HC and AS fibroblasts, RANTES levels after treatment with either HC or AS PBEC CM-RV were significantly increased ($p<0.05$) when compared to either HC or AS PBEC CM-SFM or baseline conditions (fig. 3.26). Interestingly, it was possible to observe a statistically significant increase of RANTES release with AS PBEC conditioned media (both CM-SFM and CM-RV) in both HC and AS bronchial fibroblasts.

Also IP-10 release by both HC and AS fibroblasts was significantly ($p<0.05$) triggered by RV16 conditioned media. However, it was not possible to demonstrate a significant difference in the production of this protein by RV16 conditioned media obtained by AS PBEC compared to HC PBEC (Fig. 3.26).

Finally, both RANTES and IP-10 release was not significantly altered in AS fibroblasts compared to HC fibroblasts.

Figure 3.26
RANTES and IP-10 release in conditioned media-treated fibroblasts.

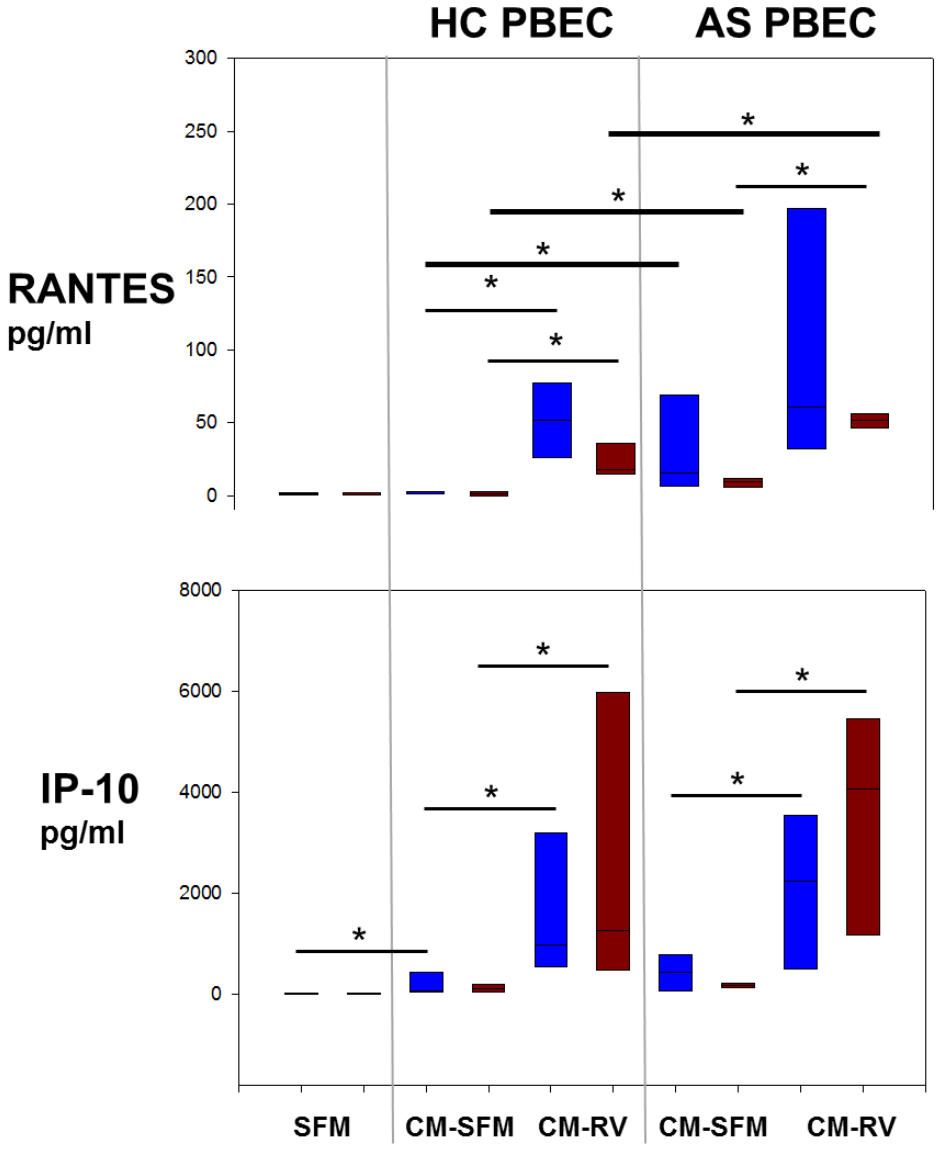

Fibroblasts obtained from 6 healthy controls (blue boxes) and 6 asthmatic subjects (brown boxes) were exposed to conditioned media acquired by either HC PBEC or AS PBEC infected with RV-16 at MOI of 2 for 24 hours (CM-RV). Non-infected epithelial conditioned media (CM-SFM, diluted 1:4 in Ultraculture) were used as control of the infected conditioned media, whereas SFM represent fibroblasts that were untreated. After 24 hours, fibroblasts growth media were collected and analysed with the cytobead arrays system. Graphs show RANTES and IIP-10 protein levels (pg/ml) after correction for the relative amount of proteins found in the PBEC conditioned media. * = $p<0.05$.

3.4.7. Conclusions.

RV infections play, without any doubt, a fundamental role in acute exacerbations of asthma and possibly in the development of the disease. Surprisingly however, there are little to none available data in the literature about a possible direct effect of viral infection on airway remodelling.

My results show that conditioned media obtained from virally infected PBEC failed to induce cell differentiation (assessed by induction of αSMA, CTGF and COL1A1 gene expression) in fibroblasts that were obtained from both healthy and asthmatic subjects. This appears to be in contrast with results obtained by other researchers. In particular, in 2011, Kuo and colleagues showed that RV has the potential, both *in vivo* and *in vitro*, to contribute to remodelling of the airways through induction of ECM deposition. In particular, the authors reported an increase in fibronectin, collagen I and VEGF gene expression after infection of BALB/c mice with RV-1b. Moreover, infection of primary fibroblasts with RV-16 increased perlecan, collagen V and VEGF deposition. RV infection did not affect fibronectin, collagen I or IV chondroitin sulphate, tenascin, versican or elastin (Kuo et al., 2011). In this experimental setup, however, RV infection was administered directly on fibroblasts. Whether *in vivo* this occurs still remains to be proven. However, fibroblasts will however certainly be exposed to a plethora of cytokines, chemokines and growth factors released by the HBEC following infection with RV. As described better above, in my experimental model, fibroblasts were not directly infected with RV16, but they were exposed to UV-irradiated conditioned media obtained from PBEC infected with the virus. A model this that I feel closer to what occurs *in vivo*.

My data suggest that epithelial infection with RV16 results in a marked amplification of the epithelial inflammatory response by the underlying fibroblasts. In particular, IL-8 and IL6 release was significantly increased in healthy and asthmatic fibroblasts treated with either CM-RV or CM-SFM from HC or AS PBEC when compared to their respective SFM controls. Moreover, CM-RV treatment resulted in a statistically significant increase of IL8 and IL6 release when compared to CM-SFM in all studied conditions. The amounts of IL8 and IL6 released by both HC and AS fibroblasts following CM-RV treatment were greatly increased compared to what was released in the CM-RV by the PBEC. Moreover, IL6 release from both

HC and AS fibroblasts following CM-SFM and CM-RV stimulation was significantly higher in conditioned media obtained from AS PBEC. In HC and AS fibroblasts, RANTES levels after treatment with either HC or AS PBEC CM-RV were significantly increased when compared to either HC or AS PBEC CM-SFM or baseline conditions. It was also possible to observe a statistically significant increase of RANTES release with AS PBEC conditioned media (both CM-SFM and CM-RV) in both HC and AS bronchial fibroblasts. Also IP-10 release by both HC and AS fibroblasts was significantly triggered by RV16 conditioned media. However, it was not possible to demonstrate a significant difference in the production of this protein by RV16 conditioned media obtained by AS PBEC compared to HC PBEC.

Very few data are present in the current scientific literature about the modulation of inflammatory response in lung fibroblasts following respiratory virus infection. However a recent article by Val Ly and colleagues has demonstrated that RV-16 infection of primary human lung fibroblasts determines induction of IL8 and IL6 proteins (assessed by ELISA) that is decreased by a concurrent treatment with dexamethasone and fluticasone (Val Ly et al, 2011).

Based on the results I obtained with this particular culture model, it seems likely that any remodelling responses occurring following RV infection arise as a secondary consequence of chronic inflammation rather than a direct effect of epithelial mediators on fibroblast differentiation. However, I have to point out that in order to have a better overall picture of these mechanisms, further studies assessing the composition of the conditioned media obtained from the virally infected PBEC are needed. In particular, these studies should involve assaying the conditioned media for known fibroblast differentiating agents, such as TGF-β2.

4. RESULTS - RESPONSES OF NORMAL AND ASTHMATIC EPITHELIAL CELLS TO OXIDATIVE STRESS.

4.1. ENVIROMENTAL STRESS AND EPITHELIAL SURVIVAL.

4.1.1. Role of oxidants in epithelial cell death.

A number of studies have indicated roles for reactive oxygen (ROS) and reactive nitrogen (RNS) species in the pathology of asthma both in terms of increased burden and decreased antioxidant defenses (Morcillo et al., 1999; Andreadis et al., 2003; Sugiura et al., 2008). A direct or a lipid peroxidation-induced increase in ROS levels could have an enhancing effect on the inflammatory response in subjects with asthma and chronic obstructive pulmonary disease (COPD) (Kirkham et al., 2006). A long-standing increase in ROS and gaseous molecule nitric oxide (NO) levels has been shown to cause RNS formation and subsequent oxidation and nitration of proteins, possibly leading to alterations in protein functions pertinent to airway injury and inflammation (Andreadis et al., 2003).

Airway responses have been shown to correlate with oxidant generation by eosinophils after antigen challenge *in vivo* (Sedgwick et al., 1992), and neutrophil superoxide generation correlates with BHR (Postma et al., 1988). In 2001, MacPherson and his group, using gas chromatography-mass spectrometry, demonstrated a 10-fold increase in 3-nitrotyrosine (3-nt) content, a marker of protein modification by RNS, in proteins recovered from bronchoalveolar lavage of severely asthmatic patients compared with non-asthmatic subjects. Moreover, anti-3-nt immunostaining was shown to colocalize with eosinophils in bronchial tissue from individuals who died of asthma (MacPherson et al., 2001).

Airway lining fluid from subjects with asthma has a lower antioxidant capacity than fluid from normal subjects (Kelly et al., 1999; Gumral et al., 2009), and

intracellular Cu,Zn superoxide dismutase (Cu,Zn-SOD) activity is decreased in asthma, but could be normalized upon corticosteroid treatment (De Raeve et al., 1997). Asthmatic individuals also display a reduction in the antioxidant enzymes that represent a fundamental first-line defense mechanism against free radicals; these include superoxide dismutases (SOD) and catalase, with lowest levels found in patients with the most severe degrees of asthma (Comhair and Erzurum, 2010). A reduced SOD activity was reported in brushed bronchial epithelial cells from patients with asthma; this occurrence was shown to strongly correlate with BHR (Smith et al., 1997; Siedlinski et al., 2009).

Although these studies have demonstrated altered oxidant defenses in asthma, most of these appear to be a consequence of the inflammatory process. While it has been hypothesized that inflammatory products could cause tissue injury and cytokine release in asthma, leading to a self-perpetuating cycle of injury and inflammation, it is unclear exactly how the kind of microenvironment necessary for establishing and maintaining the optimal conditions for persistent inflammation is created, or why are subjects with asthma particularly sensitive to inhaled environmental stimuli.

Epidemiologic studies have demonstrated important links between air pollutants, such as diesel exhaust particles (DEP), O_3, and environmental tobacco smoke (ETS), in asthma pathogenesis and exacerbation (Hiltermann et al., 1998; Bergren et al., 2009; Aubier et al., 2009; Sinclair et al., 2010); and others have shown a strong link between diets low in antioxidants and asthma (Hatch et al., 1995; Wood and Gibson, 2010). In contrast, in one of my previous studies (Bucchieri et al., 2002), PBEC were taken through several generations *in vitro* to allow recovery from any changes that had occurred *in vivo* as consequence of airway inflammation. When tested for sensitivity to oxidants, asthmatic bronchial epithelial cells had a higher susceptibility to oxidant injury suggesting a different underlying cause from those suggested by the other studies. The sensitivity of asthmatic epithelial cells to oxidant-induced apoptosis may be a key triggering mechanism that facilitates the induction and establishment of chronic inflammatory responses. Collectively, these observations could account for the involvement of environmental pollutants in asthma exacerbations and provide clues to understanding the rising trend in asthma observed over the last few decades.

4.1.2. Cigarette smoke and airways inflammation.

The principal sources of oxidants in the bronchial airways are represented by cigarette smoke, environmental pollution and local inflammation; exposure to cigarette smoke (CS) is certainly one of the primary stimuli of airway inflammation (Wood et al., 2010).

Exposure to cigarette smoke (CS) represents a considerable oxidant burden on the respiratory epithelium, which is the first line of defense to inhaled substances. CS, which is one of the most important indoor air pollutants, is a complex mixture of over 4,000 different compounds, and high levels of oxidants and ROS have been detected in both mainstream and sidestream smoke (Faux et al., 2009). It has been estimated that there are 1014 free radicals in each puff of cigarette smoke (Rahman et al., 1996).

A high toxicity has been observed for at least 52 components of CS: 18 phenols, 14 aldehydes, eight *N*-heterocyclics, seven alcohols, and five hydrocarbons (Curvall et al., 1984). Most of these compounds are capable of generating ROS during their metabolism. Thus, the mechanism of cigarette smoke toxicity is thought to incorporate oxidative stress, which mediates cell death via necrosis and apoptosis, due to the fact that cigarette smoke has been shown to cause oxidative DNA damage and cell death (Stone et al., 1994).

Some lipophilic components of CS can enter airway epithelial cells increasing intracellular ROS production by disturbing mitochondrial activity (Van der Toorn et al., 2009). The oxidative damage to cellular components occurs when The increase in ROS production causes oxidative damage in cellular components by overwhelming their antioxidant defense mechanisms; the presence of apoptosis confirms that this causes damage to DNA, nuclear DNA being one of the targets of ROS (Howard et al., 1998). However, CS-mediated DNA damage can result in uncontrolled cell proliferation and transformation (Faux et al., 2009), if the cells fail to undergo apoptosis. CS also facilitates allergen penetration across respiratory epithelium (Gangi et al., 2009) and is a potent source of oxidative stress, DNA damage and apoptosis in alveolar epithelial cells by the upregulation of Fas/APO-1 receptor and activation of caspase-3 (Jiao et al., 2006). Moreover, CS is considered a major risk factor for chronic obstructive pulmonary disease (COPD) development as

demonstrated in animal models (Wright and Churg, 2010) and it is also considered an important player in the pathogenesis of asthma as a trigger for acute symptoms, modifying inflammation that is associated with this pathology (Hellermann et al., 2002; Hu et al., 2008). Furthermore, smoking is common in asthmatic patients and it has been found to contribute to poor symptom control (Spears et al., 2010).

The link between CS and lung inflammation is therefore quite strong; however, relatively little is still known on the effects of CS on human bronchial epithelial cell survival.

4.1.3. AIMS

In view of the scarcity of studies examining the effects of CS exposure on human bronchial epithelial cell survival, the current study was designed to address this particular issue. Since epithelial survival is also affected by the ECM, and one of the limitations of my previous work was that the PBEC were grown on plastic, I have also re-evaluated the effects of oxidants and cigarette smoke extract (CSE) on epithelial cell death when cultured on different ECM components such as collagen type I, collagen type IV, laminin and fibronectin.

More specifically, my hypotheses are:

- CS induces apoptosis in PBEC through its oxidative components.

- PBECs from asthmatic donors are more susceptible to the effects of CSE.

- Antioxidants protect epithelial cells from oxidants- and CSE-induced apoptosis.

- ECM can modify survival of PBEC cells.

In order to test these hypotheses, PBEC were exposed to CSE and hydrogen peroxide in the presence or absence of antioxidants and cell survival was evaluated with the Annexin-V assay. Apoptotic mechanisms were analysed by using specific inhibitors of caspases and AIF staining.

4.1.4. Morphological observations: effects of H_2O_2 and CSE on PBEC morphology.

PBEC were plated onto 24 well trays at $5x10^4$/well and grown until 80% confluent. Cells were then serum starved for 24 hours before being treated with 400μM H_2O_2 or 20% (v/v) CSE. After 0 and 24 hours phase contrast photographs of the cells were taken with a JVC video camera.

Figure 4.1 shows that after 24 hours of treatment with H_2O_2 (b) or CSE (c), PBEC showed many characteristic signs of necrotic and apoptotic cell death. Cells display a shrunken cytoplasm with fragmented nuclei (apoptosis) or a swollen cytoplasm with enlarged nuclei (necrosis).

Figure 4.1

Morphological appearance of PBEC after 24 hrs of treatment

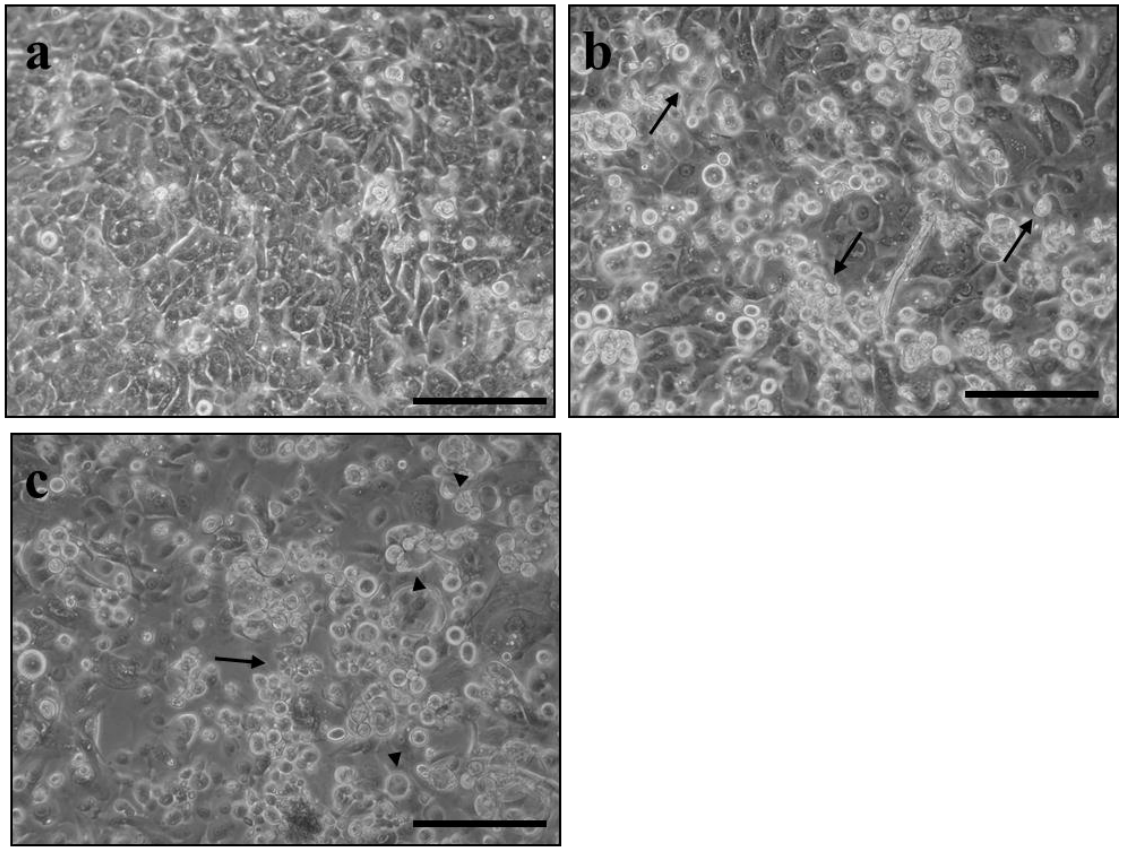

PBEC were serum starved for 24 hrs before being treated with serum free medium (a), H_2O_2 400mM (b) or CSE 20% (c) for a further 24 hrs. Arrows indicate condensed apoptotic cells; arrowheads swollen necrotic cells; bar = 100μm.

4.1.5. Evaluation of cell death: normal vs asthma differences with oxidants treatment.

Twenty subjects (10 healthy controls (HC) and 10 asthmatic subjects (AS) were recruited for this study (Table 4.1). PBEC were grown from bronchial brushings obtained by bronchoscopy and were plated onto 24 well trays, coated with collagen type I, at $5x10^4$/well and grown until 80% confluent. Cells were then serum starved for 24 hours before being treated with 400μM H_2O_2 for a further 24 hours. This dose of H_2O_2 was chosen as the most effective, based on previous dose-response curves (Bucchieri et al., 2002). Adherent cells were then harvested with trypsin/EDTA in Ca^{2+} and $Mg2^{+}$-free Hanks' balanced salt solution and combined with non-adherent cells for annexin-V FACS analysis. Basal levels of viability were similar amongst the two groups (Figure 4.2a) and there was no statistically significant difference between the groups. The same applied for the levels of EA (Figure 4.2b). Treatment with 400μM H_2O_2 induced a significant decrease in viability in both groups (p=0.011 for HS and p=0.008 for AS, N=10) (Figure 3.2a) that was accompanied by a parallel increase in the number of early apoptotic cells (p=0.015 for HC and p=0.011 for AS, N=10) (Figure 4.2b). There was no statistically significant difference between HC and AS. This was unexpected and in apparent contrast with what I had already published in 2002 with the same cell model. However, the experimental setup in 2002 was different because culture plastics had not been coated with collagen. It could therefore be hypothesized that when PBEC are plated on uncoated plastic they are more sensitive to cell death induction due to loss of the hemidesmosomal structures that will normally anchor them to their basement membrane, similarly to what happens to keratinocytes in pemphigoid disease or in lichen planopilaris (Al-Refu and Goodfield, 2009). Experiments performed subsequently and presented later in this chapter (paragraph 4.2; figure 4.12) seem to confirm this hypothesis.

Table 4.1 Clinical characteristics of volunteers.

10 subjects with moderately severe asthma and 10 healthy controls were recruited.

Subject characteristics

	Asthma	Normal	P values
Number	10	10	NA
Sex (% male)	69%	60%	P=0.6
Mean age (range)	32 (21-58)	29 (24-38)	P=0.4
Mean FEV1% predicted (SD)	77.3 (15.5)	110.3 (13.6)	P< 0.001

Subjects with asthma had mild to moderate disease, the majority (8/10) were on inhaled corticosteroids (ICS) and had relatively preserved lung function.

Characteristics of subjects with asthma

	Mild intermittent	Mild persistent	Moderate persistent
Number	2	5	3
Inhaled steroids (yes)	0	4 (80%)	3 (100%)
Mean (sd) Dose ICS BDP/day		300 (115)	617 (256)
Mean (sd) FEV1 % predicted	92.4 (6.2)	86.9 (6.6)	77.7 (17.9)

Values for FEV1 as a percentage of the predicted FEV1 are given as a mean and standard deviation of the mean. Inhaled corticosteroid dose is given as amount of beclomethasone (BDP) used per day, expressed as the mean and sd.

Figure 4.2

a **Cell viability 24hrs after treatment with H_2O_2 400µM**

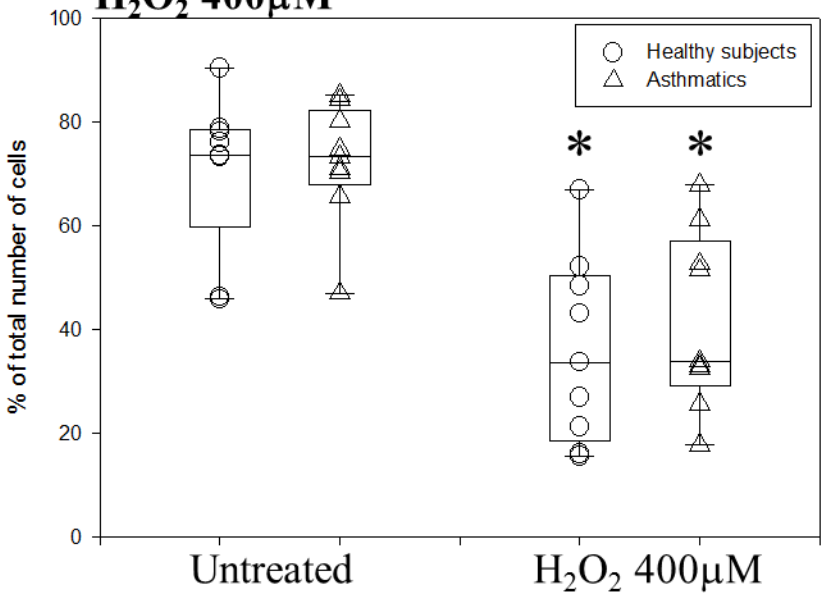

b **Early apoptosis levels 24hrs after treatment with H_2O_2 400µM**

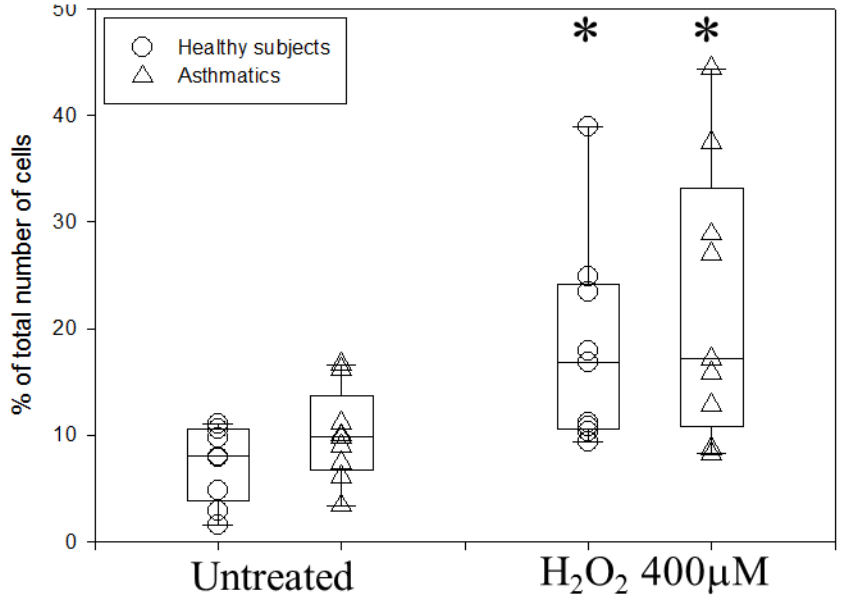

PBEC obtained from healthy controls (HC) and asthmatic subjects (AS) were treated for 24hrs with H_2O_2 400µM. Cell viability (a) and early apoptosis (b) were then evaluated with AnnexinV staining. The results are displayed as a box plot showing median, interquartile range and 5-95% confidence intervals from 10 HC (circles) and 10 AS (triangles).

* represents significance ($p<0.02$) according to Wilcoxon Signed Rank tests comparing treatment with untreated control. There was no statistical difference in both a and b comparing H_2O_2 treatment between HS and AS according to a Mann Whitney U test.

4.1.6. Evaluation of cell death: dose response curve of the effects of CSE on PBEC survival.

PBEC obtained from 8 subjects (4 HC and 4 AS) were plated onto 24 well trays, coated with collagen type I, at $5x10^4$/well and grown until 80% confluent. Cells were then serum starved for 24 hours before being treated with different concentrations of CSE (0-30%) for 24 hrs. Adherent cells were then harvested with trypsin/EDTA in Ca^{2+} and Mg^{2+}-free Hanks' balanced salt solution and combined with non-adherent cells for annexin-V FACS analysis. The graph in figure 4.3 shows a dose-response curve for this treatment. A 20% dose of CSE was selected for the following experiments because it caused a significant increase in early apoptosis without causing too many cells to become necrotic.

4.1.7. Evaluation of cell death: normal vs asthma differences with CSE treatment.

Twenty subjects (10 HC and 10 AS) were recruited for this study (table 4.1). PBEC obtained following bronchoscopic procedure were plated onto 24 well trays, coated with collagen type I, at $5x10^4$/well and grown until 80% confluent. Cells were then serum starved for 24 hours before being treated with 20% CSE for other 24 hours. Adherent cells were then harvested with trypsin/EDTA and combined with non-adherent cells for annexin-V FACS analysis.

As shown in figure 4.4a, there was no significant difference in basal viability between AS and HC. After treatment with 20% CSE, there was a decrease in viability however PBEC from asthmatic donors were more susceptible to the CSE treatment than PBECs from healthy controls (24.3±9.6 *vs* 48.5±11.9 % viable, $p=0.003$). Similarly, when EA was taken into consideration (Figure 4.4b), there was a significant increase of EA cells in the CSE treated AS group compared to the CSE treated HS group (33.1±10.4 *vs* 16.7±6.9 $p<0.05$).

Figure 4.3

Dose-response curve for CSE treatment

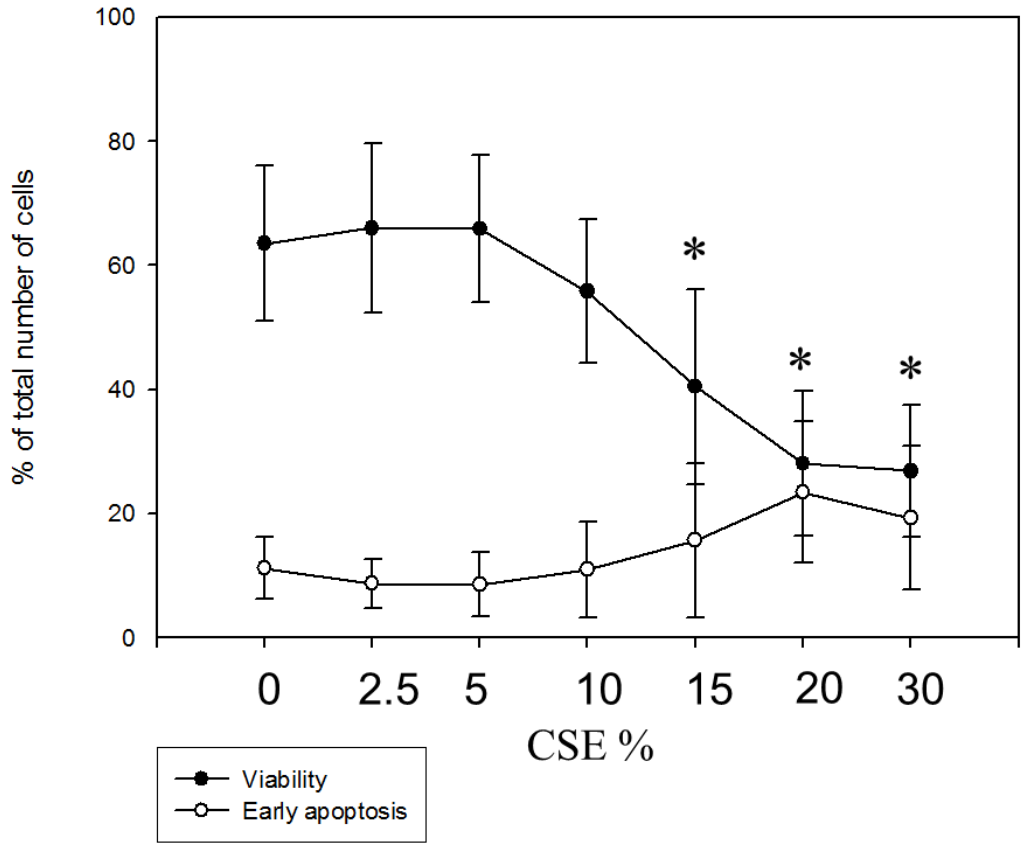

PBEC obtained from 4 HC and 4 AS were treated with increasing doses of CSE for 24 hrs. Viability and early apoptosis were then assessed with AnnexinV staining. The single curve points represent median +/- SD in all 8 subjects for both viability (black circles) and early apoptosis (white circles) levels.

* represents significance ($p<0.05$) according to Wilcoxon Signed Rank test comparing CSE treatment with untreated control (0).

CSE 20% was chosen because it was the first dose to induce significant changes in EA levels.

Figure 4.4

a **Cell viability 24hrs after treatment with CSE 20%**

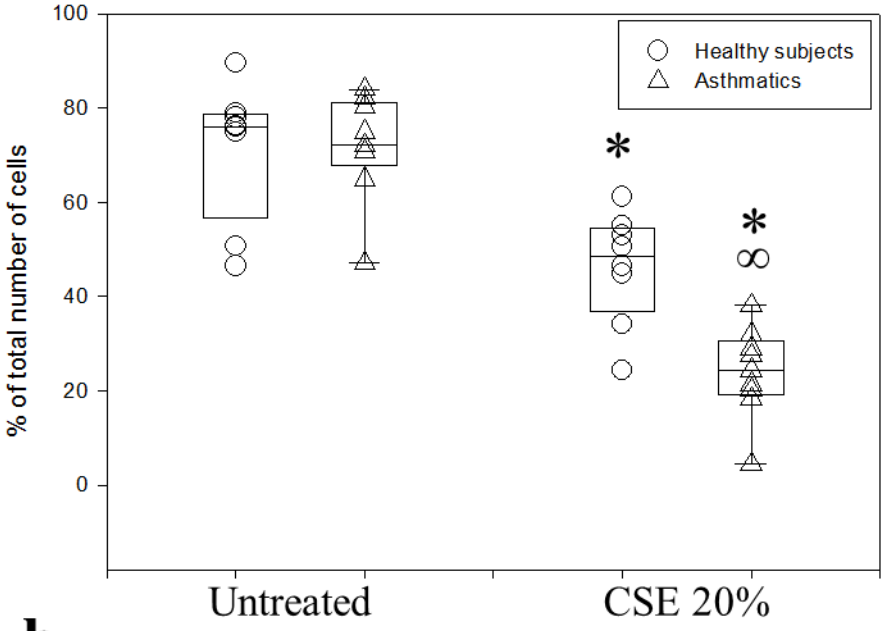

b **Early apoptosis levels 24hrs after treatment with CSE 20%**

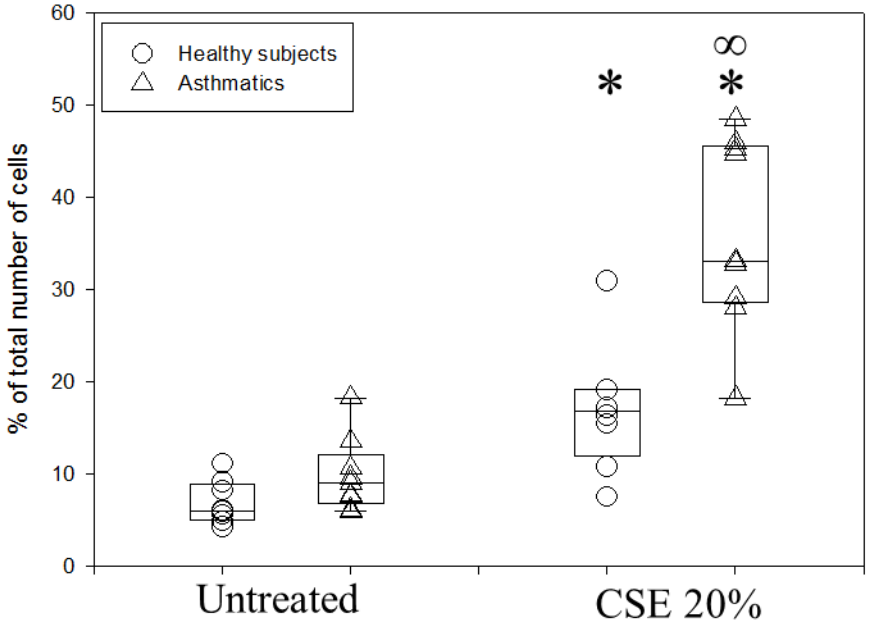

PBEC obtained from HC and AS were treated for 24hrs with CSE20%. Cell viability (a) and early apoptosis (b) were then evaluated with AnnexinV staining. The results are displayed as a box plot showing median, interquartile range and 5-95% confidence intervals from 10 HC (circles) and 10 AS (triangles).

* represents significance ($p<0.05$) according to Wilcoxon Signed Rank tests comparing treatment with untreated control.

∞ represents significance ($p=0.003$) according to a Mann Whitney U test comparing CSE treatment between HC and AS.

4.1.8. Evaluation of cell death: role of antioxidants in H2O2 and CSE-induced cell death.

To evaluate the protective role of anti-oxidants, PBEC obtained from 20 subjects (10 HC and 10 AS; table 4.1) were treated with 250nM ascorbic acid (AA) or 1mM reduced glutathione (GSH), alone or in combination with 20% CSE or 400μM H_2O_2. After 24 hours, annexin-V staining was employed to determine levels of viability and apoptosis.

Figure 4.5 shows that both GSH and AA were able to protect PBEC from H_2O_2 induced cell death. In particular, both antioxidants caused a significant ($p<0.01$) increase in cell viability when compared to H_2O_2 alone (figure 4.5a) with a concomitant statistically significant ($p=0.003$) decrease of early apoptosis levels in the HC group (figure 4.5b); the decrease of EA was also present in the AS group, but this failed to reach statistical significance. There were no significant differences between PBECs from HC or AS subjects with either antioxidant.

Figure 4.6 shows the effects of both antioxidants during CSE treatment. In this case, AA failed to protect PBEC from either HS or AS from CSE-induced cell death, as determined by both viability (figure 4.6a) and early apoptosis (figure 4.6b). In contrast, PBECs from HS or AS were significantly protected by GSH from CSE-induced cell death . In particular, GSH caused a significant increase in viability when compared to CSE alone ($p=0.005$ in HC and $p=0.003$ in AS, figure 4.6a) and, at the same time, EA levels dropped considerably ($p<0.05$ in HC and $p=0.003$ in AS) in the presence of this antioxidant (figure 4.6b). Moreover, GSH treatment caused a significantly greater ($p=0.002$) overall increase in viability in the AS group when compared to the HC group (figure 4.6a).

Figure 4.5

a **Changes in viability after 24 hrs of treatment with H_2O_2 and antioxidants**

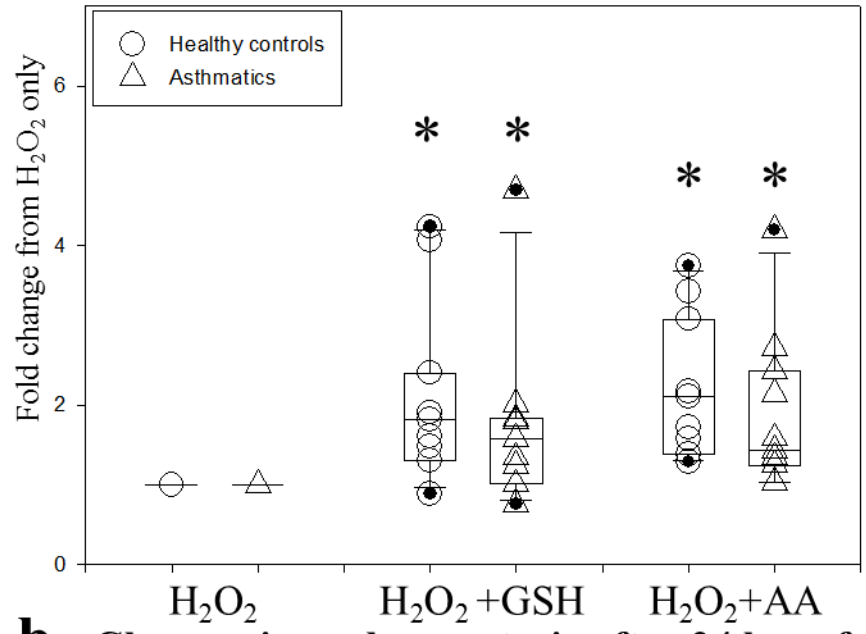

b **Changes in early apoptosis after 24 hrs of treatment with H_2O_2 and antioxidants**

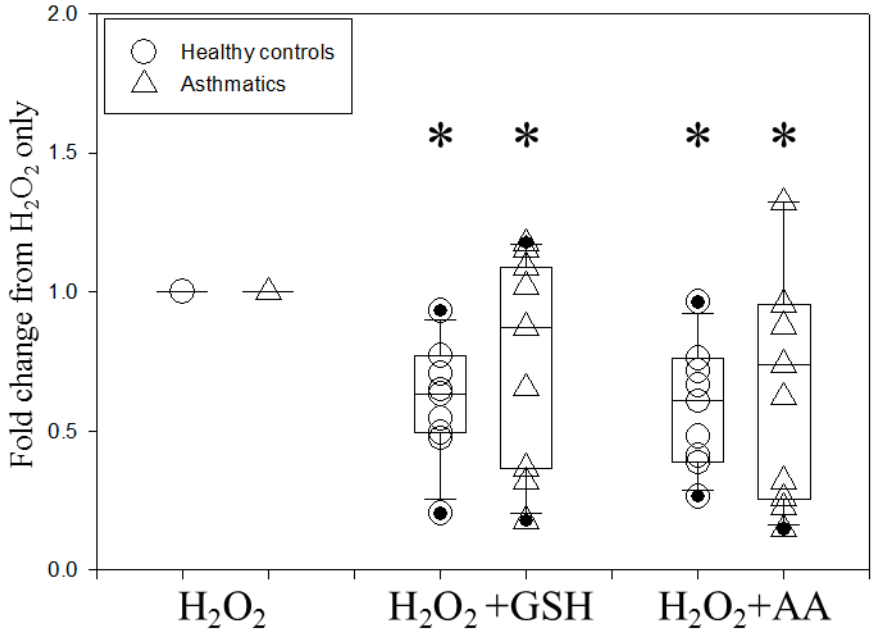

PBEC obtained from HC and AS were treated for 24hrs with H_2O_2 400µM alone or in association with reduced glutatione (GSH) 1mM and ascorbic acid (AA) 250nM. Changes in cell viability (a) and early apoptosis (b) were then evaluated with AnnexinV staining. The results are displayed as a box plot showing median, interquartile range and 5-95% confidence intervals of fold changes from H_2O_2 alone from 10 HC (circles) and 10 AS (triangles). * represents significance ($p<0.02$) according to Wilcoxon Signed Rank tests comparing antioxidants with H_2O_2 only. There was no statistical difference in both a and b comparing antioxidants treatment between HC and AS according to a Mann Whitney U test.

Figure 4.6

a **Changes in viability after 24 hrs of treatment with CSE and antioxidants**

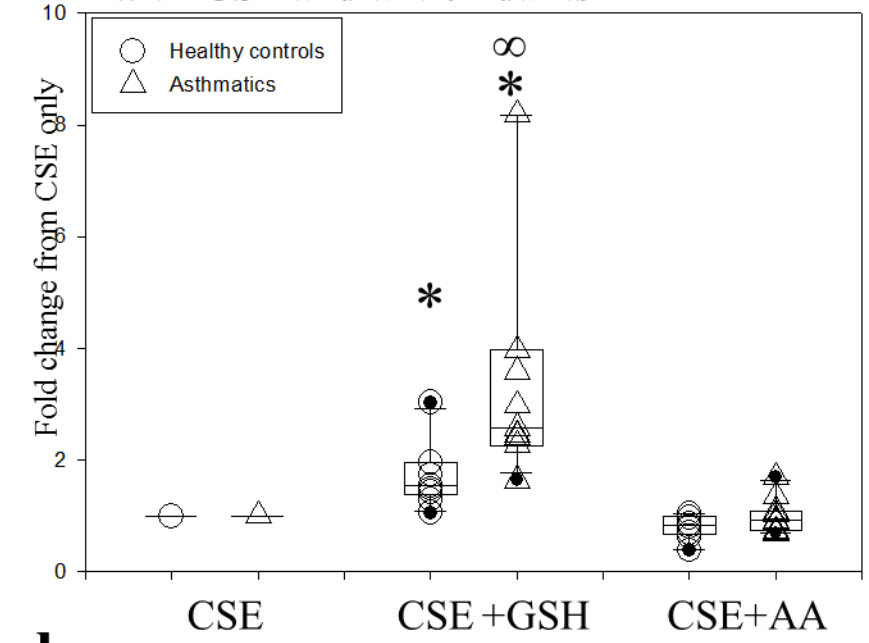

b **Changes in early apoptosis after 24 hrs of treatment with CSE and antioxidants**

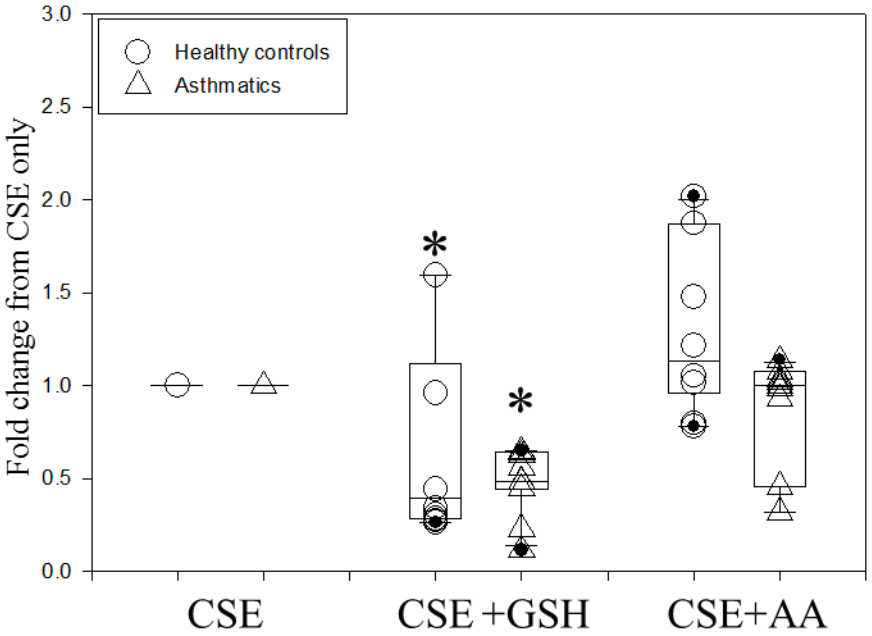

PBEC obtained from HC and AS were treated for 24hrs with CSE 20% alone or in association with reduced glutatione (GSH) 1mM and ascorbic acid (AA) 250nM. Changes in cell viability (a) and early apoptosis (b) were then evaluated with AnnexinV staining. The results are displayed as a box plot showing median, interquartile range and 5-95% confidence intervals of fold changes from CSE alone from 10 HC (circles) and 10 AS (triangles). * represents significance ($p<0.05$) according to Wilcoxon Signed Rank tests comparing GSH+CSE with CSE only. ∞ represents significance ($p<0.05$) according to a Mann Whitney U test comparing CSE+GSH treatment between HC and AS.

4.1.9. Evaluation of cell death: role of caspases 3 and 9 in H2O2 and CSE-induced cell death.

To study the molecular pathways involved in PBEC H_2O_2 and CSE-induced cell death, PBEC obtained from 8 subjects (4 HC and 4 AS) were treated with two specific cell-permeable inhibitors of caspase-3 (Ac-DEVD-CHO) and –9 (Z-LEHD-FMK), two of the most relevant components of the caspases family. PBECs were pretreated with caspase inhibitors 30 minutes prior treatment with CSE or H_2O_2 and the presence of the inhibitors was guaranteed during the duration of the treatment by a further administration of the inhibitors after the treatment with CSE and H_2O_2.

However, as shown in figures 4.7 and 4.8, the specific inhibition of both caspases with Ac-DEVD-CHO and Z-LEHD-FMK failed to induce any significant protection from H_2O_2 and CSE-induced apoptosis in both HC and AS PBEC.

Figure 4.7

a **The effects of caspase3 inhibition on H2O2-induced apoptosis 24hrs after treatment**

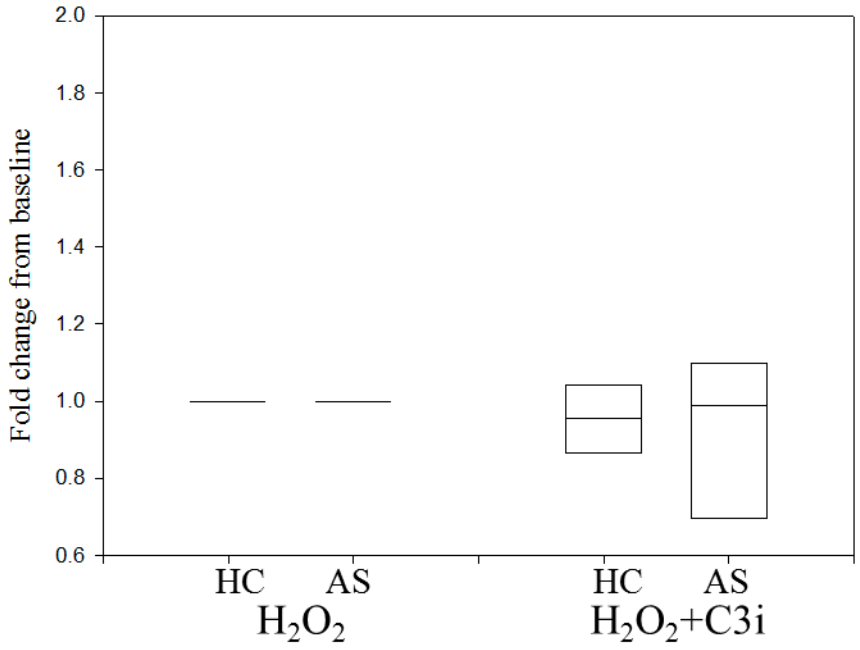

b **The effects of caspase3 inhibition on CSE-induced apoptosis 24hrs after treatment**

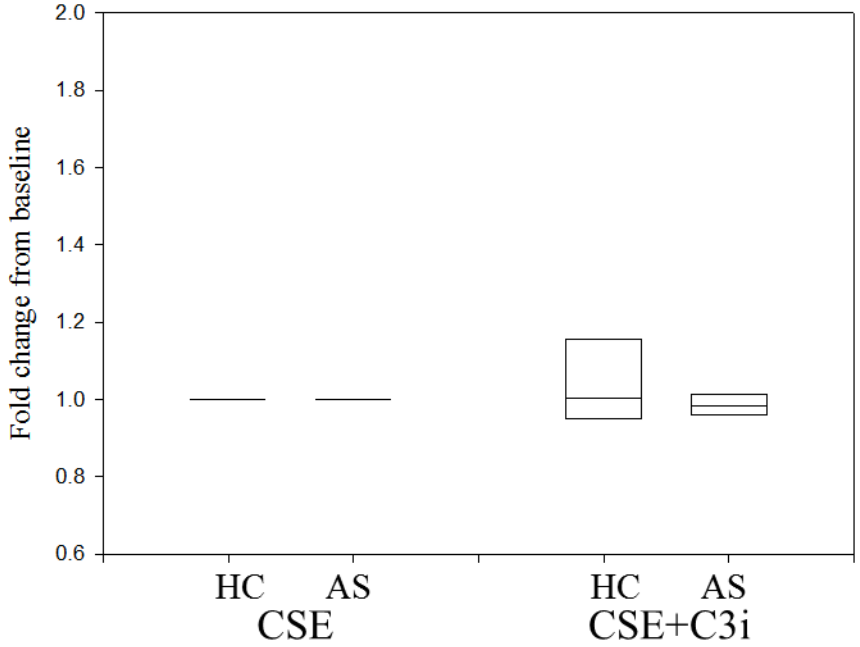

PBEC obtained from 4 HC and 4 AS were treated for 24hrs with H_2O_2 400µM alone or in combination with Ac-DEVD-CHO (C3i) (figure a), or with CSE 20% alone or in association with Ac-DEVD-CHO (C3i) (figure b). Changes in early apoptosis levels were then evaluated with AnnexinV staining. The results are displayed as a box plot showing median and 5-95% confidence intervals of fold changes from H_2O_2 or CSE only (a and b respectively) in both groups.

Figure 4.8

a **The effects of caspase9 inhibition on H2O2-induced apoptosis 24hrs after treatment**

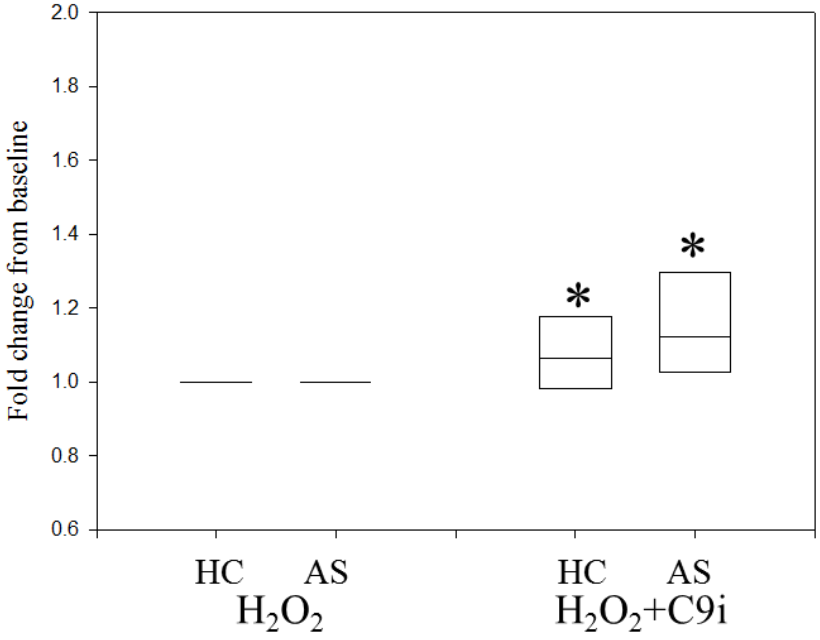

b **The effects of caspase9 inhibition on CSE-induced apoptosis 24hrs after treatment**

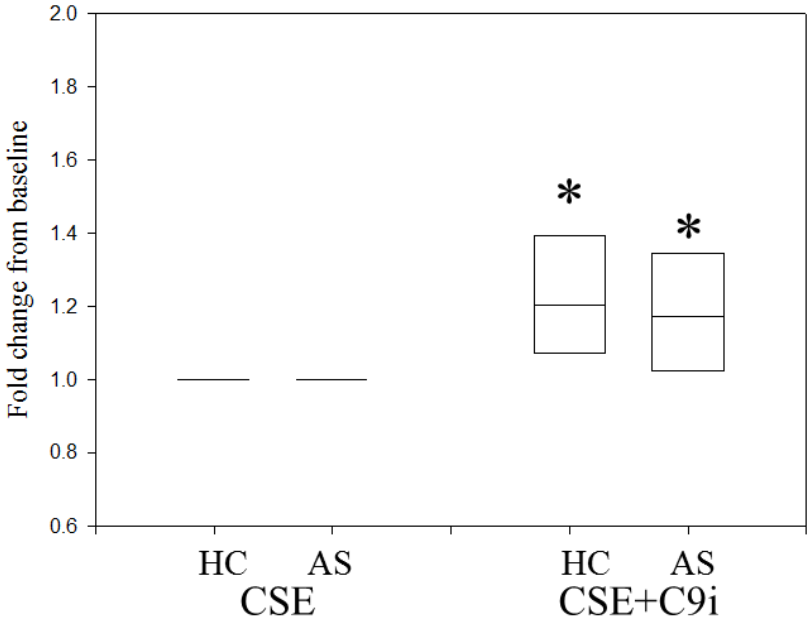

PBEC obtained from 4 HC and 4 AS were treated for 24hrs with H_2O_2 400µM alone or in combination with Z-LEHD-FMK (C9i) (figure a), or with CSE 20% alone or in association with Z-LEHD-FMK (C9i) (figure b). Changes in early apoptosis levels were then evaluated with AnnexinV staining. The results are displayed as a box plot showing median and 5-95% confidence intervals of fold changes from H_2O_2 or CSE only (a and b respectively) in both groups.

* represents significance ($p<0.05$) according to Wilcoxon Signed Rank tests comparing CSE+C9i with CSE only.

4.1.10. Evaluation of cell death: expression of AIF in normal PBEC.

Apoptosis-inducing factor (AIF) is a cell death effector molecule which operates independently of apoptotic cascades involving caspases. In non-apoptotic cells, an AIF precursor protein of 67 KDa is cleaved by local peptidase and becomes a mature AIF molecule of 57 kDa, which is confined to the mitochondrial inter-membrane space, where it functions as an oxidoreductase. Upon induction of cell death, it migrates to the nucleus, where it contributes to chromatin condensation and the apoptotic fragmentation of DNA (S.A. Susin *et al*. 1999, Daugas *et al*. 2000, Granville *et al*. 2001). In addition to this nuclear effect, AIF remaining in the cytoplasm accelerates the release of other pro-apoptotic proteins, such as cytochrome c and procaspase-9, by targeting the mitochondria [S.A. Susin *et al*. 1999]. AIF has a notable characteristic, namely, that none of these AIF effects can be blocked by caspase inhibitors [H.K. Lorenzo et al. 1999].

To determine whether oxidant-mediated apoptosis of PBEC obtained from healthy subjects involved nuclear translocation of AIF, we performed immunofluorescent microscopy with antibodies specific for AIF (see Methods section). PBEC obtained from 2 different healthy subjects were treated for 24 hrs with or without H_2O_2 400 μM.

Figure 4.9 shows that, in basal conditions, PBEC express AIF in their mitochondria (Figure 4.9 A); hydrogen peroxide treatment caused translocation of AIF from the mitochondria to the nuclei (Figure 4.9 B).

Figure 4.9

AIF staining in PBEC treated with H_2O_2 400µM.

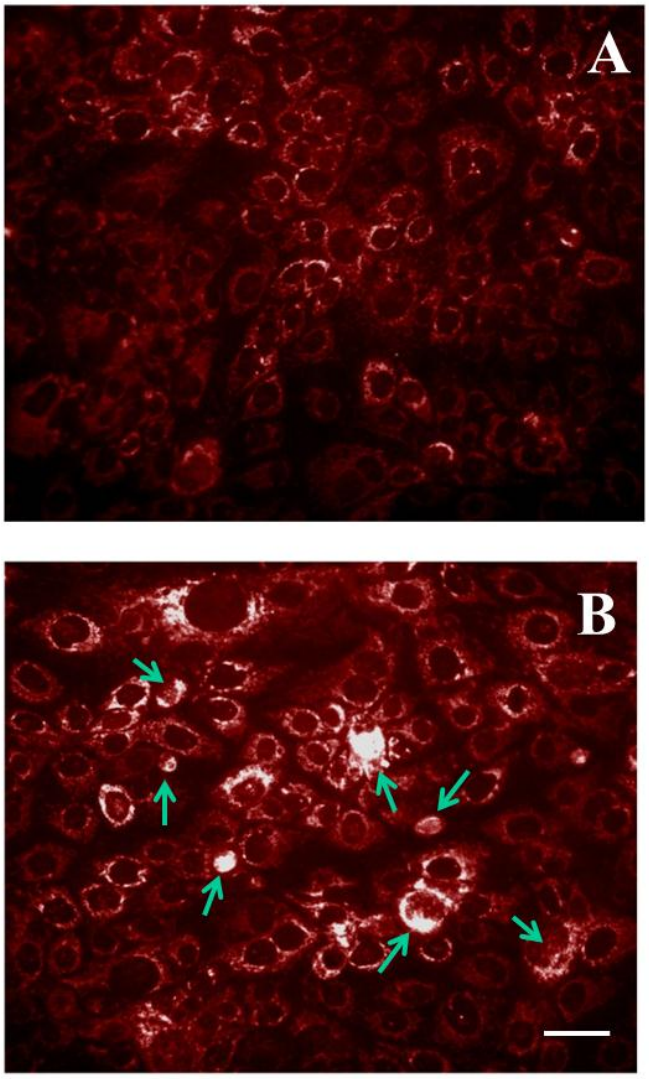

PBEC obtained from 2 different healthy subjects were treated for 24 hrs with (B) or without (A) H_2O_2 400 µM, collected, fixed and then stained with a primary antibody directed towards AIF. The figure shows that, in basal conditions, PBEC expressed AIF mainly in their mitochondria (A); hydrogen peroxide treatment instead caused translocation of AIF from the mitochondria to the nuclei (B, green arrows).
Bar = 10µm

4.1.11. Conclusions

Although many studies have demonstrated altered oxidant defences in asthma (see introduction of this chapter), most appear to be a consequence of the inflammatory process. However, previous experiments carried out in our laboratory showed that primary cultures of human asthmatic bronchial epithelial cells grown *in vitro* are more susceptible to oxidant-induced apoptosis than normal PBECs (Bucchieri et al., 2002). This sensitivity of asthmatic epithelial cells to oxidant-induced apoptosis may be a key triggering mechanism that facilitates the induction and establishment of chronic inflammatory responses. Therefore, understanding more about the underlying susceptibility of epithelial cells from asthmatic subjects to environmental stress, may help to explain the why asthmatic subjects are more prone to the effects of components of the inhaled environment.

In the present study, PBECs were treated with a 20% CSE as an additional source of oxidative stress. After 24 hours of treatment with CSE, PBEC showed many characteristic signs of necrotic and apoptotic cell death. Although there was no significant difference in basal viability between AS and HC, after treatment with 20% CSE, asthmatic PBECs showed an increased susceptibility to the CSE treatment and there was a significant increase of EA cells in the AS group treated with CSE compared to HS. In order to evaluate the role of oxidative stress, we treated PBEC with AA or reduced GSH and exposed them to 20% CSE or H_2O_2 as a positive control for oxidant-injury injury. Ax-V staining showed that the presence of AA failed to significantly protect PBEC from CSE induced apoptosis, even though it protected against apoptosis induced by H_2O_2. These findings are consistent with other studies showing that AA has some attenuating effect on inflammatory processes in the lungs but it is ineffective on CS-induced symptoms (Olatunji-Bello et al., 2008). Furthermore, there is no sufficient data available to validate a specific role for vitamin C in the treatment of asthma (Kaur et al., 2009). In contrast with AA, GSH significantly increased cell viability with a concomitant decrease in apoptosis protecting both HS and AS from CSE-induced cell death.

Free radical interactions of ROS with nucleic acids, proteins, and lipids are a cause of cell injury because they result in a whole chain of free radical reactions. Ascorbate has the ability to terminate these reactions, acting as a stable donor in free

radical-ROS interactions, converting into "semidehydroascorbate", a radical ion, and subsequently to dehydroascorbate; both of which are relatively unreactive, and not capable of inducing cellular damage. Glutathione (GSH) is a cysteine-containing tripeptide (γ-L-Glutamyl-L-cysteinylglycine); it is one of the key players in several enzymatic and nonenzymatic reactions necessary for protecting tissues against oxidative stress. The thiol portion of cysteine, in its reduced state, can donate a reducing equivalent (H^++ e-) to other unstable molecules (e.g. reactive oxygen compounds). Following such interaction, glutathione becomes reactive itself and creates glutathione disulfide (GSSG) by readily reacting with another reduced glutathione; this process is possible because of the relatively high concentration of glutathione in cells. An enzyme called glutathione reductase regenerates GSH from GSSG. The tripeptide is directly involved in the neutralization of free radicals and reactive oxygen species, as well as being able to detoxify various xenobiotics through direct conjugation. While some data suggest that the protective effect of GSH may reflect its ability to inactivate toxic substances in CSE, results obtained using A549 cells would seem to imply that volatile substances that trigger ROS generation are important contributors to the cytotoxic effects of CSE. Microarray analysis has also shown that exposure to CSE results in up-regulation of many genes involved in oxidative stress (Pierrou et al., 2007).

Canonical caspases pathways were not activated in our experimental setup in PBECs treated with CSE or H_2O_2 (apoptosis, and cell death in general, are more likely to follow the organelle dysfunction pathway, of which mitochondrial dysfunction is the best characterized (Gross et al., 1999). The specific inhibition of caspase-3 and -9 with Ac-DEVDCHO and Z-LEHD-FMK failed to induce any significant protection from CSE-induced apoptosis in both HC and AS PBEC. Instead, in the presence of oxidative stress induced by H_2O_2, PBEC displayed a migration of AIF from mitochondria towards the nucleus where, as already noted, this molecule contributes to chromatin condensation and apoptotic fragmentation of DNA. AIF would seem to be involved in acute neurotoxicity provoked by trauma, hypoglycemia, transient ischemia and chronic neurodegenerative diseases. AIF migration has also been observed in various experimental neurodegeneration models; these include retinal detachment –induced photoreceptor cell death (Hisatomi et al. , 2002), brain trauma –induced *in vivo* neuronal death (Zhang et al., 2002), cerebral

ischemia (Zhu et al., 2003), and cortical neuron death *in vitro*, induced by exposure to H_2O_2 and peroxynitrite (Zhang et al., 2002). Based on our results and these observations, it can be hypothesised that in PBECs, oxidative stress-induced apoptosis does not follow the canonical caspase pathways, but rather depends on a more direct mitochondrial damage pathway. Further and more detailed studies on AIF are necessary to better analyse this alternative pathway.

4.2 EFFECTS OF ECM ON H_2O_2-INDUCED CELL DEATH.

4.2.1 ECM and oxidative stress

The ECM is made up of an intricate combination of structural and functional macromolecules, acting as a scaffold for tissue organization (Rosso F et al., 2004). The ECM interacts with cellular receptors and with the cytoskeleton to mediate the bidirectional flow of information between the extracellular and intracellular compartments. This information regulates cell shape, cytoskeletal organization, cell motility and polarity, gene expression, proliferation, as well as survival (Rozario T and De Simone DW, 2010). Interaction with ECM from young human diploid fibroblasts reinstates an apparently youthful state in senescent cells by restoring the cells' proliferative activity, mitochondrial membrane potential, recovering growth factor responsiveness, decreasing intracellular reactive oxygen species (ROS) and increasing telomere length (Choi HR et al., 2011). When compared with normal basement membrane ECM, aberrant matrix proteins can induce cell proliferation and altered morphology in both human airway epithelial cells and fibroblasts (Royce SG et al., 2009). Moreover, epithelial cells from different epithelial tissues will die through apoptosis if removed from their cell-matrix attachments. This phenomenon, termed "anoikis", was first observed in mammary epithelium (Frisch and Francis, 1994); this apoptotic process dysregulated in many debilitating and fatal chronic diseases, such as oral squamous cell carcinoma (Bunek J et al., 2010). A similar mechanism of apoptosis induction has also been described in primary bronchial epithelial cells (PBECs) obtained from bronchial explants (Aoshiba et al., 1997) while in another study, collagens I and IV, laminin, fibronectin, and vitronectin were found to provide considerable levels of protection from apoptosis in a BEAS-2B bronchial epithelial cell line (Wadsworth SJ et al., 2004). Nevertheless, *in vivo* background apoptosis rates in intact bronchial epithelia appear to be very low (Vignola et al., 2001), suggesting that within their normal environment, epithelial cells receive strong survival signals that act by preventing the initiation of apoptosis. These signals are mediated by integrins, described as ECM receptors which cluster in multimeric complexes, called focal adhesions, recruiting kinases such as the Focal Adhesion kinase (FAK) (Gilmore AP et al., 2009). Recent results suggest that it is

not cell detachment, but the proteolytic cleavage or inhibition of FAK which is a key modulator and indicator of apoptosis in epithelial cells under oxidative stress (Mian MF et al., 2008). Moreover, several data demonstrate that different cytotoxic substances, such as arsenic (As), lead (Pb), acrylamide, methylisothiazolinone (MIT), dichlorovinylcysteine (DCVC) and halothane, seem to act by downregulating FAK tyrosine phosphorylation (Chatzizacharias NA et al., 2008). Additionally, a prolonged oxidative stress by a ROS generator called thimerosal induces a significant cleavage of FAK, accompanied by apoptosis, independently of anoikis in HeLa S cells (Mian MF et al., 2008). The principal sources of oxidants in the bronchial airways are represented by cigarette smoke (CS), environmental pollution and local inflammation. ROS have been detected in both mainstream and sidestream smoke (Faux SP et al., 2009), and after exposure to CS, fibroblasts show signs of oxidative stress damage and undergo apoptosis (Baglole CJ et al., 2006). Moreover, oxidative stress and CS exposure may trigger ECM fragmentation and elastase administration impaired lung function and exercise capacity in superoxide dismutase (SOD 3)-null mice (Yao H et al., 2010).

Beyond the proven role of CS in inducing ROS production by its components, H_2O_2 is also currently used *in vitro* as source of oxidative stress to induce cell death. Considering that the extracellular microenvironment is critically important for cell growth, survival, differentiation and morphogenesis, the aim of the current study was to determine the role of the ECM during oxidative stress-induced cell death.

4.2.2 Morphological observations: PBEC grown on different ECM components.

PBEC were plated onto 24 well trays at $5x10^4$ cells/well and grown on different ECM components or plastic for 96 hours; photographs were taken at 24 and 96 hrs. Figure 4.10 shows that after 24 hrs in culture, there were no substantial differences in PBEC morphology growth on different ECMs. Cells grown on plastic however (Fig. 4.10a), were growing slower as demonstrated by the fewer cells per microscopic field and with a tendency to form colonies. After 96 hours (Figure 4.11) the PBEC were confluent even though the cells on plastic were still slightly less in number.

4.2.3. Evaluation of cell death: effects of ECM components on H2O2-induced apoptosis.

Six PBEC cultures obtained from healthy control subjects were used to evaluate the effects of different ECM components on cell survival. PBEC were plated onto 24 well trays at $5x10^4$ cells/well and grown on collagen type I, collagen type IV, laminin, fibronectin (all 1μg/ml) or charged plastic (PBS) until 80% confluent. Cells were then serum starved for 24 hours before being treated with H_2O_2 400μM for a further 24 hours. Adherent cells were then harvested with trypsin in Ca^{2+} and Mg^{2+}-free Hanks' balanced salt solution and combined with nonadherent cells for annexin-V FACS analysis. Viability of PBECs treated with H_2O_2 400μM was significantly lower when grown on plastic than on all of the ECM components examined (Figure 4.12). In particular, the fold decrease of viability vs untreated control was 0.34±0.25 for plastic vs 0.73±0.32 for collagen I, 0.71±0.31 for laminin, 0.93±0.21 for collagen IV and 0.59±0.30 for fibronectin (N=6, $p<0.05$). The levels of early apoptosis (EA) were similar amongst the different coatings, with the exception of the cells grown on collagen IV (Figure 4.13) that showed a significant decrease of EA when compared to plastic (2.7±2.52 vs 5.59±4.21, $p=0.028$, N=6).

Figure 4.10

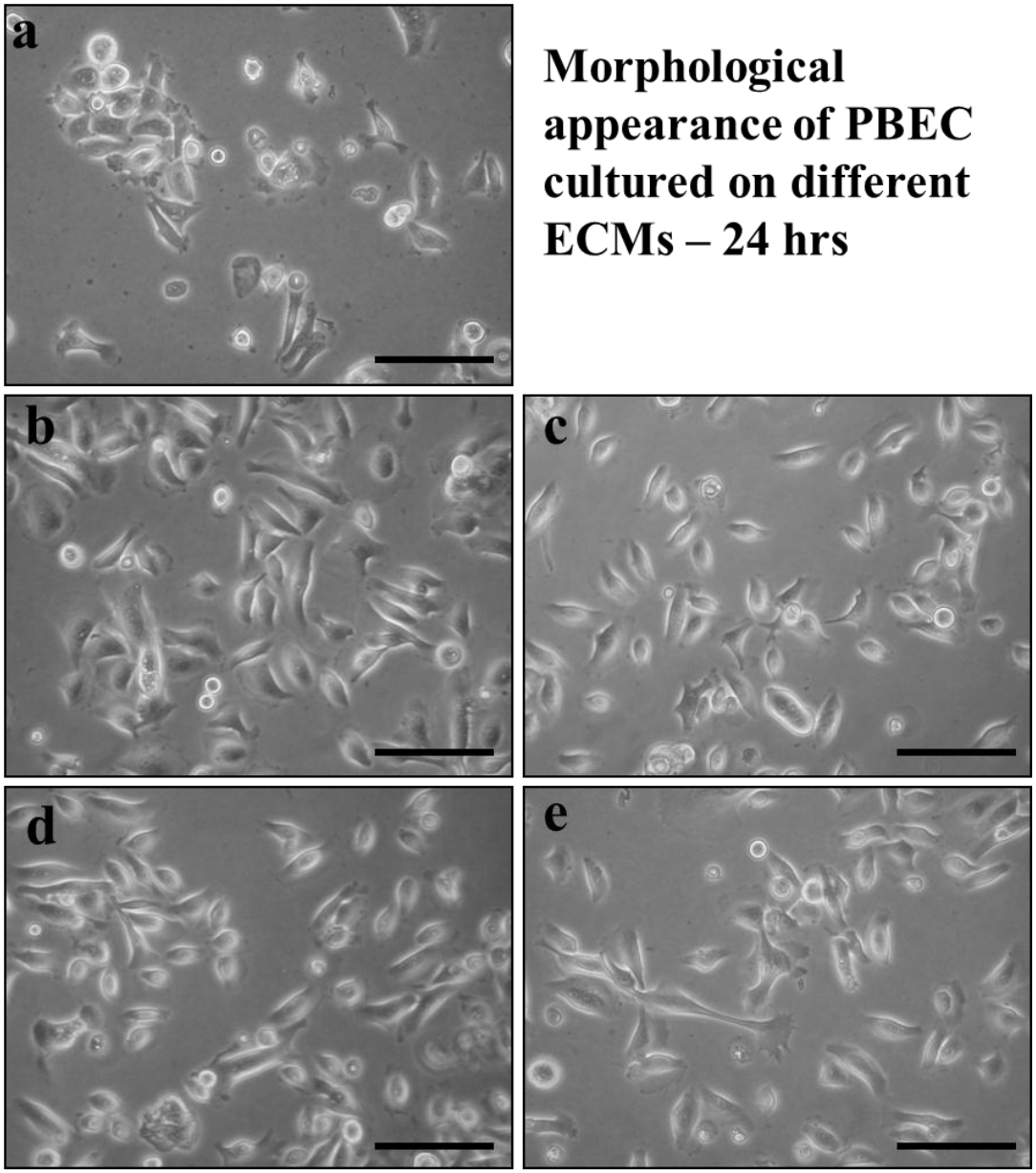

Morphological appearance of PBEC cultured on different ECMs – 24 hrs

PBEC were plated onto 24 well trays and grown on charged plastic coated with PBS only (a), collagen type I (b), collagen type IV (c), laminin (d) and fibronectin (e) all at 1µg/ml. Photographs were taken at 24 hrs. The figure shows no significant differences in growth or morphology of PBEC between the different ECMs.; bar = 100µm.

Figure 4.11

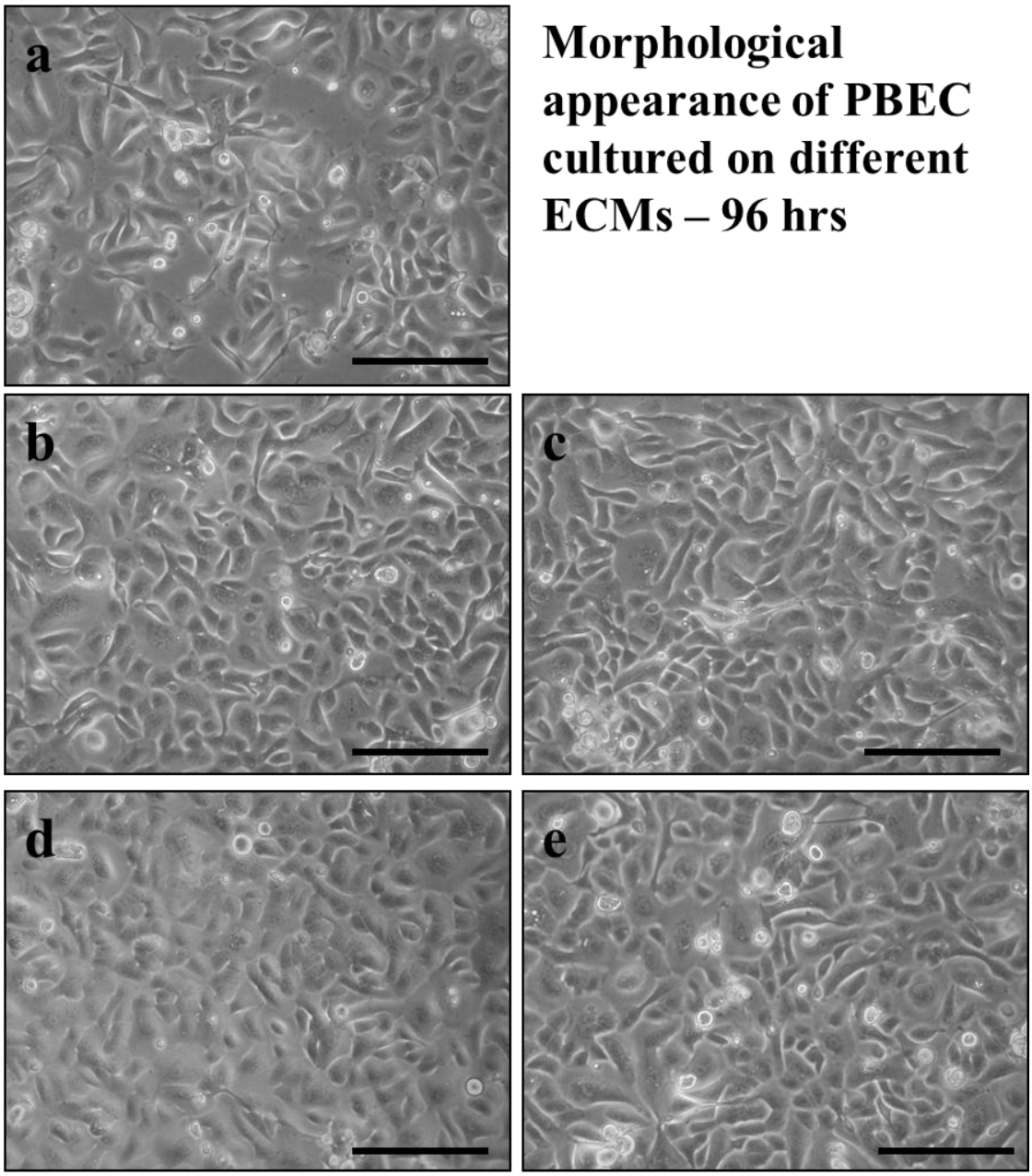

Morphological appearance of PBEC cultured on different ECMs – 96 hrs

PBEC were plated onto 24 well trays and grown on charged plastic coated with PBS only (a), collagen type I (b), collagen type IV (c), laminin (d) and fibronectin (e) all at 1µg/ml. Photographs were taken at 96 hrs. The figure shows no significant differences in growth or morphology of PBEC between the different ECMs.; bar = 100µm.

Figure 4.12

Changes in viability after 24 hrs treatment with H_2O_2

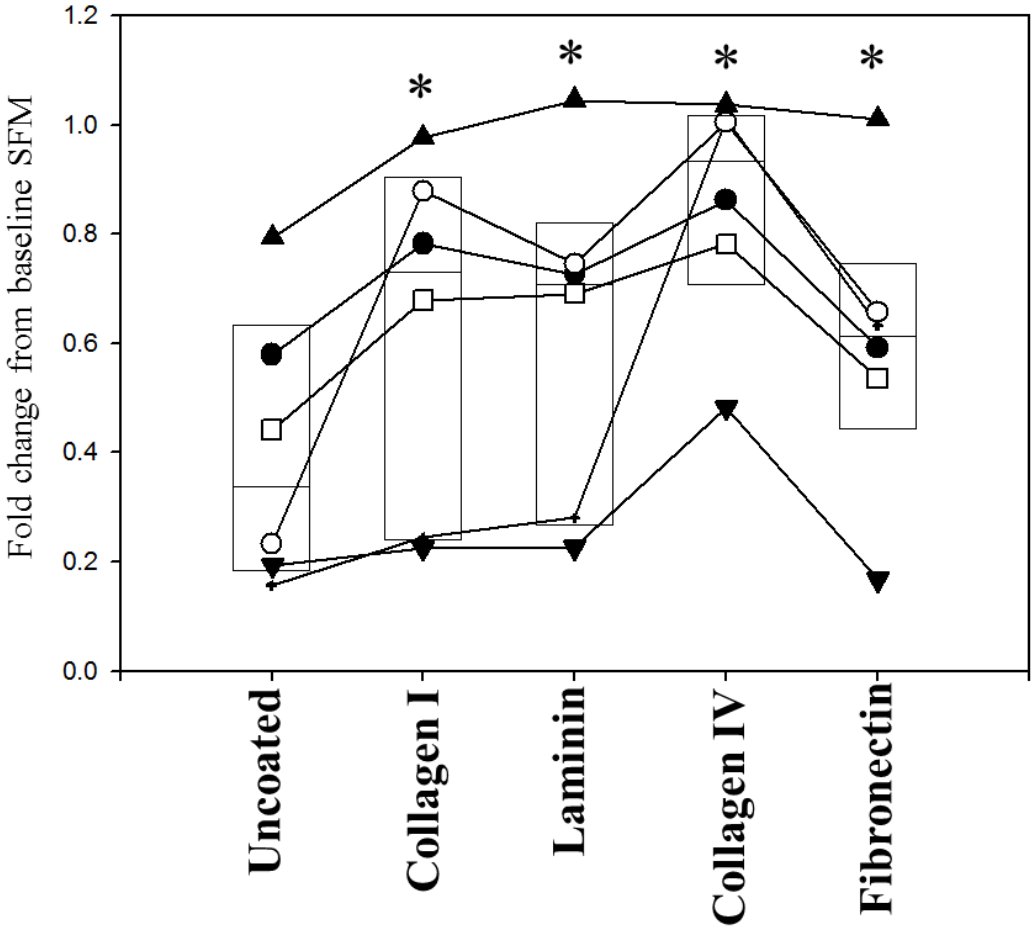

PBEC from 6 HC were grown on different ECM substrates (all at 1µg/ml) and treated with H2O2 400µM for 24 hrs. Early apoptosis levels were then quantified with flow cytometry following AnnexinV staining.
Results are plotted as fold changes from baseline SFM.
* represents significance ($p<0.05$) according to Wilcoxon Signed Rank tests comparing ECMs with uncoated.

Figure 4.13

Changes in early apoptosis after 24 hrs treatment with H_2O_2

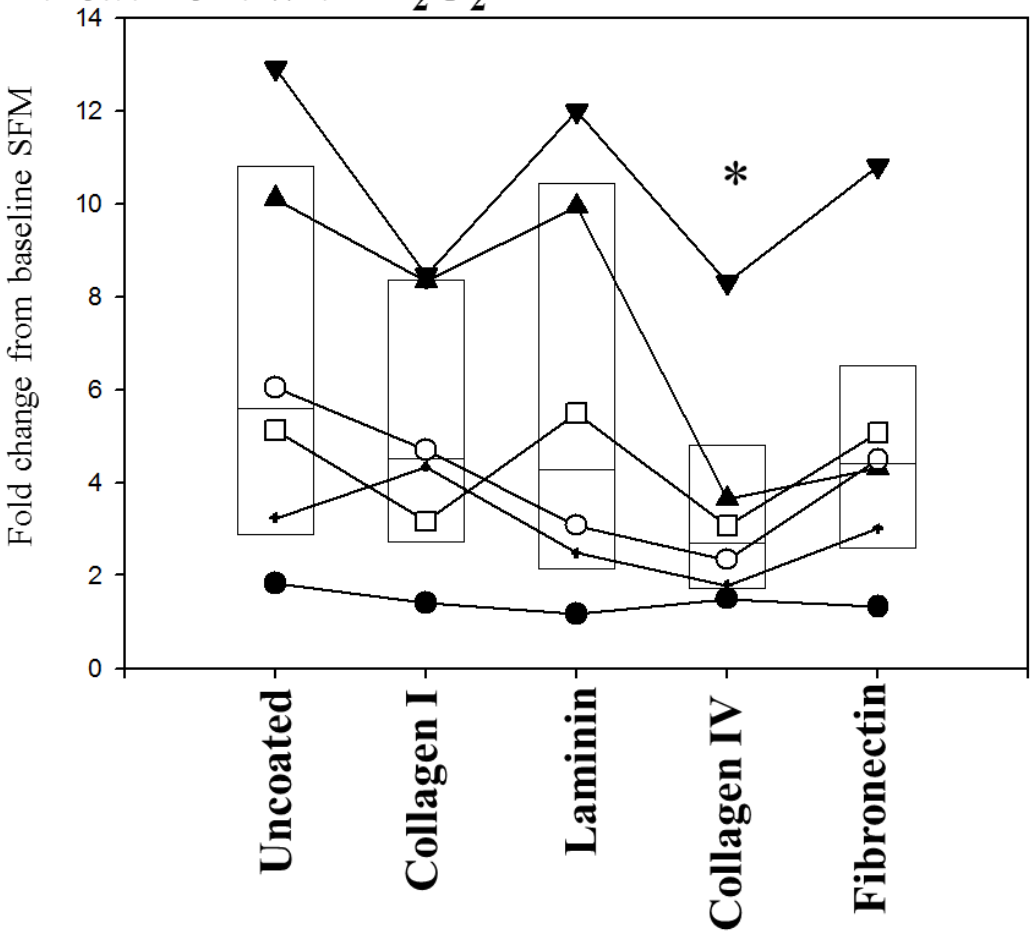

PBEC from 6 HC were grown on different ECM substrates (all at 1µg/ml) and treated with H2O2 400µM for 24 hrs. Early apoptosis levels were then quantified with flow cytometry following AnnexinV staining.
Results are plotted as fold changes from baseline SFM.
* represents significance ($p<0.03$) according to Wilcoxon Signed Rank tests comparing ECM (collagenIV) with uncoated.

4.2.4 Conclusions

The extracellular microenvironment is critically important for cell growth, survival, differentiation and morphogenesis (Rozario and De Simone, 2010).

Many growth factors such as TGFβ, fibroblast growth factor (FGF), insulin like growth factor and hepatocyte growth factor are stored in the ECM, from where they can be released allowing growth factors-regulated extracellular signalling to rapidly proceed without de novo protein synthesis (Taipale & Keski-Oja, 1997).

Wadsworth and colleagues in 2004 have demonstrated that ECM components, such as collagens I and IV, laminin, fibronectin, and vitronectin, could affect bronchial epithelial cell survival (Wadsworth et al., 2004). Using commercially available PBECs and BEAS-2B cells, these authors have shown that vitronectin for BEAS-2B cells and collagen IV for PBEC provided the strongest survival signals. This differential response was explained as a consequence of the differences in integrin expression profile between cultured PBEC and the BEAS-2B cell line. Our experimental setup was very similar to that of Wadsworth and therefore it is of no surprise that we effectively reached very similar conclusions, with collagen IV being the most effective component in reducing H_2O_2 induced apoptosis.

Another possible consequence of growing epithelial cells upon different ECM components is a change in cell phenotype, that could affect the ability of cells to maintain their cell-cell contacts and can influence cell migration (Sander et al., 1998; Streuli, 1999).

My results show that PBEC morphology was not significantly altered by the ECM in basal conditions and cell survival after oxidative stress was only modified by collagen IV. In particular, there were no substantial differences in PBEC growth morphology on different ECMs. Cells grown on plastic however were expanding at a lower rate as demonstrated by the fewer cells per microscopic field. Viability of PBECs treated with H2O2 400μM was significantly lower when grown on plastic compared to the ECM components examined, whereas early apoptosis levels were similar amongst the different coatings, with the exception of cells grown on collagen IV that showed a significant decrease of apoptosis when compared to plastic or the other ECM components.

It is possible to suppose a clear key role for the ECM in protecting airway epithelial cells from cell death. These cells are able to synthesize their own matrix but this is obviously affected by the ECM already provided to them. Changes in the components of the airways ECM such as those occurring during inflammation may alter survival signaling in both PBECs and fibroblasts. Therefore, when investigating responses in the EMTU, an integrated model, where the epithelial cells and fibroblasts are organized as closely as possible to that observed *in vivo*, is required to more accurately understand the cross talk between these cell types and the impact of epithelial injury on the overall response.

5. RESULTS - DEVELOPMENT OF MORE COMPLEX MODELS: TISSUE ENGINEERING OF THE HUMAN BRONCHIAL MUCOSA.

Early observations by Paul Weiss illustrated that blood plasma clot-cultured fibroblasts have diverse shapes, varying from stellate to bipolar, depending on the orientation of the blood clot's fibrous network. This particular led Weiss to emphasize the dynamic cell-environment interaction. In around the same period, Warren Lewis had described stress fibers, or 'tension striae' in flattened mesenchymal cells on glass coverslips. The range of variety reported by Weiss can be found in fibroblasts *in situ*, while the stress fibers similar to those observed by Lewis are seldom found in fibroblasts *in situ*, except during tissue activation occurring during situations such as wound repair and fibrosis.

However, since culturing and observing fibroblasts on glass plates is relatively simple, 2D cell cultures have paradoxically become standard practice in research. The introduction of plastic substrata for tissue culture has further strengthened this practice. Culture techniques involving extracellular matrices, such as collagen or fibrin, ensure a more intricate physical environment for fibroblast cultures, resulting in a distinctly different geometry compared to cells cultured on 2D surfaces. A three-dimensional approach also results in enhanced cell migration outcomes, which include not only cell translocation, but also remodelling of the matrix. Since the complex interactions between cell clusters and the surrounding matrix play a fundamental role in tissue mechanics, it is indispensable to fully understand these interactions if one is to consider tissues and organs as three-dimensional structures for any type of analysis pertinent to normal cell function and pathology, along with tissue engineering (Grinnell 2003).

5.1 ECM engineering

Various cell-secreted macromolecular components make up the intricate, highly hydrated polymer gel that constitutes the three-dimensional extracellular microenvironment.

One of these components is a fibrillar complex that has the task of diffusing nutrients and metabolites to and from cells; this complex, termed "ECM", is composed of cross-linked, physically immobilized sugar and protein elements

Further components include growth factors, chemokines, cytokines and other soluble effectors with important signaling functions, as well as membrane-anchored molecules, donated by neighbouring cells, that have the crucial task of enabling cell-cell communication in tissue morphogenesis.

Fibrous proteins, such as elastin, fibronectin, and laminins and collagens, and hydrophilic proteoglycans containing large glycosaminoglycan side chains, such as hyaluronic acid, are two of the principal ECM macromolecules.

While these components are present in the majority of ECMs, their form and organization, as well as biochemical and mechanical properties diverge considerably between different types of tissues. In addition to its basic functions as a solid support structure upon which cells are organized into 3D tissues, or simply as a physical boundary between neighbouring tissues, ECM also regulates multiple morphogenesis-driving cellular processes, such as cell adhesion, migration, proliferation and division, via distinct receptor-ligand interactions (Giancotti and Ruoslahti, 1999; Kleinman et al., 2003).

Furthermore, tissue dynamics are modulated by the ECM's binding, storing and sequestering capabilities on soluble growth factor proteins. For the most part, the ECM binding process involves heparan sulphate proteoglygan-related electrostatic interactions. Morphogens can be protected from enzymatic degradation-induced inactivation through binding, and the latter has also been reported to induce conformational changes that optimize receptor-ligand interaction, thus increasing biological activity in some cases. On the other hand, dynamic, bi-directional cell-matrix interaction can be established thanks to the extracellular microenvironments' ability to respond to cell-secreted signals, this ability being most apparent in situations where a protelytic degradation-related degradation of the ECM is taking place. Proteolytic enzyme secretions can selectively cleave peptide bonds of nearby

macromolecular ECM component domains. This matrix responsiveness is a key feature in 3D migration and matrix remodeling occurring during tissue formation, regeneration and several pathological processes, due to the fact that ECMs frequently serve as biophysical barriers for the cells located within . It is worth to note that non-proteolytic strategies can also induce 3D migration, with the cell type and microenvironmental situation determining the type of strategy (Friedl, 2004).

Essentially, proteolytic migration is induced through integrin-binding to the ECM, occurring in concomitance with a highly localized degradation of pericellular ECM proteins activated by cell-secreted and -activated proteolytic enzymes; these include the matrix metalloproteinase family (MMPs) (Page-McCaw et al., 2007), in addition to other enzyme families (e.g. serine proteases) (Lijnen, 2001).

Good progress has been made in the last decade or so in devising artificial ECMs. Suitable materials for productive use in three-dimensional cell cultures and *in vivo* tissue regeneration have become a reality thanks to the application of biological recognition principles.. Nonetheless, these artificial systems can still only reiterate a small portion of the key signalling and cell-response functions of natural ECMs, with at least five characteristic functions remaining beyond the grasp of the synthetic versions at the moment.

These include the near-physiological multifunctionality capabilities of the ECM; while most artificial ECMs utilize two classes of biomolecules, the natural ones are comprised of various different biochemical cues. Additionally, artificial ECMs lack in the temporal complexity in signal presentation, with the time frames and dynamics being fairly restricted in terms of longevity and complexity. Spatial complexity represents a further shortcoming of artificial ECMs. Matrix-immobilized 3D morphogen gradients are an essential factor in tissue development and regeneration, enabling several cell types and patterns to be spatially generated in relation to the original signal source, as well as controlling the migration of specific cells to specific locations. Although biomolecule gradients have been created using hydrogel surfaces (Burdick et al., 2004; DeLong et al., 2005), to date no one has succeeded in recreating them in artificial cell-responsive 3D ECMs. The versatility of artificial ECMs is also hindered by the absence of a suitable feedback system to control cell-matrix interactions. Characteristic of natural ECMs, these include, for example, features such as proteases capable of cleaving ECM components,

generating cleavage products that can have important signaling functions (Hamano et al., 2003). Moreover, most artificial ECMs presently available have some cell-specifity issues, since protease substrates of cell-responsive matrices consist of short, linear peptides with limited specificity for particular proteases; this is not the case in matrices composed of natural proteins. Therefore, most artificial ECMs are not specific to particular cells or their protease secretions, respectively.

5.2. Lungs and tissue engineering

Tissue engineering has greatly progressed in the last twenty years or so, especially with regard to replacing function in specific tissues such as exocrine pancreas, cartilage and bone, skin and blood vessels. However, it is still lacking, proper design models for engineering complex 3D ECM microenvironments to understand disease progression.

In fact, the main objectives of modern tissue engineering comprise repeating specific tissue functions for regenerative medicine and developing in vitro models of human tissues to investigate diseases' pathogenesis and for testing and screening new medications before expensive clinical trials. For these objectives to be successfully achieved, it is fundamental that the engineered models must repeat *in vitro* the complex interactions existing *in vivo* between cells and their microenvironments.

The lungs are extraordinarily complex organs that evolved for the adaptation of vertebrates to terrestrial life. While intrauterine development can proceed usually in the absence of lung tissue, life after birth depends completely upon respiration, which it is in turn dependent upon the normal architecture of the lung. The respiratory system consists of separate anatomic regions originating in the external nose and continuing into the nasal passages, pharynx, larynx, trachea, bronchi, lobar bronchi, bronchioles and peripheral airways that conduct respiratory gases to the alveoli. Gas exchanges occur across alveolar epithelial and capillary endothelial cells. Ventilation is driven by mechanical forces dependent upon neuromuscular activity that is precisely controlled by neurosensory inputs to maintain normal pCO2, pO2, and pH. Lung function is completely reliant on its extraordinary structure that exchanges millions of litres of environmental gases throughout our lifetime.

Chronic inflammatory diseases of the lungs, such as asthma, involve complex interactions between different cell types as well as extracellular matrix remodelling,

which, together with the mechanical environment that affects cell-cell and cell-matrix interactions cause the pathology.

Diseases such as asthma and COPD are difficult to study *in vivo* using animal models because there are too many important differences at various levels between animal and human cells and also it is virtually impossible to draw out mechanisms or have a great deal of control over these complex interactions.

5.3. AIMS

Our understanding of the importance of the extracellular microenvironments in regulating cell behaviour is critical in developing our understanding of the role of the EMTU in the pathogenesis of asthma. Thus, the availability of a good model of human bronchial mucosa becomes therefore paramount. For this reason our aims were to:

- design and develop a 3D outgrowth model of the human bronchial mucosa starting from bronchial biopsies acquired during bronchoscopic procedures;
- characterise, structurally and ultra-structurally, the morphological features of these outgrowths, by means of electron microscopy analysis (SEM and TEM), to verify the degree of similarity of the 3D bronchial outgrowths with the normal human bronchial mucosa;
- immunologically characterise these outgrowths by using immunofluorescence and immunogold techniques and a panel of antibodies directed towards the antigens usually expressed by the adult differentiated human bronchial mucosa;
- verify the possibility to utilize these novel 3D models to undertake functional studies to evaluate the responses of the outgrowths to environmental stress, such as that occurring during exposure to cigarette smoke and its oxidant components.

5.4. Outgrowth Model.

As reported in more details in the Methods section, bronchial biopsies, obtained though bronchoscopy, were cut into 0.5mm^3 fragments and placed onto 6.5mm Transwells, embedded in 60 μl of Matrigel^{TM} and grown in BEGM/DMEM 10% FCS (1:1) growth medium that was added underneath the membrane (Figure 5.1). The growth medium was replaced every 48hours. The expansion of the outgrowths was monitored with a contrast phase microscope.

At specific time points, the membranes with the outgrowths were prepared for Scanning Electron Microscopy (SEM), Transmission Electron Microscopy (TEM) and Immunofluorescence.

5.5. Morphological characterisation of the human bronchial outgrowths.

Phase contrast microscopy (PhaCo) revealed that the 3D outgrowths were initially formed as a network of spindly cells (likely fibroblasts) and rounder cells (possibly epithelial cells) that were growing out into the Matrigel from the biopsy which was initially placed in the middle of the transwell system (Figure 5.2). After 10-12 days, the nylon membrane covering the bottom of the insert was completely covered with the newly grown tissue and from that time the culture had a three-dimensional structure. After 30 days of culture the morphological features of the outgrowths (as observed with the PhaCo) did not change significantly. In our experience, unless specific damaging events (eg. contamination with infectious organisms), occurred during the culture period, and providing proper culture conditions were maintained, we were able to grow these 3D outgrowths for more than a year.

Figure 5.1

Three-dimensional human bronchial outgrowths

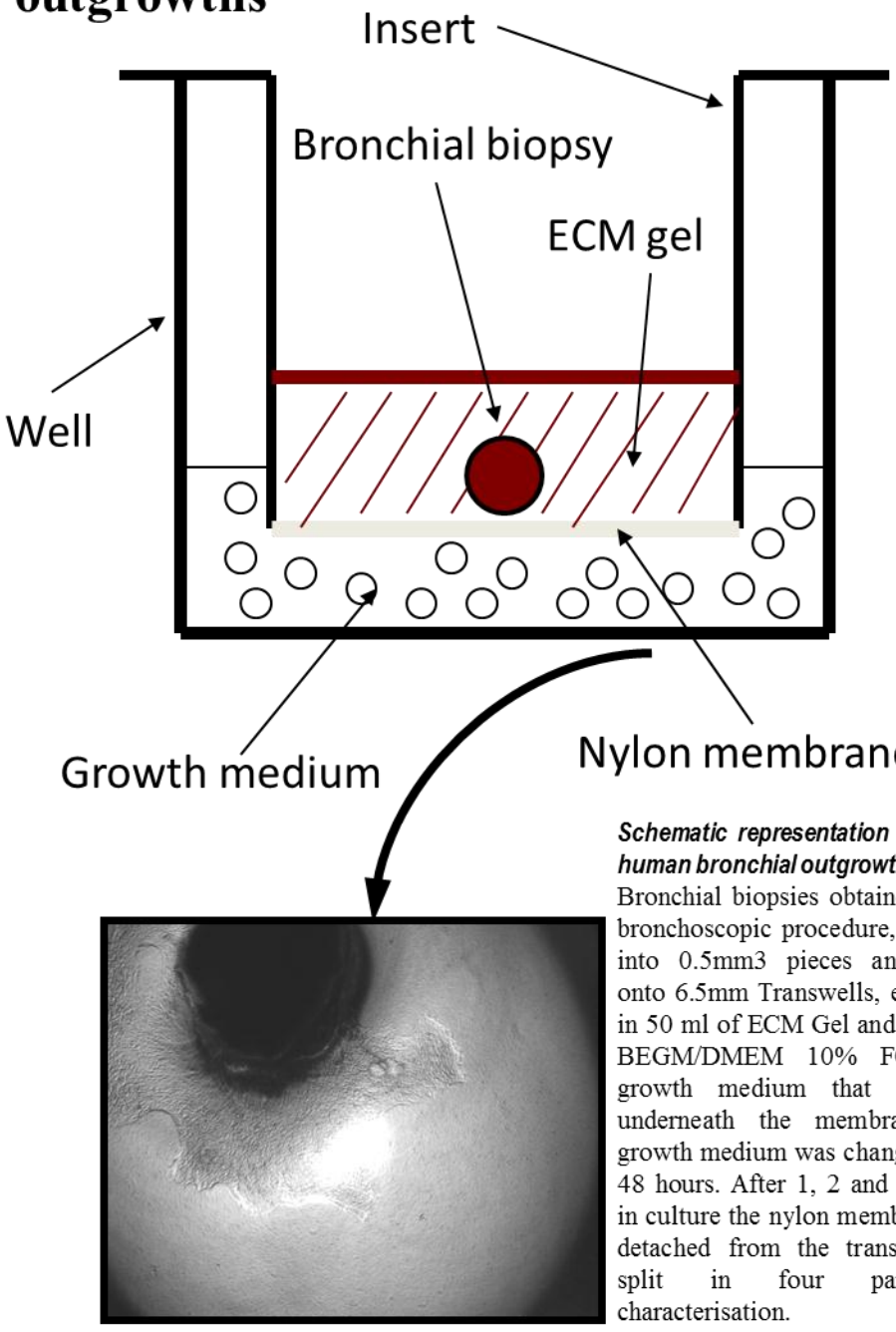

Schematic representation of the 3D human bronchial outgrowth model. Bronchial biopsies obtained during bronchoscopic procedure, were cut into 0.5mm3 pieces and placed onto 6.5mm Transwells, embedded in 50 ml of ECM Gel and grown in BEGM/DMEM 10% FCS (1:1) growth medium that was put underneath the membrane. The growth medium was changed every 48 hours. After 1, 2 and 3 months in culture the nylon membrane was detached from the transwell and split in four parts for characterisation.

Figure 5.2

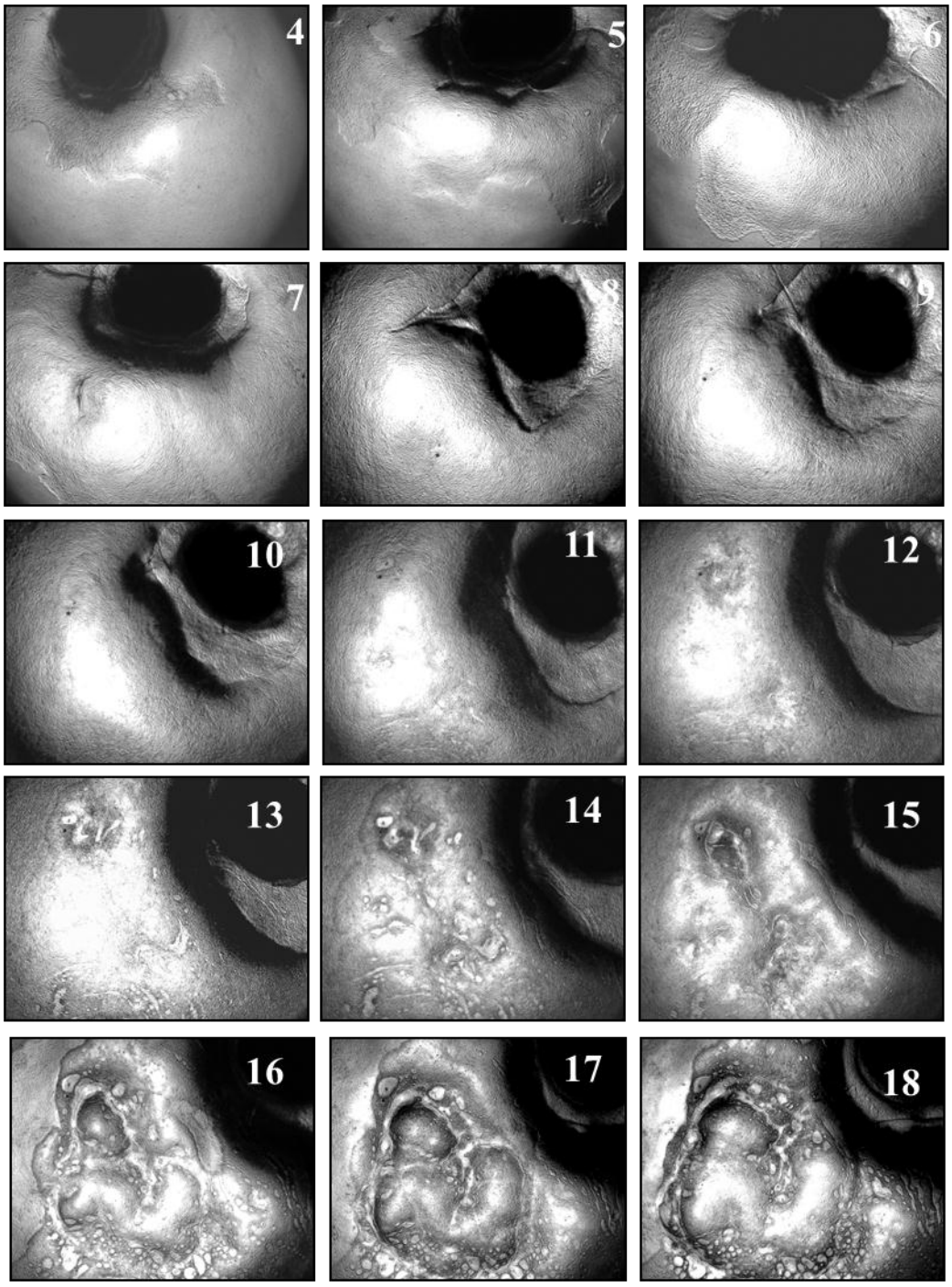

Phase contrast observation of an outgrowth during its first 18 days in culture. During the first stages, from the biopsy emerged mesenchymal cells, followed later by epithelial cells. After about ten to twelve days of culture, the cells will have covered all the nylon membrane of the insert. Subsequently, the growth will become three-dimensional.

5.5.1. SEM Analysis.

The next step consisted of morphological evaluation of the bronchial 3D outgrowths using electron microscopy. Electron microscopy enabled us to study the typical ultra-structural features of these culture models and to compare them to those of the normal well differentiated adult human bronchial mucosa.

SEM analysis is usually limited to surfaces studies, and in our case it resulted very useful in evaluating and screening the growth of our 3D models. As shown in Figure 5.3, the 3D outgrowths showed a progressive development and differentiation of their apical surface. After 10 days this surface was completely covered with microvilli of epithelial cells (Fig.5.3 A,B and C). It was also possible to clearly identify the cell borders. Around 20 days the apical surface started to present very few ciliated elements (Fig.5.3 C, D and E) that represented around 40% ot the total surface area after 30 days in culture (Fig.5.3, F, G and H). This ratio between ciliated cells and cells with microvilli (40:60) did not change significantly after this time point. The cilia measured around 8 μm (Fig.5.3 F, orange line) which is comparable with the normal length of cilia of the normal bronchial epithelium.

By fracturing the outgrowths layer after fixation we were also able to observe the inner structures. Figure 5.4 A shows the presence of a complex cell network of elongated cells underneath the epithelial cells layer in an outgrowth that has been cultured for 32 days. The elongated, spindly elements rest on the nylon membrane of the plastic insert and their cytoplasmic membrane is full of long processes that seem to reach for the other cells and also for the epithelial cells above, that, in stark contrast with the elongated cells, present tight intracellular junctions typical of epithelial cells (Figure 5.4 B). The appearance and location of the elongated cells instead suggest a mesenchymal/fibroblastic phenotype. It was not possible to observe other cell types.

Figure 5.3

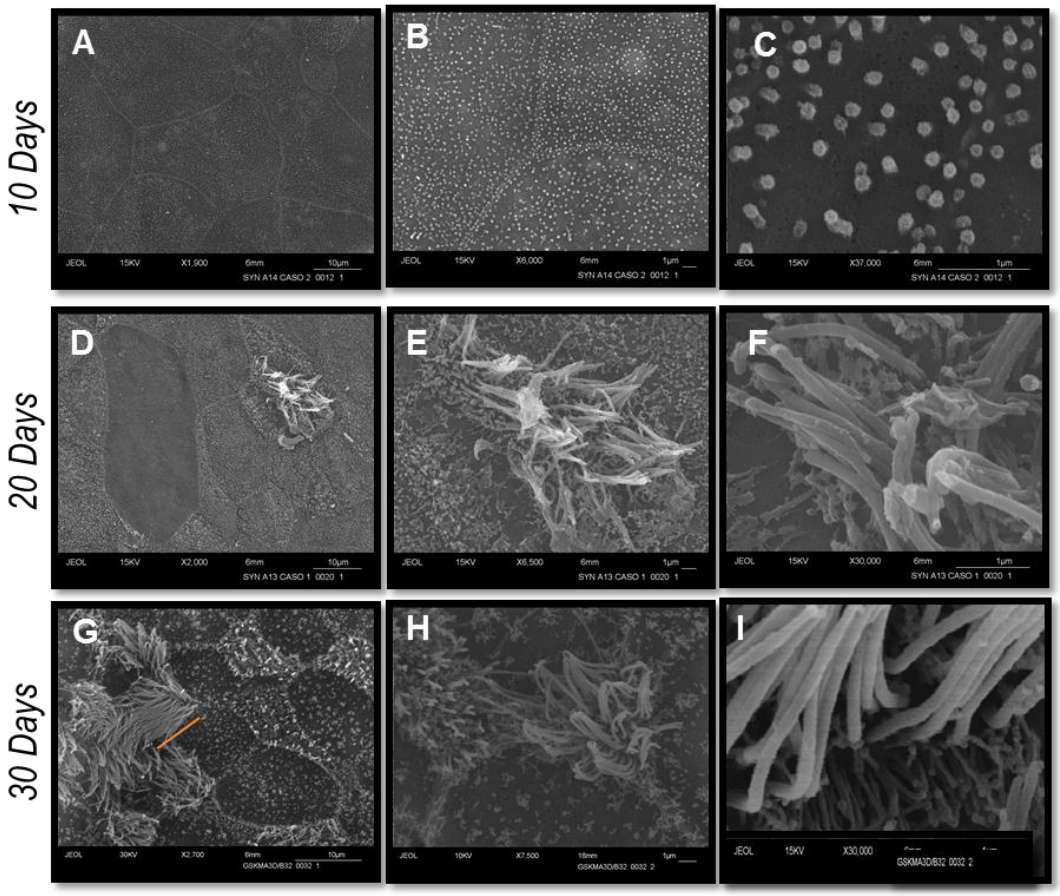

SEM screening during the first 30 days in culture. Formation of ciliate elements begins after around 20 days in culture and is completed after 1 month.

Figure 5.4

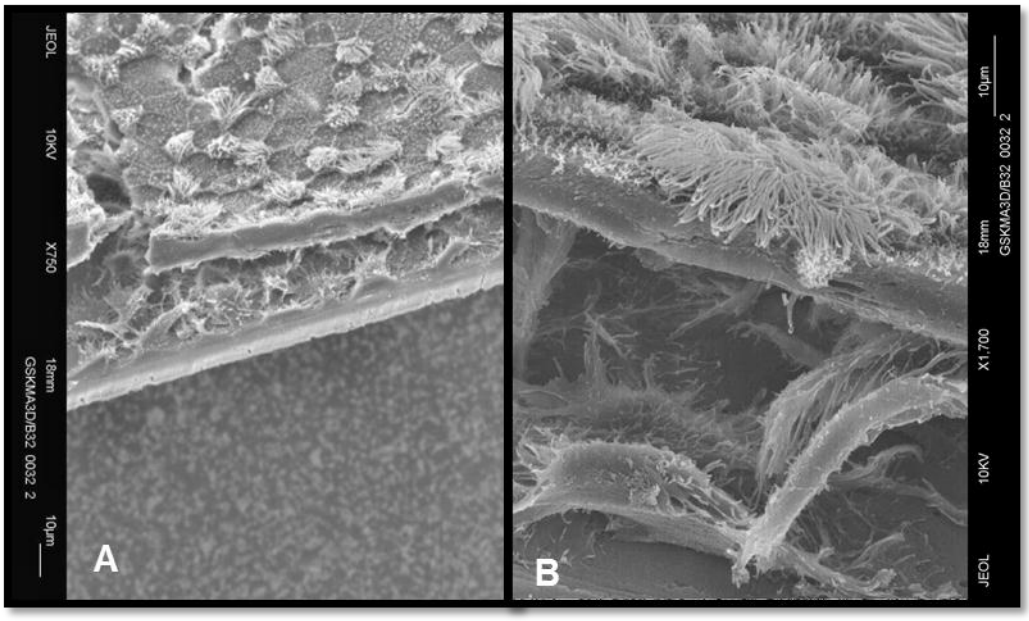

SEM analysis of the outgrowths. After 30 days of culture, it is possible to observe a complex cell layer with elongated cells (fibroblasts) growing underneath a layer of epithelial cells.

5.5.2. TEM analysis.

TEM analysis enabled us to have a better understanding of the structural characteristics of the 3D bronchial outgrowth. Figure 5.5 shows a panoramic view of a 30 days old outgrowth: it is possible to clearly identify two distinct strata, the top one formed of two layers of epithelial-like cells, a basal and an apical one, and the bottom one where fibroblast-like cells are dispersed in a highly organized ECM. The two layers are separated by a well-developed basement membrane. In Figure 5.6 it is possible to analyze the epithelial component more in details. In particular, the apical epithelial elements present microvilli and cilia that are structurally well formed. The basal epithelial cells are separated from the mesenchymal layer by a well-developed basement membrane to which basal epithelial cells are attached via hemidesmosomes (Fig.5.6 C). The latero-lateral surfaces present adhesive junctions (desmosomes, clearly visible in fig.5.6 E) that keep the surfaces of adjacent cells well attached, and enlargements where desmosomes are missing and where it is possible to discern exo- and endocytosis occurrences (Fig.5.6 D).

The lower layer (mesenchymal layer) has a completely different structure with fibroblasts dispersed in a well-defined ECM (Figure 5.7). In fig.5.7 B, it is possible to observe high magnification details of a fibroblastic cytoplasmic process: it is quite clear that the proteic material that will eventually form the ECM is extruded into the extracellular space from caveolae-like structures present on the cytoplasmic membrane of the fibroblasts.

It was not possible to identify any other cytotypes (such as immune or inflammatory cells) apart from the ones already described. As better detailed in the Discussion session of this chapter, this is another strong point of this model because it enables study of cellular processes devoid of the presence of inflammatory cells.

Figure 5.5

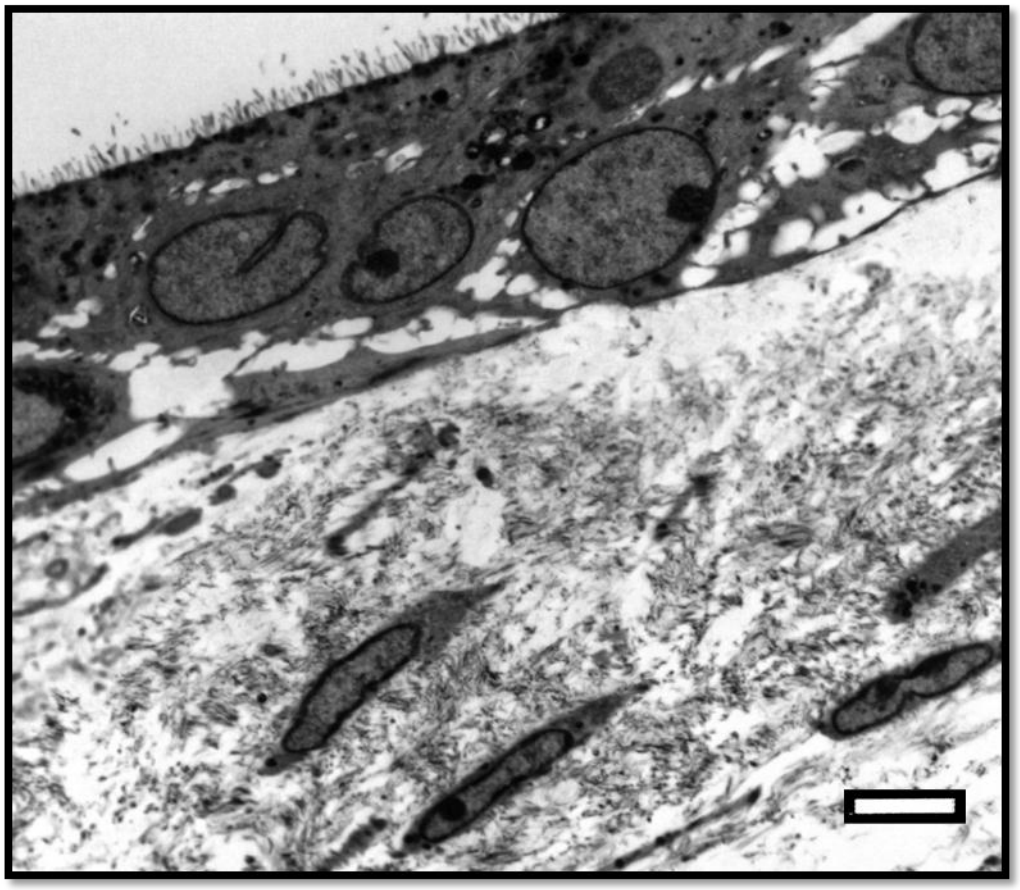

Overview by TEM of a 3D outgrowth after 30 days of culture. Clearly visible in the apical part of this image is the stratified epithelial layer, separated, by a basement membrane, from the layer of connective tissue with fibroblast cells surrounded by ECM.
Bar = 2um

Figure 5.6

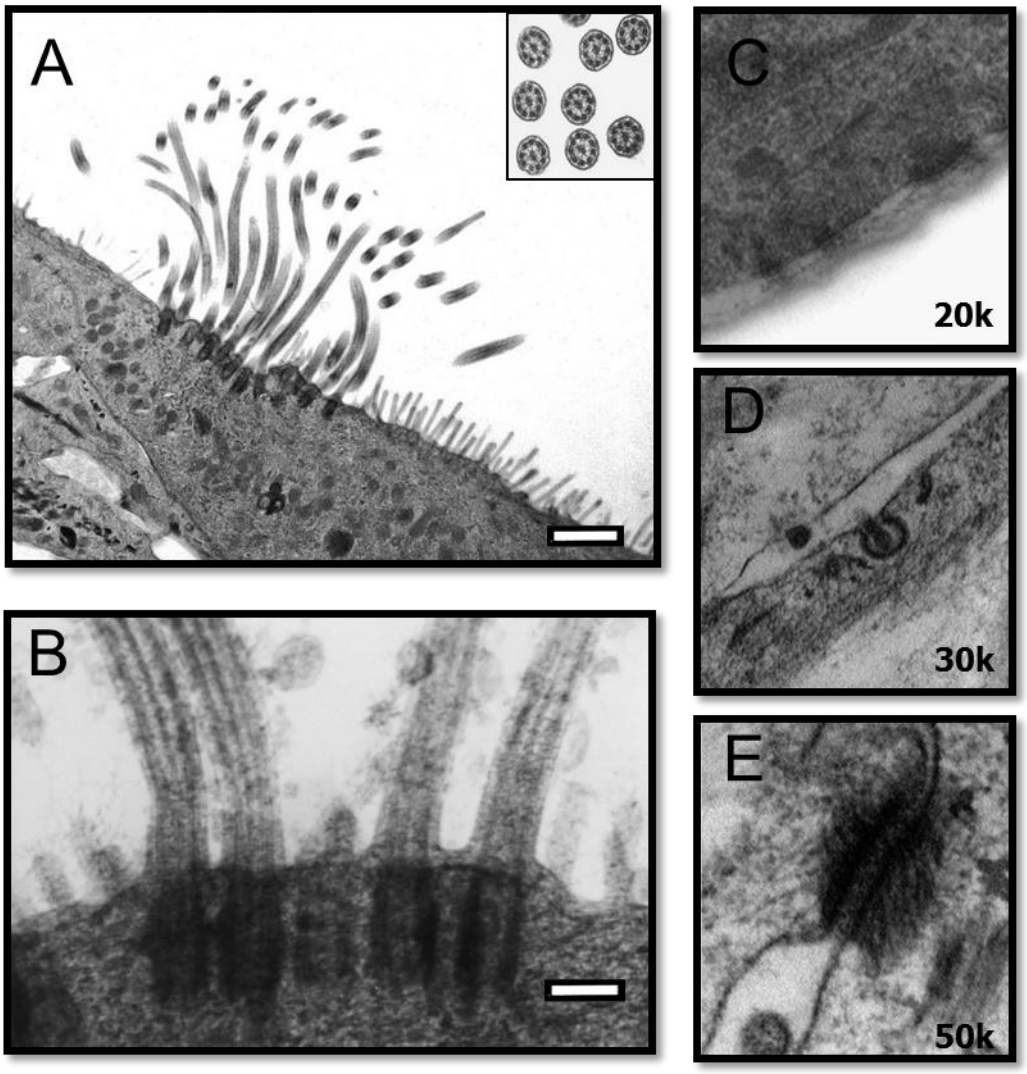

Epithelial elements with different apical structures. Both microvilli and cilia are visible (A), the inset shows a particular of the cilia, displaying their internal structure; in figure B, it is possible to observe the presence of basal bodies of the ciliated structures. C shows a well developed basement membrane to which basal epithelial cells are attached via emi-desmosomes. In D is possible to observe an enlargement of the later-lateral surface inside which is possible to detect exo/endocytosis of cytoplasmic materials. E shows a complete desmosome just above the abovementioned enlargement, that keeps the latero-lateral surfaces of two adjacent cells well attached. Bars = 1um in A and 200nm in B.

Figure 5.7

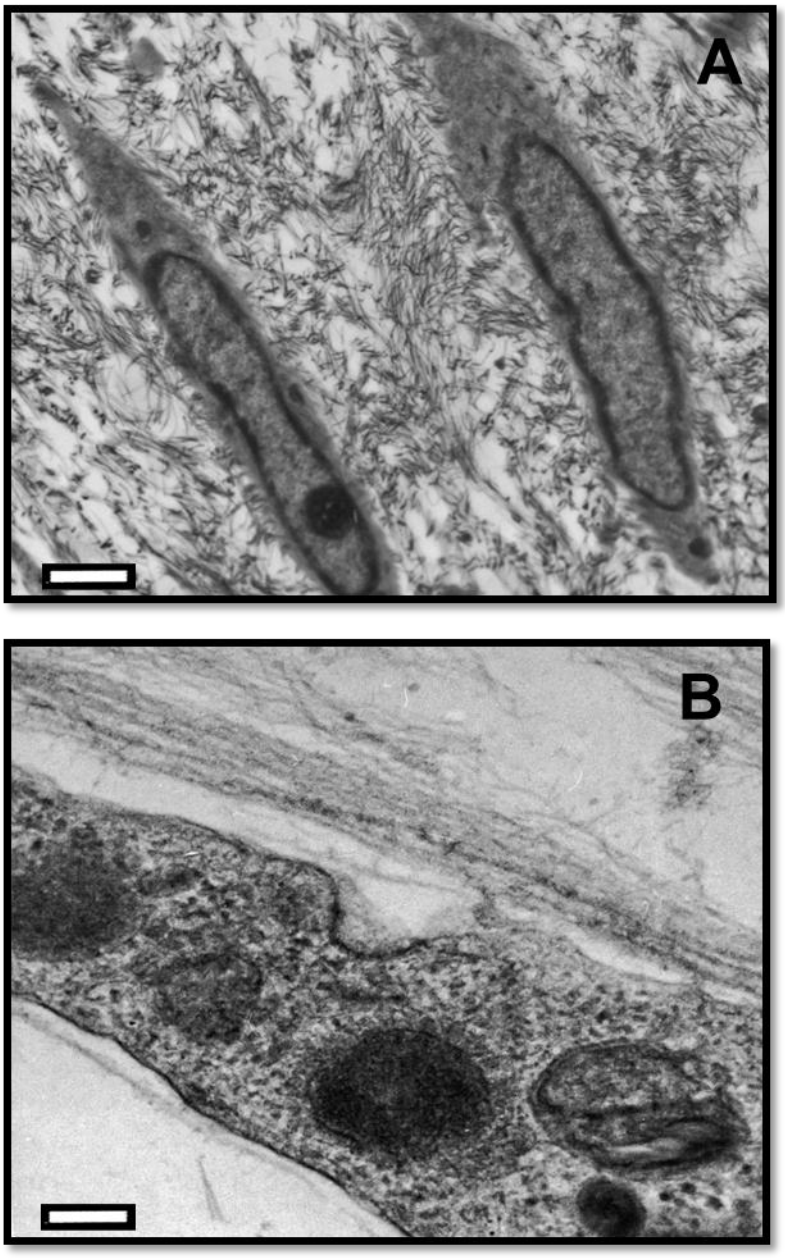

Particular of two fibroblasts from the mesenchymal layer. They appear to be surrounded by ECM proteins (A) that, as illlustrated in figure B, are produced by the fibroblasts themselves. The cytoplasms of the fibroblasts contain vacuoles filled with proteic material and their cytoplasmic membranes present caveolae-like structures, from where the assembled proteins are released into the extracellular space. Bars = 1um in A and 200nm in B.

5.6. Immunocharacterisation.

In order to better characterize the 3D bronchial outgrowths, these were studied by immunofluorescence, with a series of primary antibodies directed against the main antigens of interest. See the Methods section for a detailed description of the protocols and antibodies utilized. In particular, we used immunofluorescence and confocal microscopy observations to characterize the outgrowths. Figure 5.8 shows that the epithelial layers were positive for CK13 (A) and CK18 (B), whereas the underlying fibroblast layer was positive for Collagen I (C) and Laminin (D). The outgrowths did not express CD3, CD4, CD8, CD18, CD28, CD 45, CD64, CD68 and MPO (markers of different kind of leukocytes, lymphocytes, macrophages and neutrophils) and this was in accordance with the morphological observations.

Figure 5.8

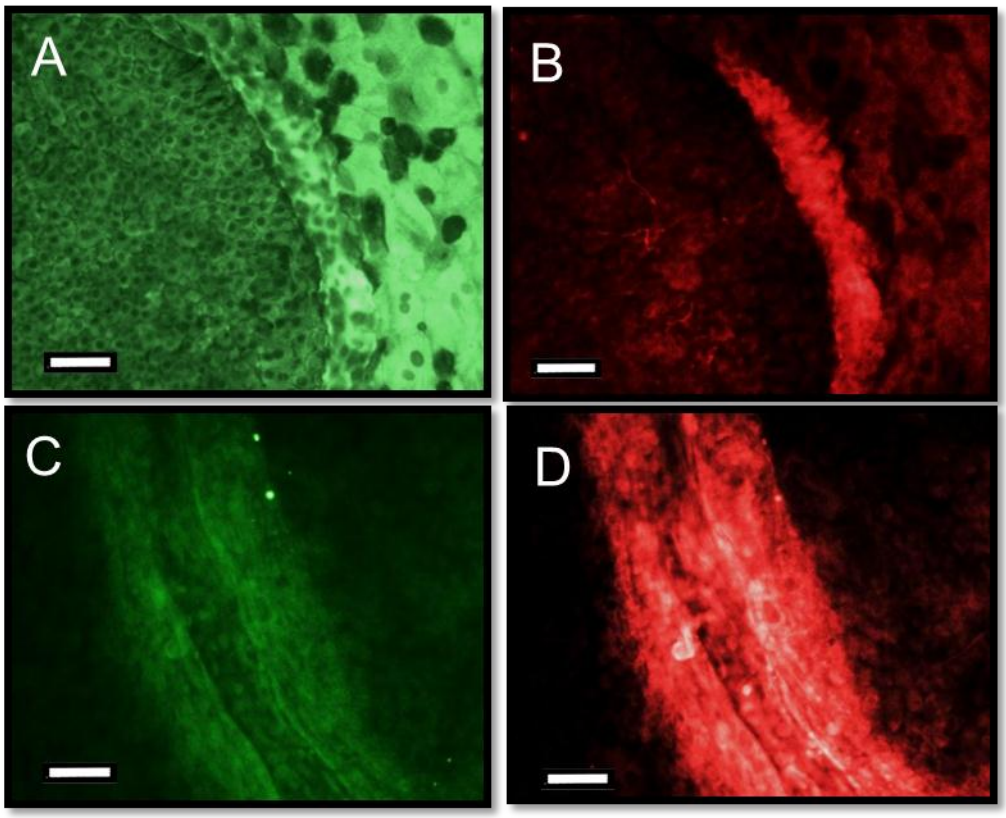

Immunofluorescence staining of the epithelial (A and B) and fibroblast (C and D) layers. The epithelial cells resulted positive for CK13 (A) and CK18 (B), whereas the fibroblasts expressed Collagen Type I (C) and Laminin (D). Bars = 40 um.

5.7. FUNCTIONAL STUDIES.

As pointed out earlier, one of the main limitations of traditional cell culture models is not being able to follow cell treatments for long time points due to the fact that after a few days at most any cell culture would have reached confluency and therefore the effects of whatever we want to test will be marred/biased by physiologically occurring cell growth inhibition phenomena. The bronchial 3D outgrowth that we have developed instead is apparently free from this limitation given its ability to grow indefinitely. Moreover, the contemporary presence of bronchial epithelial and fibroblast cells in their natural microenvironment puts us in the position of being able to study the effects of medium/long term exposures on a model that closely mimic the human bronchial mucosa and where it is actually fairly easy to highlight eventual alteration of the EMTU.

5.7.1. Study of the effects of long term CSE exposure on 3D outgrowths survival and differentiation.

Given the results obtained earlier in terms of effects on cell death and survival of traditional primary cultures of bronchial epithelial cells or fibroblasts after exposure to CSE and oxidants, our first functional evaluation of the 3D bronchial outgrowth was carried out after stimulation with CSE.

3D outgrowths were cultured for one month, in order to let them properly differentiate, before exposing them to CSE 15% for 21 days. This dose and time point was decided after a preliminary experiment where outgrowths were exposed to three doses of CSE (10, 15 and 20%) and monitored daily with a phase contrast microscope. In this preliminary experiment no significant differences were observed between the three doses of CSE.

During the exposure time, fresh medium containing CSE 15% or not (Control) was added to the outgrowths every 48 hours. All the conditioned media were catalogued and stored at -80 degree C for later studies.

Long term exposure with CSE did not cause any cell death amongst the two cell populations. This was unexpected after the studies carried out earlier with the

traditional cell culture models. However, the long term treatment caused a partial remodeling of the architecture of the 3D outgrowths. In particular, the apical epithelial cells completely lost their ciliated structures that were replaced by thick microvilli entirely covered by mucus (Fig.5.9 A). Moreover, the fibroblast increased their production of collagens and this resulted in a clear thickening of the basement membrane and in a complete disarray of the fibroblast layer (Fig.5.9 B and inset). These structural modifications are compatible with those occurring after a chronic inflammatory insult. Interestingly though, our 3D outgrowth models are void of any immune or inflammatory cell components, as shown earlier.

Figure 5.9

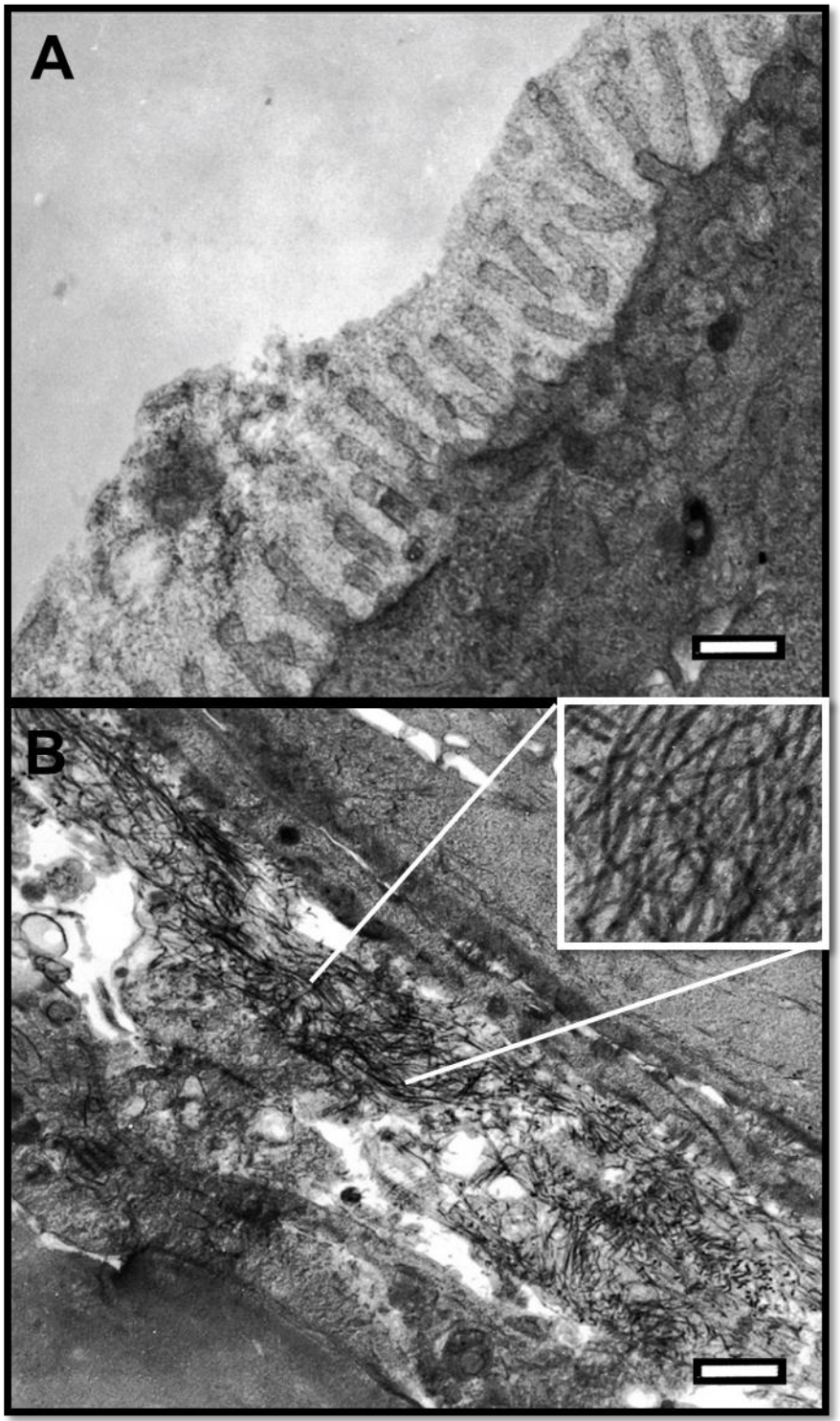

Effects of CSE treatment on outgrowths' ultrastructure. Outgrowths were cultured for one month before being treated for 21 days with CSE 15%. It is possible to see the modifications to the normal structures described earlier. In particular, the apical epithelial cells completely lose their ciliated structures, subsequently replaced by thick microvilli entirely covered by mucus (A). There is also an increase in the production of collagens by the fibroblasts that results in the thickening of the basement membrane and a disarray of the fibroblast layer. Bars = 200nm in A and 1um in B.

5.8. Conclusions.

The complexity of the mechanisms that contribute to airway remodeling is still only partially understood. Inflammatory factors clearly play a key role in the pathogenesis of asthma as already discussed in the introduction of this thesis, but it is quite difficult to correctly interpret the importance of these factors in matrix remodeling in experimental models where the true three-dimensional environment is missing. For example, the environmental stress could determine a variation of the remodeling response by coordinating cell responses to stress itself (Swartz et al., 2001). Moreover, two-way cell-cell communications are fundamental in mediating remodeling responses, as PBEC and fibroblasts could each "see" stress differently and therefore play different roles in ECM remodeling. The 3D ECM is therefore critical for the modulation of a stress environment for the cells that reside in it, and thus the full role played by environmental stress in the remodeling of the airways cannot be determined in the absence of a proper 3D tissue environment.

For these reasons, I have established a novel in vitro model, mimicking the bronchial mucosa, that could result particularly useful in the study of the pathogenesis of lung diseases such as asthma, where the importance of alterations of the EMTU has already been suggested but not yet fully understood.

My results show that during the culture period, the outgrowths displayed a progressive development and differentiation of their apical surface that after one month in culture was completely covered with well formed microvilli and cilia; the ratio between ciliated cells and cells with microvilli (40:60) did not change significantly after this time point. The cilia were properly functional and measured around 8 μm which is comparable with the normal length of cilia of the human bronchial epithelium. Underneath the epithelial cell layer, it was possible to observe a complex network of elongated cells showing a typical mesenchymal/fibroblastic phenotype. The epithelial layer was formed of two layers, a basal (positive for CK13) and an apical one (that expressed CK18), and it was separated from the fibroblastic layer by a well-developed basement membrane to which basal epithelial cells were attached via hemidesmosomes. The latero-lateral surface of the epithelial layer presented adhesive junctions (desmosomes) that were keeping the surfaces of adjacent cells well attached; in enlargements where desmosomes were missing, it was possible to observe exo- and endocytosis occurrences. The lower (mesenchymal)

layer showed a completely different structure with fibroblasts dispersed in a well-defined ECM (expressing collagen type I and laminin) whose proteic components were clearly extruded into the extracellular space from caveolae-like structures present on the cytoplasmic membrane of the fibroblasts. No other cytotypes (such as immune or inflammatory cells) were found, and the immunostaining results confirmed this since the outgrowths did not express CD3, CD4, CD8, CD18, CD28, CD 45, CD64, CD68 and MPO.

This model offers the possibility to conduct long term experiments, to evaluate interactions between different cell populations in a three-dimensional environment and to administer exogenous molecules. My data demonstrate that long term exposure to CSE did not cause any cell death amongst fibroblasts and epithelial cells. However, the long term treatment caused a remodeling of the architecture of the 3D outgrowths, with a complete loss of cilia (replaced by thick microvilli) from the apical epithelial cells and enhanced secretion of mucus that completely covered the microvilli. The fibroblasts instead increased their production of collagens and this resulted in a thickening of the basement membrane as well as in a complete disarray of the fibroblast layer. These structural modifications are comparable to those occurring after a chronic inflammatory insult. However, as stated above, the 3D outgrowth models are void of any immune or inflammatory cells and this would suggest that these cells might not be required for priming tissue remodeling after a long term exposure to CSE.

6. FINAL DISCUSSION

The main aim of this thesis was to investigate epithelial mesenchymal signalling in *in vitro* models of asthma, with particular attention to environmental influences. Our hypothesis was that epithelial susceptibility to environmental injury and a prolonged tissue repair response might result in activation of the EMTU, therefore promoting airway wall remodelling. In order to test our main hypothesis, we carried out our first experiments using primary cultures of human PBEC and bronchial fibroblasts obtained from both HC and AS. The choice of these cell culture models was dictated by the limited availability at that time of more complex and well characterised models of the human bronchial mucosa. Moreover, primary cell cultures have many advantages compared to cell lines, including the ability to preserve their original phenotype *in vitro* for many generations, observed during our earlier studies (Bucchieri et al., 2002), as well as the possibility of studying disease-related modification by using cells obtained from different groups of patients (i.e. AS and HC), etc.

Using these models, in this thesis, we demonstrate that there are several differences in bronchial epithelial susceptibility to environmental injuries (such as those induced by CS, oxidative stress and RV infection) and this translates into varying effects on fibroblasts. In particular, we found that AS PBEC are more susceptible to CSE-induced cell death, and that GSH is more effective in rescuing cells from CSE-induced apoptosis in the AS group. We also demonstrated that oxidant- or CSE-induced cell death in PBEC does not follow the canonical caspase pathways, but rather depends on a more direct mitochondrial damage pathway, and that apoptosis of these cells is dependent on the ECM components, with collagen IV being the most effective in sustaining higher levels of viability. Using the same cell model, we also found that infection of AS PBEC with RV-16 determined a statistically significant decrease in apoptosis when compared to infection of HC PBEC, and, consequently, that RV duplicates more efficiently in AS PBEC, determining higher rates of infection in AS.

In bronchial fibroblasts, we found that ECM was important in defining fibroblast activity and that collagen type I and fibronectin in particular determined a significant increase in adhesion rates, while laminin reduced differentiation of

fibroblasts into myofibroblasts. We also found that AS fibroblasts expressed more αSMA than HC fibroblasts; however, no significant difference in terms of fibroblast differentiation was found when different ECM components, relevant to asthma pathogenesis, were studied. Finally, we designed a sequential exposure experiment where bronchial fibroblasts were exposed to conditioned media obtained from PBEC infected with RV16; this resulted in a marked amplification of the epithelial inflammatory response by the underlying fibroblasts mainly due to increased release of IL8, IL6, RANTES and IP-10, and we concluded suggesting that any *in vivo* remodelling responses, following a RV infection, arise as a secondary consequence of chronic inflammation, rather than as a direct effect of epithelial mediators on fibroblast differentiation.

Primary cultures or cell lines still represent the most commonly used *in vitro* human models to study responses of cell systems to specific stimuli. However, the main limitations of these models are the absence of the extracellular components and the loss of proper cell-cell communication that arises from the former. In fact, in our first experiments we studied the responses of the single cell type, and while this approach can sometimes be useful to isolate specific factors of interest, we could not properly evaluate the cell-cell interactions whose modifications are at the basis of the development of complex diseases such as asthma and COPD. The use of relatively simple sequential exposure models, such as the one that we employed to study the responses of bronchial fibroblasts to the conditioned media released by the PBEC, can only partially address this issue. Furthermore, in these experiments, the epithelial cells were undifferentiated, and so did not have the benefit of protection by the epithelial mucus secretions and the physical barrier formed by the epithelial tight junctions. For this reason, in the second part of our project, we were constantly driven by the need to develop better and more complex *in vitro* models of the human bronchial mucosa. In the last few years this necessity has been motivating other groups, as evidenced by the progressively increasing number of publications on this regard. Of particular interest, in the field of tissue engineering of the lung, is the research work by Huh and colleagues on the alveolar-endothelial membrane, or more anatomically relevant to the objective of this thesis, the research by Choe and colleagues on human bronchial airways. In the latter paper, the Authors developed a tissue-engineered human airway wall model, where differentiated bronchial epithelial

cells were sitting on top of a collagen gel containing lung fibroblasts. Lateral compressive strain was then applied using a novel straining device and responses studied in terms of ECM remodelling. Their interesting results showed that dynamic strain induced increased deposition of collagen type III and IV as well as secretion of matrix metalloproteinase-2 and -9. Their conclusion was that "in a physiologically relevant three-dimensional model of the bronchial wall, dynamic compressive strain induced tissue remodeling that mimics many features of remodeling seen in asthma, in the absence of inflammation and dependent on epithelial–fibroblast signalling" (Choe et al., 2006).

In this experimental model however, bronchial epithelial cells and fibroblasts were first cultured separately and then co-cultured in an artificial collagen gel. This model, along with recently employed similar ones, is limited by the fact that the ECM is artificially laid out, the cells are already phenotypically modified before to even enter the three-dimensional system, and their life is quite short and therefore is not possible to undertake long-term experiments. In our model instead, both PBEC and fibroblasts outgrow autonomously from a bronchial biopsy into a3D gel (Matrigel), whose composition is very similar to that of the normal ECM of the bronchial airways. Moreover, after the initial expansion phase, fibroblasts start to lay out a newly formed ECM that is architecturally and structurally compatible with that of the human bronchial airways. In the meantime, the PBEC start differentiating because of the air-liquid interface, and after around 30 days of culture the outgrowths present a properly differentiated bronchial epithelium, separated, by a functional basement membrane, from a newly constituted *lamina propria* where fibroblasts lay the ECM.

However, in our model there are two limitations. First of them is the complete absence of the immune cells, and the second being the lack of circulation. The latter could be easily overcome by the employment of microfluidics (as seen in Huh et al., 2010), while the former may be considered an advantage, giving us the opportunity to selectively add, whether in the epithelial or in the mesenchymal layer, cytokines, chemokines or any other factor whose effects one might want to research. In our case, this lack of any immune or inflammatory elements has permitted us to verify that after a long-term exposure to CS, the newly formed bronchial mucosa undergoes a series of morphological changes (such as thickening of the basement membrane,

loss of ciliated cells, increase of mucus production, disarray of the *lamina propria*) typical of the inflamed and remodelled mucosa seen in chronic inflammatory lung diseases, but without immune cell intervention.

In the last few years, based on the increased knowledge of the allergic pathways of asthmatic inflammation, a number of new molecules have been identified as potential targets for the development of novel therapeutic strategies for asthma. Leukotriene modifiers (Iwona and Tomasz, 2008; Duroudier et al., 2009), IgE blockers, such as omalizumab (Babu et al., 2001; Bullerkotte et al., 2010), Mepolizumab, a monoclonal antibody directed to IL-5 with dramatic effects in reducing circulating and lung eosinophils (Flood-Page et al., 2007; Nair et al., 2009; Haldar et al., 2009), humanized or human blocking monoclonal antibodies against IL-13 or the shared IL-4rα (Corren et al., 2010; Wenzel et al., 2007), TNFα blockers such as etanercept (Berry et al., 2006; Morjaria et al., 2008), immunosuppressant drugs (Polosa and Benfatto, 2009) and allergen immunotherapy (Canonica et al., 2009) have all produced excellent results in research laboratories, only to fail more or less disappointingly in clinical application.

With all these overall negative results, it becomes legitimate to wonder whether the main pathogenetical hypotheses followed so far might be flawed in one way or another. Certainly, simple allergen sensitization and challenges in animals are very far from the reality of clinical asthma (Wenzel and Holgate, 2006) and the only animal in which asthma occurs naturally, the cat (Reinero et al., 2009), has not yet been explored as a potential model system. Greater attention should therefore now be given to the development of novel and more accurate *in vitro* systems of the bronchial airways to be used as baseline models in which to replicate the structural and biological features of asthma.

Recently, in both asthmatic biopsies and in an *in vitro* model of differentiated bronchial epithelium, a defect in epithelial tight junction formation, associated with impaired barrier function, has been reported (Holgate, 2007). In asthmatic subjects, the bronchial epithelium is also more sensitive to oxidant stress (Bucchieri et al., 2002), and it does not generate IFN-β and IFN-λ in response to virus infection (Wark et al., 2005). Therefore, most of the inflammatory and structural responses that occur in chronic asthma could be the consequence of a defective epithelium, in turn leading

to a chronic wound reaction to recurrent environmental damage (Swindle et al., 2009).

The discovery that many asthma-susceptibility genes, recently identified through positional cloning and genome-wide association studies, are expressed by epithelial cells and bronchial fibroblasts, further adds to our paradigm that assigns to the EMTU a central role in the pathogenesis of asthma (Cookson, 2004; Holgate et al., 2007). Moreover, the majority of the most frequent risk factors responsible for the development, exacerbation and chronicity of asthma, such as irritants (household and industrial chemicals), environmental tobacco smoke, respiratory viruses and certain bacteria (*Chlamydia* and *Mycoplasma*), active allergens (from house dust mite, fungal and pollens), as well as environmental pollutants (ozone, nitrogen oxides), act through the EMTU (Eder et al., 2006; Nadeem et al., 2008). One possible example of gene-environment interactions involved in asthma pathogenesis is the finding that the asthma susceptibility gene, ADAM33, which is expressed in mesenchymal cells undergoes ectodomain shedding in the presence of TGF-β2 (Puxeddu et al 2009). In this study, it was postulated epithelial susceptibility to injury would lead to an increase in epithelial TGFβ2 release which would drive ectodomain shedding of the ADAM33 metalloprotease leading to a disease-related gain of function involving increased angiogenesis. Understanding the complex interactions between epithelial susceptibility genes and the environment and how this impacts on the EMTU should be a focus of future research.Our final finding, that most of the typical features of a chronically inflamed mucosa can be reproduced in our 3D in vitro model without the presence of the cells naturally considered responsible for these modifications, seems to confirm this paradigm.

Unfortunately, due to the large number of experiments that were performed for the first part of this thesis, and to the long time necessary to first develop and then characterise the 3D outgrowth model, little time was left during the course of this PhD study for functional studies using this model. Future work will therefore be focused on repeating most of what we have already done on the primary cultures (RV infection, oxidative stress and eventual protective effect of antioxidants), on the 3D outgrowth model. It would also be of great interest to apply the outgrowth model to other tissues in order to study other diseases, where, similarly to asthma, little is known about the true interactions between resident and immune cells. The model is

particularly relevant to COPD pathogenesis and would be of great interest for studies of cystic fibrosis. Furthermore, it would be of interest to test whether similar models of the enteric mucosa can be developed and used for the study of the pathogenesis of the celiac disease that shares some similarities with asthma.

REFERENCES

- Al-Refu K, Goodfield M. Basement membrane changes in lichen planopilaris. J Eur Acad Dermatol Venereol. 2009 Nov;23(11):1289-93.
- Andreadis AA, Hazen SL, Comhair SA, Erzurum SC. Oxidative and nitrosative events in asthma. Free Radic Biol Med. 2003 Aug 1;35(3):213-25.
- Andrews AL, Nasir T, Bucchieri F, Holloway JW, Holgate ST, Davies DE. IL-13 receptor alpha 2: a regulator of IL-13 and IL-4 signal transduction in primary human fibroblasts. J Allergy Clin Immunol. 2006;118(4):858-65.
- Aoshiba K, Rennard SI, and Spurzem JR. Cell-matrix and cell-cell interactions modulate apoptosis of bronchial epithelial cells. *Am J Physiol Lung Cell Mol Physiol* 272: L28-L37, 1997.
- Araujo BB, Dolhnikoff M, Silva LF, et al. Extracellular matrix components and regulators in the airway smooth muscle in asthma. European Respiratory Journal. 2008;32(1):61–69.
- Aubier M. Traffic-related pollutants and their impact on allergic respiratory diseases. Bull Acad Natl Med. 2009;193(6):1303-13.
- Babu KS, Arshad SH, Holgate ST. Omalizumab, a novel anti-IgE therapy in allergic disorders. *Expert Opin Biol Ther* 1(6):1049-58, 2001.
- Bayram H., J.L. Devalia, O.A. Khair, M.M. Abdelaziz, R.J. Sapsford, M. Sagai, R.J. Davies, Comparison of ciliary activity and inflammatory mediator release from bronchial epithelial cells of nonatopic nonasthmatic subjects and atopic asthmatic patients and the effect of diesel exhaust particles in vitro, J. Allergy Clin. Immunol. 102 (1998) 771–782.
- Bazán-Perkins B, Sánchez-Guerrero E, Vargas MH, Martínez-Cordero E, Ramos-Ramírez P, Alvarez-Santos M, Hiriart G, Gaxiola M, Hernández-Pando R. Beta1-integrins shedding in a guinea-pig model of chronic asthma with remodelled airways. Clin Exp Allergy. 2009 May;39(5):740-51.
- Beate E, D Kessler, M Aumailley and T Krieg. Interactions of fibroblasts with the extracellular matrix: implications for the understanding of fibrosis. Springer Semin Immunopathol (2000) 21:415-429.

- Bedke N, Haitchi HM, Xatzipsalti M, Holgate ST, Davies DE. Contribution of bronchial fibroblasts to the antiviral response in asthma. J Immunol. 2009;182(6):3660-7.
- Begueret H, Berger P, Vernejoux JM, Dubuisson L, Marthan R, Tunon-De-Lara JM. Inflammation of bronchial smooth muscle in allergic asthma. Thorax. 2007;62(1):8–15.
- Beqaj S, Jakkaraju S, Mattingly RR, Pan D, Schuger L. High RhoA activity maintains the undifferentiated mesenchymal cell phenotype, whereas RhoA down-regulation by laminin-2 induces smooth muscle myogenesis. J Cell Biol 2002;156:893-903.
- Bergren DR. Environmental tobacco smoke exposure and airway hyperresponsiveness. Inflamm Allergy Drug Targets. 2009;8(5):340-7
- Berry MA, Hargadon B, Shelley M, Parker D, Shaw DE, Green RH, Bradding P, Brightling CE, Wardlaw AJ, Pavord ID. Evidence of a role of tumor necrosis factor alpha in refractory asthma. *N Engl J Med* 354(7):697-708, 2006.
- Billington CK, Penn RB. m3 muscarinic acetylcholine receptor regulation in the airway. Am J Respir Cell Mol Biol 2002;26:269-72.
- Bochkov YA, Hanson KM, Keles S, Brockman-Schneider RA, Jarjour NN, Gern JE. Rhinovirus-induced modulation of gene expression in bronchial epithelial cells from subjects with asthma. Mucosal Immunol. 2010;3(1):69-80.
- Bono, P., Rubin, K., Higgins, J. M. and Hynes, R. O. (2001). Layilin, a novel integral membrane protein, is a hyaluronan receptor. *Mol. Biol. Cell* 12, 891-900.
- Boodoo S, Spannhake EW, Powell JD, Horton MR Differential regulation of hyaluronan-induced IL-8 and IP-10 in airway epithelial cells. Am J Physiol Lung Cell Mol Physiol. 2006 Sep;291(3):L479-86.
- Borowsky, M. L. and Hynes, R. O. (1998). Layilin, a novel talin-binding transmembrane protein homologous with C-type lectins, is localized in membrane ruffles. *J. Cell Biol.* 143, 429-442.

- Bourdin A, Neveu D, Vachier I, Paganin F, Godard P, Chanez P. Specificity of basement membrane thickening in severe asthma. *J Allergy Clin Immunol* 2007;119:1367–1374.
- Boxall C, Holgate ST, Davies DE. The contribution of transforming growth factor-beta and epidermal growth factor signalling to airway remodelling in chronic asthma. *Eur Respir J* 2006;27:208–229.
- Brewster, C. E., Howarth, P. H., Djukanovic, R., Wilson, J., Holgate, S. T. and Roche, W. R. (1990). Myofibroblasts and subepithelial fibrosis in bronchial asthma. *Am. J. Respir. Cell Mol. Biol.* 3, 507-511.
- Britten, K. M., P. H. Howarth, and W. R. Roche. 1993. Immunohistochemistry on resin sections: a comparison of resin embedding techniques for small mucosal biopsies. *Biotech. Histochem.* 68:271–280.
- Bryan SA, Kanabar V, Matti S, Leckie MJ, Khan J, Rolfe L, et al. Effect of recombinant human interleukin-12 on eosinophils, airway hyper-responsiveness and the late asthmatic response. Lancet 2000;356:2149-53.
- Bucchieri F, Puddicombe SM, Lordan JL, Richter A, Buchanan D, Wilson SJ, Ward J, Zummo G, Howarth PH, Djukanović R, Holgate ST, Davies DE.Asthmatic bronchial epithelium is more susceptible to oxidant-induced apoptosis. Am J Respir Cell Mol Biol. 2002;27(2):179-85
- Bullerkotte U, Wieczorek D, Kapp A, Wedi B. Effective treatment of refractory severe heat urticaria with omalizumab. *Allergy,* 2010 Jul;65(7):931-2. Epub 2009 Nov 23.
- Buoro S, Ferrarese P, Chiavegato A, Roelofs M, Scatena M, Pauletto P, et al. Myofibroblast-derived smooth muscle cells during remodelling of rabbit urinary bladder wall induced by partial outflow obstruction. Lab Invest 1993;69:589-602.
- Burdick, J.A., Khademhosseini, A. and Langer, R. Fabrication of gradient hydrogels using a microfluidics/photopolymerization process. *Langmuir* 20(13), 5153–5156 (2004).
- Camoretti-Mercado B, Liu HW, Halayko AJ, Forsythe SM, Kyle JW, Li B, et al. Physiological control of smooth muscle-specific gene expression through regulated nuclear translocation of serum response factor. *J Biol Chem* 2000;275:30387-93.

- Canonica GW, Bousquet J, Casale T, Lockey RF, Baena-Cagnani CE, Pawankar R, Potter PC, Bousquet PJ, Cox LS, Durham SR, Nelson HS, Passalacqua G, Ryan DP, Brozek JL, Compalati E, Dahl R, Delgado L, van Wijk RG, Gower RG, Ledford DK, et al. Sub-lingual immunotherapy: World Allergy Organization Position Paper 2009. *Allergy* 64(Suppl 91):1-59, 2009.
- Carp, H. & Janoff, A. (1978) Possible mechanisms of emphysema in smokers. *In vitro* suppression of serum elastase-inhibitory capacity by fresh cigarette smoke and its prevention by antioxidants. *Am. Rev. Respir. Dis.* 118, 617-621.
- Carroll N, Elliot J, Morton A, James A. The structure of large and small airways in nonfatal and fatal asthma. Am Rev Respir Dis 1993;147:405-10.
- Chakir J, Laviolette M, Boutet M, Laliberté R, Dubé J, Boulet LP. Lower airways remodeling in nonasthmatic subjects with allergic rhinitis. Lab Invest. 1996 Nov;75(5):735-44.
- Chamley JH, Campbell GR, McConnell JD, Groschel-Stewart U. Comparison of vascular smooth muscle cells from adult human, monkey and rabbit in primary culture and in subculture. Cell Tissue Res 1977;177:503-22.
- Chaudhary N, Richter A, Collins JE, Roche WR, Davies DE, Holgate ST. Phenotype comparison of asthmatic and nonasthmatic (myo)fibroblasts [abstract]. Am J Respir Crit Care Med 2001;163:A473.
- Choe MM, Sporn PH, Swartz MA. Extracellular matrix remodeling by dynamic strain in a three-dimensional tissue-engineered human airway wall model. *Am J Respir Cell Mol Biol* 2006;35:306–313.
- Choi HR, Cho KA, Kang HT, Lee JB, Kaeberlein M, Suh Y, Chung IK, Park SC. Restoration of senescent human diploid fibroblasts by modulation of the extracellular matrix. Aging Cell. 2011 Feb;10(1):148-57.
- Chung KF, P.J. Barnes, Cytokines in asthma, Thorax 54 (1999) 825–857.
- Cokugras H, Akcakaya N, Seckin, Camcioglu Y, Sarimurat N, Aksoy F. Ultrastructural examination of bronchial biopsy specimens from children with moderate asthma. Thorax 2001;56:25-9.
- COMEAP (Committee on the Medical Effects of Air Pollution). Asthma and outdoor air pollution. London: Her Majesty's Stationery Office; 1995.

- Comhair SA, Erzurum SC. Redox control of asthma: molecular mechanisms and therapeutic opportunities. Antioxid Redox Signal. 2010;12(1):93-124.
- Cookson W. The immunogenetics of asthma and eczema: a new focus on the epithelium. *Nat. Rev. Immunol.* 2004;4:978–988.
- Cordes N, Blaese MA, Plasswilm L, Rodemann HP, Van Beuningen D. Fibronectin and laminin increase resistance to ionizing radiation and the cytotoxic drug Ukrain in human tumour and normal cells in vitro. Int J Radiat Biol. 2003 Sep;79(9):709-20.
- Corne, J.M., C. Marshall, S. Smith, J. Schreiber, G. Sanderson, S.T. Holgate, and S.L. Johnston. 2002. Frequency, severity, and duration of rhinovirus infections in asthmatic and non-asthmatic individuals: a longitudinal cohort study. *Lancet* 359:831.
- Corren J, Busse W, Meltzer EO, Mansfield L, Bensch G, Fahrenholz J, Wenzel SE, Chon Y, Dunn M, Weng HH, Lin SL. A randomized, controlled, phase 2 study of AMG 317, an IL-4Ralpha antagonist, in patients with asthma. *Am J Respir Crit Care Med* 181(8):788-96, 2010.
- Curvall, M., Enzell, C.R. & Petterson, B. (1984) An evaluation of the utility of four *in vitro* short term tests for predicting the cytotoxicity of individual compounds derived from tobacco smoke. *Cell Biol. Toxicol.* 1, 173-193.
- Darby I, Skalli O, Gabbiani G. Alpha-smooth muscle actin is transiently expressed by myofibroblasts during experimental wound healing. Lab Invest 1990;63:21-9.
- Davies DE. The role of the epithelium in airway remodeling in asthma. Proc Am Thorac Soc. 2009;6(8):678-82
- De Clerk, L.S., C.H. Bridts, A.M. Mertens, M.M. Moens, and W.J. Stevens 1999. Use of fluorescent dyes in the determination of adherence of human leucocytes to endothelial cells and the effect of fluorochromes on cellular function. *J. Immunol. Methods* 172: 115-124.
- De Raeve, H. R., F. B. Thunnissen, F. T. Kaneko, F. H. Guo, M. Lewis, M. S. Kavuru, M. Secic, M. J. Thomassen, and S. C. Erzurum. 1997. Decreased Cu,Zn-SOD activity in asthmatic airway epithelium: correction by inhaled corticosteroid in vivo. *Am. J. Physiol.* 272:L148–L154.

- De Silva D, Dagher H, Ghildyal R, Lindsay M, Li X, Freezer NJ, Wilson JW, Bardin PG. Vascular endothelial growth factor induction by rhinovirus infection. J Med Virol. 2006;78(5):666-72.
- DeLong, S.A., Moon, J.J. and West, J.L. Covalently immobilized gradients of bFGF on hydrogel scaffolds for directed cell migration. *Biomaterials* **26**(16), 3227–3234 (2005).
- Derdak S, Dixon P, Watts H, Penney D, Phipps R. CD4 expression in lung fibroblasts. Lancet. 1991 Feb 9;337(8737):374.
- Dezateux C, Stocks J. Lung development and early origins of respiratory illness. Br Med Bull 1997;53:40-57.
- Dhawan J. and Farmer S.R., Regulation of alpha 1 (I)-collagen gene expression in response to cell adhesion in Swiss 3T3 fibroblasts. *J Biol Chem* 265 (1990), pp. 9015–9021.
- Dhawan J., Lichtler A.C., Rowe D.W. and Farmer S.R., Cell adhesion regulates pro-alpha 1 (I) collagen mRNA stability and transcription in mouse fibroblasts. *J Biol Chem* 266 (1991), pp. 8470–8475.
- Djukanovic R. Airway inflammation in asthma and its consequences: implications for treatment in children and adults. J Allergy Clin Immunol 2002;109(suppl 6):S539-48.
- Dosanjh A. Transforming growth factor-beta expression induced by rhinovirus infection in respiratory epithelial cells. Acta Biochim Biophys Sin (Shanghai). 2006 Dec;38(12):911-4.
- Doull, I.J.M., F.C. Lampe, S. Smith, J. Schreiber, N.J. Freezer, and S.T. Holgate. 1997. Effect of inhaled corticosteroids on episodes of wheezing associated with viral infection in school age children: randomised double blind placebo controlled trial. *BMJ* 315, no. 7112:858.
- Dunnill MS. The pathology of asthma. Ciba Foundation Study Group. 1971;38:35-46.
- Duroudier NP, Tulah AS, Sayers I.Leukotriene pathway genetics and pharmacogenetics in allergy. Allergy. 2009 Jun;64(6):823-39. Epub 2009 Mar 26.
- Eder W., Ege M. J., von Mutius E. The asthma epidemic. *N. Engl. J. Med.* 2006;355:2226–2235.

- Fang F, Orend G, Watanabe N, Hunter T, Ruoslahti E. Dependence of cyclin E-CDK2 kinase activity on cell anchorage. *Science* 1996; 271: 499–502.
- Faux SP, Tai T, Thorne D, Xu Y, Breheny D, Gaca M. The role of oxidative stress in the biological responses of lung epithelial cells to cigarette smoke. Biomarkers. 2009;14 Suppl 1:90-6
- Fedorov IA, Wilson SJ, Davies DE, Holgate ST. Epithelial stress and structural remodelling in childhood asthma.*Thorax* 2005;60:389–394.
- Flood-Page M, Menzies-Gow S, Phipps S, Compton C, Walls C, Barnes N, et al. Reduction of tissue eosinophils in mild atopic asthmatics by an ant-IL-5 monoclonal antibody (mepolizumab) is associated with inhibition of tenascin deposition within the bronchial epithelial basement membrane [abstract]. Am J Respir Crit Care Med 2002;165:B42.
- Flood-Page P, Swenson C, Faiferman I, Matthews J, Williams M, Brannick L, Robinson D, Wenzel S, Busse W, Hansel TT, Barnes NC; International Mepolizumab Study Group. A study to evaluate safety and efficacy of mepolizumab in patients with moderate persistent asthma. *Am J Respir Crit Care Med*176(11):1062-71, 2007.
- Fraenkel, D.J., P. Bardin, G. Sanderson, S.T. Holgate, and S.L. Johnston. 1995. Lower airway inflammation during rhinovirus colds in normal and in asthmatic subjects. *Am J Respir Crit Care Med* 151:879.
- Freyer AM, Johnson SR, Hall IP. Effects of growth factors and extracellular matrix on survival of human airway smooth muscle cells. Am J Respir Cell Mol Biol 2001;25:569-76.
- Friedl, P. Prespecification and plasticity: shifting mechanisms of cell migration. *Curr. Opin. Cell Biol.* **16**(1), 14–23 (2004).
- Frisch SM and Francis H. Disruption of epithelial cell-matrix interactions induces apoptosis. *J Cell Biol* 124: 619-626, 1994.
- Gabbiani G. The myofibroblast in wound healing and fibrocontractive diseases. *J Pathol* 2003;200:500–503.
- Gailit, J. and Clark, R. A. (1994). Wound repair in the context of extracellular matrix. *Curr. Opin. Cell Biol.* 6, 717-725.
- Gangl K, Reininger R, Bernhard D, Campana R, Pree I, Reisinger J, Kneidinger M, Kundi M, Dolznig H, Thurnher D, Valent P, Chen KW, Vrtala

S, Spitzauer S, Valenta R, Niederberger V. Cigarette smoke facilitates allergen penetration across respiratory epithelium. Allergy. 2009;64(3):398-405.

- Gern, J.E., D.M. Galagan, N.N. Jarjour, E.C. Dick, and W.W. Busse. 1997. Detection of rhinovirus RNA in lower airway cells during experimentally induced infection. *Am J Respir Crit Care Med* 155:1159-61.
- Giancotti, F.G. and Ruoslahti, E. Integrin signaling. *Science* **285**(5430), 1028–1032 (1999).
- Girodet PO, Ozier A, Bara I, Tunon De Lara JM, Marthan R, Berger P. Airway remodeling in asthma: new mechanisms and potential for pharmacological intervention. Pharmacology and Therapeutics. 2011;130(3):325–337
- Gizycki, M. J., Adelroth, E., Rogers, A. V., O'Byrne, P. M. and Jeffery, P. K. (1997). Myofibroblast involvement in the allergen-induced late response in mild atopic asthma. *Am. J. Respir. Cell Mol. Biol.* 16, 664-673.
- Grinnell F. Fibroblast biology in three-dimensional collagen matrices. Trends Cell Biol. 2003 May;13(5):264-9.
- Grinnell F., Fibroblasts, myofibroblasts, and wound contraction. *J Cell Biol* 124 (1994), pp. 401–440.
- Gross A, Yin XM, Wang K, Wei MC, Jockel J, Milliman C, Erdjument-Bromage H, Tempst P, Korsmeyer SJ. Caspase cleaved BID targets mitochondria and is required for cytochrome c release, while BCL-XL prevents this release but not tumor necrosis factor-R1/Fas death. *J Biol Chem*. 1999 Jan 8;274(2):1156-63.
- Grunberg, K., H.H. Smits, M.C. Timmers, E.P. de Klerk, R.J. Dolhain, E.C. Dick, P.S. Hiemstra, and P.J. Sterk. 1997. Experimental rhinovirus 16 infection: effects on cell differentials and soluble markers in sputum in asthmatic subjects. *Am J Respir Crit Care Med* 156:609.
- Guadagno T.M. and Assoian R.K., G1/S control of anchorage-independent growth in the fibroblast cell cycle. *J Cell Biol* 115 (1991), pp. 1419–1425.
- Guadagno TM, Ohtsubo M, Roberts JM, Assoian RK. A link between cyclin A expression and adhesion-dependent cell cycle progression. *Science* 1993; 262: 1572–5.

- Gumral N, Naziroglu M, Ongel K, Beydilli ED, Ozguner F, Sutcu R, Caliskan S, Akkaya A. Antioxidant enzymes and melatonin levels in patients with bronchial asthma and chronic obstructive pulmonary disease during stable and exacerbation periods. Cell Biochem Funct. 2009;27(5):276-83.
- Haldar P, Brightling CE, Hargadon B, Gupta S, Monteiro W, Sousa A, Marshall RP, Bradding P, Green RH, Wardlaw AJ, Pavord ID. Mepolizumab and exacerbations of refractory eosinophilic asthma. *N Engl J Med* 360(10):973-84, 2009.
- Halwani R, Al-Muhsen S, Al-Jahdali H, Hamid Q. Role of transforming growth factor-β in airway remodeling in asthma. Am Journal of Resp Cell and Mol Biol. 2011;44(2):127–133.
- Hamano, Y., Zeisberg, M., Sugimoto, H., Lively, J.C., Maeshima, Y., Yang, C.Q. *et al.* Physiological levels of tumstatin, a fragment of collagen IV alpha 3 chain, are generated by MMP-9 proteolysis and suppress angiogenesis via alpha V beta 3 integrin. *Cancer Cell* **3**(6), 589–601 (2003).
- Hamilton LM, Puddicombe SM, Dearman RJ, Kimber I, Sandström T, Wallin A, Howarth PH, Holgate ST, Wilson SJ, Davies DE. Altered protein tyrosine phosphorylation in asthmatic bronchial epithelium. Eur Respir J. 2005 Jun;25(6):978-85.
- Hatch, G. E. 1995. Asthma, inhaled oxidants, and dietary antioxidants. *Am. J. Clin. Nutr*. 61:625S–630S.
- Haughland, R.P., Handbook of Fluorescent Probes and Research Chemicals. Sixth ed. ed. M.T.Z. Spence. 1996, Eugene: *Molecular Probes, Inc.* 377-384.
- Hayward IP, Bridle KR, Campbell GR, Underwood PA, Campbell JH. Effect of extracellular matrix proteins on vascular smooth muscle cell phenotype. Cell Biol Int 1995;19:839-46.
- Heijink IH, van Oosterhout A, Kapus A. Epidermal growth factor receptor signalling contributes to house dust mite-induced epithelial barrier dysfunction. Eur Respir J. 2010 Nov;36(5):1016-26.
- Hellermann GR, Nagy SB, Kong X, Lockey RF, Mohapatra SS. Mechanism of cigarette smoke condensate-induced acute inflammatory response in human bronchial epithelial cells. Respir Res. 2002;3:22.

- Herard AL, Pierrot D, Hinnrasky J *et al*. Fibronectin and its alpha 5 beta 1-integrin receptor are involved in the wound-repair process of airway epithelium. *Am. J. Physiol.* 1996; 271: L726–33.
- Hiltermann, T. J., J. Stolk, S. C. van der Zee, B. Brunekreef, C. R. de Bruijne, P. H. Fischer, C. B. Ameling, P. J. Sterk, P. S. Hiemstra, and L. van Bree. 1998. Asthma severity and susceptibility to air pollution. *Eur. Respir. J.* 11:686–693.
- Hinz B, Mastrangelo D, Iselin CE, Chaponnier C, Gabbiani G. Mechanical tension controls granulation tissue contractile activity and myofibroblast differentiation. Am J Pathol 2001;159:1009-20.
- Hisatomi T, Sakamoto T, Goto Y, Yamanaka I, Oshima Y, Hata Y, Ishibashi T, Inomata H, Susin SA, Kroemer G. Critical role of photoreceptor apoptosis in functional damage after retinal detachment. Curr Eye Res. 2002 Mar;24(3):161-72.
- Holgate S. T. Epithelium dysfunction in asthma. *J. Allergy Clin. Immunol.* 2007;120:1233–1244.
- Holgate S. T., Davies D. E., Powell R. M., Howarth P. H., Haitchi H. M., Holloway J. W. Local genetic and environmental factors in asthma disease pathogenesis: chronicity and persistence mechanisms. *Eur. Respir. J.* 2007;29:793–803.
- Holgate S.T., D.E. Davies, Epithelial desquamation in asthma, Am. J. Respir. Crit. Care Med. 164 (2001) 1997.
- Holgate ST, D. E. Davies, S. Puddicombe, A. Richter, P. Lackie, J. Lordan and P. Howarth. Mechanisms of airway epithelial damage: epithelial-mesenchymal interactions in the pathogenesis of asthma. Eur Respir J. September 20, 2003 vol. 22 no. 44 suppl 24s-29s.
- Holgate ST, Holloway J, Wilson S, Bucchieri F, Puddicombe S, Davies DE Epithelial-mesenchymal communication in the pathogenesis of chronic asthma. Proc Am Thorac Soc. 2004;1(2):93-8.
- Holgate ST, Roberts G, Arshad HS, Howarth PH, Davies DE. The role of the airway epithelium and its interaction with environmental factors in asthma pathogenesis. Proc Am Thorac Soc 2009;6:655-659.

- Holgate ST. Asthma: more than an inflammatory disease. Curr Opin Allergy Clin Immunol 2002;2:27-9.
- Holgate ST. Genetic and environmental interaction in allergy and asthma. J Allergy Clin Immunol 1999;104:1139-46.
- Holgate ST. Pathogenesis of asthma. Clin Exp Allergy. 2008;38(6):872-97.
- Holgate, S. T., D. E. Davies, P. M. Lackie, S. J. Wilson, S. M. Puddicombe, and J. L. Lordan. 2000. Epithelial-mesenchymal interactions in the pathogenesis of asthma. *J. Allergy Clin. Immunol.* 105:193–204.
- Horiba K, Fukuda Y. Synchronous appearance of fibronectin, integrin alpha 5 beta 1, vinculin and actin in epithelial cells and fibroblasts during rat tracheal wound healing. *Virchows Arch.* 1994; 425: 425–34.
- Howard, D.J., Briggs, L.A. & Pritsos, C.A. (1998) Oxidative DNA damage in mouse heart, liver, and lung tissue due to acute side-stream tobacco smoke exposure. *Arch. Biochem. Biophys.* 352, 293-297.
- Howarth PH, Wilson J, Djukanovic R, Wilson S, Britten K, Walls A, et al. Airway inflammation and atopic asthma: a comparative bronchoscopic investigation. Int Arch Allergy Appl Immunol 1991;94:266-9.
- Hu W, Xie J, Zhao J, Xu Y, Yang S, Ni W. Involvement of Bcl-2 family in apoptosis and signal pathways induced by cigarette smoke extract in the human airway smooth muscle cells. DNA Cell Biol. 2009;28(1):13-22.
- Huang X-Z, Wu J, Zhu W, Pytela R, Sheppard D. Expression of the human integrin beta 6 subunit in alveolar type II cells and bronchiolar epithelial cells reverses lung inflammation in beta6 knockout mice. *Am. J. Respir. Cell Mol. Biol.* 1998; 19: 636–42.
- Huang X-Z, Wu JF, Cass D *et al*. Inactivation of the integrin B6 sub-unit gene reveals a role of epithelial integrins in regulating inflammation in lungs and skin. *J. Cell Biol.* 1996; 133: 921–8.
- Hughes CS, Postovit LM, Lajoie GA. Matrigel: a complex protein mixture required for optimal growth of cell culture. Proteonomics 2010;10:1886-1890.
- Huh D, Matthews BD, Mammoto A, Montoya-Zavala M, Hsin HY, Ingber DE. Reconstituting organ-level lung functions on a chip. Science. 2010 Jun 25;328(5986):1662-8.

- Hulbert, W. M., T. McLean, and J. C. Hogg. 1985. The effect of acute airway inflammation on bronchial reactivity in guinea pigs. *Am. Rev. Respir. Dis.* 132: 7-11.
- Hunninghake, G. W., and R. G. Crystal. 1983. Cigarette smoking and lung destruction: accumulation of neutrophils in the lungs of cigarette smokers. *Am. Rev. Respir. Dis.* 128: 833-838
- Hurd, S. Z. 1991. Workshop summary and guidelines: investigative use of bronchoscopy, lavage, and bronchial biopsies in asthma and other airway diseases. *J. Allergy Clin. Immunol.* 88:808–814.
- Hynes, R. O. (1992). Integrins: versatility, modulation, and signaling in cell adhesion. *Cell* 69, 11-25.
- Iwona S, Tomasz G. Antileukotriene treatment in children with asthma--new patents. Recent Pat Inflamm Allergy Drug Discov. 2008;2(3):202-11.
- Jeffery P. Structural alterations and inflammation of bronchi in asthma. Int J Clin Pract Suppl 1998;96:5-14.
- Jeffery, P. K., A. J. Wardlaw, F. C. Nelson, J. V. Collins, and A. B. Kay. 1989. Bronchial biopsies in asthma: an ultrastructural, quantitative study and correlation with hyperreactivity. *Am. Rev. Respir. Dis.* 140:1745–1753.
- Jiao ZX, Ao QL, Xiong M Cigarette smoke extract inhibits the proliferation of alveolar epithelial cells and induces apoptosis. Sheng Li Xue Bao. 2006;58(3):244-54.
- Johnson PR, Roth M, Tamm M, Hughes M, Ge Q, King G, et al. Airway smooth muscle cell proliferation is increased in asthma. Am J Respir Crit Care Med 2001;164:474-7.
- Johnson PRA, Burgess JK. Airway smooth muscle and fibroblasts in the pathogenesis of asthma. *Curr Allergy Asthma Rep* 2004;4:102–108.
- Johnston, S.L., P.K. Pattemore, G. Sanderson, S. Smith, F. Lampe, L. Josephs, P. Symington, S. O'Toole, S.H. Myint, D.A.J. Tyrell, and S.T. Holgate. 1995. Community study of the role of viral infections in exacerbations of asthma in 9-11year old children. *BMJ* 310:1225.
- Johnston, S.L., P.K. Pattemore, G. Sanderson, S. Smith, M.J. Campbell, L.K. Josephs, A. Cunningham, B.S. Robinson, S.H. Myint, M.E. Ward, D.A. Tyrrell, and S.T. Holgate. 1996. The relationship between upper respiratory

infections and hospital admissions for asthma: a time-trend analysis. *Am J Respir Crit Care Med* 154:654.

- Kaur B, Rowe BH, Arnold E. Vitamin C supplementation for asthma. Cochrane Database Syst Rev. 2009;21;(1):CD000993
- Kelly MM, Leigh R, Bonniaud P, Ellis R, Wattie J, Smith MJ, Martin G, Panju M, Inman MD, Gauldie J. Epithelial expression of profibrotic mediators in a model of allergen-induced airway remodeling. *Am J Respir Cell Mol Biol* 2005;32:99–107.
- Kelly, F. J., I. Mudway, A. Blomberg, A. Frew, and T. Sandstrom. 1999. Altered lung antioxidant status in patients with mild asthma. *Lancet* 354: 482–483.
- Kim ES, Kim SH, Kim KW, Park JW, Kim YS, Sohn MH, Kim KE. Basement membrane thickening and clinical features of children with asthma. *Allergy* 2007;62:635–640.
- Kim KK, Kugler MC, Wolters PJ, Robillard L, Galvez MG, Brumwell AN, Sheppard D, Chapman HA. Alveolar epithelial cell mesenchymal transition develops in vivo during pulmonary fibrosis and is regulated by the extracellular matrix. Proc Natl Acad Sci U S A. 2006 Aug 29;103(35):13180-5. Epub 2006 Aug 21.
- Kirkham P, Rahman I. Oxidative stress in asthma and COPD: antioxidants as a therapeutic strategy. Pharmacol Ther. 2006;111(2):476-9-
- Kitamura H, Cambier S, Somanath S, Barker T, Minagawa S, Markovics J, Goodsell A, Publicover J, Reichardt L, Jablons D, Wolters P, Hill A, Marks JD, Lou J, Pittet JF, Gauldie J, Baron JL, Nishimura SL. Mouse and human lung fibroblasts regulate dendritic cell trafficking, airway inflammation, and fibrosis through integrin αvβ8-mediated activation of TGF-β. J Clin Invest. 2011 Jul;121(7):2863-75.
- Kleinman, H.K., Philp, D. and Hoffman, M.P. Role of the extracellular matrix in morphogenesis. *Curr. Opin. Biotechnol.* **14**(5), 526–532 (2003).
- Kloek J, Mortaz E, Van Ark I, Lilly CM, Nijkamp FP, Folkerts G. Glutathione prevents the early asthmatic reaction and airway hyperresponsiveness in guinea pigs. J Physiol Pharmacol. 2010;61(1):67-72.

- Korpi-Steiner NL, Valkenaar SM, Bates ME, Evans MD, Gern JE, Bertics PJ Human monocytic cells direct the robust release of CXCL10 by bronchial epithelial cells during rhinovirus infection. Clin Exp Allergy. 2010;40(8):1203-13.
- Kuo C, Lim S, King NJ, Bartlett NW, Walton RP, Zhu J, Glanville N, Aniscenko J, Johnston SL, Burgess JK, Black JL, Oliver BG. Rhinovirus infection induces expression of airway remodelling factors in vitro and in vivo. Respirology. 2011;16(2):367-77. doi: 10.1111/j.1440-1843.2010.01918.x.
- Kuo C, Lim S, King NJ, Bartlett NW, Walton RP, Zhu J, Glanville N, Aniscenko J, Johnston SL, Burgess JK, Black JL, Oliver BG. Rhinovirus infection induces expression of airway remodelling factors in vitro and in vivo. Respirology. 2011 Feb;16(2):367-77.
- Lachowicz-Scroggins ME, Boushey HA, Finkbeiner WE, Widdicombe JH. Interleukin-13-induced mucous metaplasia increases susceptibility of human airway epithelium to rhinovirus infection. Am J Respir Cell Mol Biol. 2010;43(6):652-61.
- Lackie P.M., J.E. Baker, U. Günthert, S.T. Holgate, Expression of CD44 isoforms is increased in the airway epithelium of asthmatic subjects, Am. J. Respir. Cell. Mol. Biol. 16 (1997) 14–22.
- Lange P, Parner J, Vestbo J, Schnohr P, Jensen G. A 15-year follow-up study of ventilatory function in adults with asthma. N Engl J Med 1998;339:1194-200.
- Laprise C, Laviolette M, Boutet M, et al. Asymptomatic airway hyperresponsiveness: relationships with airway inflammation and remodelling. Eur Respir J 1999;14:63-73.
- Larsen K, Malmstrom J, Wildt M, Dahlqvist C, Hansson L, Marko-Varga G, Bjermer L, Scheja A, Westergren-Thorsson G. Functional and phenotypical comparison of myofibroblasts derived from biopsies and bronchoalveolar lavage in mild asthma and scleroderma. *Respir Res* 2006;7:11.
- Law L, Zheng L, Orsida B, Levvey B, Oto T, Kotsimbos AT, Snell GI, Williams TJ. Early changes in basement membrane thickness in airway walls post-lung transplantation. *J Heart Lung Transplant* 2005;24:1571–1576.

- Leckie MJ, Brinke AT, Khan J, Diamant Z, O'Connor B, Walls CM, et al. Effects of an interleukin-5 blocking monoclonal antibody on eosinophils, airways hyper-responsiveness, and the late asthmatic response. Lancet 2000;356:2144-8.
- Lee KS, Kim SR, Park SJ, Min KH, Lee KY, Jin SM, Yoo WH, Lee YC. Antioxidant down-regulates interleukin-18 expression in asthma. Mol Pharmacol. 2006;70(4):1184-93.
- Lijnen, H.R. Elements of the fibrinolytic system. *Ann. N. Y. Acad. Sci.* **936**, 226–236 (2001).
- Loubaki L, Semlali A, Boisvert M, Jacques E, Plante S, Aoudjit F, Mourad W, Chakir J. Crosstalk between T cells and bronchial fibroblasts obtained from asthmatic subjects involves CD40L/alpha 5 beta 1 interaction. Mol Immunol. 2010 Jul;47(11-12):2112-8.
- MacPherson JC, Comhair SA, Erzurum SC, Klein DF, Lipscomb MF, Kavuru MS, Samoszuk MK, Hazen SL Eosinophils are a major source of nitric oxide-derived oxidants in severe asthma: characterization of pathways available to eosinophils for generating reactive nitrogen species. J Immunol. 2001;166(9):5763-72.
- McAnulty RJ, Chambers RC & Laurent GJ. Regulation of fibroblast procollagen production. Transforming growth factor-beta 1 induces prostaglandin E2 but not procollagen synthesis via a pertussis toxin-sensitive G-protein. *Biochem. J.* 1995; 307: 63–8.
- McParland BE, Macklem PT, Pare PD. Airway wall remodeling: friend or foe? Journal of Applied Physiology. 2003;95(1):426–434.
- Meiss RA. Influence of intercellular tissue connections on airway muscle mechanics. Journal of Applied Physiology. 1999;86(1):5–15.
- Merendino AM, Bucchieri F, Gagliardo R, Daryadel A, Pompeo F, Chiappara G, Santagata R, Bellia V, David S, Farina F, Davies DE, Simon HU, Vignola AM. CD40 ligation protects bronchial epithelium against oxidant-induced caspase-independent cell death. Am J Respir Cell Mol Biol. 2006 Aug;35(2):155-64. Epub 2006 Mar 16.
- Message SD, Johnston SL. Viruses in asthma. Br Med Bull 2002;61:29-43.

- Michalik M, Pierzchalska M, Legutko A, Ura M, Ostaszewska A, Soja J, Sanak M. Asthmatic bronchial fibroblasts demonstrate enhanced potential to differentiate into myofibroblasts in culture. Med Sci Monit. 2009 Jul;15(7):BR194-201.
- Michalik M, Pierzchalska M, Włodarczyk A, Wójcik KA, Czyż J, Sanak M, Madeja Z. Transition of asthmatic bronchial fibroblasts to myofibroblasts is inhibited by cell-cell contacts. Respir Med. 2011 Oct;105(10):1467-75.
- Mochitate K, Pawelek P, Grinnell F. Stress relaxation of contracted collagen gels: disruption of actin filament bundles, release of cell surface fibronectin, and down- regulation of DNA and protein synthesis. Exp Cell Res 1991;193:198-207.
- Moharamzadeh K, Brook IM, Van Noort R, Scutt AM, Smith KG, Thornhill MH. Development, optimization and characterization of a full-thickness tissue engineered human oral mucosal model for biological assessment of dental biomaterials. J Mater Sci Mater Med. 2008;19(4):1793-801.
- Montefort, S., J. A. Roberts, R. Beasley, S. T. Holgate, and W. R. Roche. 1992. The site of disruption of the bronchial epithelium in asthmatic and non-asthmatic subjects. *Thorax* 47:499–503.
- Morcillo, E. J., J. Estrela, and J. Cortijo. 1999. Oxidative stress and pulmonary inflammation: pharmacological intervention with antioxidants. *Pharmacol. Res.* 40:393–404.
- Morioka M, Parameswaran H, Naruse K, Kondo M, Sokabe M, Hasegawa Y, Suki B, Ito S. Microtubule dynamics regulate cyclic stretch-induced cell alignment in human airway smooth muscle cells. PLoS One. 2011;6(10):e26384.
- Morjaria JB, Chauhan AJ, Babu KS, Polosa R, Davies DE, Holgate ST. The role of a soluble TNFalpha receptor fusion protein (etanercept) in corticosteroid refractory asthma: a double blind, randomised, placebo controlled trial. *Thorax* 63(7):584-91, 2008.
- Mutsaers SE, Bishop JE, McGrouther G, Laurent GJ. Mechanisms of tissue repair: from wound healing to fibrosis. *Int. J. Biochem. Cell Biol.* 1997; **29**: 5–17.

- Myohanen, H. T., Stephens, R. W., Hedman, K., Tapiovaara, H., Ronne, E., Hoyer-Hansen, G., Dano, K. and Vaheri, A. (1993). Distribution and lateral mobility of the urokinase-receptor complex at the cell surface. *J. Histochem. Cytochem.* 41, 1291-1301.
- Nadeem A, Chhabra SK, Masood A, Raj HG. Increased oxidative stress and altered levels of antioxidants in asthma. J Allergy Clin Immunol. 2003;111(1):72-8.
- Nadeem A, Masood A, Siddiqui N. Oxidant--antioxidant imbalance in asthma: scientific evidence, epidemiological data and possible therapeutic options. Ther Adv Respir Dis. 2008;2(4):215-35.
- Nadeem A., Masood A., Siddiqui N. Oxidant–antioxidant imbalance in asthma: scientific evidence, epidemiological data and possible therapeutic options. *Ther. Adv. Respir. Dis.* 2008;2:215–235.
- Nair P, Pizzichini MM, Kjarsgaard M, Inman MD, Efthimiadis A, Pizzichini E, Hargreave FE, O'Byrne PM. Mepolizumab for prednisone-dependent asthma with sputum eosinophilia. *N Engl J Med*360(10):985-93, 2009.
- Nicholson, K.G., J. Kent, and D.C. Ireland. 1993. Respiratory viruses and exacerbations of asthma in adults. *BMJ* 307:982.
- Olatunji-Bello II, Olayemi SO, Daramola AO, Ogungbemi AO Ascorbic acid and the effect of cigarette smoke on tissues--a preliminary report. West Afr J Med. 2008;27(2):78-81.
- Ordonez, C., R. Ferrando, D. M. Hyde, H. H. Wong, and J. V. Fahy. 2000. Epithelial desquamation in asthma: artifact Or pathology? *Am. J. Respir. Crit. Care Med.* 162:2324–2329.
- Page-McCaw, A., Ewald, A.J. and Werb, Z. Matrix metalloproteinases and the regulation of tissue remodelling. *Nat. Rev. Mol. Cell Biol.* **8**(3), 221–233 (2007).
- Papadopoulos NG, Bates PJ, Bardin PG, Papi A, Leir SH, Fraenkel DJ, Meyer J, Lackie PM, Sanderson G, Holgate ST, Johnston SL. Rhinoviruses infect the lower airways. J Infect Dis. 2000;181(6):1875-84.
- Papadopoulos NG, Papi A, Meyer J, Stanciu LA, Salvi S, Holgate ST, Johnston SL. Rhinovirus infection up-regulates eotaxin and eotaxin-2 expression in bronchial epithelial cells. Clin Exp Allergy. 2001;31(7):1060-6.

- Papi, A. & Johnston, S.L. Respiratory epithelial cell expression of vascular cell adhesion molecule-1 and its up-regulation by rhinovirus infection via NF-kB and GATA transcription factors. *J Biol Chem* 274, 9707-9720 (1999).
- Pepe C, Foley S, Shannon J, Lemiere C, Olivenstein R, Ernst P, Ludwig MS, Martin JG, Hamid Q. Differences in airway remodeling between subjects with severe and moderate asthma. *J Allergy Clin Immunol* 2005;116:544–549.
- Persson CG. On the medical history of xanthines and other remedies for asthma: a tribute to HH Salter. Thorax. 1985;40(12):881-6.
- Phan, S. H. (1996). Role of the myofibroblast in pulmonary fibrosis. *Kidney Int. Suppl.* 54, S46-48.
- Phipps RP, Penney DP, Keng P, Quill H, Paxhia A, Derdak S, Felch ME. Characterization of two major populations of lung fibroblasts: distinguishing morphology and discordant display of Thy 1 and class II MHC. Am J Respir Cell Mol Biol. 1989 Jul;1(1):65-74.
- Pierrou S, Broberg P, O'Donnell RA, Pawłowski K, Virtala R, Lindqvist E, Richter A, Wilson SJ, Angco G, Möller S, Bergstrand H, Koopmann W, Wieslander E, Strömstedt PE, Holgate ST, Davies DE, Lund J, Djukanovic R. Expression of genes involved in oxidative stress responses in airway epithelial cells of smokers with chronic obstructive pulmonary disease. Am J Respir Crit Care Med. 2007 Mar 15;175(6):577-86. Epub 2006 Dec 7.
- Pilewski JM, Latoche JD, Arcasoy SM, Albelda SM. Expression of integrin cell adhesion receptors during human airway epithelial repair in vivo. *Am. J. Physiol.* 1997; 273: L256–L263.
- Pohunek P, Roche WR, Tarzikova J, Kurdmann J, Warner JO. Eosinophilic inflammation in the bronchial mucosa in children with bronchial asthma [abstract]. Eur Respir J 2000;11(suppl 25):160s.
- Polosa R, Benfatto GT. Managing patients with chronic severe asthma: rise to the challenge. *Eur J Intern Med* 20(2):114-24, 2009.
- Postma, D. S., T. E. Renkema, J. A. Noordhoek, H. Faber, H. J. Sluiter, and H. Kauffman. 1988. Association between nonspecific bronchial hyperreactivity and superoxide anion production by polymorphonuclear leukocytes in chronic air-flow obstruction. *Am. Rev. Respir. Dis.* 137:57–61.

- Proud D. Role of rhinovirus infections in asthma. Asian Pac J Allergy Immunol. 2011 Sep;29(3):201-8.
- Puddicombe, S. M., R. Polosa, A. Richter, M. T. Krishna, P. H. Howarth, S. T. Holgate, and D. E. Davies. 2000. The involvement of the epidermal growth factor receptor in epithelial repair in asthma. *FASEB J.* 14:1362–1374.
- Puxeddu I, Berkman N, Nissim Ben Efraim AH, Davies DE, Ribatti D, Gleich GJ, Levi-Schaffer F. The role of eosinophil major basic protein in angiogenesis. Allergy. 2009 Mar;64(3):368-74. Epub 2008 Dec 17.
- Qian J, Kumar A, Szucsik JC, Lessard JL. Tissue and developmental specific expression of murine smooth muscle gamma-actin fusion genes in transgenic mice. Dev Dyn 1996;207:135-44.
- Quint JK, Donaldson GC, Goldring JJ, Baghai-Ravary R, Hurst JR, Wedzicha JA. Serum IP-10 as a biomarker of human rhinovirus infection at exacerbation of COPD. Chest. 2010;137(4):812-22.
- Rahman I, MacNee W. Oxidative stress and regulation of glutathione in lung inflammation. Eur Respir J 2000;16:534-54.
- Rahman, I., C. A. Smith, M. F. Lawson, D. J. Harrison, and W. MacNee. 1996. Induction of gamma-glutamylcysteine synthetase by cigarette smoke is associated with AP-1 in human alveolar epithelial cells. *FEBS Lett.* 396: 21-25.
- Ramos-Barbón D, Fraga-Iriso R, Brienza NS, Montero-Martínez C, Verea-Hernando H, Olivenstein R, Lemiere C, Ernst P, Hamid QA, Martin JG. T Cells localize with proliferating smooth muscle alpha-actin+ cell compartments in asthma. Am J Respir Crit Care Med. 2010 Aug 1;182(3):317-24.
- Reddel, H., S. Ware, G. Marks, C. Salome, C. Jenkins, and A. Woolcock. 1999. Differences between asthma exacerbations and poor asthma control. *Lancet* 353:364.
- Redington AE, Madden J, Frew AJ, Djukanovic R, Roche WR, Holgate ST, et al. Transforming growth factor-beta 1 in asthma. Measurement in bronchoalveolar lavage fluid. Am J Respir Crit Care Med 1997;156:642-7.

- Reinero CR, DeClue AE, Rabinowitz P. Asthma in humans and cats: is there a common sensitivity to aeroallegens in shared environments? *Environ Res* 109(5):634-40, 2009.
- Richter A, Puddicombe SM, Lordan JL, Bucchieri F, Wilson SJ, Djukanovic R, et al. The contribution of interleukin (IL)-4 and IL-13 to the epithelial-mesenchymal trophic unit in asthma. Am J Respir Cell Mol Biol 2001;25:385-91.
- Roche, W. R., Beasley, R., Williams, J. H. and Holgate, S. T. (1989). Subepithelial fibrosis in the bronchi of asthmatics. *Lancet* i, 520-524.
- Rowe RG, Keena D, Sabeh F, Willis AL, Weiss SJ. Pulmonary fibroblasts mobilize the membrane-tethered matrix metalloprotease, MT1-MMP, to destructively remodel and invade interstitial type I collagen barriers. Am J Physiol Lung Cell Mol Physiol. 2011 Nov;301(5):L683-92..
- Royce SG, Tan L, Koek AA, Tang ML. Effect of extracellular matrix composition on airway epithelial cell and fibroblast structure: implications for airway remodeling in asthma. Ann Allergy Asthma Immunol. 2009 Mar;102(3):238-46.
- Rozario T, DeSimone DW. The extracellular matrix in development and morphogenesis: a dynamic view. Dev Biol. 2010 May 1;341(1):126-40. Epub 2009 Oct 23.
- Saetta, M., A. Di Stefano, P. Maestrelli, A. Ferraresso, R. Drigo, A. Potena, A. Ciaccia, and L. M. Fabbri. 1993. Activated T-lymphocytes and macrophages in bronchial mucosa of subjects with chronic bronchitis. *Am. Rev. Respir. Dis.* 147: 301-306.
- Saetta, M., A. Di Stefano, P. Maestrelli, G. Turato, M. P. Ruggieri, A. Roggeri, P. Calcagni, C. E. Mapp, A. Ciaccia, and L. M. Fabbri. 1994. Airway eosinophilia in chronic bronchitis during exacerbations. *Am. J. Respir. Crit. Care Med.* 150: 1646-1652.
- Saglani S, Malmström K, Pelkonen AS, Malmberg LP, Lindahl H, Kajosaari M, Turpeinen M, Rogers AV, Payne DN, Bush A, *et al.* Airway remodeling and inflammation in symptomatic infants with reversible airflow obstruction. *Am J Respir Crit Care Med* 2005;171:722–72.

- Saglani S, Payne DN, Zhu J, Wang Z, Nicholson AG, Bush A, Jeffery PK. Early detection of airway wall remodeling and eosinophilic inflammation in preschool wheezers. *Am J Respir Crit Care Med* 2007;176:858–864.
- Salter HH. On Asthma: Its Pathology and Treatment. London: John Churchill, 1860.
- Salvi SS, Sampson AP, Holgate ST. Asthma. In: Encyclopedia of Life Sciences. Nature Publishing Group, 2001;1-8. DOI: 10.1038/npg.els.0002305.
- Sander EE, van Delft S, ten Klooster JP, Reid T, van der Kammen RA, Michiels F, and Collard JG. Matrix-dependent Tiam1/Rac signaling in epithelial cells promotes either cell-cell adhesion or cell migration and is regulated by phosphatidylinositol 3-kinase. *J Cell Biol* 143: 1385-1398, 1998.
- Sappino AP, Schurch W, Gabbiani G. Differentiation repertoire of fibroblastic cells: expression of cytoskeletal proteins as marker of phenotypic modulations. Lab Invest 1990;63:144-61..
- Scaffidi AK, Moodley YP, Weichselbaum M, Thompson PJ, Knight DA. Regulation of human lung fibroblast phenotype and function by vitronectin and vitronectin integrins. J Cell Sci 2001;114:3507-16.
- Schmitt-Gräff A, Desmoulière A, Gabbiani G. Heterogeneity of myofibroblast phenotypic features: an example of fibroblastic cell plasticity. Virchows Arch. 1994;425(1):3-24.
- Schroth MK, Grimm E, Frindt P, Galagan DM, Konno SI, Love R, Gern JE. Rhinovirus replication causes RANTES production in primary bronchial epithelial cells. Am J Respir Cell Mol Biol. 1999;20(6):1220-8.
- Sedgwick JB, Calhoun WJ, Gleich GJ, Kita H, Abrams JS, Schwartz LB, Volovitz B, Ben-Yaakov M, Busse WW Immediate and late airway response of allergic rhinitis patients to segmental antigen challenge. Characterization of eosinophil and mast cell mediators. Am Rev Respir Dis. 1991;144(6):1274-81.
- Sedgwick, J. B., W. J. Calhoun, R. F. Vrtis, M. E. Bates, P. K. McAllister, and W. W. Busse. 1992. Comparison of airway and blood eosinophil function after in vivo antigen challenge. *J. Immunol.* 149:3710–3718.

- Serini, G. and Gabbiani, G. (1999). Mechanisms of myofibroblast activity and phenotypic modulation. *Exp. Cell Res*. 250, 273-283.
- Sheppard D. Epithelial integrins. *Bioessays* 1996; 18: 655–60.
- Sheppard D. Roles of airway epithelial integrins in health and disease. *Chest* 1996; 109: 29S–32S.
- Siedlinski M, van Diemen CC, Postma DS, Vonk JM, Boezen HM. Superoxide dismutases, lung function and bronchial responsiveness in a general population. Eur Respir J. 2009 May;33(5):986-92.
- Sigurs, N. 2002. Clinical perspectives on the association between respiratory syncytial virus and reactive airways disease. *Respir Res* 3(Suppl 1):S8-S14.
- Skadhuage LR, Christensen K, Kyvik KO, Sigsgaard T. Genetic and environmental influence on asthma: a population based study of 11,688 Danish twin pairs. Eur Respir J 1999;13:8-14.
- Smith, L. J., M. Shamsuddin, P. H. Sporn, M. Denenberg, and J. Anderson. 1997. Reduced superoxide dismutase in lung cells of patients with asthma. *Free Radic. Biol. Med.* 22:1301–1307.
- Snyder JC, Zemke AC, Stripp BR. Reparative capacity of airway epithelium impacts deposition and remodeling of extracellular matrix. *Am J Respir Cell Mol Biol* 2009;40:633–642.
- Sont JK, Willems LN, Bel EH, van Krieken JH, Vandenbroucke JP, Sterk PJ. Clinical control and histopathologic outcome of asthma when using airway hyperresponsiveness as an additional guide to long-term treatment. The AMPUL Study Group. Am J Respir Crit Care Med 1999;159:1043-51.
- Soutar A, Seaton A, Brown K. Bronchial reactivity and dietary antioxidants. Thorax 1997;52:166-70.
- Spanakis E, Brouty-Boyé D. Discrimination of fibroblast subtypes by multivariate analysis of gene expression. Int J Cancer. 1997 May 2;71(3):402-9.
- Spanakis E, Brouty-Boyé D. Quantitative variation of proto-oncogene and cytokine gene expression in isolated breast fibroblasts. Int J Cancer. 1995 May 29;61(5):698-705.
- Spears M, Cameron E, Chaudhuri R, Thomson NC. Challenges of treating asthma in people who smoke. Expert Rev Clin Immunol 2010; 6(2):257-68.

- Spurrell JC, Wiehler S, Zaheer RS, Sanders SP, Proud D. Human airway epithelial cells produce IP-10 (CXCL10) in vitro and in vivo upon rhinovirus infection. Am J Physiol Lung Cell Mol Physiol. 2005;289(1):L85-95.
- Stevens PT, Kicic A, Sutanto EN, Knight DA, Stick SM. Dysregulated repair in asthmatic paediatric airway epithelial cells: the role of plasminogen activator inhibitor-1. *Clin Exp Allergy* 2008;38:1901–1910.
- Stone, K., Bermudez, E. & Pryor, W.A. (1994) Aqueous extracts of cigarette tar containing the tar free radical cause DNA nicks in mammalian cells. *Environ. Health Perspect.* 102, 173-178.
- Streuli C. Extracellular matrix remodelling and cellular differentiation. *Curr Opin Cell Biol* 11: 634-640, 1999.
- Sumino KC, Walter MJ, Mikols CL, Thompson SA, Gaudreault-Keener M, Arens MQ, Agapov E, Hormozdi D, Gaynor AM, Holtzman MJ, Storch GA. Detection of respiratory viruses and the associated chemokine responses in serious acute respiratory illness. Thorax. 2010;65(7):639-44.
- Swartz MA, Tschumperlin DJ, Kamm RD, Drazen JM. Mechanical stress is communicated between different cell types to elicit matrix remodeling. Proc Natl Acad Sci U S A 2001;98:6180-5.
- Swartz MA, Tschumperlin DJ, Kamm RD, Drazen JM.Mechanical stress is communicated between different cell types to elicit matrix remodelling. *Proc Natl Acad Sci USA* 2001;98:6180–6185.
- Swindle E. J., Collins J. E., Davies D. E. Breakdown in epithelial barrier function in patients with asthma: identification of novel therapeutic approaches. *J. Allergy Clin. Immunol.* 2009;124:23–34.
- Swindle EJ, Collins JE, Davies DE. Breakdown in epithelial barrier function in patients with asthma: identification of novel therapeutic approaches. J Allergy Clin Immunol. 2009 Jul;124(1):23-34.
- Taipale, J., & Keski-Oja, J. (1997). Growth factors in the extracellular matrix. FASEB J 11(1), 51−59.
- Takeyama, K., K. Dabbagh, S. J. Jeong, T. Dao-Pick, I. F. Ueki, and J. A. Nadel. 2000. Oxidative stress causes mucin synthesis via transactivation of epidermal growth factor receptor: role of neutrophils. *J. Immunol.* 164: 1546-1552.

- Tang, H., Kerins, D. M., Hao, Q., Inagami, T. and Vaughan, D. E. (1998). The urokinase-type plasminogen activator receptor mediates tyrosine phosphorylation of focal adhesion proteins and activation of mitogen-activated protein kinase in cultured endothelial cells. *J. Biol. Chem.* 273, 18268-18272.
- Teran L.M., Mochizuki M., Bartels J., Valencia E.L., Nakajima T., Hirai K. and Schroder J.M. Th1- and Th2-type cytokines regulate the expression and production of eotaxin and RANTES by human lung fibroblasts. *Am J Respir Cell Mol Biol* 20 4 (1999), pp. 777–786.
- The Childhood Asthma Management Program Research Group. Long-term effects of budesonide or nedocromil in children with asthma. N Engl J Med 2000;343:1054-63.
- The Global Initiative for Asthma. Global strategy for asthma management and prevention; a six part asthma management program. Bethesda, Md: National Institutes of Health; 2002. NHLBI publication no. 02-3659:93-172.
- Thompson HG, Mih JD, Krasieva TB, Tromberg BJ, George SC. Epithelial-derived TGF-beta2 modulates basal and wound-healing subepithelial matrix homeostasis. *Am J Physiol Lung Cell Mol Physiol* 2006;291:L1277-L1285.
- Thompson, A. B., D. Daughton, R. A. Robbins, M. A. Ghafouri, M. Oehlerking, and S. I. Rennard. 1989. Intraluminal airway inflammation in chronic bronchitis: characterization and correlation with clinical parameters. *Am. Rev. Respir. Dis.* 140: 1527-1537.
- Tomasek JJ, Gabbiani G, Hinz B, Chaponnier C, Brown RA. Myofibro-blasts and mechano-regulation of connective tissue remodelling. Nat Rev Mol Cell Biol 2002;3:349-63.
- Torry D.J., Richards C.D., Podor T.J. and Gauldie J., Anchorage-independent colony growth of pulmonary fibroblasts derived from fibrotic human lung tissue. *J Clin Invest* 93 (1994), pp. 1525–1532
- Tschumperlin DJ, Drazen JM. Mechanical stimuli to airway remodeling. Am J Respir Crit Care Med 2001;164(suppl):S90-4.
- Tschumperlin DJ, Oswari J, Margulies AS. Deformation-induced injury of alveolar epithelial cells. Effect of frequency, duration, and amplitude. *Am J Respir Crit Care Med* 2000;162:357–362.

- Tschumperlin DJ, Shively JD, Kikuchi T, Drazen JM. Mechanical stress triggers selective release of fibrotic mediators from bronchial epithelium. *Am J Respir Cell Mol Biol* 2003;28:142–149.
- Van Ganse E, Laforest L, Pietri G, Boissel JP, Gormand F, Ben Joseph R, et al. Persistent asthma: disease control, resource utilisation and direct costs. Eur Respir J 2002;20:260-7.
- Van Ly D, King NJ, Moir LM, Burgess JK, Black JL, Oliver BG. Effects of β(2) Agonists, Corticosteroids, and Novel Therapies on Rhinovirus-Induced Cytokine Release and Rhinovirus Replication in Primary Airway Fibroblasts. J Allergy (Cairo). 2011;2011:457169.
- Vermes, I., C. Haanen, H. Steffens-Nakken, and C. Reutelingsperger. 1995. A novel assay for apoptosis: flow cytometric detection of phosphatidylserine expression on early apoptotic cells using fluorescein labelled Annexin V. *J. Immunol. Methods* 184:39–51.
- Vignola AM, Chiappara G, Siena L, Bruno A, Gagliardo R, Merendino AM, Polla BS, Arrigo AP, Bonsignore G, Bousquet J, and Chanez P. Proliferation and activation of bronchial epithelial cells in corticosteroid-dependent asthma. *J Allergy Clin Immunol* 108: 738-746, 2001.
- Wadsworth SJ, Anette M. Freyer, Randolph L. Corteling and Ian P. Hall. Biosynthesized matrix provides a key role for survival signaling in bronchial epithelial cells. *Am J Physiol Lung Cell Mol Physiol* 286: L596-L603, 2004.
- Warburton D, Schwarz M, Tefft D, et al. The molecular basis of lung morphogenesis. Mech Dev 2000;92:55-81.
- Wark PA, Johnston SL, Bucchieri F, Powell R, Puddicombe S, Laza-Stanca V, Holgate ST, Davies DE. Asthmatic bronchial epithelial cells have a deficient innate immune response to infection with rhinovirus. J Exp Med. 2005;201(6):937-47.
- Wark, P. A. B., S. L. Johnston, I. Moric, J. L. Simpson, M. J. Hensley, and P. G. Gibson. 2002. Neutrophil degranulation and cell lysis is associated with clinical severity in virus-induced asthma. *Eur Respir J* 19:68-75.
- Wei, Y., Yang, X., Liu, Q., Wilkins, J. A. and Chapman, H. A. (1999). A role for caveolin and the urokinase receptor in integrin-mediated adhesion and signaling. *J. Cell Biol.* 144, 1285-1294.

- Welch, M. P., Odland, G. F. and Clark, R. A. (1990). Temporal relationships of F-actin bundle formation, collagen and fibronectin matrix assembly, and fibronectin receptor expression to wound contraction. *J. Cell Biol.* 110, 133-145.
- Wenzel S, Holgate ST. The mouse trap: It still yields few answers in asthma. *Am J Respir Crit Care Med* 174(11):1173-6, 2006.
- Wenzel S, Wilbraham D, Fuller R, Getz EB, Longphre M. Effect of an interleukin-4 variant on late phase asthmatic response to allergen challenge in asthmatic patients: results of two phase 2a studies. *Lancet* 370(9596):1422-31, 2007.
- Werb Z, Tremble PM, Behrendtsen O, Crowley E, Damsky CH. Signal transduction through the fibronectin receptor induces collagenase and stromelysin gene expression. *J. Cell Biol.* 1989; 109: 877–89.
- Werb Z, Tremble PM, Behrendtsen O, Crowley E, Damsky CH. Signal transduction through the fibronectin receptor induces collagenase and stromelysin gene expression. *J. Cell Biol.* 1989; **109**: 877–89.
- Westergren-Thorsson G, Larsen K, Nihlberg K, Andersson-Sjöland A, Hallgren O, Marko-Varga G, Bjermer L. Pathological airway remodelling in inflammation. Clin Respir J. 2010 May; 4 Suppl 1:1-8.
- Wewers, M. D., and J. E. Gadek. 1987. The protease theory of emphysema. *Ann. Intern. Med.* 107: 761-763.
- Wicks J, Haitchi HM, Holgate ST, Davies DE, Powell RM. Enhanced upregulation of smooth muscle related transcripts by TGF beta2 in asthmatic (myo) fibroblasts. Thorax. 2006 Apr;61(4):313-9. Epub 2006 Jan 31.
- Wicks J, Haitchi HM, Holgate ST, Davies DE, Powell RM. Enhanced upregulation of smooth muscle related transcripts by TGF beta2 in asthmatic (myo) fibroblasts. Thorax. 2006 Apr;61(4):313-9. Epub 2006 Jan 31.
- Wiggs BR, Bosken C, Pare PD, James A, Hogg JC. A model of airway narrowing in asthma and in chronic obstructive pulmonary disease. Am Rev Respir Dis 1992;145:1251-8.
- Wilson JW, Li X, Pain MC. The lack of distensibility of asthmatic airways. American Review of Respiratory Disease. 1993;148(3):806–809.

- Wood LG, Powell H, Grissell TV, Davies B, Shafren DR, Whitehead BF, Hensley MJ, Gibson PG. Persistence of rhinovirus RNA and IP-10 gene expression after acute asthma. Respirology. 2011;16(2):291-9.
- Wood LG, Simpson JL, Wark PA, Powell H, Gibson PG. Characterization of innate immune signalling receptors in virus-induced acute asthma. Clin Exp Allergy. 2010 Dec 3.
- Woods, A. and Couchman, J. R. (1994). Syndecan 4 heparan sulfate proteoglycan is a selectively enriched and widespread focal adhesion component. *Mol. Biol. Cell* 5, 183-192.
- Woods, A. and Couchman, J. R. (1998). Syndecans: synergistic activators of cell adhesion. *Trends Cell Biol.* 8, 189-192.
- Woods, A., Longley, R. L., Tumova, S. and Couchman, J. R. (2000). Syndecan-4 binding to the high affinity heparin-binding domain of fibronectin drives focal adhesion formation in fibroblasts. *Arch. Biochem. Biophys.* 374, 66-72.
- Xiao C, Puddicombe SM, Field S, Haywood J, Broughton-Head V, Puxeddu I, Haitchi HM, Vernon-Wilson E, Sammut D, Bedke N, Cremin C, Sones J, Djukanović R, Howarth PH, Collins JE, Holgate ST, Monk P, Davies DE. Defective epithelial barrier function in asthma. J Allergy Clin Immunol. 2011 Sep;128(3):549-56.e1-12.
- Yamashita J, Itoh H, Hirashima M, Ogawa M, Nishikawa S, Yurugi T, et al. Flk1-positive cells derived from embryonic stem cells serve as vascular progenitors. Nature 2000;408:92-6.
- Yang Y, Beqaj S, Kemp P, Ariel I, Schuger L. Stretch-induced alternative splicing of serum response factor promotes bronchial myogenesis and is defective in lung hypoplasia. J Clin Invest 2000;106:1321-30.
- Yebra, M., Goretzki, L., Pfeifer, M. and Mueller, B. M. (1999). Urokinase-type plasminogen activator binding to its receptor stimulates tumor cell migration by enhancing integrin-mediated signal transduction. *Exp. Cell Res.* 250, 231-240.
- Zaheer RS, Koetzler R, Holden NS, Wiehler S, Proud D. Selective transcriptional down-regulation of human rhinovirus-induced production of

CXCL10 from airway epithelial cells via the MEK1 pathway. J Immunol. 2009;182(8):4854-64

- Zhang HY, Phan SH. Inhibition of myofibroblast apoptosis by transforming growth factor beta(1). Am J Respir Cell Mol Biol 1999;21:658-65.
- Zhang J, O'Shea S, Liu J, Schuger L. Bronchial smooth muscle hypoplasia in mouse embryonic lungs exposed to a laminin beta1 chain antisense oligonucleotide. Mech Dev 1999;89:15-23.
- Zhang M, Zhang Z, Pan HY, Wang DX, Deng ZT, Ye XL. TGF-beta1 induces human bronchial epithelial cell-to-mesenchymal transition in vitro. Lung. 2009 May-Jun;187(3):187-94. Epub 2009 Feb 28.
- Zhang X, Chen J, Graham SH, Du L, Kochanek PM, Draviam R, Guo F, Nathaniel PD, Szabó C, Watkins SC, Clark RS. Intranuclear localization of apoptosis-inducing factor (AIF) and large scale DNA fragmentation after traumatic brain injury in rats and in neuronal cultures exposed to peroxynitrite. J Neurochem. 2002 Jul;82(1):181-91.
- Zhu C, Qiu L, Wang X, Hallin U, Candé C, Kroemer G, Hagberg H, Blomgren K. Involvement of apoptosis-inducing factor in neuronal death after hypoxia-ischemia in the neonatal rat brain. J Neurochem. 2003 Jul;86(2):306-17.
- Zimmermann, P. and David, G. (1999). The syndecans, tuners of transmembrane signaling. *FASEB J.* 13 Suppl., S91-S100.